

University of Warwick institutional repository: <http://go.warwick.ac.uk/wrap>

**A Thesis Submitted for the Degree of PhD at the University of Warwick**

<http://go.warwick.ac.uk/wrap/56212>

This thesis is made available online and is protected by original copyright.

Please scroll down to view the document itself.

Please refer to the repository record for this item for information to help you to cite it. Our policy information is available from the repository home page.

***STRUCTURAL STUDIES OF  
MAIN GROUP METAL  
CARBOXYLATES AND DITHIOCARBAMATES***

by

**Stephen Mark Roe**

**A thesis submitted in partial fulfilment of the requirements for the degree of Doctor of Philosophy.**

**Department of Chemistry,  
University of Warwick,  
Coventry. CV4 7AL.**

**October 1989**

For Jinks.

## Table of Contents

<b>Chapter 1: Introduction</b> .....	1
1.1 General Chemistry of Organotin Complexes .....	1
1.2 General Chemistry of Organotellurium Complexes .....	4
1.3 Carboxylic Acids and Dithiocarbamates .....	5
1.4 Secondary Bonding .....	9
References .....	11
<b>Chapter 2: The Crystal Structures of Four Triphenyltin and One Triphenyltellurium Carboxylates</b> .....	13
2.1 Introduction .....	13
2.2 Results .....	14
2.3 Experimental .....	17
References .....	40
<b>Chapter 3: The Crystal Structures of Two Diphenyltin Dicarboxylates and One Diphenyltellurium Dicarboxylate</b> .....	43
3.1 Introduction .....	43
3.2 Results .....	44
3.3 Experimental .....	46
References .....	64
<b>Chapter 4: The Crystal Structures of Three Diphenyltellurium Bisdithiocarbamates</b> .....	66
4.1 Introduction .....	66
4.2 Results .....	66
4.3 Experimental .....	68
References .....	88
<b>Chapter 5: The Crystal Structures of Six Hydrolysis Products of Organotin Compounds</b> .....	90
5.1 Introduction .....	90
5.2 Results .....	91
5.3 Experimental .....	94
References .....	131
<b>Chapter 6: Experimental Section</b> .....	135
6.1 Choice of Crystal .....	135
6.2 Crystal Mounting and Data Collection Procedure .....	136
References .....	141
<b>Chapter 7: Conclusions and Further Areas of Study</b> .....	142
7.1 Conclusions .....	142
7.2 Areas of Further Study .....	143
<b>Appendix A: Crystallographic Theory and Structure Solution</b> .....	145



A.1 Diffraction of X-Rays .....	145
A.2 Symmetry and Space Groups .....	146
A.3 Data Reduction .....	149
A.4 The Structure Factor and Patterson Function .....	151
A.5 Structure Solution and Refinement .....	152
References .....	155
<b>Appendix B: Thermal Parameter Tables .....</b>	<b>156</b>
<b>Appendix C: Final Structure Factor Tables .....</b>	<b>175</b>

## List of Tables

<b>Table</b>	<b>Title</b>	<b>Page</b>
Table 1.1	Coordination modes of Carboxylic acids	7
Table 2.1	Crystal Data and Data Collection Parameters for [1]-[5]	28
Table 2.2	Atomic Coordinates for [1]	29
Table 2.3	Atomic Coordinates for [2]	30
Table 2.4	Atomic Coordinates for [3]	31
Table 2.5	Atomic Coordinates for [4]	32
Table 2.6	Atomic Coordinates for [5]	33
Table 2.7	Bond Lengths and Angles for [1]	34
Table 2.8	Bond Lengths and Angles for [2]	35
Table 2.9	Bond Lengths and Angles for [3]	36
Table 2.10	Bond Lengths and Angles for [4]	37
Table 2.11	Bond Lengths and Angles for [5]	38
Table 2.12	Infra-red and <sup>1</sup> H-n.m.r. data	39
Table 2.12	Selected Bond Lengths	39
Table 3.1	Crystal Data and Data Collection Parameters for [6]-[8]	56
Table 3.2	Atomic Coordinates for [6]	57
Table 3.3	Atomic Coordinates for [7]	58
Table 3.4	Atomic Coordinates for [8]	59
Table 3.5	Bond Lengths and Angles for [6]	60
Table 3.6	Bond Lengths and Angles for [7]	61
Table 3.7	Bond Lengths and Angles for [8]	62
Table 3.8	Infra-red and <sup>1</sup> H-n.m.r. data	63
Table 4.1	Crystal Data and Data Collection Parameters for [9]-[11]	77
Table 4.2	Atomic Coordinates for [9]	78
Table 4.3	Atomic Coordinates for [10]	79
Table 4.4	Atomic Coordinates for [11]	80

Table 4.4	cont.	81
Table 4.5	Bond Lengths and Angles for [9]	82
Table 4.6	Bond Lengths and Angles for [10]	84
Table 4.7	Bond Lengths and Angles for [11]	85
Table 4.7	cont.	86
Table 4.8	Selected Bond Lengths	87
Table 4.9	Deviations from Mean Planes	87
Table 5.1	Crystal Data and Data Collection Parameters for [12]-[17]	112
Table 5.2	Atomic Coordinates for [12]	113
Table 5.3	Atomic Coordinates for [13]	114
Table 5.4	Atomic Coordinates for [14]	115
Table 5.5	Atomic Coordinates for [15]	116
Table 5.5	cont.	117
Table 5.6	Atomic Coordinates for [16]	118
Table 5.7	Atomic Coordinates for [17]	119
Table 5.8	Bond Lengths and Angles for [12]	120
Table 5.9	Bond Lengths and Angles for [13]	121
Table 5.9	cont.	122
Table 5.10	Bond Lengths and Angles for [14]	123
Table 5.10	cont.	124
Table 5.11	Bond Lengths and Angles for [15]	125
Table 5.11	cont.	126
Table 5.11	cont.	127
Table 5.12	Bond Lengths and Angles for [16]	128
Table 5.13	Bond Lengths and Angles for [17]	129
Table 5.13	cont.	130
Table 5.13	cont.	131
Table 7.1	Selected Bond Lengths	144
Table A.1	The Seven Crystal Systems	147

<b>Table B.1</b>	<b>Anisotropic thermal parameters for [1]</b>	<b>157</b>
<b>Table B.2</b>	<b>Anisotropic thermal parameters for [2]</b>	<b>158</b>
<b>Table B.3</b>	<b>Anisotropic thermal parameters for [3]</b>	<b>159</b>
<b>Table B.4</b>	<b>Anisotropic thermal parameters for [4]</b>	<b>160</b>
<b>Table B.5</b>	<b>Anisotropic thermal parameters for [5]</b>	<b>161</b>
<b>Table B.6</b>	<b>Anisotropic thermal parameters for [6]</b>	<b>162</b>
<b>Table B.7</b>	<b>Anisotropic thermal parameters for [7]</b>	<b>163</b>
<b>Table B.8</b>	<b>Anisotropic thermal parameters for [8]</b>	<b>164</b>
<b>Table B.9</b>	<b>Anisotropic thermal parameters for [9]</b>	<b>165</b>
<b>Table B.10</b>	<b>Anisotropic thermal parameters for [10]</b>	<b>166</b>
<b>Table B.11</b>	<b>Anisotropic thermal parameters for [11]</b>	<b>167</b>
<b>Table B.12</b>	<b>Anisotropic thermal parameters for [12]</b>	<b>168</b>
<b>Table B.13</b>	<b>Anisotropic thermal parameters for [13]</b>	<b>169</b>
<b>Table B.14</b>	<b>Anisotropic thermal parameters for [14]</b>	<b>170</b>
<b>Table B.15</b>	<b>Anisotropic thermal parameters for [15]</b>	<b>171</b>
<b>Table B.15</b>	<b>cont.</b>	<b>172</b>
<b>Table B.16</b>	<b>Anisotropic thermal parameters for [16]</b>	<b>173</b>
<b>Table B.17</b>	<b>Anisotropic thermal parameters for [17]</b>	<b>174</b>

## List of Figures

<b>Figure</b>	<b>Title</b>	<b>Page</b>
Scheme 1.1	Hydrolysis Pathways for $R_3SnX$ and $R_2SnX_2$	2
Figure 1.1	Proposed structures for $R_2Sn(OCOR)_2$	3
Figure 1.2	Carboxylate Bridging with Metal-Metal bonding	8
Figure 1.3	Resonance Behaviour in Dithiocarbamates	9
Figure 2.1	View of the Molecule of [1]	20
Figure 2.2	View of the Polymeric Chain of [1]	21
Figure 2.3	View of the Molecule of [2]	22
Figure 2.4	View of the Polymeric Chain of [2]	23
Figure 2.5	View of the Molecule of [3]	24
Figure 2.6	View of the Hydrogen Bonded Chain of [3]	25
Figure 2.7	View of the Molecule of [4]	26
Figure 2.8	View of the Dimer formed by [5]	27
Figure 3.1	View of the Molecule of [6]	50
Figure 3.2	Packing Diagram for [6]	51
Figure 3.3	View of the Molecule of [7]	52
Figure 3.4	View of the Packing of [7]	53
Figure 3.5	View of the Dimer formed by [8]	54
Figure 3.6	Packing Diagram for [8]	55
Figure 4.1	View of the Molecule of [9]	71
Figure 4.2	Packing Diagram for [9]	72
Figure 4.3	View of the Molecule of [10]	73
Figure 4.4	Packing Diagram for [10]	74
Figure 4.5	View of the Molecule of [11]	75
Figure 4.6	Packing Diagram for [11]	76
Figure 5.1	View of the Dimer formed by [12]	99

Figure 5.2	View of the Dimer formed by [13]	100
Figure 5.3	View of [13] with Phenyl groups removed	101
Figure 5.4	Packing Diagram for [13]	102
Figure 5.5	View of the Dimer formed by [14]	103
Figure 5.6	View of [14] with Phenyl groups removed	104
Figure 5.7	Packing Diagram for [14]	105
Figure 5.8	View of the Dimer formed by [15]	106
Figure 5.9	View of [15] with Phenyl groups removed	107
Figure 5.10	Top View of the Hexamer formed by [16]	108
Figure 5.11	Side View of the Hexamer formed by [16]	109
Figure 5.12	View of the Dimer formed by [17]	110
Figure 5.13	View of [17] with Phenyl groups removed	111
Scheme 5.1-5	Possible Hydrolysis Schemes for [12] to [16]	131
Figure 6.1	The Goniometer Head	137
Figure 6.2	The Four Circles of the Diffractometer	137
Figure 6.3	Example of a Rotation Photograph	138
Figure A.1	Diffraction of X-Rays from Crystal Planes	145
Figure A.2	Derivation of Miller Indices For Any Plane of Reflection	146
Figure A.3	The Fourteen Bravais Lattices	148
Figure A.4	Primary Extinction in a Crystal	153

## **Declaration**

**The work described in this thesis is entirely original and my own, except where otherwise indicated.**

## **Publications**

Parts of the work contained in this thesis have been published in the scientific literature under the following references:

Nathaniel W. Alcock and S. Mark Roe, *J. Chem. Soc., Dalton Trans.*, 1989, 1589.

S. M. Roe and N.W. Alcock, *Proceedings of the Sixth ICOCC of Ge, Sn and Pb*, Brussels 1989.



## Acknowledgments

I would like to thank my supervisor Dr. N.W. Alcock for his help and guidance in the field of crystallography. My thanks also to my wife and our parents, for their encouragement and support throughout my period of research. Lastly, my thanks also to everyone in the Chemistry department for their assistance and friendship.

This thesis has been written using the *troff* word processing program, with the preprocessors *tbl* and *eqn*, running under the UNIX operating system and printed on an Agfa P400PS postscript printer. I would like to thank the operators for their help during the last four years.

I am indebted to the S.E.R.C. for financial support for the research.

## Abstract

The work contained in this thesis describes the crystal structures of a number of tin(IV) and tellurium(IV) carboxylates and dithiocarbamates. The results show the regularity at which these types of compounds form secondary bonds (weak interactions), and the effect of the lone pair of tellurium(IV) on the geometries formed. The area has been studied through the determination of the following crystal structures:

- i) monocarboxylates:  $\text{Ph}_3\text{SnOCOCH}_2\text{Cl}$ ,  $\text{Ph}_3\text{SnOCOCHCl}_2$ ,  $\text{Ph}_3\text{SnOCOCCl}_3 \cdot \text{MeOH}$ ,  $\text{Ph}_3\text{SnOCOCCl}_3$  and  $\text{Ph}_3\text{TeOCOCCl}_3$ .
- ii) dicarboxylates:  $\text{Ph}_2\text{Sn}(\text{OCOCH}_3)_2$ ,  $\text{Ph}_2\text{Sn}(\text{OCOCH}_2\text{Cl})_2$  and  $\text{Ph}_2\text{Te}(\text{OCOCCl}_3)_2$ .
- iii) dithiocarbamates:  $\text{Ph}_2\text{Te}(\text{S}_2\text{CNEt}_2)_2$ ,  $\text{Ph}_2\text{Te}(\text{S}_2\text{CN}(\text{Et})(\text{Ph}))_2$  and  $\text{Ph}_2\text{Te}(\text{S}_2\text{CNPh}_2)_2$ .

In addition to these, six hydrolysis products of  $\text{Ph}_3\text{SnOCOCCl}_3$  are reported. These compounds show the varied results that are obtained from the facile dearylation of the organotin compound by a strong organic acid in the presence of water. The following structures are reported:  $\text{Ph}_2\text{Sn}(\text{OH})(\text{OCOCCl}_3)$ ,  $\{[\text{Ph}_2\text{Sn}(\text{OCOCCl}_3)]_2\text{O}\}_2$  (two isomers),  $[(\text{PhSn})_3(\text{O})_2(\text{OCOCCl}_3)_5]_2$ ,  $[\text{PhSn}(\text{O})(\text{OCOCCl}_3)]_6$  and  $[(\text{Ph}_2\text{Sn})_2(\text{OH})(\text{OCOCCl}_3)_3]_2$ .

# CHAPTER 1

## Introduction

### 1.1 General Chemistry and Geometry of OrganoTin Complexes

Tin is a group 14 metallic element. It has the electronic structure  $[\text{Kr}] 4d^{10} 5s^2 5p^2$ , and thus has two main oxidation states,  $\text{Sn}^{\text{II}}$  and  $\text{Sn}^{\text{IV}}$ . The  $\text{Sn}^{\text{III}}$  state is known for only one compound,  $[(\text{Me}_3\text{Si})_2\text{CH}]_3\text{Sn}$ , the radical surviving due to shielding from the bulky organo groups. This thesis will be concerned with the +IV oxidation state only.

Syntheses in organotin(IV) chemistry usually start from the corresponding organotin halide compound  $\text{R}_n\text{SnX}_{4-n}$ . These can be formed by a metathesis reaction by mixing appropriate amounts of the tetraorganotin compound (formed from tin tetrahalide by reaction with excess Grignard reagent) and tin tetrahalide<sup>1</sup>. The diorganotin dihalide can also be simply prepared by reacting an organohalide with tin metal. This was first studied by Frankland<sup>2</sup>, who termed it 'Direct Synthesis'. The halides can then be replaced by a wide variety of substituents, including oxides, hydroxides, hydrides, amines or other organo groups.

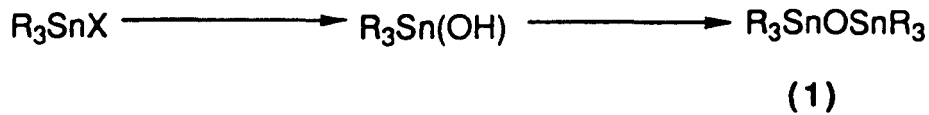
A further route into organotin chemistry is by cleavage of the Sn-C bond in a tetraorganotin compound. This can be accomplished by a wide variety of compounds including halogens, to form  $\text{R}_3\text{SnX}$ ,  $\text{R}_2\text{SnX}_2$  or  $\text{RSnX}_3$  depending on conditions, group I and III metal halides, e.g.  $\text{AlCl}_3$ , halides, e.g.  $\text{VOCl}_3$ ,  $\text{CuBr}_2$  to form  $\text{R}_3\text{SnX}$ , inorganic acids and, to a lesser extent, organic acids<sup>3-8</sup>.

A major problem with organotin halides is their susceptibility to hydrolysis. This is due to the strength of the Sn-O bond<sup>9</sup> and the drive to the formation of the stable  $\text{Sn}_2\text{O}_2$  stannoxane ring unit. Scheme 1.1 shows the hydrolysis pathways for  $\text{R}_3\text{SnX}$  and  $\text{R}_2\text{SnX}_2$ . Structure types (1), (2), (3) and (4) can all dimerise to form  $\text{Sn}_2\text{O}_2$  rings, e.g. (6). The dihydroxide can not be isolated, due to very rapid loss of  $\text{H}_2\text{O}$  to form  $\text{R}_2\text{SnO}$ , but all the others have been identified structurally.

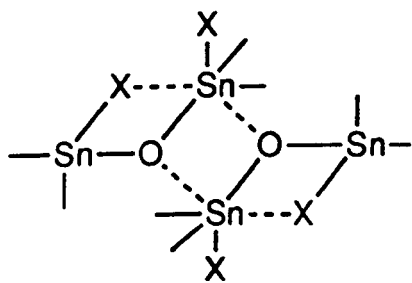
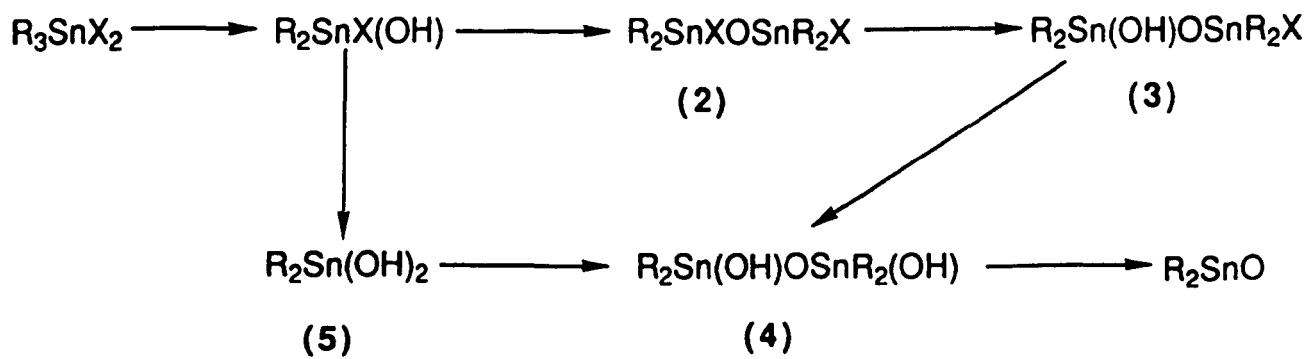
There are four main routes for preparing organotin carboxylates. These are:-

- (i) the reaction of the carboxylic acid with either the organotin oxide or hydroxide in refluxing toluene, with the use of a Dean-Stark separator to remove water from the reaction,
- (ii) from organotin halides (usually chlorides) by reaction with the metal salt of an acid ( $\text{M}=\text{Ag}$ ,  $\text{Na}$ ,  $\text{K}$ ,  $\text{Tl}$ ),

**Scheme 1**



**Scheme 2**



(6)

**Scheme 1.1:** Hydrolysis pathways of  $\text{R}_3\text{SnX}$  and  $\text{R}_2\text{SnX}_2$

- (iii) reaction of the organotin hydride with the carboxylic acid to produce the ester and liberate hydrogen gas or
- (iv) cleavage of the Sn-C bond in a tetraorganotin compound by a carboxylic acid.

In this work variations of methods (i) and (ii) were generally used because (iii) and (iv) were found to give many side reactions with the strong acids used (halocarboxylates).

Tin differs from its lower group members by its willingness to expand its coordination shell from four up to five, six and seven. Some eight coordinate complexes have also been reported<sup>10-12</sup>. This facile increase in coordination is for two reasons. Firstly, more groups can be accommodated around the Sn(IV) atom than around the Si(IV) or Ge(IV) centres, due to a large increase in the covalent radius (Si=1.17Å, Ge=1.22Å, Sn=1.40Å)<sup>9</sup>, and, secondly, the Sn centre is a strong Lewis acid ( $R_4Sn \ll R_3SnCl < R_2SnCl_2 < RSnCl_3 < SnCl_4$ ), unlike Si and Ge which are not. In fact, four coordination only occurs for tin compounds that either have no secondary coordinating ability, i.e.  $Sn(C_6F_5)_4$ , or have bulky groups preventing further coordination<sup>13,14</sup>. To achieve this extra coordinating ability the tin uses its d-orbitals to expand the valence shell from  $sp^3$ , for tetrahedral structures, to  $sp^3d^4$ , for eight coordinate complexes.

In triorganotin carboxylates the most common structure involves the carboxylate group bridging between two tin atoms, thus creating a linear chain with trigonal bipyramidal tin centres<sup>15</sup>. No diorganotin carboxylates or organotin tricarboxylate structures had been reported at the start of this work, but three structures had been proposed on the basis of IR and Moessbauer data for the dicarboxylates. They are shown in Figure 1.1. Two dicarboxylate complexes are reported here and show that the solution structure (I) is retained in the solid state. Tricarboxylates have been synthesised<sup>16</sup> but are extremely sensitive to moisture, and have not been studied in any detail.

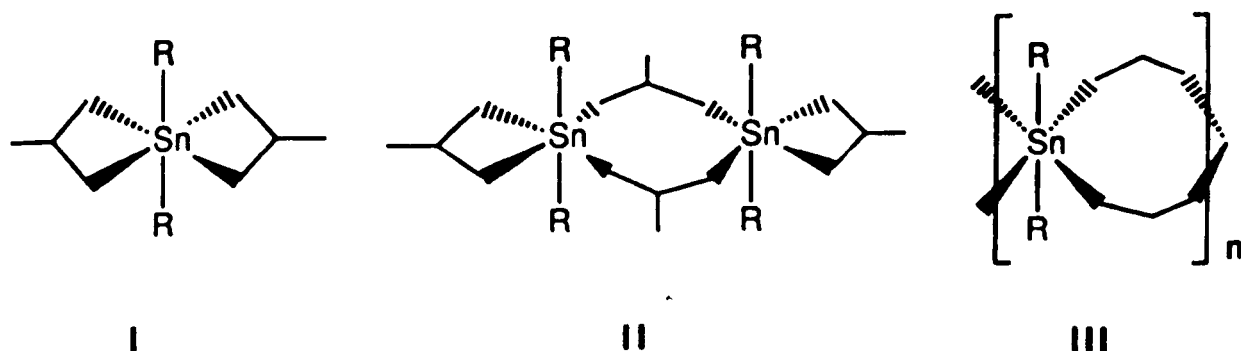


**Figure 1.1:** Proposed structures for  $R_2Sn(OCOR)_2$

Triorganotin dithiocarbamates have a distorted tetrahedral geometry<sup>17-20</sup>, with the second sulphur forming a secondary bond to the tin. Diorganotin dithiocarbamates have been reported as six coordinate, with the dithiocarbamates equatorial and bidentate<sup>19,21,22</sup>.

Impetus in the area of organotin carboxylate chemistry has come mainly from the pharmaceutical and agricultural industries. Triorganotin and, to a lesser extent, diorganotin compounds have been found to be extremely toxic in small doses to such diverse systems as fungi and mammals. For instance,  $\text{Et}_3\text{SnOAC}$  is very toxic to mammals and  $\text{Ph}_3\text{Sn}$  compounds have been used in small doses as effective fungicides against Potato Blight since the early 1960's<sup>23</sup>. Organotin compounds are important biocides for three reasons. Firstly, the toxicity is dependent on the organotin moiety, not the tin itself. Secondly, they inhibit a fundamental biological process, namely the transportation of electrons in the cell, thus disrupting photosynthesis in plants, for example. Thirdly, the tin compounds are easily broken down in the environment, by either sunlight or soil microbes, to produce harmless inorganic compounds, unlike their mercury analogues. The dependency of the toxic effects on the organo groups in the compound is the most important of the three reasons, because this creates the possibility to synthesise many different compounds with varying organo groups to maximise the effect of the compound for specific situations. Tin compounds are also used for the stabilisation of polymers and act by trapping any free radicals or  $\text{HCl}$  produced by the action of sunlight on the polymer.

## 1.2 General Chemistry and Geometry of Organotellurium Complexes

Tellurium is a group 16 element. Unlike tin, tellurium was only discovered in the 18<sup>th</sup> Century<sup>24</sup>, and has been investigated to lesser extent. The main interest in tellurium compounds stems from their use as vulcanising agents in rubber. It has the electronic structure  $[\text{Kr}] 4d^{10}5s^25p^4$  and can have formal oxidation states of -2, +1, +2, +4 and +6. Tellurium is a borderline metallic/non-metallic element. With the formal oxidation state -2, tellurium acts like  $\text{O}^{2-}$ , i.e. forms  $\text{H}_2\text{Te}$ . The +1 oxidation state is known for many organo compounds, i.e.  $\text{RTeTeR}$ <sup>25</sup>, but the halo complexes are much less stable. The +6 state is only known for  $\text{TeF}_6$ . The +2 and +4 states are the most stable. This thesis will only be concerned with the +4 oxidation state, using the tellurium as a metal centre, to compare with analogous tin compounds.

Organotellurium chemistry, like tin, usually proceeds from the halide compound. The main methods of preparation are listed below.

- (i) mono, di or triorganotellurium species can be formed by the reaction of the appropriate amounts of  $\text{RMgX}$ ,  $\text{RHgX}$  or  $\text{RLi}$  compounds on  $\text{TeCl}_4$ .
- (ii) triaryl compounds can be formed by the direct reaction of  $\text{TeCl}_4$  on an activated aromatic compound, i.e.  $\text{PhOEt}$  to give  $p\text{-EtOC}_6\text{H}_4\text{TeCl}_3$ . This is a facile reaction involving electrophilic attack of  $\text{Cl}_3\text{Te}^+$ . The reaction does not proceed past the trihalide. Bromo or iodo complexes do not react as well as chloro complexes.
- (iii) diorgano compounds can be specifically formed by the reaction of  $\text{R}_2\text{Hg}$  on  $\text{TeCl}_4$ , the oxidative addition of  $\text{X}_2$  on to  $\text{R}_2\text{Te}$  or the action of a diazonium salt  $(\text{ArN}_2)\text{Cl}$  on  $\text{Te}$  metal.

To form compounds with halides other than chloride, it is usually easier to synthesise the chloride then carry out a halide exchange reaction. The di and trihalide compounds are slightly susceptible to hydrolysis. The triorgano compounds, on the other hand, are completely stable, often being recrystallised from boiling water. The triorgano compounds are essentially ionic in nature and exist as  $\text{R}_3\text{Te}^+ \text{X}^-$  in solution.

Tellurium carboxylates have been synthesised in three ways. Firstly, the reaction of the chloride with a metal salt of the acid, usually  $\text{Ag}$ . Secondly, the disproportionation of an acid chloride with  $\text{R}_2\text{Te}$  to form  $\text{R}_2\text{Te}(\text{acid})_2$  and  $\text{R}_2\text{TeCl}_2$ . Thirdly,  $\text{Te}(\text{acid})_4$  has been produced by the reaction of a carboxylic acid on  $\text{TeCl}_4$  in benzene.

Tellurium, in the +4 oxidation state, has a lone pair of electrons. Thus the expected structure, from VSEPR theory, for a tetraalkyl tellurium compound is trigonal bipyramidal, with the lone pair in an equatorial position, and this has been proved to be the case, e.g.  $\text{Ph}_4\text{Te}$ <sup>26</sup>. Tellurium though, like tin, is also prone to increasing its valence shell above four coordination, using secondary interactions.  $\text{TeF}_6(\text{NMe}_3)_2$  and  $\text{Te}(\text{motc})_4$  ( $\text{motc}=\text{N}-(2\text{-hydroxyethyl})\text{-N-methyl-dithiocarbamate}$ ) have been reported as stable eight coordinate complexes<sup>27,28</sup>. A further possibility in the geometry of tellurium compounds is that the lone pair may become stereochemically inert, for instance  $(\text{NH}_4)_2\text{TeCl}_6$  has an octahedral geometry<sup>29</sup>. This phenomenon has been discussed by Urch<sup>30</sup>.

### 1.3 Carboxylic Acids and Dithiocarbamates

Carboxylic acids,  $\text{RCOOH}$ , have been used as coordination ligands from the 19<sup>th</sup> Century onwards<sup>31</sup>. They make up a large and varied section of the coordination chemistry papers

reported. This is due to three reasons. Firstly, the carboxylic acids, and their derivative salts, are easy to handle and purify, and the physical properties of the carboxylates can be easily changed by altering the substituent groups. Secondly, they are readily available by a variety of methods, including oxidation of alcohols, insertion of CO<sub>2</sub> and hydrolysis of esters<sup>32</sup>. Finally, and perhaps most importantly, they have a very varied coordination behaviour, with ten types of coordination characterised (Table 1.1).

The neutral carboxylic acid has, in a simplistic view, one single and one double C-O bond. From Paulings standard covalent radii, the bond lengths should be 1.45Å, for the C-O, and 1.21Å, for the C=O. However these values are never achieved in reality, there is always some degree of delocalisation present, due to resonance behaviour, the average values for the neutral molecule being 1.23Å and 1.33Å. In the anion the carboxylate becomes totally delocalised and the average C-O bond length has been reported as 1.26Å<sup>33</sup>.

This delocalisation has been used to categorise the carboxylate complexes by infra-red spectroscopy<sup>34</sup>. In complexes where the carboxylate acts as a unidentate ligand, it should have a spectrum similar to a neutral carboxylate. Thus, there is a large difference between the strengths of the (nominal) C-O and C=O bonds, leading to a large difference ( $\Delta$ ) between the corresponding symmetric and antisymmetric stretches in the infra-red spectrum. Compounds that have chelating or bridging carboxylates will have similar strength C-O bonds and, therefore, a small difference ( $\Delta$ ) between the IR stretches. For acetate complexes it has been reported that compounds with  $\Delta > 200\text{cm}^{-1}$ , the carboxylate will be unidentate and below this level, either bidentate or chelating<sup>34</sup>. Ranges were proposed to distinguish chelating and bidentate complexes, however these are not reliable<sup>35</sup>. Care also has to be taken when comparing results from different carboxylic acids, since changes in the substituents can cause large changes in the position of the peaks in the IR spectrum. For instance changing from acetate to trifluoroacetate changes the limits, such that unidentate coordination takes place when  $\Delta > 260\text{cm}^{-1}$ . The changes stem from the electronic effects of the substituent on the carboxylate group. Electron withdrawing substituents stabilise the anion and can increase the acidity of the carboxylate quite markedly. For instance there is a change of  $\text{pK}_a$  in RCOOH from 4.75 for R=CH<sub>3</sub> to 0.65 for R=CCl<sub>3</sub>. It was not until the use of X-ray diffraction techniques that the full range of bonding modes were realised.



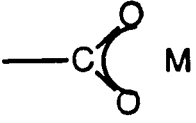
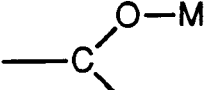
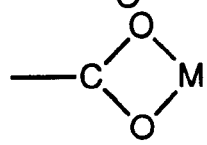
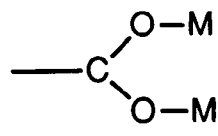
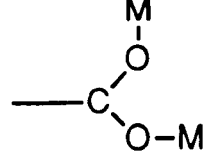
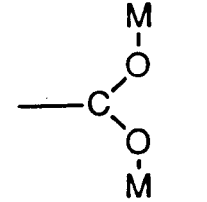
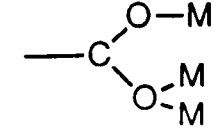
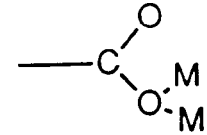
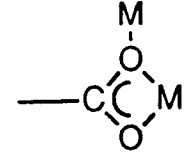
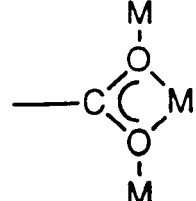
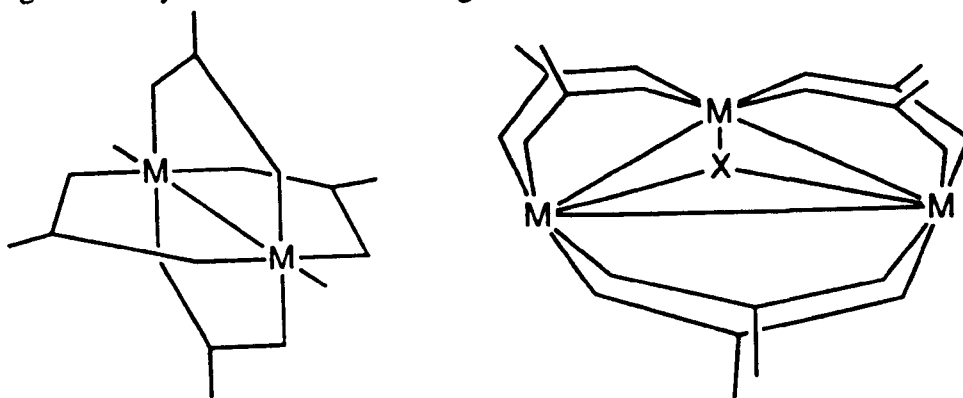
Type	Description	Example*
	Ionic	Na(HCOO) [Co(imidazole) <sub>6</sub> (O <sub>2</sub> CMe) <sub>2</sub> H <sub>2</sub> O] [Ti(SC(NH <sub>2</sub> ) <sub>2</sub> ) <sub>4</sub> ](O <sub>2</sub> CPh)
	Unidentate	B(O <sub>2</sub> CMe) <sub>2</sub> (acac) Ph <sub>3</sub> Sb(O <sub>2</sub> CMe) <sub>2</sub>
	Chelating	Zn(O <sub>2</sub> CMe) <sub>2</sub> .2H <sub>2</sub> O Sn(O <sub>2</sub> CMe) <sub>4</sub>
	Bridging syn/syn	[Cr(O <sub>2</sub> CMe) <sub>2</sub> H <sub>2</sub> O] <sub>2</sub> [Os(O <sub>2</sub> CMe)(CO) <sub>3</sub> ] <sub>2</sub>
	Bridging syn/anti	Cu(O <sub>2</sub> CH) <sub>2</sub> Me <sub>3</sub> Sn(O <sub>2</sub> CMe)
	Bridging anti/anti	Cu(O <sub>2</sub> CH) <sub>2</sub> .4H <sub>2</sub> O Mn(O <sub>2</sub> CMe) <sub>2</sub> (H <sub>2</sub> O) <sub>4</sub>
	Tridentate	Cu(O <sub>2</sub> CMe)
	Monatomic	[Cu(O <sub>2</sub> CMe)L] <sub>2</sub> L=salicyaldimine deriv. Hg(O <sub>2</sub> CMe) <sub>2</sub> [(C <sub>6</sub> H <sub>11</sub> ) <sub>3</sub> P]
	Bridging/Chelating	Cd(O <sub>2</sub> CMe) <sub>2</sub> (H <sub>2</sub> O) <sub>2</sub>
	Bridging/Chelating	Me <sub>2</sub> Tl(O <sub>2</sub> CMe)

Table 1.1: Coordination modes of Carboxylates. (\*= examples taken from references 31,32)

Of the three types of coordination, unidentate, chelating and bridging, the bridging modes are the most common and, of these, the syn/syn bridge is the largest group. This type of coordination often occurs with metal-metal bonding (Figure 1.2). Unidentate coordination occurs usually only when there is no further bonding site available or steric requirements preclude coordination. True chelating complexes are the least common group. This is probably explained by the steric strain generated by the four membered ring.



**Figure 1.2:** Carboxylate bridging with metal-metal bonding.

Dithiocarbamates,  $R_2NCS_2$ , also have a rich coordination chemistry. This is for three reasons, the complexes tend to be stable, the ligand itself is inert to attack and, in the transition metals, the dithiocarbamate also has some redox properties. They have two types of coordination, either chelating or unidentate. The chelating complexes all occur with either transition metals or f-block elements, where  $p\pi-d(f)\pi$  overlap is possible between the ligand and metal. In the main group elements, where this is not possible, the bonding is all unidentate. Bonati and Ugo<sup>36</sup> suggested that infra-red could be used to distinguish the different coordination modes. This has since been discounted by Kellner et al<sup>37</sup>, who showed, from a study of X-ray structures, that the dithiocarbamate ligand always had  $C_1$  symmetry and, therefore, the infra-red spectra would be similar.

Most work reported in the literature centres on the transition element complexes, due to the chelating ability and the variations and redox properties this brings. For instance, by using aromatic groups on the nitrogen, or having the nitrogen as part of the aromatic system, the donating ability of the dithiocarbamate can be greatly reduced. This is due to the lone pair of the nitrogen being involved in the  $\pi$ -system, thus reducing the effectiveness of the resonance structure (c) (Figure 1.3)<sup>38</sup>. This can also be shown using infra-red spectra, where the C-N bond stretch is lowered by  $\sim 300\text{cm}^{-1}$  when aromatic groups are present, indicating a weaker C-N bond. The

redox properties also stem from the resonance structure (c), where high oxidation state metal centres can be stabilised by removal of positive charge from the metal to the nitrogen<sup>39</sup>. In main group complexes the resonance structures do not apply, since the ligands are unidentate.

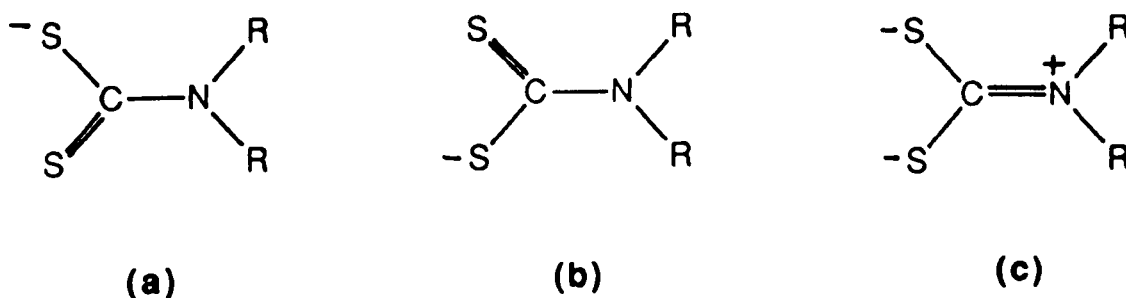


**Figure 1.3:** Resonance behaviour in Dithiocarbamates.

#### 1.4 Secondary Bonding

Secondary bonding<sup>40</sup> is an interaction between two atoms that do not have a primary bond between them, but are nevertheless affecting the geometry of each other. The term secondary bonding is usually used for interactions where relatively high coordination numbers are involved, i.e. trigonal bipyramidal, octahedral and higher. Smaller systems, such as hydrogen bonding, are normally covered by the term donor-acceptor interactions. These two concepts are theoretically similar.

The distance between the two atoms usually lies in the range between the sum of the covalent and the sum of the Van der Waals radii, though some have been reported at longer than this. For instance,  $\text{Et}_2\text{SnI}_2$  is nearly tetrahedral in the gas phase. On crystallisation though, the molecule becomes almost octahedral, a change of approximately  $15^\circ$  in the bond angles. The length of the Sn-I interaction in this case is  $4.28\text{\AA}$ , almost  $0.2\text{\AA}$  longer than the Van der Waal distance<sup>41</sup>. The interactions form a continuous distribution from the standard bond length to longer than the Van der Waals distance<sup>42</sup>.

The interactions must be approximately linear with a primary bond, i.e.  $\text{X-A---Y}$  where  $\text{A---Y}$  is the secondary bond, and the atom involved in the secondary bond should occupy a stereochemically significant position not already occupied by a primary bond or a lone pair. The secondary bond also causes a change in the trans primary bond as stated by Bent:

"..a reciprocal relationship, the lengthening of an intramolecular interaction ( $r_1$ ) with a shortening of a trans-intermolecular interaction ( $r_2$ )"<sup>43</sup>.

The bond is suggested<sup>40</sup> as forming from the donation of a lone pair of electrons on Y into the  $\sigma^*$  orbital formed from the A-X bond. Considering both primary and secondary bonds there are three molecular orbitals formed, containing two electron pairs. The primary bonding pair occupies the lowest orbital, the  $\sigma$ -bonding, to form the strong bond, and the secondary bonding pair occupies the middle orbital, the  $\sigma$ -non bonding, to form a weak interaction. This is similar to the scheme proposed for hydrogen bonding<sup>44</sup>.

These effects can only be investigated by the use of X-ray diffraction, where the whole cell, and the interactions within it, can be studied. Moessbauer and n.m.r. may also be used to give an indication of the geometry of the complex.

The strength of the interactions are difficult to determine quantitatively because it is difficult to determine unambiguously what the relative Van der Waals and covalent radii should be for a given system. This is because other substituents in the system may affect the values, by withdrawing electron density off the central atom for instance. An estimate of the bond order of an interaction can be made by the use of Paulings equation<sup>41</sup>:

$$r = r_o - c \log n \quad 1.1$$

where  $r$  = measured bond length

$r_o$  = standard bond length

$c$  = constant

$n$  = measure of the bond strength.

$c$  and  $r_o$  are constant for a particular pair of atoms.

## References

- 1) K.A. Kocheskov, *Ber.*, 1926, **62**, 996.
- 2) E. Frankland, *Ann.*, 1849, **71**, 171.
- 3) M. Gielen, J. Nasielski, *Bull. Chem. Soc. Belges*, 1962, **71**, 32.
- 4) O. Buchman, M. Grosjean, J. Nasielski, *Bull. Chem. Soc. Belges*, 1963, **72**, 286.
- 5) G. Bahr, *Z. Anorg. Chem.*, 1948, **256**, 107.
- 6) R.W. Bott, C. Eaborn, P.M. Greasley, *J. Chem. Soc.*, 1964, 4804.
- 7) R. Sasin, G.S. Sasin, *J. Org. Chem.*, 1965, **20**, 770.
- 8) M.M. Koton. *Zh. Obshch. Khim.*, 1956, **26**, 3581.
- 9) *Comprehensive Organometallic Chemistry*, ed. G. Wilkinson, F.G.A. Stone, E.W. Abel, Vol. 2, p. 523, Pergamon Press, Oxford, 1982.
- 10) C.D. Garner, D. Sutton, S.C. Wallwork, *J. Chem. Soc.(A)*, 1967, 1949.
- 11) N.W. Alcock, V.L. Tracy, *Acta Cryst.(B)*, 1979, **35**, 80.
- 12) W.J. Kroenke, M.E. Kenney, *Inorg. Chem.*, 1964, **3**, 251.
- 13) A. Karpides, C. Forman, R.H.P. Thomas, A.T. Reed, *Inorg. Chem.*, 1974, **13**, 811.
- 14) K.C. Molloy, T.G. Purcell, E. Hahn, H. Schumann, J.J. Zuckerman, *Organometallics*, 1986, **5**, 85.
- 15) S.W. Ng, C. Wei, V.G.K. Das, *J. Organomet. Chem.*, 1988, **345**, 59.
- 16) H.H. Anderson, *Inorg. Chem.*, 1964, **3**, 912.
- 17) G.M. Sheldrick, W.S. Sheldrick, *J. Chem. Soc.(A)*, 1970, 490.
- 18) G.M. Sheldrick, W.S. Sheldrick, R.F. Dalton, K. Jones, *J. Chem. Soc.(A)*, 1970, 493.
- 19) P.F. Lindley, P. Carr, *J. Cryst. Mol. Struct.*, 1974, **4**, 173.
- 20) V.G.K. Das, C. Wei, E. Sinn, *J. Organomet. Chem.*, 1985, **290**, 291.
- 21) T. Kimura, N. Yasuoka, N. Kasai, M. Kakudo, *Bull. Chem. Soc. Jpn.*, 1972, **45**, 1649.
- 22) J.S. Morris, E.O. Schlemper, *J. Cryst. Mol. Struct.*, 1980, **9**, 13.
- 23) *Comprehensive Organometallic Chemistry*, ed. G. Wilkinson, Vol. 2, p. 608, Pergamon Press, Oxford, 1982.
- 24) *The Chemistry Of Selenium, Tellurium and Polonium*, K.W. Bagnall, Elsevier, Amsterdam, 1966.
- 25) *Tellurium*, W.C. Cooper, p. 224-235, Van Nostrand-Reinhold, New York, 1971.
- 26) C.S. Smith, J.S. Lee, D.D. Titus, R.F. Ziolo, *Organometallics*, 1982, **1**, 350.

- 27) E.L. Muetterties, W.D. Phillips, *J. Am. Chem. Soc.*, 1957, **79**, 2975.
- 28) S. Husebye, *Acta Chem. Scand.*, 1979, **33**, 485.
- 29) A.C. Hazell, *Acta Chem. Scand.*, 1966, **20**, 165.
- 30) D.S. Urch, *J. Chem. Soc.*, 1964, 5775.
- 31) *Comprehensive Coordination Chemistry*, ed. G. Wilkinson, Vol. 2, p. 436, Pergamon Press, Oxford, 1987.
- 32) *Comprehensive Organic Chemistry*, ed. D. Barton, W.D. Ollis, Vol. 2, p. 594, Pergamon Press, Oxford, 1979.
- 33) J.C. Speakman, *Struct. Bonding*, 1972, **12**, 141.
- 34) G.B. Deacon, R.J. Phillips, *Coord. Chem. Rev.*, 1980, **33**, 227.
- 35) *Comprehensive Coordination Chemistry*, ed. G. Wilkinson, Vol. 2, p. 438, Pergamon Press, Oxford, 1987.
- 36) F. Bonati, R. Ugo, *J. Organomet. Chem.*, 1967, **10**, 257.
- 37) R. Kellner, G. St. Nikolov, N. Tredafilova, *Inorg. Chim. Acta*, 1984, **84**, 233.
- 38) D. Coucouvanis, *Prog. Inorg. Chem.*, 1970, **11**, 233.
- 39) J. Willemse, J.A. Cras, J.J. Steggerda, C.P. Keijzers, *Struct. Bonding*, 1976, **28**, 83.
- 40) N.W. Alcock, *Adv. Inorg. Chem. Radiochem.*, 1972, **15**, 1.
- 41) P. Murray-Rust, *Chem. Soc. Spec. Per. Rep.; Mol. Struct. by Diffr. Methods*, **6**, 154.
- 42) H.B. Burgi, *Agnew. Chem. Intl. Ed. Eng.*, 1975, **14**, 460.
- 43) H.A. Bent, *Chem. Rev.*, 1968, **68**, 587.
- 44) *Hydrogen Bonding*, S.N. Vinogradov, R.H. Linnell, Van Nostrand-Reinhold, New York, 1971.

## CHAPTER 2

### The Crystal Structures of Four Triphenyltin and One Triphenyltellurium Carboxylates

#### 2.1 Introduction

Many triorganotin carboxylate compounds have been synthesised since 1860 when Cahours<sup>1</sup> made the first  $R_3SnOCOR$  complex. Initial studies using infra-red by Okawara<sup>2</sup> indicated that the compounds existed as planar  $R_3Sn$  groups with ionic carboxylates. However, Beattie and Gilson<sup>3</sup> interpreted the spectra as having bridging carboxylate groups and this was supported by Janssen et al<sup>4</sup> with viscosity measurements. This has since been confirmed by Moessbauer<sup>5</sup> and X-ray determinations<sup>6</sup>.

The first structure for a triorganotin carboxylate,  $CH_3SnO_2CH$ , was reported by Okawara and Wada<sup>7</sup> in 1967. Since this time many compounds have been studied, and most have been found to have the polymeric form. If a bulky carboxylate is present in the molecule<sup>8</sup>, then it is possible to break the chain. The carboxylate then usually chelates to the tin, thus preserving the five coordination of the tin. Only one structure has been reported thus far with a four coordinate tin centre,  $(C_6H_{11})_3SnO_2CCH_2(C_8H_6N)$ <sup>8</sup>, which uses both bulky organo and carboxyl groups. Ford and Sams<sup>9</sup> synthesised  $Ph_3SnO_2CCCl_3$  which, from infra-red and Moessbauer data, they characterised as a tetracoordinate monomer. Thus it was of interest to see if this was indeed the case.

Interest in this area of chemistry is mostly stimulated by the agrochemical industry.  $R_3Sn$  compounds are very efficient and safe biocides<sup>10</sup>. With the exception of methyl and ethyl organo groups, the tin compounds are non-toxic to mammals.  $Ph_3SnOCOCCH_3$  (marketed under the trade name Brestan by Hoechst A.G.) has been used against Potato Blight<sup>11</sup>. Their safety comes from their simple break down pathway to non-toxic inorganic tin compounds in the environment, unlike their organoarsenic and mercury analogues which form volatile toxic methylated compounds<sup>12</sup>.

In contrast to the tin carboxylates, the tellurium analogues have not been studied in any detail. These are of interest for three reasons. Firstly, with the lone pair, the tellurium compounds should form different geometries, secondly, they should form secondary bonds of the type noticed by Alcock et al.<sup>13</sup>, and thirdly, no triorganotellurium carboxylates have so far been structurally

characterised.

This chapter describes the preparation and crystal study of a series of triphenyltin carboxylates, [1]-[4], and one triphenyltellurium carboxylate, [5]. This carboxylic acids used were monochloroacetic, for [1], dichloroacetic, for [2], and trichloroacetic, for [3], [4] and [5]. These acids were chosen to investigate the effects of the strength and the change in steric bulk of the acid. Compound [4] has a methanol molecule adducted to the tin. Views of the molecules are in Figures 2.1-2.8.  $\text{Ph}_3\text{SnOCOCH}_2\text{Cl}$ , [2], was reported by Ng<sup>14</sup> in 1989 at the 6<sup>th</sup> ICOCC of Ge, Sn and Pb. The structure reported was identical to that discussed below.

## 2.2 Results

From Infra-red studies made by Deacon and Phillips<sup>15</sup> on carboxylate complexes a value of greater than  $200\text{-}260\text{cm}^{-1}$  for  $\nu_{\text{asym}} - \nu_{\text{sym}}$  in halocarboxylates indicated a unidentate carboxylate (the lower limit for the acetate, the higher for the trihalo derivatives). From Table 2.12 it can be seen that both the trichloroacetate complexes are greater than the limit as are the adducts with MeCN and MeOH. Thus it was expected that the trichloroacetate structures [3], [4], [5] and the MeCN complex would have unidentate and the mono and dichloroacetate complexes [1], [2] and the tellurium acetate complex would have bidentate carboxylates. This is borne out in the structural studies.

Compounds [1] and [2],  $\text{Ph}_3\text{SnOCOCH}_2\text{Cl}$  and  $\text{Ph}_3\text{SnOCOCHCl}_2$  (Figures 2.1 and 2.3), are five coordinate, trigonal bipyramidal complexes. The tin forms a strong bond to the neighbouring carbonyl oxygen in the carboxylate and increases its coordination from four to five, thus creating an infinite chain in the solid state (Figures 2.2 and 2.4). With [3],  $\text{Ph}_3\text{SnOCOCCl}_3 \cdot \text{MeOH}$  (Figure 2.5), the tin atom forms an adduct with the oxygen in the methanol solvent. This also forms an infinite chain via a hydrogen bond between the carboxyl oxygen and the methoxy hydrogen ( $\text{O}2\text{-O}3=2.705\text{\AA}$ ) (Figure 2.6). The chains propagate in the b, c and b directions for [1], [2] and [3] respectively. In [1] and [2] there is also a weak interaction between Sn1 and the carbonyl oxygen. This is indicated by the fact that although the difference in the C-O bond lengths is small ( $\Delta\text{C-O}=0.009, 0.013\text{\AA}$  for [1], [2]), the difference in Sn-O distances is large ( $\Delta\text{Sn-O}=0.169, 0.130\text{\AA}$ ). Thus there must be an extra interaction from the carboxylate to the tin to reduce the electron density in the carbonyl group. Therefore the carboxylate also has a small chelating effect. The Sn-



O(2) distances are 3.232 and 3.536 Å for [1] and [2], which are approaching the Van der Waals distance at 3.62 Å. However, this interaction does cause significant widening of the C-Sn-C angle from the trigonal bipyramidal 120° to 135.1 and 124.6° for [1] and [2] respectively. The phenyl groups take up the equatorial positions of the complex and the oxygens the axial. This is expected since it is known that the more electronegative elements/groups take up the axial positions<sup>16</sup>. The carboxylates all adopt the syn/anti conformation in the bridge. The phenyl rings adopt the usual 'paddle wheel' formation to reduce the steric hindrance between them. The tin atom sits slightly above the plane of C11, C21 and C31. For [2] the effect is very small, 0.0268 Å, but [1] and [3], have significant deviations out of plane, toward the carboxylate, of 0.0996 and 0.1293 Å. In [1] the chelation effect causes the tin to be drawn out of the plane. In [3] the effect is due to more weakly interacting MeOH causing the geometry to be somewhere between trigonal bipyramidal and tetrahedral.

Compounds of the type formed by [1] and [2] are well known in tin carboxylate chemistry, and many have been studied structurally. Generally the more sterically hindered the carboxylate and the organo groups on the tin, the greater the asymmetry of the Sn-O bond lengths<sup>17</sup>. Thus [2] would be expected to be more asymmetric than [1]. This is not the case though (Table 2.13) and the most likely reason for this is the chelating effect in [1] withdrawing electron density from the acyl oxygen, and so reducing the donating ability. The repeat distance of [2] is much larger than [1] (5.557 to 5.086 Å for Sn-Sn') and outside the average found by Ng et al<sup>18</sup> at 5.19 +/- 0.2 Å. It is, therefore, a borderline polymeric carboxylate. This is also indicated by its high  $\Delta\nu$  value from the infra-red studies (Table 2.12), which is approaching the unidentate/bidentate limit. Two other compounds have been classified as being on the borderline, (C<sub>6</sub>H<sub>5</sub>CH<sub>2</sub>)<sub>3</sub>SnO<sub>2</sub>CCH<sub>3</sub><sup>19</sup> and (C<sub>6</sub>H<sub>11</sub>)<sub>3</sub>SnO<sub>2</sub>CCF<sub>3</sub><sup>20</sup>. These are presumably nearly monomeric due to the bulkiness of the cyclohexyl groups.

[4], Ph<sub>3</sub>SnOCOCCl<sub>3</sub>, forms a distorted tetrahedral monomeric unit (Figure 2.7). The distortion arises from a long interaction from the acyl oxygen to the tin to form a chelated ring. The distance is 2.955 Å, which is much shorter than the Van der Waals distance of 3.62 Å. The interaction also causes the C11-Sn1-C21 angle to open up from the tetrahedral 109.6° to 117.9(2)°. The difference in C-O bond lengths is quite marked, at 0.084 Å, as would be expected from a predominantly unidentate carboxylate. The nearest intermolecular contact is at 5.048 Å.

With [4] the chain has been broken to produce a monomeric unit. This is due to the large steric effects of the CCl<sub>3</sub> and phenyl groups. Molloy et al<sup>8</sup> claimed the first four coordinate triorganotin carboxylate in 1986. This has bulky cyclohexyl organo groups and also contains an

intermolecular hydrogen bond to tie up the acyl oxygen. He claims that, although the distance between the tin and the oxygen is only 2.929 Å, the interaction is not electronic, but steric. This is based on the pattern of angular and bond length changes, which do not show a systematic move towards a trigonal bipyramidal geometry. The same argument can be used for [4], where the C-Sn-C angles all increase from the expected 109.6° to 117.9(2), 112.0(1) and 113.8(2)°, instead of two of the angles decreasing towards 90° and one increasing to 120° as would be expected in the tbp geometry. Also the asymmetry in the C-O bond lengths in the carboxylate is large (0.084 Å), indicating single/double bond character, rather than delocalised bidentate bonding.

[5],  $\text{Ph}_3\text{TeOCOCCL}_3$ , forms a dimer in the solid state (Figure 2.8). The geometry at the tellurium centre is a distorted octahedron. There are three primary Te-C bonds, two secondary Te-O bonds in cis formation and a lone pair opposite one of the Te-C bonds. The dimer is held together by two bidentate bridging carboxylates. The Te-O bond lengths (2.735, 3.225 Å) are longer than the expected covalent bond length (2.11 Å) and in solution the complex would be expected to break up into  $\text{Ph}_3\text{Te}^+ \text{ } ^-\text{O}_2\text{CCCL}_3$  as is the case with  $\text{Ph}_3\text{TeCl}^{21}$ . The plane of the carboxylates is at an angle of 55.9° with respect to the plane formed by Te1,C1,Te1A,C1A. They form an eight membered ring which has a chair type conformation.

There are two compounds with similar structures to [5]. They are  $\text{Ph}_3\text{Te}(\text{NCO})^{22}$  and  $\text{Ph}_3\text{Te}(\text{SCN})^{23}$ . The thiocyanate complex forms dimers and tetramers in the solid state, while the cyanate only forms tetramers.  $\text{Et}_3\text{TeBr}^{24}$  also adopts a tetrameric structure based on cubane. That the carboxylate only forms dimers is probably due to the steric effect of the  $\text{CCl}_3$  group. Another compound which may have been expected to dimerise is acetylphenoxatellurine nitrate<sup>25</sup>, but this is present as discrete ionic monomers in the solid state. In all structures of the type  $\text{R}_3\text{TeX}$  the compounds are predominantly ionic, with long interactions holding the structures together.

Comparing the tin and tellurium monocarboxylates reported, it is obvious that both prefer to increase their coordination sphere via the use of secondary interactions. In the case of tin, the coordination is increased to five, with the creation of an infinite chain in the solid state. With tellurium the coordination is increased to six, including the lone pair, by the formation of a dimer. In both cases the secondary interaction is with the acyl oxygen of the carboxylate, i.e. the carboxylate forms a bidentate bridge. The tellurium system is essentially ionic and, due to the distance from the tellurium centre, the bulkiness of the carboxylate does not affect the geometry of

the molecule. In the tin system this is not the case, with the increasing bulk of the carboxylate leading to the breaking of the polymeric chain with trichloroacetate.

## 2.3 Experimental

### 2.3.1 Synthesis of Compounds

$\text{Ph}_3\text{SnOH}$  was prepared from  $\text{Ph}_3\text{SnCl}$  by the method of Kushlefsky et al.<sup>26</sup>.

#### Triphenyltin Carboxylates

$\text{Ph}_3\text{SnO}_2\text{CCH}_2\text{Cl}$ , [1],  $\text{Ph}_3\text{SnO}_2\text{CCHCl}_2$ , [2], and  $\text{Ph}_3\text{SnO}_2\text{CCCl}_3\cdot\text{MeOH}$ , [3], were prepared by stirring  $\text{Ph}_3\text{SnOH}$  and the appropriate acid (1:1) in aqueous methanol ( $30\text{cm}^3$ ) for 3hrs. An adduct with MeCN was made similarly by stirring in MeCN. The solvent was removed and the white product recrystallised from MeCN, EtOH and MeOH respectively.  $\text{Ph}_3\text{SnO}_2\text{CCCl}_3$ , [4], was prepared from [3] by the method of Ford et al.<sup>27</sup>. [4] was also prepared by the method of Srivastava et al.<sup>28</sup>. Crystals from the former method were used for the structure determination.

#### Triphenyltellurium Carboxylates

$\text{Ph}_3\text{TeCl}$ , prepared from  $\text{TeCl}_4$  and  $\text{PhLi}$  (1:3) at  $-77^\circ\text{C}$ , was stirred with the silver salt of the respective acid in dry  $\text{CH}_2\text{Cl}_2$ . The precipitated  $\text{AgCl}$  was filtered off and the solvent reduced to a minimum. Crystals of  $\text{Ph}_3\text{TeO}_2\text{CCCl}_3$ , [5], were grown by the liquid diffusion method using petroleum ether (30/40°bpt.) as the precipitating solvent. Crystals of  $\text{Ph}_3\text{TeO}_2\text{CCH}_3$  were grown in the same manner but were very platy and structure determination was not attempted.

### 2.3.2 Spectroscopic Data

Infra-red data was recorded on a Perkin-Elmer 580B spectrophotometer in the range  $4000\text{-}400\text{cm}^{-1}$  using KBr discs with Nujol Mull.  $^1\text{H-n.m.r.}$  spectra in the range  $0\text{-}10\text{ppm}$  were recorded on a Perkin-Elmer R34. Results are listed in Table 2.12.

### 2.3.3 X-Ray Crystallography

All data sets were recorded at 293K with Mo-K $\alpha$  radiation at 0.71069Å except for [5] which was recorded at 298K with 0.71073Å radiation. Standard reflections were measured every 200 reflections and showed slight changes during the data collection (1,3,5,3 and 4% for [1], [2], [3], [4] and [5] respectively). The data was processed using profile analysis and corrected for Lorentz, polarisation and absorption effects, the last by the Gaussian method. The cell parameters were calculated from 15 reflections with  $2\theta$  between 20 and 22°. All non-hydrogen atoms were refined anisotropically. Hydrogen atoms were inserted at calculated positions and not refined. Their temperature factors were fixed at 0.07Å<sup>2</sup>. The methyl group in [3] was treated as a rigid CH<sub>3</sub> unit, its initial orientation taken from the strongest H-atom peaks on a difference Fourier synthesis. Computing was with SHELXTL<sup>29</sup> on a Data General DG30 for [1], [2] and [3] and with SHELXTL PLUS<sup>30</sup> on a DEC MicroVax II for [4] and [5]. Scattering factors in the analytical form and anomalous dispersion factors taken from International Tables<sup>31</sup>. Data collection parameters are listed in Table 2.1. Atomic coordinates are in Tables 2.2-2.6 and bond lengths and angles in Tables 2.7-2.11 for [1], [2], [3], [4] and [5] respectively. Selected bond lengths are in Table 2.13.

### **Triphenyltin Monochloroacetate [1]**

Analysis of the systematic absences gave the space group as P2<sub>1</sub>/c. The tin atom was located using the Patterson routine and the remaining non-hydrogen atoms were located using difference Fourier syntheses. The residual electron density was located around the tin atom.

### **Triphenyltin Dichloroacetate [2]**

The systematic absences gave the space group as P2<sub>1</sub>/c. The tin atom was found using the Patterson interpretation section of SHELXTL and the remaining non-hydrogen atoms were located on successive Fourier syntheses. The residual electron density, approximately 1.2 electrons, was located in the rotation cone of the dichloro group indicating a small amount of disorder, though not enough to warrant refinement with partial occupancy of the chlorine positions.

### **Triphenyltin Trichloroacetate Methanol Adduct [3]**

The space group was determined to be  $P2_1/c$  by analysis of the systematic absences. All hydrogen atoms were inserted at calculated positions except for H3, the methoxy hydrogen. This was located on a difference Fourier map and allowed to refine its position. Its isotropic temperature factor was fixed at  $0.07\text{\AA}^2$ .

#### **Triphenyltin Trichloroacetate [4]**

Two crystals were used for this structure determination. The cell parameters were calculated from the first, but during the data collection the crystal decomposed to approximately 50% of the original intensity with a sharp cut-off after 25hrs. Thus the data was retaken with a second crystal at high speed,  $12^\circ\text{min}^{-1}$ , to ensure little decomposition, the mean drop in intensity being only 3%. No systematic absences in the data proved the space group to be either  $P1$  or  $P\bar{1}$ . Analysis of the E-statistics indicated a non-centrosymmetric space group, but density calculations indicated the number of molecules in the unit cell to be 2. Thus  $P\bar{1}$  was initially chosen and excellent refinement showed this to be the correct choice. Residual electron density lies in the rotation cone of the trichloro group, showing there is a small amount of rotational disorder, and also near the tin atom.

#### **Triphenyltellurium Trichloroacetate [5]**

Initial analysis of a small part of the data ( $20^\circ < 2\theta < 22^\circ$ ) showed the cell was C-centred and the data was collected accordingly. Study of the systematic absences gave the space group as  $Cc$  or  $C2/c$ . The E-statistics indicated a centrosymmetric space group and the density calculations required 8 molecules per unit cell. Therefore  $C2/c$  was initially chosen and proven correct by good refinement. Most of the residual electron density lies close to the tellurium atom.

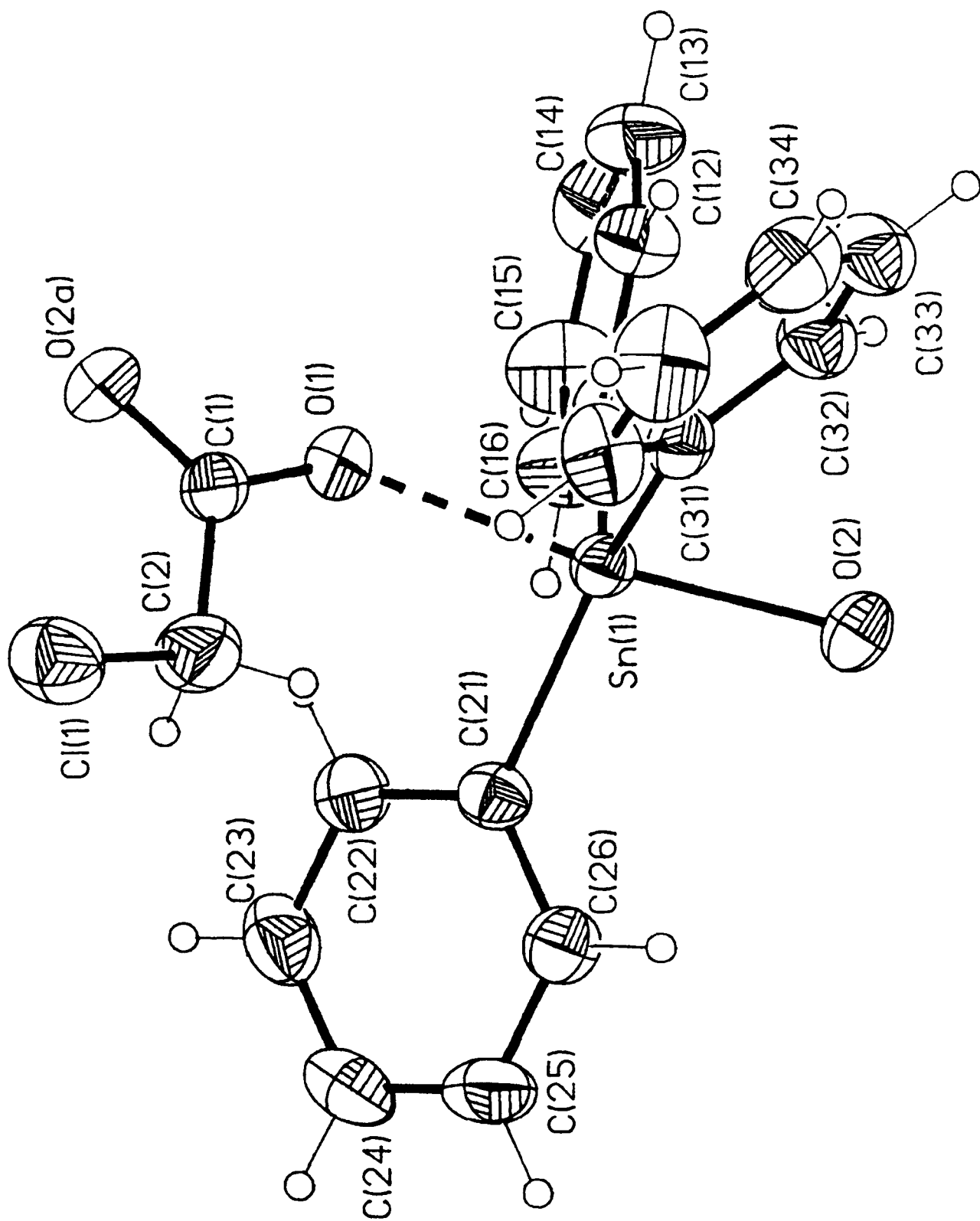


**FIGURE 2.1** View of the molecule of [1], showing atomic numbering scheme.

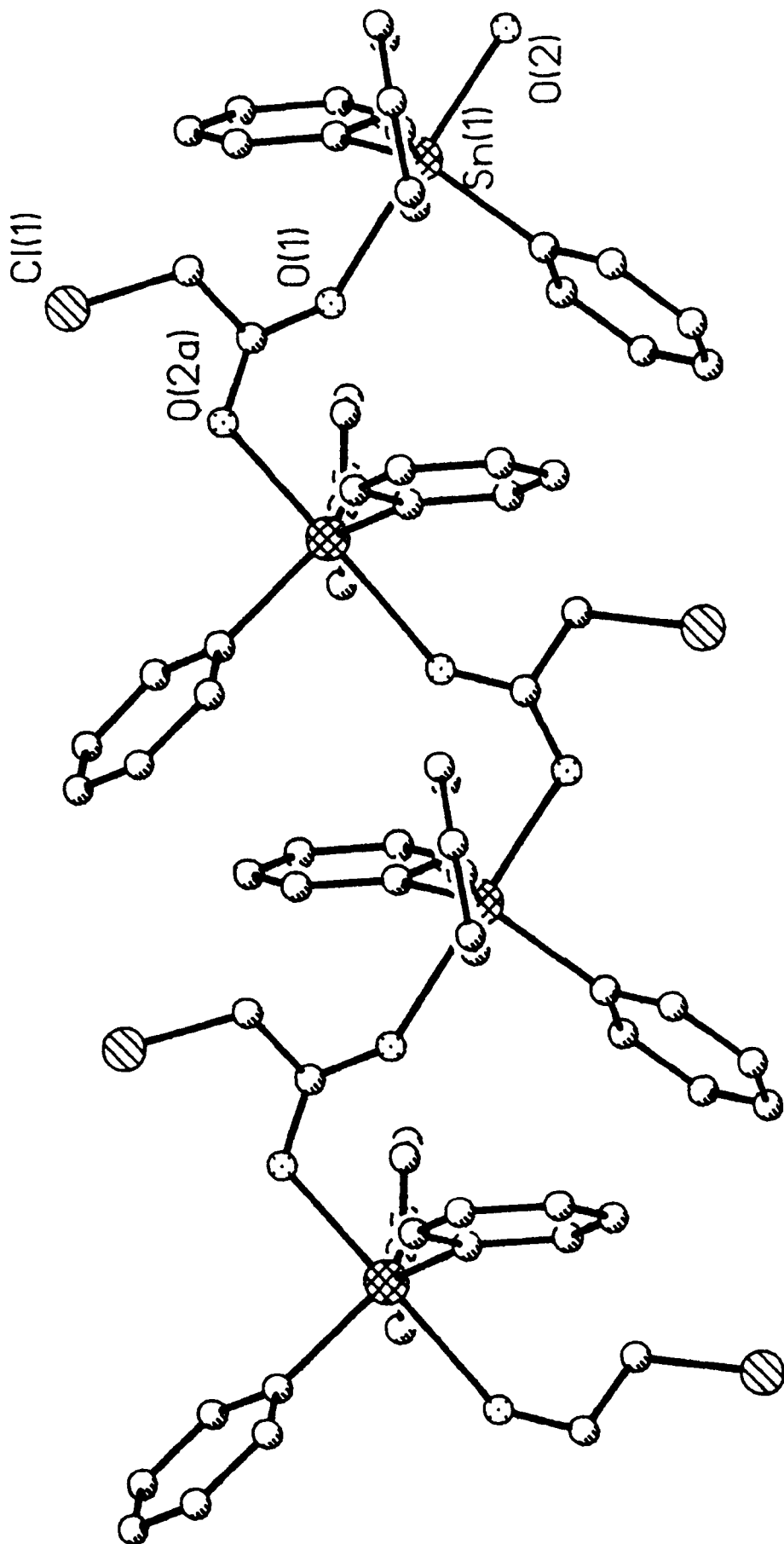
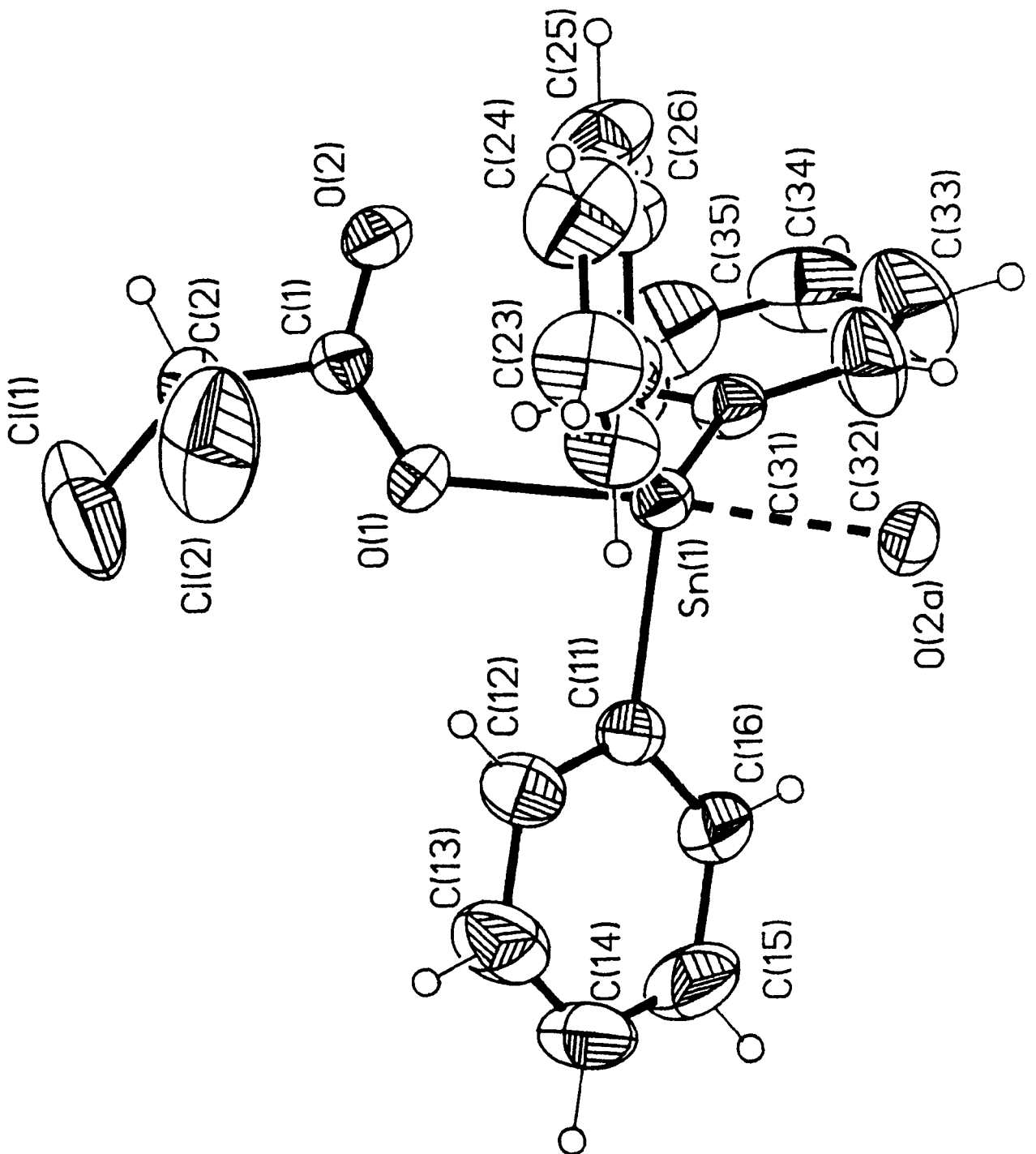


FIGURE 2.2 View of the polymeric chain of [1].



**FIGURE 2.3** View of the molecule of [2], showing atomic numbering scheme.



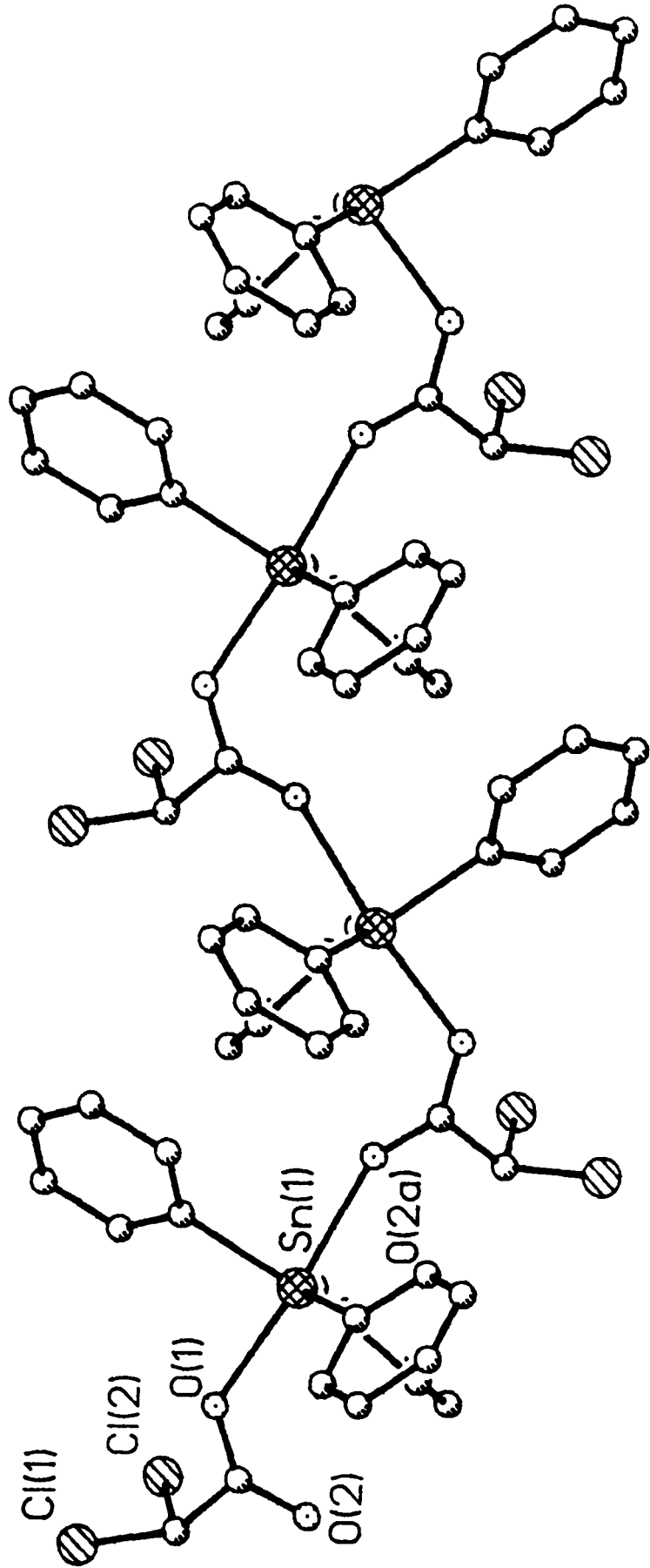
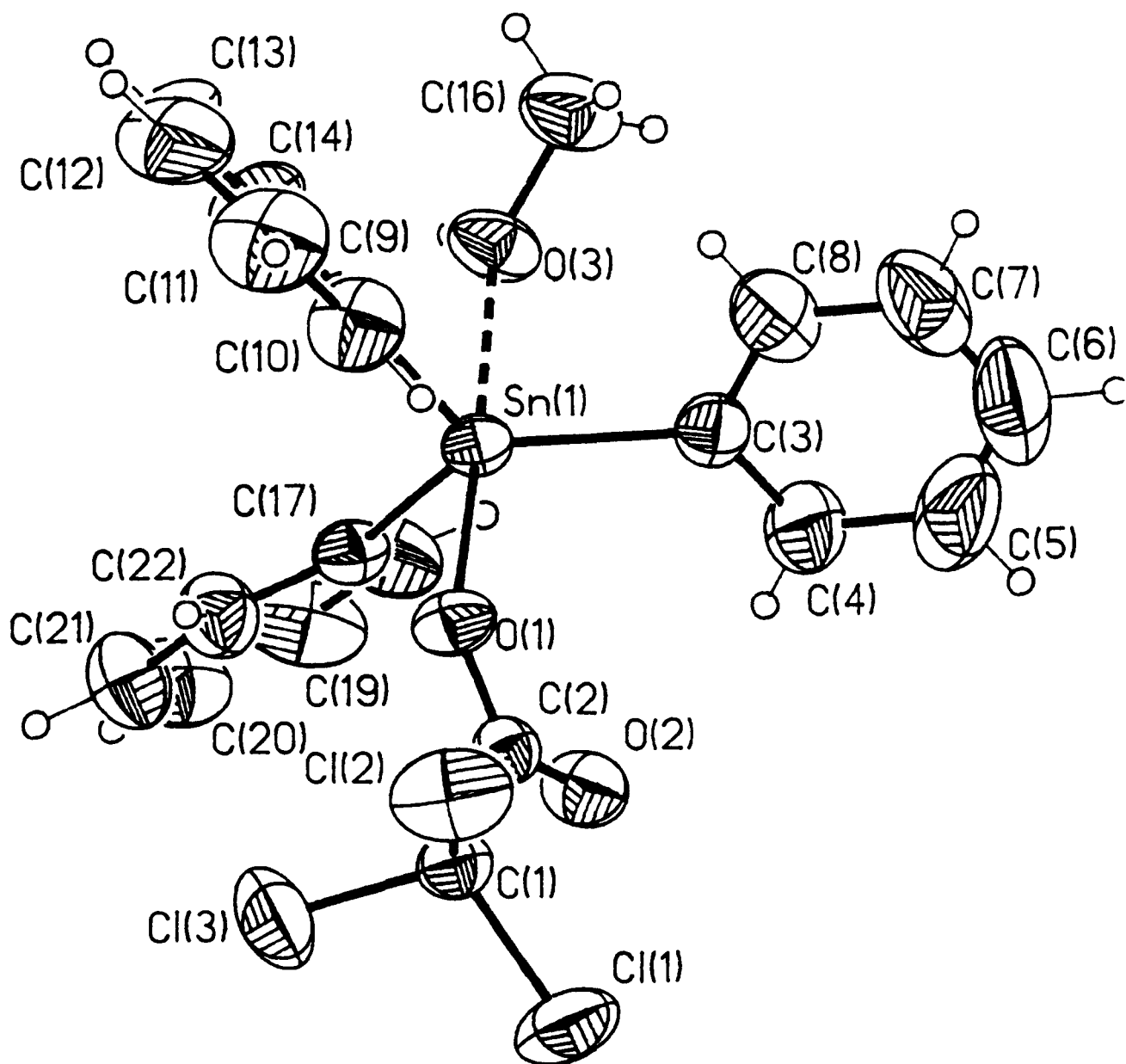


FIGURE 2.4 View of the polymeric chain of [2].



**FIGURE 2.5** View of the molecule of [3], showing atomic numbering scheme.

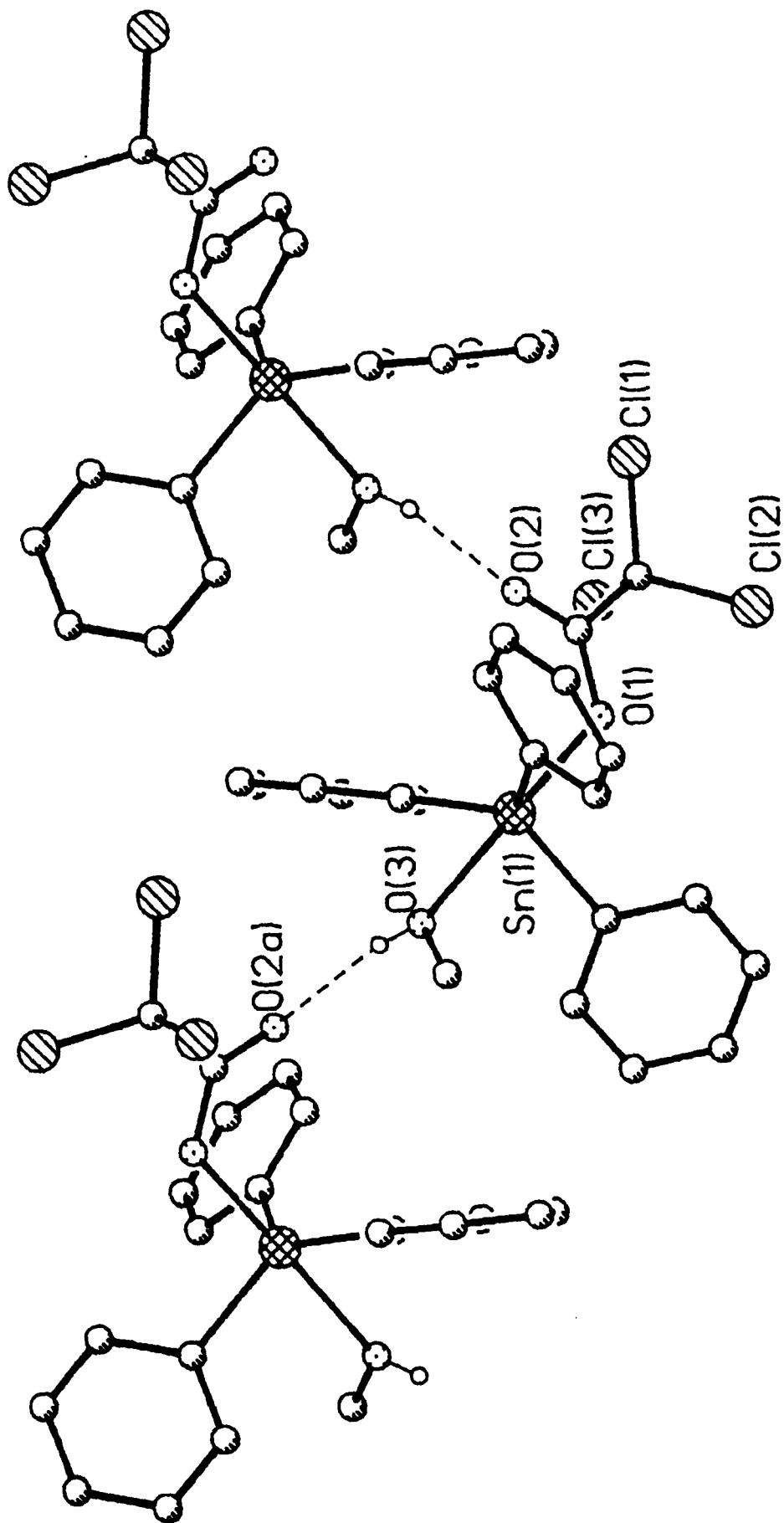


FIGURE 2.6 View of the Hydrogen Bonded chain of [3].

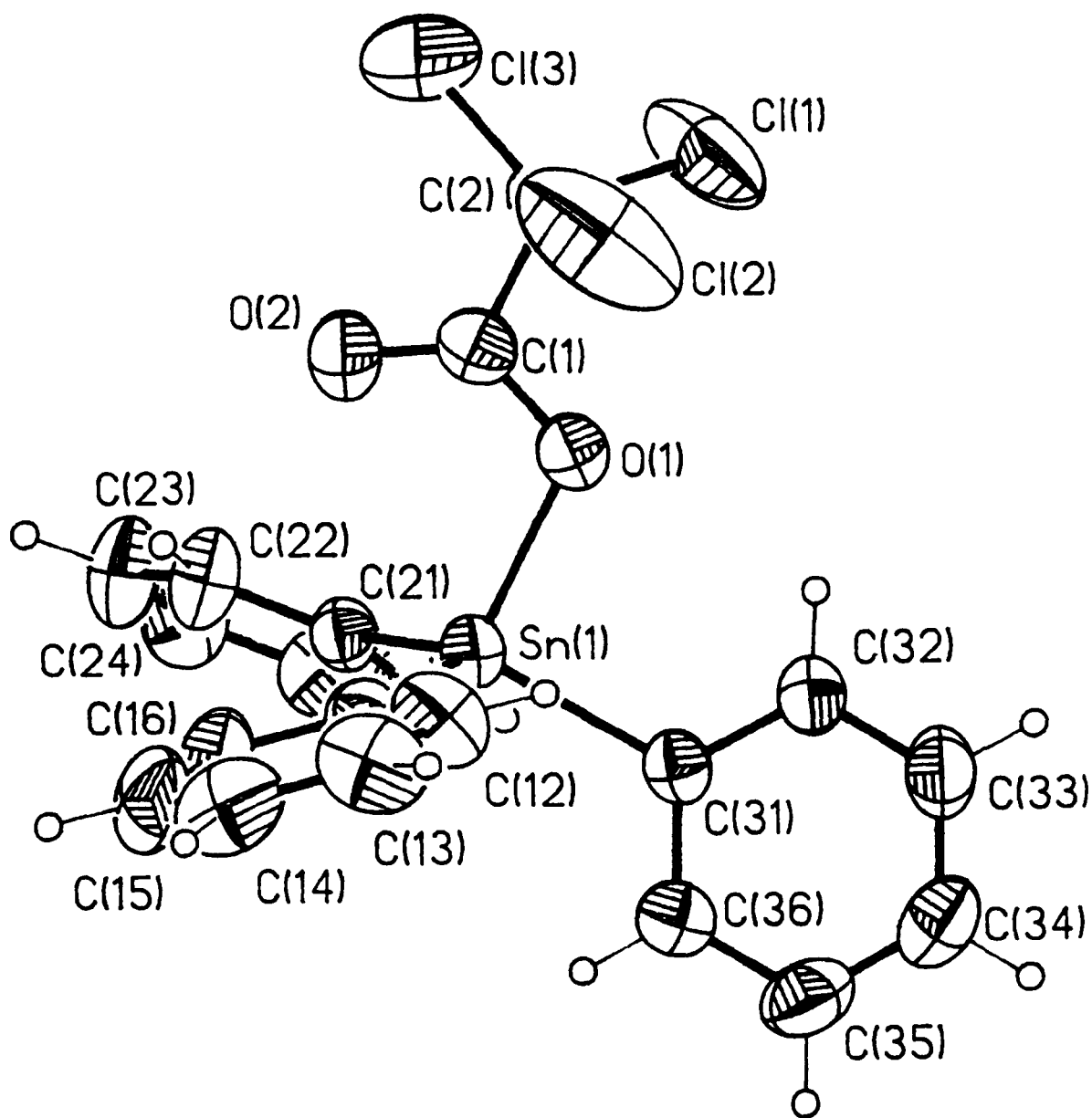


FIGURE 2.7 View of the molecule of [4], showing atomic numbering scheme.

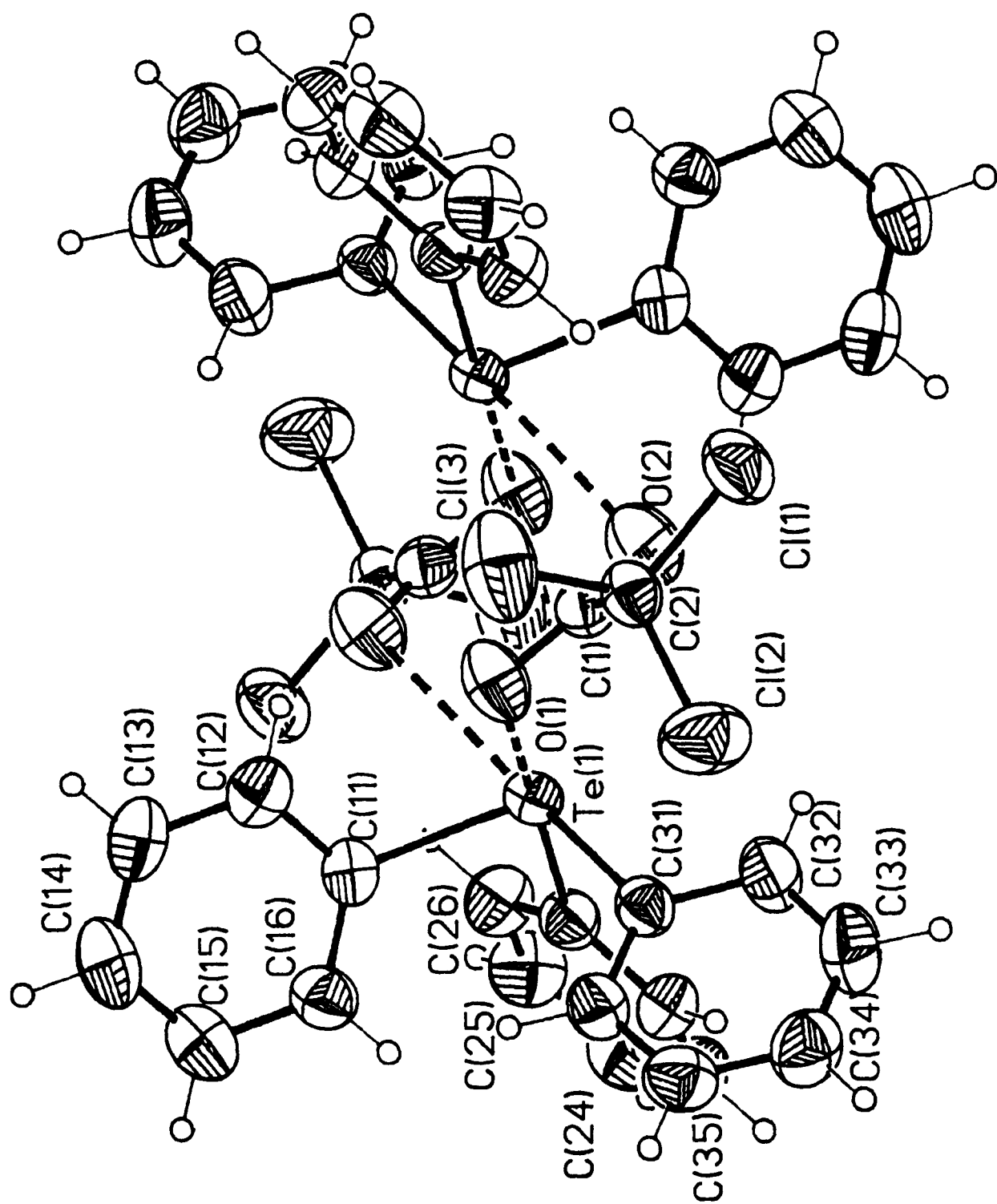


FIGURE 2.8 View of the dimer of [5], showing atomic numbering scheme.

**Table 2.1: Crystal Data and Data Collection Parameters**

Compound	[1]	[2]	[3]	[4]	[5]
Formula	C <sub>20</sub> H <sub>17</sub> O <sub>2</sub> Cl <sub>3</sub> Sn	C <sub>20</sub> H <sub>16</sub> O <sub>2</sub> Cl <sub>2</sub> Sn	C <sub>20</sub> H <sub>15</sub> O <sub>2</sub> Cl <sub>3</sub> Sn.CH <sub>3</sub> OH	C <sub>20</sub> H <sub>15</sub> O <sub>2</sub> Cl <sub>3</sub> Sn	C <sub>20</sub> H <sub>15</sub> O <sub>2</sub> Cl <sub>3</sub> Te
Mass	443.45	478.05	544.48	512.44	521.44
D <sub>calc</sub> (gcm <sup>-3</sup> )	1.63	1.62	1.56	1.62	1.75
Z	4	4	4	2	8
Crystal System	Monoclinic	Monoclinic	Monoclinic	Triclinic	Monoclinic
Systematic Absences	h0l l=2n+1 0k0 k=2n+1	h0l l=2n+1 0k0 k=2n+1	h0l l=2n+1 0k0 k=2n+1	none	hkl h+l=2n+1 hol l=2n+1
Space Group	P2 <sub>1</sub> /c	P2 <sub>1</sub> /c	P2 <sub>1</sub> /c	P $\bar{1}$	C2/c
a(Å)	9.004(3)	15.127(2)	10.196(2)	9.783(5)	21.374(13)
b(Å)	10.171(4)	12.537(2)	12.672(2)	9.810(5)	8.509(5)
c(Å)	19.748(4)	11.115(2)	17.913(3)	11.845(5)	21.797(16)
α(°)	-	-	-	101.90(4)	-
β(°)	92.37(2)	111.75(1)	91.59(2)	98.26(4)	93.42(6)
γ(°)	-	-	-	104.84(4)	-
U(Å <sup>3</sup> )	1807.0(1.0)	1957.7(0.6)	2313.6(0.8)	1051.7(0.9)	3957.7(4.2)
μ(cm <sup>-1</sup> )	15.75	15.94	14.74	16.10	17.2
F(000)	880	944	1076	504	2016
Crystal Size	0.5×0.8×0.8	0.2×0.2×0.4	0.2×0.2×0.4	0.4×0.3×0.6	-
Max. Trans.	0.9276	0.8548	0.7915	0.9805	0.8412
Min. Trans.	0.8773	0.7814	0.7464	0.9515	0.6827
Scan Range(°)	+/- 1.0	+/- 1.0	-0.95,+0.95	+/-0.8	-1.0,+1.1
Scan Rate(°min <sup>-1</sup> )	2.0	2.0	4	12	3
Max. 2θ(°)	50	50	50	50	50
Refs. Collected	3486	3444	2258	3726	3449
Refs. Observed	2513	2622	1770	3453	2966
R(final)	0.0297	0.0404	0.00041	0.00270	0.00139
R <sub>w</sub>	0.0295	0.0430	0.0296	0.0368	0.0305
S	0.00027	0.00073	0.0327	0.0428	0.0364
Max. on final Fourier	+/- 0.6	+/- 1.2	+0.3,-0.25	+/-0.8	+0.55,-0.42
Max. δ/σ	0.004	0.004	0.105	0.004	0.001
No. of Parameters	217	226	103	235	235

TABLE 2.2

Atomic coordinates ( $\times 10^4$ ) for [1] (with standard deviations in parentheses).

Atom	x	y	z	U
Sn(1)	887.0(3)	7006.4(3)	7369.1(1)	30(1)*
Cl(1)	3720.6(13)	10387.7(13)	6046.2(6)	58(1)*
O(1)	2068.9(29)	8673.3(25)	6934.7(14)	39(1)*
O(2)	456.5(30)	10156.2(26)	7268.2(13)	39(1)*
C(1)	1488(4)	9787(4)	6903(2)	33(1)*
C(2)	1979(5)	10745(4)	6373(2)	53(2)*
C(11)	2423(4)	5678(4)	6960(2)	32(1)*
C(12)	2155(5)	5070(4)	6341(2)	43(1)*
C(13)	3163(5)	4199(5)	6085(2)	56(2)*
C(14)	4473(5)	3930(5)	6444(3)	58(2)*
C(15)	4758(5)	4506(5)	7064(3)	64(2)*
C(16)	3747(5)	5382(5)	7307(2)	51(2)*
C(21)	1429(4)	7409(4)	8410(2)	34(1)*
C(22)	1873(5)	6365(4)	8821(2)	46(2)*
C(23)	2344(5)	6573(5)	9485(2)	53(2)*
C(24)	2385(5)	7816(5)	9753(2)	53(2)*
C(25)	1952(5)	8859(5)	9351(2)	53(2)*
C(26)	1490(5)	8661(4)	8681(2)	44(1)*
C(31)	-971(4)	7399(4)	6694(2)	35(1)*
C(32)	-672(5)	7634(4)	6019(2)	45(1)*
C(33)	-1802(5)	7858(5)	5544(2)	57(2)*
C(34)	-3253(6)	7842(5)	5725(3)	63(2)*
C(35)	-3574(5)	7625(5)	6378(3)	67(2)*
C(36)	-2442(5)	7404(5)	6872(2)	53(2)*

\* Equivalent isotropic U defined as one third of the trace of the orthogonalised  $U_{ij}$  tensor.

**TABLE 2.3**

**Atomic coordinates ( $\times 10^4$ ) for [2] (with standard deviations in parentheses).**

atom	x	y	z	U
Sn(1)	2780.0(2)	6989.6(3)	7303.8(3)	34(1)*
Cl(1)	2424(2)	4229(2)	3590(3)	124(1)*
Cl(2)	782(2)	5291(3)	3686(3)	124(1)*
O(1)	2701(3)	5955(3)	5645(3)	40(1)*
O(2)	2741(3)	7055(3)	4104(4)	45(2)*
C(1)	2488(4)	6227(4)	4489(5)	37(2)*
C(2)	1866(5)	5443(5)	3481(6)	55(3)*
C(11)	2788(4)	5575(4)	8347(5)	39(2)*
C(12)	2094(4)	4802(5)	7816(6)	51(3)*
C(13)	2097(5)	3874(5)	8494(7)	71(3)*
C(14)	2807(6)	3727(6)	9698(7)	78(4)*
C(15)	3476(6)	4468(6)	10227(7)	75(3)*
C(16)	3479(5)	5409(5)	9559(6)	54(3)*
C(21)	1435(4)	7626(4)	6140(5)	38(2)*
C(22)	615(4)	7202(5)	6226(7)	59(3)*
C(23)	-252(5)	7592(7)	5440(8)	77(4)*
C(24)	-330(5)	8381(7)	4572(8)	90(4)*
C(25)	469(6)	8816(6)	4494(7)	76(4)*
C(26)	1348(5)	8448(5)	5260(6)	53(2)*
C(31)	4106(4)	7705(4)	7549(5)	41(2)*
C(32)	4450(5)	8581(6)	8305(7)	71(3)*
C(33)	5326(6)	9016(6)	8453(9)	91(4)*
C(34)	5849(5)	8581(7)	7830(8)	80(4)*
C(35)	5524(5)	7707(7)	7059(8)	76(3)*
C(36)	4654(4)	7274(5)	6917(7)	57(3)*

\* Equivalent isotropic U defined as one third of the trace of the orthogonalised  $U_{ij}$  tensor.



TABLE 2.4

Atomic coordinates ( $\times 10^4$ ) for [3] (standard deviations in parentheses).

atom	x	y	z	U
Sn(1)	1712.3(3)	7372.2(2)	7467.4(3)	36(1)*
C1(1)	3309.6(16)	11432.6(10)	6369.7(13)	80(1)*
C1(2)	5040.0(13)	9671.1(13)	6248.0(14)	83(1)*
C1(3)	2665(2)	9769(2)	5347(2)	90(1)*
O(1)	2880(3)	8479(2)	6845(2)	44(2)*
O(2)	1733(3)	9907(3)	7145(3)	55(2)*
C(1)	3389(5)	10054(4)	6227(4)	44(3)*
C(2)	2574(4)	9461(4)	6811(4)	33(3)*
C(4)	1470(4)	8948(3)	8756(4)	82(2)
C(5)	1770	9381	9456	113(6)*
C(6)	2711	8903	9925	114(6)*
C(7)	3351	7992	9693	93(6)*
C(8)	3050	7559	8993	58(5)*
C(3)	2110	8037	8525	41(3)*
C(10)	4282(3)	6356(3)	7001(3)	64(3)*
C(11)	5088	5570	6719	98(4)*
C(12)	4576	4572	6559	106(5)*
C(13)	3256	4360	6681	99(5)*
C(14)	2450	5146	6963	67(4)*
C(9)	2963	6144	7123	38(3)*
C(18)	-1236(4)	7669(3)	7074(3)	55(3)*
C(19)	-2340	7746	6600	67(5)*
C(20)	-2201	7715	5827	72(6)*
C(21)	-958	7608	5530	89(3)
C(22)	146	7531	6005	58(2)
C(17)	7	7562	6777	36(4)*
O(3)	399(3)	6113(3)	8117(3)	50(2)*
C(16)	841(6)	5523(5)	8760(4)	75(4)*

\* Equivalent isotropic U defined as one third of the trace of the orthogonalised  $U_{ij}$  tensor.

TABLE 2.5

Atomic coordinates ( $\times 10^4$ ) for [4] (standard deviations in parentheses).

	x	y	z	U (eq)
Sn(1)	8560.7(2)	6224.7(2)	7439.0(2)	40.5(1)
C1(1)	6563(2)	1001(2)	7335(2)	117(1)
C1(2)	9602(2)	1828(3)	8078(3)	155(1)
C1(3)	8319(4)	493(2)	5674(3)	169(2)
O(1)	8037(3)	4083(3)	7571(3)	54(1)
O(2)	8839(5)	3546(4)	5934(3)	71(2)
C(1)	8374(4)	3229(4)	6756(4)	48(1)
C(2)	8192(5)	1687(5)	6951(5)	59(2)
C(11)	10851(4)	6892(4)	7752(3)	46(1)
C(12)	11637(6)	6730(6)	8761(5)	70(2)
C(13)	13104(6)	7195(6)	8997(6)	81(3)
C(14)	13820(6)	7852(7)	8258(6)	81(2)
C(15)	13081(6)	8001(7)	7261(5)	82(2)
C(16)	11573(5)	7537(6)	6999(4)	63(2)
C(21)	7417(4)	6403(4)	5846(3)	44(1)
C(22)	7881(5)	6100(6)	4799(4)	61(2)
C(23)	7112(6)	6253(7)	3773(4)	73(2)
C(24)	5883(6)	6688(6)	3793(4)	68(2)
C(25)	5423(5)	6977(5)	4824(4)	61(2)
C(26)	6179(5)	6834(5)	5850(4)	52(2)
C(31)	7780(4)	7018(4)	8954(3)	43(1)
C(32)	7053(5)	6093(5)	9554(3)	52(2)
C(33)	6599(5)	6660(6)	10552(4)	64(2)
C(34)	6845(6)	8117(6)	10964(4)	66(2)
C(35)	7563(6)	9052(5)	10391(5)	69(2)
C(36)	8039(5)	8500(5)	9386(4)	58(2)

\* Equivalent isotropic U defined as one third of the trace of the orthogonalised  $U_{ij}$  tensor.

TABLE 2.6

Atomic coordinates ( $\times 10^4$ ) for [5] (standard deviations in parentheses).

	x	y	z	U(eq)
Te(1)	1916.1(1)	-751.8(3)	5467.6(1)	37.7(1)
Cl(1)	1435.2(6)	-1716.1(1.6)	2791.9(5)	66.8(4)
Cl(2)	595.7(7)	-154.4(1.9)	3559.1(7)	85.9(5)
Cl(3)	563.2(7)	-3512.1(1.9)	3431.3(6)	88.5(5)
O(1)	1267(1)	-2324(4)	4538(1)	61(1)
O(2)	2071(1)	-1729(4)	3984(2)	67(1)
C(1)	1525(2)	-1992(4)	4065(2)	46(1)
C(2)	1057(2)	-1861(5)	3482(2)	47(1)
C(11)	1337(2)	-2065(4)	6024(2)	43(1)
C(12)	1246(2)	-3632(5)	5890(2)	55(1)
C(13)	905(2)	-4529(5)	6277(2)	62(2)
C(14)	659(2)	-3876(6)	6784(2)	65(2)
C(15)	745(2)	-2303(6)	6908(2)	61(2)
C(16)	1089(2)	-1383(5)	6526(2)	52(1)
C(21)	2259(2)	744(4)	6194(2)	43(1)
C(22)	2158(2)	2350(5)	6185(2)	50(1)
C(23)	2459(2)	3277(5)	6629(2)	58(2)
C(24)	2841(2)	2626(6)	7075(2)	65(2)
C(25)	2930(2)	1033(6)	7091(2)	61(2)
C(26)	2648(2)	91(5)	6649(2)	53(1)
C(31)	1278(2)	949(4)	5112(2)	42(1)
C(32)	1515(2)	1995(6)	4697(2)	61(2)
C(33)	1139(2)	3215(6)	4483(2)	69(2)
C(34)	550(2)	3376(6)	4660(2)	64(2)
C(35)	311(2)	2315(5)	5063(2)	59(2)
C(36)	680(2)	1093(5)	5296(2)	49(1)

\* Equivalent isotropic U defined as one third of the trace of the orthogonalised  $U_{ij}$  tensor.

TABLE 2.7

**Bond lengths (Å) and angles (°) for [1]**  
(standard deviations in parentheses).

**a) Bond lengths**

Sn(1)-O(1)	2.195(3)	Sn(1)-C(11)	2.117(4)
Sn(1)-C(21)	2.134(4)	Sn(1)-C(31)	2.134(4)
Sn(1)-O(2a)	2.364(3)	Cl(1)-C(2)	1.758(5)
O(1)-C(1)	1.248(5)	O(2)-C(1)	1.257(5)
O(2)-Sn(1a)	2.364(3)	C(1)-C(2)	1.509(6)
C(11)-C(12)	1.383(5)	C(11)-C(16)	1.384(6)
C(12)-C(13)	1.378(6)	C(13)-C(14)	1.378(7)
C(14)-C(15)	1.371(7)	C(15)-C(16)	1.375(7)
C(21)-C(22)	1.385(6)	C(21)-C(26)	1.381(6)
C(22)-C(23)	1.378(6)	C(23)-C(24)	1.370(7)
C(24)-C(25)	1.372(6)	C(25)-C(26)	1.386(6)
C(31)-C(32)	1.391(6)	C(31)-C(36)	1.384(6)
C(32)-C(33)	1.374(6)	C(33)-C(34)	1.369(7)
C(34)-C(35)	1.351(8)	C(35)-C(36)	1.400(7)

**b) Bond angles**

O(1)-Sn(1)-C(11)	90.5(1)	O(1)-Sn(1)-C(21)	97.6(1)
C(11)-Sn(1)-C(21)	111.3(1)	O(1)-Sn(1)-C(31)	89.5(1)
C(11)-Sn(1)-C(31)	112.9(1)	C(21)-Sn(1)-C(31)	135.1(1)
O(1)-Sn(1)-O(2a)	174.6(1)	C(11)-Sn(1)-O(2a)	87.6(1)
C(21)-Sn(1)-O(2a)	87.7(1)	C(31)-Sn(1)-O(2a)	86.6(1)
Sn(1)-O(1)-C(1)	120.8(2)	C(1)-O(2)-Sn(1a)	144.2(2)
O(1)-C(1)-O(2)	124.1(4)	O(1)-C(1)-C(2)	119.1(4)
O(2)-C(1)-C(2)	116.7(3)	Cl(1)-C(2)-C(1)	114.3(3)
Sn(1)-C(11)-C(12)	122.0(3)	Sn(1)-C(11)-C(16)	120.8(3)
C(12)-C(11)-C(16)	117.2(4)	C(11)-C(12)-C(13)	121.2(4)
C(12)-C(13)-C(14)	120.1(4)	C(13)-C(14)-C(15)	120.0(4)
C(14)-C(15)-C(16)	119.1(4)	C(11)-C(16)-C(15)	122.5(4)
Sn(1)-C(21)-C(22)	117.8(3)	Sn(1)-C(21)-C(26)	123.6(3)
C(22)-C(21)-C(26)	118.4(4)	C(21)-C(22)-C(23)	120.6(4)
C(22)-C(23)-C(24)	120.8(4)	C(23)-C(24)-C(25)	119.2(4)
C(24)-C(25)-C(26)	120.5(4)	C(21)-C(26)-C(25)	120.6(4)
Sn(1)-C(31)-C(32)	116.9(3)	Sn(1)-C(31)-C(36)	125.2(3)
C(32)-C(31)-C(36)	117.9(4)	C(31)-C(32)-C(33)	121.0(4)
C(32)-C(33)-C(34)	120.4(4)	C(33)-C(34)-C(35)	119.8(5)
C(34)-C(35)-C(36)	120.8(5)	C(31)-C(36)-C(35)	120.1(4)

**TABLE 2.8**

**Bond lengths (Å) and angles (°) for [2]**  
(standard deviations in parentheses).

**a) Bond lengths**

Sn(1)-O(1)	2.221(4)	Sn(1)-C(11)	2.116(6)
Sn(1)-C(21)	2.121(5)	Sn(1)-C(31)	2.121(6)
Sn(1)-O(2a)	2.351(4)	Cl(1)-C(2)	1.723(7)
Cl(2)-C(2)	1.747(8)	O(1)-C(1)	1.250(6)
O(2)-C(1)	1.237(7)	O(2)-Sn(1a)	2.351(4)
C(1)-C(2)	1.525(7)	C(11)-C(12)	1.389(8)
C(11)-C(16)	1.381(7)	C(12)-C(13)	1.386(10)
C(13)-C(14)	1.383(10)	C(14)-C(15)	1.339(11)
C(15)-C(16)	1.395(10)	C(21)-C(22)	1.385(10)
C(21)-C(26)	1.394(9)	C(22)-C(23)	1.369(9)
C(23)-C(24)	1.355(13)	C(24)-C(25)	1.359(13)
C(25)-C(26)	1.366(9)	C(31)-C(32)	1.364(9)
C(31)-C(36)	1.379(10)	C(32)-C(33)	1.385(12)
C(33)-C(34)	1.345(14)	C(34)-C(35)	1.365(11)
C(35)-C(36)	1.378(10)		

**b) Bond angles**

O(1)-Sn(1)-C(11)	87.3(2)	O(1)-Sn(1)-C(21)	88.2(2)
C(11)-Sn(1)-C(21)	117.3(2)	O(1)-Sn(1)-C(31)	96.3(2)
C(11)-Sn(1)-C(31)	118.1(2)	C(21)-Sn(1)-C(31)	124.6(2)
O(1)-Sn(1)-O(2a)	173.4(1)	C(11)-Sn(1)-O(2a)	87.6(2)
C(21)-Sn(1)-O(2a)	90.4(2)	C(31)-Sn(1)-O(2a)	89.8(2)
Sn(1)-O(1)-C(1)	127.4(3)	C(1)-O(2)-Sn(1a)	146.2(3)
O(1)-C(1)-O(2)	126.1(4)	O(1)-C(1)-C(2)	115.7(5)
O(2)-C(1)-C(2)	118.2(5)	Cl(1)-C(2)-Cl(2)	110.7(4)
Cl(1)-C(2)-C(1)	111.4(4)	Cl(2)-C(2)-C(1)	109.1(5)
Sn(1)-C(11)-C(12)	120.1(4)	Sn(1)-C(11)-C(16)	120.6(4)
C(12)-C(11)-C(16)	119.3(5)	C(11)-C(12)-C(13)	120.4(5)
C(12)-C(13)-C(14)	118.9(6)	C(13)-C(14)-C(15)	121.5(7)
C(14)-C(15)-C(16)	120.3(6)	C(11)-C(16)-C(15)	119.7(6)
Sn(1)-C(21)-C(22)	119.7(4)	Sn(1)-C(21)-C(26)	121.7(5)
C(22)-C(21)-C(26)	118.6(5)	C(21)-C(22)-C(23)	119.3(7)
C(22)-C(23)-C(24)	121.7(8)	C(23)-C(24)-C(25)	119.6(7)
C(24)-C(25)-C(26)	120.5(7)	C(21)-C(26)-C(25)	120.3(7)
Sn(1)-C(31)-C(32)	123.1(6)	Sn(1)-C(31)-C(36)	119.1(4)
C(32)-C(31)-C(36)	117.7(6)	C(31)-C(32)-C(33)	121.4(8)
C(32)-C(33)-C(34)	119.8(8)	C(33)-C(34)-C(35)	120.4(8)
C(34)-C(35)-C(36)	119.6(8)	C(31)-C(36)-C(35)	121.1(6)

TABLE 2.9

**Bond lengths (Å) and angles (°) for [3]**

(standard deviations in parentheses).

**a) Bond lengths**

Sn(1)-O(1)	2.168(3)	Sn(1)-C(3)	2.102(6)
Sn(1)-C(9)	2.115(3)	Sn(1)-C(17)	2.120(4)
Sn(1)-O(3)	2.404(4)	C1(1)-C(1)	1.768(5)
C1(2)-C(1)	1.751(5)	C1(3)-C(1)	1.761(7)
O(1)-C(2)	1.283(5)	O(2)-C(2)	1.200(7)
C(1)-C(2)	1.548(8)	C(4)-C(5)	1.395
C(4)-C(3)	1.395	C(5)-C(6)	1.395
C(6)-C(7)	1.395	C(7)-C(8)	1.395
C(8)-C(3)	1.395	C(10)-C(11)	1.395
C(10)-C(9)	1.395	C(11)-C(12)	1.395
C(12)-C(13)	1.395	C(13)-C(14)	1.395
C(14)-C(9)	1.395	C(18)-C(19)	1.395
C(18)-C(17)	1.395	C(19)-C(20)	1.395
C(20)-C(21)	1.395	C(21)-C(22)	1.395
C(22)-C(17)	1.395	O(3)-C(16)	1.435(8)

**b) Bond angles**

O(1)-Sn(1)-C(3)	96.2(2)	O(1)-Sn(1)-C(9)	89.0(1)
C(3)-Sn(1)-C(9)	117.1(2)	O(1)-Sn(1)-C(17)	94.6(1)
C(3)-Sn(1)-C(17)	127.9(2)	C(9)-Sn(1)-C(17)	113.9(2)
O(1)-Sn(1)-O(3)	178.0(2)	C(3)-Sn(1)-O(3)	85.8(2)
C(9)-Sn(1)-O(3)	90.1(1)	C(17)-Sn(1)-O(3)	84.2(1)
Sn(1)-O(1)-C(2)	121.0(3)	C1(1)-C(1)-C1(2)	108.6(3)
C1(1)-C(1)-C1(3)	108.2(3)	C1(2)-C(1)-C1(3)	109.9(4)
C1(1)-C(1)-C(2)	110.8(4)	C1(2)-C(1)-C(2)	112.7(4)
C1(3)-C(1)-C(2)	106.6(4)	O(1)-C(2)-O(2)	127.5(5)
O(1)-C(2)-C(1)	111.6(5)	O(2)-C(2)-C(1)	120.8(4)
C(5)-C(4)-C(3)	120.0	C(4)-C(5)-C(6)	120.0
C(5)-C(6)-C(7)	120.0	C(6)-C(7)-C(8)	120.0
C(7)-C(8)-C(3)	120.0	Sn(1)-C(3)-C(4)	121.3(1)
Sn(1)-C(3)-C(8)	118.7(1)	C(4)-C(3)-C(8)	120.0
C(11)-C(10)-C(9)	120.0	C(10)-C(11)-C(12)	120.0
C(11)-C(12)-C(13)	120.0	C(12)-C(13)-C(14)	120.0
C(13)-C(14)-C(9)	120.0	Sn(1)-C(9)-C(10)	119.7(1)
Sn(1)-C(9)-C(14)	120.1(1)	C(10)-C(9)-C(14)	120.0
C(19)-C(18)-C(17)	120.0	C(18)-C(19)-C(20)	120.0
C(19)-C(20)-C(21)	120.0	C(20)-C(21)-C(22)	120.0
C(21)-C(22)-C(17)	120.0	Sn(1)-C(17)-C(18)	121.8(1)
Sn(1)-C(17)-C(22)	118.1(1)	C(18)-C(17)-C(22)	120.0
Sn(1)-O(3)-C(16)	124.6(3)		

TABLE 2.10

Bond lengths (Å) and angles (°) for [4]

(standard deviations in parentheses).

a) Bond lengths

Sn(1)-O(1)	2.076 (3)	Sn(1)-C(11)	2.120 (4)
Sn(1)-C(21)	2.115 (4)	Sn(1)-C(31)	2.129 (4)
Cl(1)-C(2)	1.728 (6)	Cl(2)-C(2)	1.733 (6)
Cl(3)-C(2)	1.753 (6)	O(1)-C(1)	1.281 (5)
O(2)-C(1)	1.197 (6)	C(1)-C(2)	1.547 (7)
C(11)-C(12)	1.387 (7)	C(11)-C(16)	1.371 (7)
C(12)-C(13)	1.357 (7)	C(13)-C(14)	1.361 (10)
C(14)-C(15)	1.348 (9)	C(15)-C(16)	1.395 (7)
C(21)-C(22)	1.383 (6)	C(21)-C(26)	1.381 (7)
C(22)-C(23)	1.392 (8)	C(23)-C(24)	1.376 (9)
C(24)-C(25)	1.363 (7)	C(25)-C(26)	1.382 (7)
C(31)-C(32)	1.384 (6)	C(31)-C(36)	1.381 (6)
C(32)-C(33)	1.382 (7)	C(33)-C(34)	1.357 (7)
C(34)-C(35)	1.364 (8)	C(35)-C(36)	1.397 (8)

b) Bond angles

O(1)-Sn(1)-C(11)	103.9(2)	O(1)-Sn(1)-C(21)	111.5(1)
C(11)-Sn(1)-C(21)	117.9(2)	O(1)-Sn(1)-C(31)	94.8(1)
C(11)-Sn(1)-C(31)	112.0(1)	C(21)-Sn(1)-C(31)	113.8(2)
Sn(1)-O(1)-C(1)	113.0(3)	O(1)-C(1)-O(2)	126.1(4)
O(1)-C(1)-C(2)	113.1(4)	O(2)-C(1)-C(2)	120.7(4)
Cl(1)-C(2)-Cl(2)	109.5(3)	Cl(1)-C(2)-Cl(3)	109.5(2)
Cl(2)-C(2)-Cl(3)	108.4(3)	Cl(1)-C(2)-C(1)	111.9(4)
Cl(2)-C(2)-C(1)	107.2(3)	Cl(3)-C(2)-C(1)	110.2(4)
Sn(1)-C(11)-C(12)	119.5(3)	Sn(1)-C(11)-C(16)	121.2(3)
C(12)-C(11)-C(16)	119.2(4)	C(11)-C(12)-C(13)	120.4(6)
C(12)-C(13)-C(14)	120.4(6)	C(13)-C(14)-C(15)	120.3(5)
C(14)-C(15)-C(16)	120.5(6)	C(11)-C(16)-C(15)	119.2(5)
Sn(1)-C(21)-C(22)	121.5(3)	Sn(1)-C(21)-C(26)	119.3(3)
C(22)-C(21)-C(26)	119.2(4)	C(21)-C(22)-C(23)	119.8(5)
C(22)-C(23)-C(24)	120.3(5)	C(23)-C(24)-C(25)	119.8(5)
C(24)-C(25)-C(26)	120.5(5)	C(21)-C(26)-C(25)	120.4(4)
Sn(1)-C(31)-C(32)	122.0(3)	Sn(1)-C(31)-C(36)	119.8(3)
C(32)-C(31)-C(36)	118.2(4)	C(31)-C(32)-C(33)	120.0(4)
C(32)-C(33)-C(34)	121.5(5)	C(33)-C(34)-C(35)	119.7(5)
C(34)-C(35)-C(36)	119.6(5)	C(31)-C(36)-C(35)	121.0(5)

TABLE 2.11

## Bond lengths (Å) and angles (°) for [5]

(standard deviations in parentheses).

## a) Bond lengths

Te(1)-O(11)	2.735 (4)	Te(1)-O(2a)	3.225 (4)
Te(1)-C(11)	2.106 (4)	Te(1)-C(21)	2.127 (4)
Te(1)-C(31)	2.104 (4)	Cl(1)-C(2)	1.753 (4)
Cl(2)-C(2)	1.769 (4)	Cl(3)-C(2)	1.757 (4)
O(1)-C(1)	1.231 (5)	O(2)-C(1)	1.211 (5)
C(1)-C(2)	1.574 (5)	C(11)-C(12)	1.377 (6)
C(11)-C(16)	1.371 (6)	C(12)-C(13)	1.377 (7)
C(13)-C(14)	1.370 (7)	C(14)-C(15)	1.376 (7)
C(15)-C(16)	1.387 (6)	C(21)-C(22)	1.384 (5)
C(21)-C(26)	1.372 (6)	C(22)-C(23)	1.377 (6)
C(23)-C(24)	1.352 (7)	C(24)-C(25)	1.369 (7)
C(25)-C(26)	1.366 (6)	C(31)-C(32)	1.386 (6)
C(31)-C(36)	1.367 (6)	C(32)-C(33)	1.376 (7)
C(33)-C(34)	1.346 (7)	C(34)-C(35)	1.378 (7)
C(35)-C(36)	1.383 (6)		

## b) Bond angles

C(11)-Te(1)-C(21)	94.4(2)	C(11)-Te(1)-C(31)	100.8(2)
C(21)-Te(1)-C(31)	92.9(1)	O(1)-C(1)-O(2)	130.2(4)
O(1)-C(1)-C(2)	113.5(4)	O(2)-C(1)-C(2)	116.2(3)
Cl(1)-C(2)-Cl(2)	108.2(2)	Cl(1)-C(2)-Cl(3)	108.0(2)
Cl(2)-C(2)-Cl(3)	109.1(2)	Cl(1)-C(2)-C(1)	113.2(3)
Cl(2)-C(2)-C(1)	108.2(3)	Cl(3)-C(2)-C(1)	110.1(3)
Te(1)-C(11)-C(12)	118.1(3)	Te(1)-C(11)-C(16)	120.2(3)
C(12)-C(11)-C(16)	121.6(4)	C(11)-C(12)-C(13)	118.7(4)
C(12)-C(13)-C(14)	120.8(4)	C(13)-C(14)-C(15)	120.0(5)
C(14)-C(15)-C(16)	120.0(4)	C(11)-C(16)-C(15)	119.0(4)
Te(1)-C(21)-C(22)	122.3(3)	Te(1)-C(21)-C(26)	117.5(3)
C(22)-C(21)-C(26)	119.8(4)	C(21)-C(22)-C(23)	119.4(4)
C(22)-C(23)-C(24)	120.6(4)	C(23)-C(24)-C(25)	120.0(4)
C(24)-C(25)-C(26)	120.6(4)	C(21)-C(26)-C(25)	119.7(4)
Te(1)-C(31)-C(32)	115.4(3)	Te(1)-C(31)-C(36)	123.3(3)
C(32)-C(31)-C(36)	121.2(4)	C(31)-C(32)-C(33)	118.5(4)
C(32)-C(33)-C(34)	121.1(5)	C(33)-C(34)-C(35)	120.3(4)
C(34)-C(35)-C(36)	120.1(4)	C(31)-C(36)-C(35)	118.8(4)



**Table 2.12:** Infra-red( $\text{cm}^{-1}$ ) and  $^1\text{H}$ -n.m.r.(ppm) data.

M,R	$\nu_{\text{asymm}}$	$\nu_{\text{symm}}$	$\Delta\nu$	Int.	$\delta$
Sn,CH <sub>3</sub> <sup>11</sup>	1548	1420	128	-	-
Sn,CH <sub>2</sub> Cl [1]	1575	1400	155	15,1.9	7.5-8.0,4.2
Sn,CHCl <sub>2</sub> [2]	1595	1330	195	15,0.8	7.5-8.0,6.05
Sn,CCl <sub>3</sub> [4]	1680	1330	350	-	7.5-8.0
Te,CH <sub>3</sub>	1640(b)	1370	270	-	-
		1290	350		
Te,CCl <sub>3</sub> [5]	1660	1305	355	-	7.5-8.0

**Table 2.13:** Selected bond lengths for tin carboxylates.

Compound		[1]	[2]	[4]
R	CH <sub>3</sub> <sup>11</sup>	CH <sub>2</sub> Cl	CHCl <sub>2</sub>	CCl <sub>3</sub>
Sn-O1	2.219(6)	2.195(3)	2.221(3)	2.076(3)
Sn-O2	2.349(3)	2.364(3)	2.351(4)	-
$\Delta\text{Sn-O}$	0.130	0.169	0.130	-
C-O1	1.263(5)	1.248(5)	1.250(6)	1.281(5)
C-O2	1.251(5)	1.257(5)	1.237(7)	1.197(6)
$\Delta\text{C-O}$	0.012	0.009	0.013	0.084
repeat dist.	5.488	5.086	5.557	-

## References

- 1) A. Cahours, *Ann.*, 1860, **114**, 354.
- 2) R. Okawara, D.E. Webster, E.G. Rochow, *J. Am. Chem. Soc.*, 1960, **82**, 3287.
- 3) I.R. Beattie, T. Gilson, *J. Chem. Soc.*, 1961, 2585.
- 4) M.J. Janssen, J.G.A. Luijten, G.J.M. van der Kerk, *Rec. Trav. Chim.*, 1963, **82**, 90.
- 5a) B.F.E. Ford, B.V. Liengme, J.R. Sams, *J. Organomet. Chem.*, 1969, **19**, 53.
- 5b) C. Poder, J.R. Sams, *J. Organomet. Chem.*, 1969, **19**, 67.
- 5c) B.F.E. Ford, J.R. Sams, *J. Organomet. Chem.*, 1971, **31**, 47.
- 6) P.A. Cusack, P.J. Smith, J.D. Donaldson, S.M. Grimes, *A Bibliography of X-Ray Crystal Structures of Tin Compounds*, International Tin Research Institute Publication Number 588.
- 7) R. Okawara, M. Wada, *Adv. Organomet. Chem.*, 1967, **5**, 150.
- 8) K.C. Molloy, T.G. Purcell, E. Hahn, H. Schumann, J.J. Zuckerman *Organometallics*, 1986, **5**, 85.
- 9) B.F.E. Ford, J.R. Sams, *Inorg. Chim. Acta.*, 1978, **28**, L173.
- 10) *Comprehensive Organometallic Chemistry*, Vol. 2, p. 608, ed. G. Wilkinson, F.G.A. Stone, E.W. Abel, Pergamon Press Ltd. 1982
- 11) K.C. Molloy, T.G. Purcell, K. Quill, I.W. Nowell, *J. Organomet. Chem.*, 1984, **267**, 237.

- 12) J.S. Thayer, F.E. Brinkman, *Adv. Organomet. Chem.*, 1982, **20**, 313.
- 13) N.W. Alcock, W.D. Harrison, C. Howes, *J. Chem. Soc., Dalton*, 1984, 1709.
- 14) S.W. Ng, K.L. Chin, C. Wei, V.G.K. Das, K.J. Butcher, submitted for publication in *J. Organomet. Chem.*
- 15) G.B. Deacon, R.J. Phillips, *Coord. Chem. Rev.*, 1980, **33**, 227.
- 16a) R.J. Gillespie, *J. Chem. Ed.*, 1970, **47**, 18.
- 16b) E.L. Muetterties, W. Mahler, R. Schmutzler, *Inorg. Chem.*, 1963, **2**, 613.
- 17) K.C. Molloy, K. Quill, I.W. Nowell, *J. Chem. Soc., Dalton*, 1987, 101.
- 18) S.W. Ng, C. Wei, V.G.K. Das, *J. Organomet. Chem.*, 1988, **345**, 59.
- 19) N.W. Alcock, R.E. Timms, *J. Chem. Soc. (A)*, 1968, 1873.
- 20) S. Calogero, P. Ganis, V. Peruzzo, G. Tagliavini, *J. Organomet. Chem.*, 1980, **191**, 381.
- 21) W.C. Cooper, *Tellurium*, New York, Van Nostrand-Reinhold, 1971.
- 22) D.D. Titus, J-S. Lee, R.F. Ziolo, *J. Organomet. Chem.*, 1976, **120**, 381.
- 23) J-S. Lee, D.D. Titus, R.F. Ziolo, *Inorg. Chem.*, 1977, **16**, 2487.
- 24) R.K. Chadha, J.E. Drake, M.A. Khan, G. Singh, *J. Organomet. Chem.*, 1984, **260**, 73.
- 25) M.R. Smith, M.M. Mangion, E.A. Meyers, *J. Hetrocyc. Chem.*, 1973, **10**, 537.

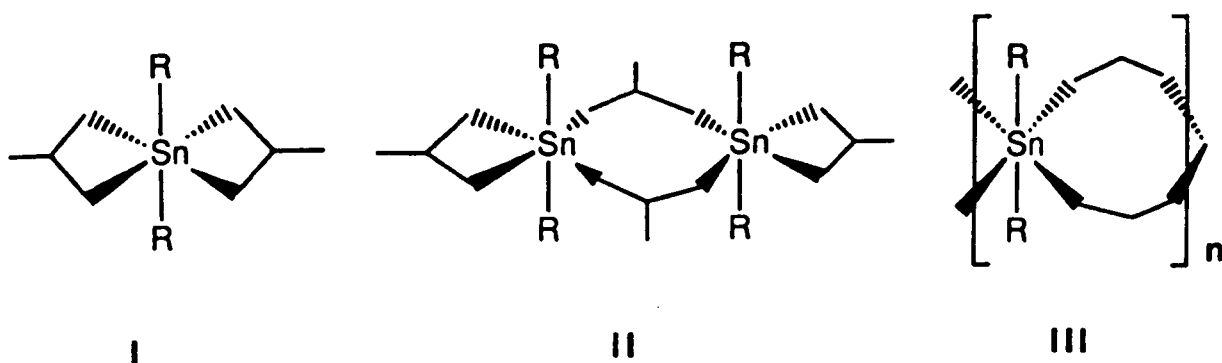
- 26) B. Kushlefsky, I. Simmons, A. Ross, *Inorg. Chem.*, 1963, **2**, 189.
- 27) B.F.E. Ford, J.R. Sams, *J. Organomet. Chem.*, 1971, **31**, 47.
- 28) T.N. Srivastava, J. Singh, *Indian J. Chem.*, 1983, **22A**, 674.
- 29) G.M. Sheldrick (1983). *SHELXTL Users Manual*, Nicolet XRD Corporation, Madison, Wisconsin.
- 30) G.M. Sheldrick (1986). *SHELXTL PLUS Users Manual*, Nicolet XRD Corporation, Madison, Wisconsin.
- 31) *International Tables for X-ray Crystallography* (1974). Vol. IV. Birmingham: Kynoch Press. (Present distributor D. Reidel, Dordrecht.)

## CHAPTER 3

### The Crystal Structure of Two Diphenyltin Dicarboxylates and One Diphenyltellurium Dicarboxylate

#### 3.1 Introduction

Diorganotin biscarboxylates have been known for many years, the first preparations being by Cahours<sup>1</sup> and Kulmiz<sup>2</sup> in 1860. Since then many studies have taken place using IR<sup>3</sup>, Moessbauer<sup>4</sup>, <sup>13</sup>C- and <sup>119</sup>Sn-n.m.r.<sup>5,6,7</sup>. Many of the compounds prepared used alkyl organo groups, since these have proved more industrially useful. These types of compound tend to be highly hygroscopic and do not show sharp melting points. Biscarboxylates are used extensively in industry for the light stabilisation of PVC sheeting and there is also interest in their structure due to their catalytic use in the isocyanate/hydroxyl reaction<sup>8</sup>. Until 1987, when Lockhart et al.<sup>9</sup> published the structure of Me<sub>2</sub>Sn(OAc)<sub>2</sub>, no structures were known. The data collected from the other techniques supported a monomeric structure (I) in solution, but three structures had been proposed for the solid state (I, II and III). Lockhart found structure (I) in the solid state as well. Very recently, a further compound was structurally characterised, (n-Bu)<sub>2</sub>Sn(o-NH<sub>2</sub>C<sub>6</sub>H<sub>4</sub>COO)<sub>2</sub><sup>10</sup>. This is reported as being a bicapped tetrahedron or a very distorted octahedron. In addition to the long interactions to the acyl oxygens, there are also intermolecular interactions distorting the structure.



The first diorganotellurium biscarboxylates were prepared by Vernon<sup>11</sup> in 1920 when he synthesised the dimethyltellurium bisbenzoate and picrate complexes by the use of silver carboxylates. In 1926, Drew<sup>12</sup> prepared a diacetate with the tellurium as part of a cyclic organic moiety. Although these, unlike the tin complexes, were stable, moderately high melting point

crystals, the first structure was not undertaken until 1984 when Bulgarevich et al<sup>13</sup> and Alcock et al<sup>14</sup> examined the diphenyltellurium bistrifluoroacetate and bis-p-methoxyphenyltellurium bistrifluoroacetate respectively.

It was of interest to extend the range of structures known, especially in the case of tin where different possibilities were available for the structure, and compare the tin and tellurium complexes to study the differences the lone pair on the tellurium produces. Of further interest was the secondary bonding that tin and tellurium complexes have already been shown to adopt to increase the electron density on the metal. To this end three structures have been characterised, diphenyltin bisacetate [6], diphenyltin bismonochloroacetate [7] and diphenyltellurium bistrichloroacetate [8].

### 3.2 Results

From Infra-red studies (Table 3.8) it can be seen that all the carboxylate stretches have a  $\Delta\nu$  greater than  $200\text{cm}^{-1}$ . As stated earlier in Chapter 2, Deacon and Phillips<sup>15</sup> proposed that a value greater than  $200\text{-}260\text{cm}^{-1}$  for halocarboxylate complexes indicated unidentate behaviour. This is proved correct in all of the structures, which have primarily unidentate carboxylates, the secondary bonds being quite long. The increasing value for  $\Delta\nu$  down the table is expected due to the increased acidity of the carboxylate. The exception,  $\text{Ph}_2\text{Sn}(\text{O}_2\text{CCHCl}_2)_2$ , is probably due to the mull being of the crude, uncrystallised product.

The structure of [6],  $\text{Ph}_2\text{Sn}(\text{O}_2\text{CCH}_3)_2$  (Figure 3.1), is based on a very distorted tetrahedron. The distortion arises from long interactions between the Sn and the carbonyl oxygens (average distance =  $2.555\text{\AA}$ ). This forces the phenyl carbon atoms apart, opening the angle between them to  $131.4(2)^\circ$ , and closing the angle between the primary bonded oxygens, O2 and O3, to  $82.0(2)^\circ$ . The angle between the planes C11-Sn1-C21 and O2-Sn1-O3 is only altered slightly, with a  $3.9^\circ$  deviation from the expected  $90.0^\circ$  position. The molecule forms discrete monomeric units in the solid state as is shown in the packing diagram (Figure 3.2).

The structure of [7],  $\text{Ph}_2\text{Sn}(\text{OCOCH}_2\text{Cl})_2$  (Figure 3.3), is similar to that of [6] except that the C11-Sn1-C21 angle opens out further to  $147.2(2)^\circ$ , the O2-Sn1-O3 angle staying close to that of [6] at  $82.3(2)^\circ$ . The angle between the planes is again  $93.9^\circ$ . However, in the solid state the molecules are ordered along the c-axis, instead of being discrete, by means of Van der Waals

interactions between the tin bonded oxygens, O2 and O3, and the neighbouring tin atom (Figure 3.4). These interactions, 3.461(6)Å and 3.552(6)Å respectively, are approaching, but less than the sum of the Van der Waals radii<sup>16</sup>, and clearly have a large effect in the packing of the molecule in the lattice. In contrast, the nearest intermolecular contact for [6] is 5.396Å.

Structure [6] is similar to two compounds already reported,  $\text{Me}_2\text{Sn}(\text{OAc})_2$  and  $\text{Me}_2\text{Sn}(\text{NO}_3)_2$ , with the bidentate ligands bonding to the primary tin atom only, giving monomeric units<sup>9,17</sup>. [7], which would also be expected to adopt this structure forms two extra secondary bonds to a neighbouring tin atom forming a chain structure in the solid state. This is reflected in the increased density of this compound over [6] due to the more ordered packing. These long interactions are presumably due to the more electronegative carboxylate removing electron density from the tin atom, requiring it to make extra bonds to be stable.  $\text{Et}_2\text{SnI}_2$  also adopts this type of packing, raising the coordination of the tin from four to six to assuage the Lewis acidity of the tin<sup>18</sup>.  $\text{Et}_2\text{SnCl}_2$  and  $\text{Et}_2\text{SnBr}_2$  also increase their coordination from four to six, though the structure adopted is slightly different since the halogens bond to two different neighbouring tin atoms<sup>18</sup>. In this way a better octahedral geometry is formed, presumably this is not possible for [7] or the iodo-compound due to steric reasons. Interestingly  $\text{Ph}_2\text{SnCl}_2$ <sup>9</sup> forms discrete monomeric units. Since the phenyl moiety is more electronegative than the ethyl this must be a consequence of the increased steric bulk of the phenyl group.

The asymmetric unit for [8],  $\text{Ph}_2\text{Te}(\text{OCOCCl}_3)_2$ , consists of two half molecules, the other halves being generated by the 2-fold axis. The molecules sit close together in the solid state, with the phenyl rings pointing out from the centre of the dimer, while the carboxylates point in (Figure 3.5). The carbonyl oxygens are bonded to both tellurium atoms by long range interactions which are shorter than the sum of the Van der Waals radii at 3.60Å (range=3.032-3.250Å). The geometry of the tellurium atoms can be thought of in two ways. Firstly, considering only the primary bonds the molecules are based on distorted trigonal bipyramids, as expected from VSEPR theory<sup>20</sup>, the bond angles O3-Te1-O3A and C5-Te1-C5A being reduced from 180 and 120° to 167.3(2) and 98.9(3)° respectively due to the effect of the lone pair which sits on the axis between the tellurium atoms. Secondly, it is possible for the lone pair to be non-sterically active<sup>21</sup>. If this is the case then the structure is a distorted octahedral complex. O3 and O3A are the axial groups, with C5, C5A, O2 and O2A making up the equatorial plane. The angles are all near 180° to 167.3(2), 161.4(2) and 161.4(2)° respectively. The distortions arise from the two secondary bonds

from O2 and O2A not being in the primary coordination sphere. This is perhaps the most plausible explanation because with the Te1-Te2 distance being 3.793(4)Å, shorter than the sum of the Van der Waals radii (4.40Å) the lone pair/lone pair repulsion would be expected to be quite large. The actual answer probably lies somewhere between these two extremes. The trichloroacetates themselves are skewed with respect to each other by an angle of 53.3°. The packing diagram (Figure 3.6) shows the molecules lying in planes bounded by chlorines. The closest intermolecular distance between these planes is Cl(6)-Cl(6)=3.376Å. The tellurium compound, [8], increases its coordination by forming a dimer rather than a chain. This has been noted for two previous structures,  $\text{Ph}_2\text{Te}(\text{O}_2\text{CCF}_3)_2^3$  and  $(p\text{-MeOC}_6\text{H}_4)_2\text{Te}(\text{O}_2\text{CCF}_3)_2^4$ . In both these structures, though, only one carboxylate is participating in secondary bonding, the other hangs free. In this geometry there is a vacant site left for the lone pair, trans to one of the aryl groups, pointing out of the dimer, and therefore the lone pair is sterically active. In [8] the short Te1-Te2 bond distance and four bridging carboxylates precludes the possibility of the lone pair being totally sterically active. Non-sterically, or partially, active lone pairs have been witnessed previously by Drew et al<sup>22</sup> and Schmidt et al<sup>23</sup> and discussed by Shustorovich and Dobosh<sup>21</sup> as "quasi lone pairs" (QLP's).

The comparison of the tin and tellurium dicarboxylate systems is simplified by the fact that the lone pair of the tellurium is sterically inactive. Both systems form four primary and two secondary bonds. The average primary Sn-O bond (2.087Å) and average primary Te-O bond (2.156Å) show a difference of ~0.07Å, which is compatible with the difference in size of the Sn<sup>IV</sup> and Te<sup>IV</sup> covalent centres. The difference between the two systems arises from the secondary bonds. In the case of tin, the secondary bonds are formed to the acyl oxygen of the bound carboxylate, thus forming a monomeric unit. In the tellurium system a dimer is formed and the secondary bonds are to a neighbouring acyl oxygen.

### 3.3 Experimental

#### 3.3.1 Synthesis of Compounds

$\text{Ph}_2\text{SnCl}_2$  was purchased from Aldrich and used as received.

#### Silver Carboxylates



$\text{Ag}_2\text{O}$  and the appropriate acid were stirred in distilled water. The water was reduced using a rotary evaporator until crystallisation occurred. The flask was cooled in a refrigerator and the product filtered off. Repeated reduction of the solvent volume and filtration gave a good yield of white crystals. These were used immediately or stored wrapped in foil in a dessicator. Infra-red spectra show that these compounds are anhydrous.

### **Diphenyltin dicarboxylates**

$\text{Ph}_2\text{SnCl}_2$  and  $\text{AgO}_2\text{CMe}$  (1:2) were refluxed in dry hexane for 3hrs. The hot solution was filtered to remove  $\text{AgCl}$  and then removed on a rotary evaporator. The product was recrystallised from hot petroleum ether (30-40°bpt.). For the mono-chloroacetate compound  $\text{CH}_2\text{Cl}_2$  was used as the solvent. Crystals were obtained by liquid diffusion using  $\text{CH}_2\text{Cl}_2$ /petroleum ether (30-40°bpt.). Suitable crystals could not be isolated for the di-chloroacetate complex, most solvents giving very thin platy crystals, and the spectroscopic data recorded is from the crude product. The bistrichloroacetate complex was not isolated. Hydrolysis of the product is suspected here, from comparison with the monocarboxylates.

### **Diphenyltellurium dicarboxylates**

$\text{Ph}_2\text{TeCl}_2$  and the sodium salt of the respective acid (acetic and trichloroacetic) (1:2) were stirred in dry benzene (30cm<sup>3</sup>) for 24hrs. The solution was filtered through Celite to remove the  $\text{NaCl}$  and the solvent removed by rotary evaporation. The white product was recrystallised from  $\text{CCl}_4$ /Hexane by liquid diffusion.

#### **3.3.2 Spectroscopic Data**

Infra-red data was recorded on a Perkin-Elmer 580B spectrophotometer in the range 4000-400cm<sup>-1</sup> using KBr discs with Nujol Mull. <sup>1</sup>H-n.m.r. spectra in the range 0-10ppm were recorded on a Perkin-Elmer R34. Results are listed in Table 3.8.

#### **3.3.3 X-Ray Crystallography**

All data sets were recorded at 293K with Mo-K $\alpha$  radiation at 0.71069Å. Standard reflections were measured every 200 reflections and showed slight changes during the data collection (1, 1 and 10% for [6],[7] and [8] respectively). The data was processed using profile analysis and corrected for Lorentz, polarisation and absorption effects, the last by the Gaussian method. The cell parameters were calculated from 15 reflections with  $2\theta$  between 20 and 22°. All non-hydrogen atoms were refined anisotropically. Hydrogen atoms were inserted at calculated positions and not refined. Their temperature factors were fixed at 0.07Å<sup>2</sup>. Methyl groups in [6] were treated as rigid CH<sub>3</sub> units, their initial orientation taken from the strongest H-atom peaks on a difference Fourier synthesis. Computing was with SHELXTL<sup>24</sup> on a Data General DG30. Scattering factors in the analytical form and anomalous dispersion factors were taken from International Tables<sup>25</sup>. Data collection parameters are listed in Table 3.1. Atomic coordinates are in Tables 3.2-3.4 and bond lengths and angles in Tables 3.5-3.7 for [6], [7] and [8] respectively. Views of the molecules and packing diagrams are shown in Figures 3.1-3.6.

### **Diphenyltin Diacetate [6]**

Systematic absences  $h00, h=2n+1$ ,  $0k0, k=2n+1$ ,  $00l, l=2n+1$  gave the space group as  $P2_12_12_1$ . The Patterson synthesis gave the heavy atom at 0.855,0.500,0.604.  $P2_12_12_1$  has no special positions and so the y coordinate was not fixed. This finally refined to 0.48369(4). The remaining non-hydrogen atoms were located by difference Fourier synthesis.

### **Diphenyltin Bis-monochloroacetate [7]**

Systematic absences  $h0l, l=2n+1$  and  $hk0, h=2n+1$  indicate space groups  $P2_1ca$  or  $Pmca$ . These are non-standard settings of  $Pca2_1$  and  $Pbcm$  respectively. From density calculations the expected number of molecules per unit cell was 4, giving  $\rho=1.81$ .  $Pca2_1$  was therefore initially chosen for the refinement but did not give encouraging results. The space group was changed to  $Pbcm$  with the condition that the heavy atom must lie on  $z=1/4$ . The Patterson synthesis gave the heavy atom at (1/4,1/4,1/4). Since x and y are not tied to 1/4 they were given initial values of 0.246 and 0.254. Refinement then proceeded smoothly.

### **Diphenyltellurium Bis-trichloroacetate [8]**

The data was taken as an I-centred monoclinic cell (original cell 21.2173Å, 11.2422Å, 19.2085Å, 90°, 103.61°, 90°). After the data collection this was transformed to give a C-centred monoclinic cell using the cell transformation program 'CRYSTAL'. Analysis of the systematic absences for the I-centred cell gave probable space groups of Ia or I2/a. From density calculations eight molecules were expected. This gave I2/a as the most likely choice. On transformation of the cell this gives the standard space group C2/c. This choice was proved correct by good refinement. Two heavy atoms were found by the Patterson synthesis, with half occupancy at 0,y,3/4. These positions were used and gave good refinement. Residual electron density is located in the rotation circles of the CCl<sub>3</sub> groups.

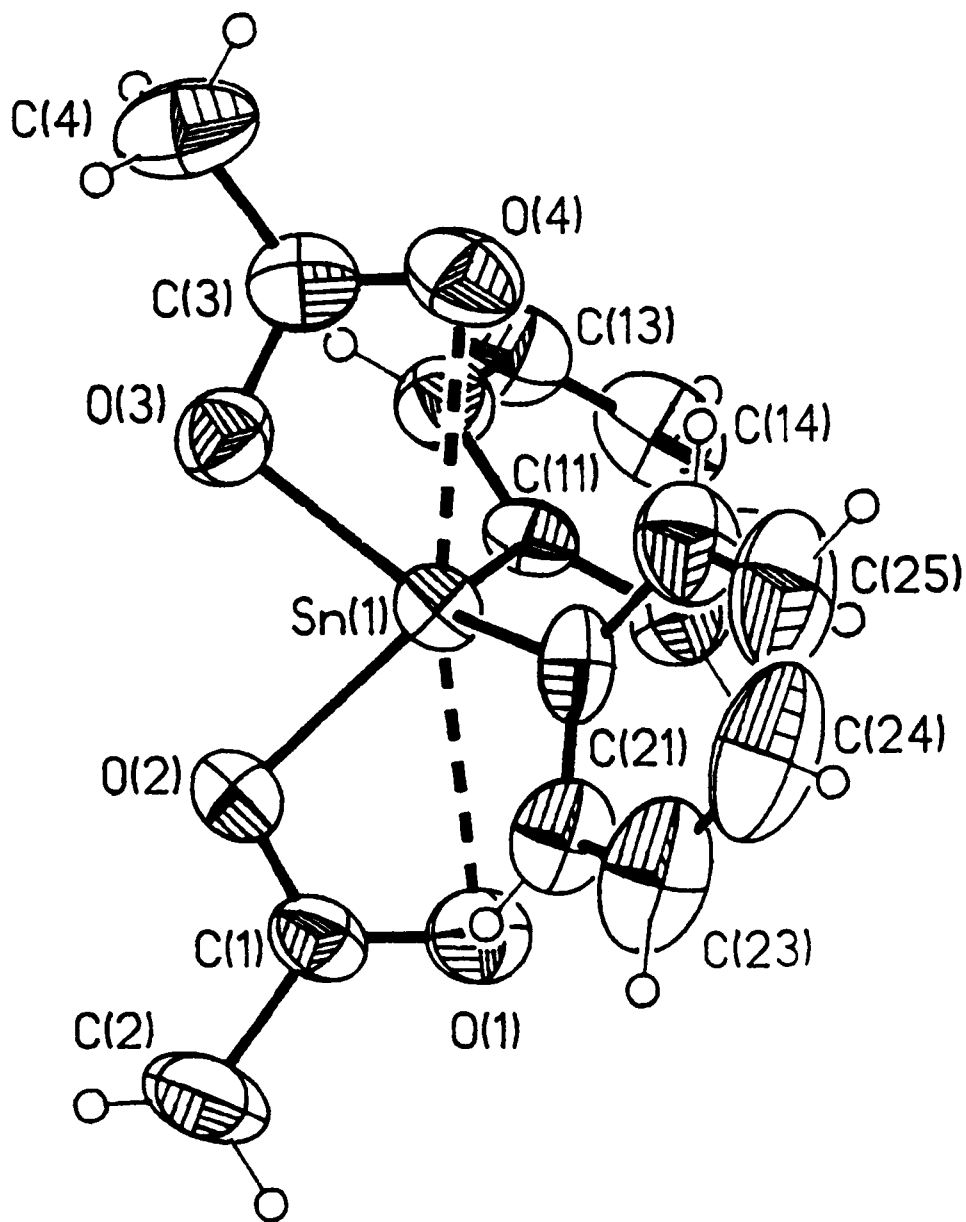
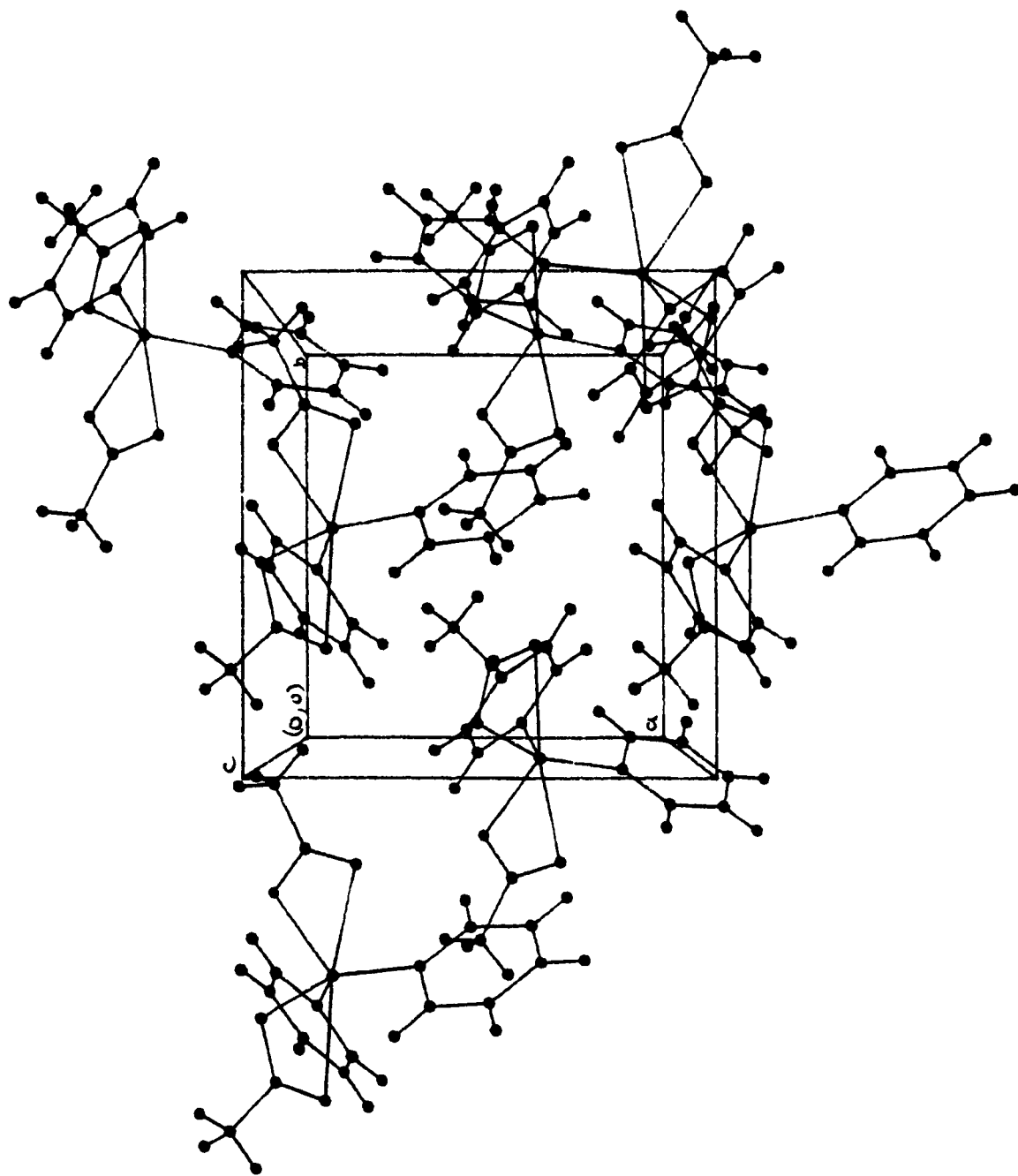


FIGURE 3.1 View of the molecule of [6], showing atomic numbering scheme.



**FIGURE 3.2** Packing diagram for [6].

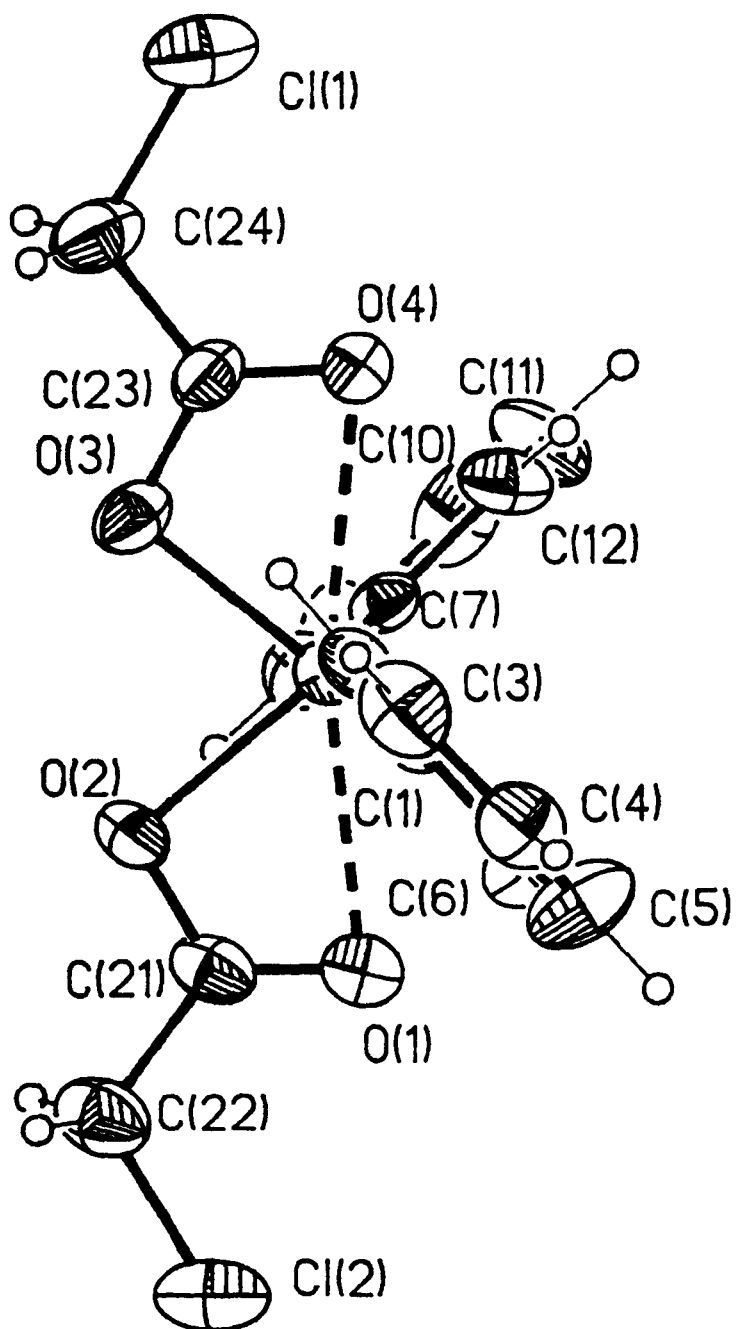
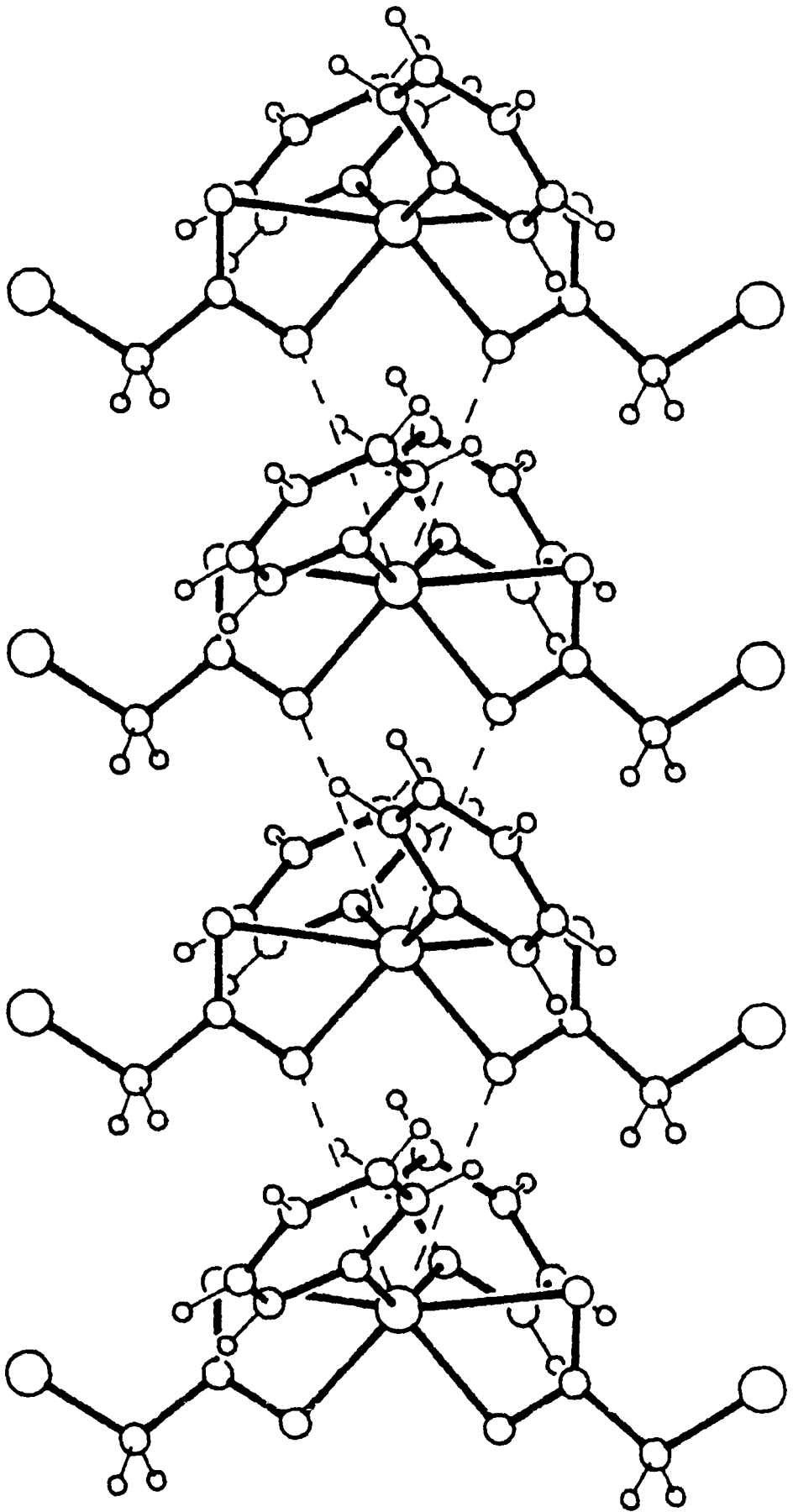


FIGURE 3.3 View of one molecule of [7], showing atomic numbering scheme.



**FIGURE 3.4** View of the packing of [7].

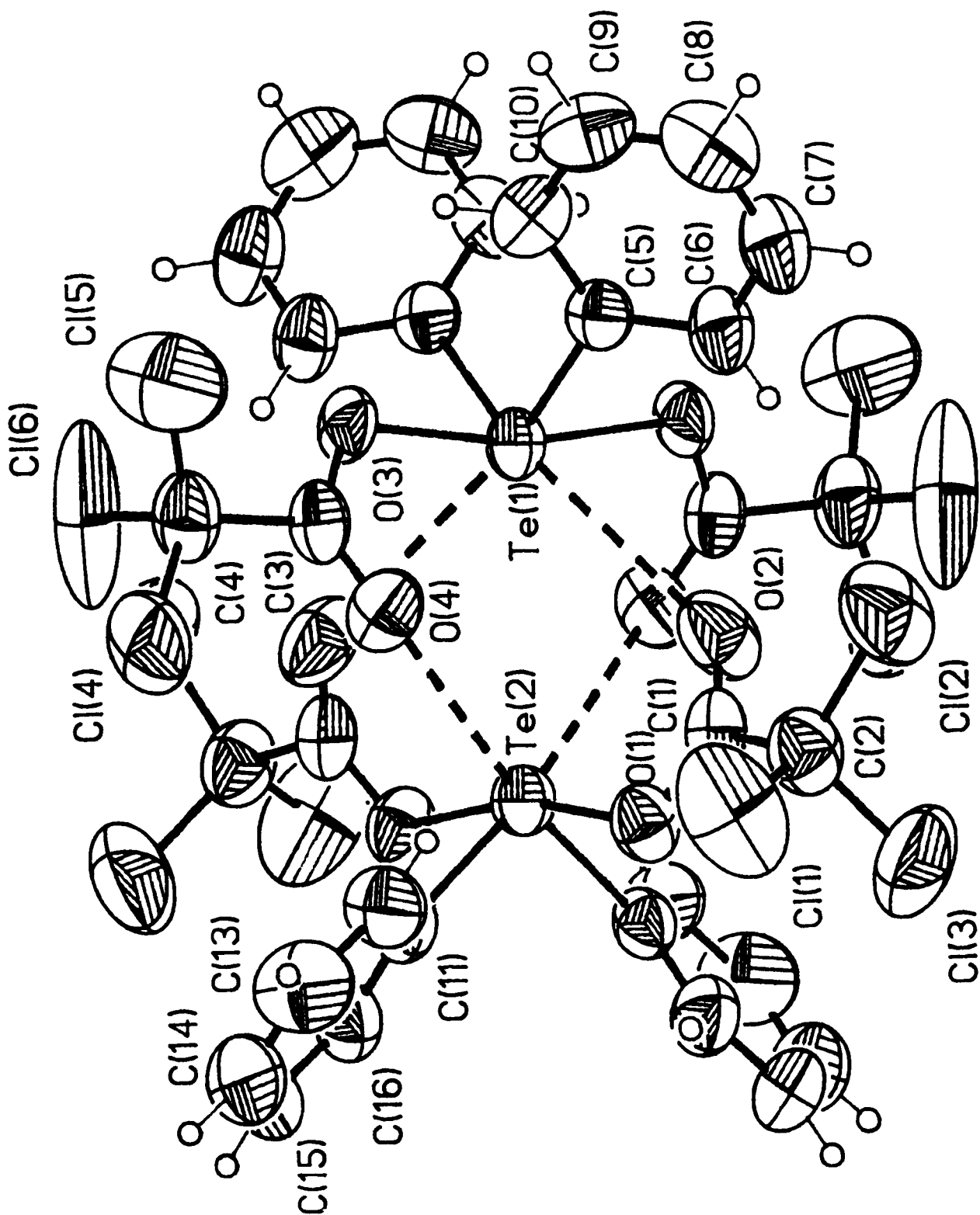


FIGURE 3.5 View of the dimer of [8], showing atomic numbering scheme.



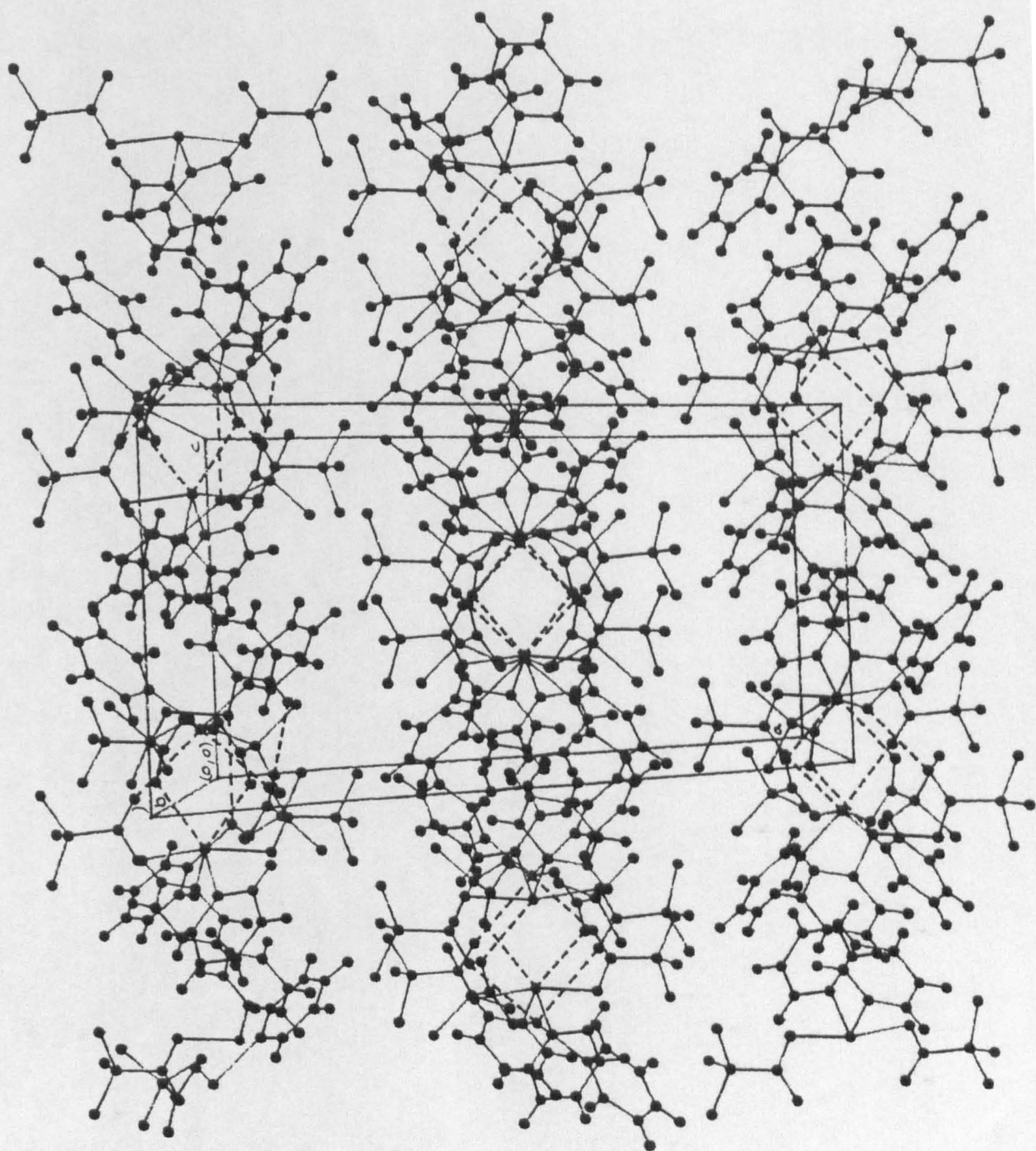


FIGURE 3.6 Packing diagram for [8].

**Table 3.1: Crystal data and data collection parameters**

<b>Compound</b>	<b>[6]</b>	<b>[7]</b>	<b>[8]</b>
Formula	C <sub>16</sub> H <sub>16</sub> O <sub>4</sub> Sn	C <sub>16</sub> H <sub>14</sub> O <sub>4</sub> Cl <sub>2</sub> Sn	C <sub>16</sub> H <sub>10</sub> O <sub>4</sub> Cl <sub>6</sub> Te
Mass(gmol <sup>-1</sup> )	390.99	459.88	606.85
D <sub>calc.</sub> (gcm <sup>-3</sup> )	1.58	1.81	1.81
Z	4	4	8
Crystal System	Orthorhombic	Orthorhombic	Monoclinic
Systematic Absences	h00 h=2n+1 0k0 k=2n+1 00l l=2n+1	h0l l=2n+1 hk0 h=2n+1	hkl h+k=2n+1 h0l h,l=2n+1
Space Group	P2 <sub>1</sub> 2 <sub>1</sub> 2 <sub>1</sub>	Pbcm (rot)	C2/c (trans)
a(Å)	8.512(2)	9.909(6)	25.047(9)
b(Å)	9.038(2)	17.782(11)	11.242(8)
c(Å)	21.309(6)	9.599(7)	19.208(6)
α(°)	-	-	-
β(°)	-	-	124.58(3)
γ(°)	-	-	-
U(Å <sup>3</sup> )	1639.2(0.7)	1691.5(1.7)	4453.2(4.3)
μ(cm <sup>-1</sup> )	15.7	18.5	21.3
F(000)	776	904	2336
Crystal Size(mm)	0.5×0.3×0.1	0.6×0.4×0.4	0.2×0.4×0.2
Max. Trans.	0.8739	0.6318	0.6887
Min. Trans.	0.6942	0.5511	0.5201
Scan Range(°)	+/- 1.0	+1.2,-1.0	+1.2,-1.0
Scan Rate(°min <sup>-1</sup> )	2.0	2.0	3.0
Max. 2θ(°)	50	50	50
Refs. Collected	1704	1596	3937
Refs. Observed	1575	1409	2916
R(final)	0.0283	0.0462	0.0424
R <sub>w</sub>	0.0311	0.0493	0.0475
g	0.00074	0.03656	0.00044
Max. on final Fourier	+0.3,-0.8	+0.6,-2.3	+0.5,-0.6
Max. δ/σ	0.013	0.011	0.019
No. of Parameters	196	207	100

rot - rotated from Pmca, trans - transformed from I2/a

**TABLE 3.2**

**Atomic coordinates ( $\times 10^4$ ) for [6] (with standard deviations in parentheses).**

atom	x	y	z	U
Sn(1)	8567.0(4)	4836.9(4)	6040.1(2)	41(1)*
O(1)	8681(5)	7517(5)	6458(2)	61(1)*
O(2)	10163(5)	5624(4)	6697(2)	55(1)*
O(3)	9975(5)	2963(4)	6100(2)	57(1)*
O(4)	8062(6)	2444(5)	5460(2)	70(2)*
C(1)	9797(7)	7033(7)	6750(3)	51(2)*
C(2)	10782(10)	7933(10)	7181(3)	81(3)*
C(3)	9270(9)	2049(7)	5717(3)	59(2)*
C(4)	10043(13)	611(8)	5617(4)	93(3)*
C(11)	9039(6)	5746(5)	5143(2)	42(2)*
C(12)	10115(7)	5084(7)	4760(3)	53(2)*
C(13)	10366(8)	5659(8)	4166(3)	65(2)*
C(14)	9537(9)	6850(8)	3957(3)	74(3)*
C(15)	8452(9)	7525(8)	4346(3)	69(2)*
C(16)	8196(8)	6976(6)	4940(3)	56(2)*
C(21)	6438(7)	4512(7)	6528(3)	53(2)*
C(22)	6183(7)	5256(8)	7104(3)	62(2)*
C(23)	4796(9)	5098(12)	7407(4)	89(3)*
C(24)	3618(10)	4266(11)	7156(5)	109(4)*
C(25)	3831(9)	3581(11)	6611(5)	105(4)*
C(26)	5257(9)	3685(8)	6283(4)	75(3)*

\* Equivalent isotropic U defined as one third of the trace of the orthogonalised  $U_{ij}$  tensor.

TABLE 3.3

Atomic coordinates ( $\times 10^4$ ) for [7] (with standard deviations in parentheses).

Atom	x	y	z	U
Sn(1)	2423.8(4)	2526.8(2)	2500.0	30(1)*
C1(1)	-2550(2)	3510(2)	1597(5)	62(1)*
C1(2)	7310(2)	1494(2)	1376(5)	63(1)*
O(1)	4825(4)	2054(3)	2731(5)	47(1)*
O(2)	3760(6)	2370(3)	825(7)	36(1)*
O(3)	1049(5)	2718(4)	887(6)	40(1)*
O(4)	12(4)	2991(3)	2844(5)	43(1)*
C(21)	4787(6)	2084(4)	1468(6)	38(2)*
C(22)	5883(7)	1816(5)	489(8)	53(2)*
C(23)	24(6)	2986(4)	1573(6)	38(2)*
C(24)	-1102(7)	3256(5)	660(8)	53(2)*
C(1)	1842(5)	1434(3)	3092(7)	30(2)*
C(2)	704(5)	1118(3)	2562(7)	39(2)*
C(3)	318(7)	390(4)	2883(7)	55(2)*
C(4)	1043(7)	-10(3)	3817(7)	50(2)*
C(5)	2190(7)	283(4)	4374(8)	60(3)*
C(6)	2611(7)	1002(4)	4019(9)	54(3)*
C(7)	3028(5)	3614(3)	3151(7)	30(2)*
C(8)	4083(5)	3967(3)	2467(7)	39(2)*
C(9)	4482(6)	4668(4)	2895(6)	47(2)*
C(10)	3834(7)	5024(3)	3975(7)	54(2)*
C(11)	2803(7)	4691(5)	4644(9)	57(3)*
C(12)	2351(6)	3994(4)	4251(8)	48(2)*

\* Equivalent isotropic U defined as one third of the trace of the  
the orthogonalised  $U_{ij}$  tensor.

TABLE 3.4

Atomic coordinates ( $\times 10^4$ ) for [8] (with standard deviations in parentheses).

Atom	x	y	z	U
Te(1)	00.0	1724.4(5)	7500.0	53(1)*
Te(2)	00.0	-1649.7(5)	7500.0	53(1)*
Cl(1)	413(2)	-1787(3)	10363(2)	149(2)*
Cl(2)	1352.0(14)	44.8(20)	10823.8(13)	118(2)*
Cl(3)	1607.0(13)	-2322.3(27)	10563.8(15)	151(2)*
Cl(4)	-2336.2(11)	-72.6(20)	6844.9(17)	117(2)*
Cl(5)	-2209.9(13)	2388.9(25)	6929.0(26)	175(3)*
Cl(6)	-2293.3(11)	1153.6(45)	5596.2(14)	194(2)*
O(1)	361(2)	-1886(4)	8815(2)	65(2)*
O(2)	816(3)	-108(4)	9057(3)	93(3)*
O(3)	-999(2)	1936(4)	7052(3)	62(2)*
O(4)	-959(2)	177(4)	7601(3)	74(3)*
C(1)	703(3)	-1020(6)	9277(3)	63(3)*
C(2)	986(3)	-1250(7)	10214(4)	81(4)*
C(3)	-1247(3)	1028(5)	7167(3)	57(3)*
C(4)	-1997(3)	1109(6)	6661(4)	73(4)*
C(5)	242(3)	2942(5)	8471(4)	53(3)*
C(6)	805(3)	2774(6)	9262(4)	68(4)*
C(7)	966(4)	3576(7)	9897(4)	81(4)*
C(8)	576(5)	4521(8)	9743(5)	89(6)*
C(9)	8(4)	4676(6)	8956(5)	81(5)*
C(10)	-157(3)	3888(6)	8323(4)	69(4)*
C(11)	-735(3)	-2844(5)	7272(4)	57(3)*
C(12)	-1028(3)	-2653(6)	7696(4)	77(4)*
C(13)	-1534(4)	-3389(7)	7500(6)	104(7)*
C(14)	-1739(4)	-4264(8)	6916(6)	111(6)*
C(15)	-1448(4)	-4458(7)	6512(5)	96(5)*
C(16)	-937(3)	-3730(6)	6686(4)	72(4)*

\* Equivalent isotropic U defined as one third of the trace of the orthogonalised  $U_{ij}$  tensor.

**TABLE 3.5**

**Bond lengths (Å) and angles (°) for [6]**

(standard deviations in parentheses).

**a) Bond lengths**

Sn(1)-O(1)	2.583(4)	Sn(1)-O(2)
Sn(1)-O(3)	2.079(4)	Sn(1)-O(4)
Sn(1)-C(11)	2.119(5)	Sn(1)-C(21)
O(1)-C(1)	1.216(8)	O(2)-C(1)
O(3)-C(3)	1.307(8)	O(4)-C(3)
C(1)-C(2)	1.487(10)	C(3)-C(4)
C(11)-C(12)	1.365(8)	C(11)-C(16)
C(12)-C(13)	1.386(8)	C(13)-C(14)
C(14)-C(15)	1.382(10)	C(15)-C(16)
C(21)-C(22)	1.417(9)	C(21)-C(26)
C(22)-C(23)	1.353(10)	C(23)-C(24)
C(24)-C(25)	1.329(15)	C(25)-C(26)

**b) Bond angles**

O(1)-Sn(1)-O(2)	54.7(1)	O(1)-Sn(1)-O(3)
O(2)-Sn(1)-O(3)	82.0(2)	O(1)-Sn(1)-O(4)
O(2)-Sn(1)-O(4)	137.2(2)	O(3)-Sn(1)-O(4)
O(1)-Sn(1)-C(11)	86.6(2)	O(2)-Sn(1)-C(11)
O(3)-Sn(1)-C(11)	105.2(2)	O(4)-Sn(1)-C(11)
O(1)-Sn(1)-C(21)	89.6(2)	O(2)-Sn(1)-C(21)
O(3)-Sn(1)-C(21)	110.6(2)	O(4)-Sn(1)-C(21)
C(11)-Sn(1)-C(21)	131.4(2)	Sn(1)-O(1)-C(1)
Sn(1)-O(2)-C(1)	103.5(3)	Sn(1)-O(3)-C(3)
Sn(1)-O(4)-C(3)	83.5(4)	O(1)-C(1)-O(2)
O(1)-C(1)-C(2)	124.0(6)	O(2)-C(1)-C(2)
O(3)-C(3)-O(4)	118.9(6)	O(3)-C(3)-C(4)
O(4)-C(3)-C(4)	124.8(7)	Sn(1)-C(11)-C(12)
Sn(1)-C(11)-C(16)	119.5(4)	C(12)-C(11)-C(16)
C(11)-C(12)-C(13)	119.0(6)	C(12)-C(13)-C(14)
C(13)-C(14)-C(15)	120.0(6)	C(14)-C(15)-C(16)
C(11)-C(16)-C(15)	119.5(6)	Sn(1)-C(21)-C(22)
Sn(1)-C(21)-C(26)	121.6(5)	C(22)-C(21)-C(26)
C(21)-C(22)-C(23)	119.8(6)	C(22)-C(23)-C(24)
C(23)-C(24)-C(25)	119.9(8)	C(24)-C(25)-C(26)
C(21)-C(26)-C(25)	119.1(8)	

TABLE 3.6

**Bond lengths (Å) and angles (°) for [7]**

(standard deviations in parentheses).

**a) Bond lengths**

Sn(1)-O(2)	2.101(6)	Sn(1)-O(3)	2.090(6)
Sn(1)-C(1)	2.105(6)	Sn(1)-C(7)	2.118(6)
Cl(1)-C(24)	1.753(8)	Cl(2)-C(22)	1.747(8)
O(1)-C(21)	1.214(8)	O(2)-C(21)	1.294(8)
O(3)-C(23)	1.301(8)	O(4)-C(23)	1.220(7)
C(21)-C(22)	1.514(10)	C(23)-C(24)	1.498(10)
C(1)-C(2)	1.359(7)	C(1)-C(6)	1.401(10)
C(2)-C(3)	1.385(9)	C(3)-C(4)	1.351(9)
C(4)-C(5)	1.361(10)	C(5)-C(6)	1.387(11)
C(7)-C(8)	1.385(8)	C(7)-C(12)	1.421(9)
C(8)-C(9)	1.370(8)	C(9)-C(10)	1.374(9)
C(10)-C(11)	1.344(10)	C(11)-C(12)	1.371(11)

**b) Bond angles**

O(2)-Sn(1)-O(3)	82.3(2)	O(2)-Sn(1)-C(1)	104.9(2)
O(3)-Sn(1)-C(1)	99.9(2)	O(2)-Sn(1)-C(7)	99.7(2)
O(3)-Sn(1)-C(7)	104.8(2)	C(1)-Sn(1)-C(7)	147.2(2)
Sn(1)-O(2)-C(21)	100.5(5)	Sn(1)-O(3)-C(23)	101.2(4)
O(1)-C(21)-O(2)	121.2(6)	O(1)-C(21)-C(22)	125.7(6)
O(2)-C(21)-C(22)	113.1(6)	Cl(2)-C(22)-C(21)	112.4(5)
O(3)-C(23)-O(4)	121.0(6)	O(3)-C(23)-C(24)	113.8(5)
O(4)-C(23)-C(24)	125.2(6)	Cl(1)-C(24)-C(23)	113.1(5)
Sn(1)-C(1)-C(2)	120.5(4)	Sn(1)-C(1)-C(6)	121.9(4)
C(2)-C(1)-C(6)	117.5(6)	C(1)-C(2)-C(3)	122.2(6)
C(2)-C(3)-C(4)	119.6(6)	C(3)-C(4)-C(5)	120.2(6)
C(4)-C(5)-C(6)	120.5(7)	C(1)-C(6)-C(5)	119.9(7)
Sn(1)-C(7)-C(8)	119.2(4)	Sn(1)-C(7)-C(12)	121.3(4)
C(8)-C(7)-C(12)	119.5(5)	C(7)-C(8)-C(9)	119.2(6)
C(8)-C(9)-C(10)	120.7(6)	C(9)-C(10)-C(11)	120.8(6)
C(10)-C(11)-C(12)	121.0(7)	C(7)-C(12)-C(11)	118.7(6)

TABLE 3.7

**Bond lengths (Å) and angles (°) for [8]**

(standard deviations in parentheses).

**a) Bond lengths**

Te(1)-O(3)	2.149(4)	Te(1)-C(5)	2.106(6)
Te(2)-O(1)	2.163(4)	Te(2)-C(11)	2.114(7)
Cl(1)-C(2)	1.724(10)	Cl(2)-C(2)	1.764(7)
Cl(3)-C(2)	1.771(8)	Cl(4)-C(4)	1.719(9)
Cl(5)-C(4)	1.712(9)	Cl(6)-C(4)	1.735(8)
O(1)-C(1)	1.267(7)	O(2)-C(1)	1.204(9)
O(3)-C(3)	1.278(8)	O(4)-C(3)	1.202(7)
C(1)-C(2)	1.535(9)	C(3)-C(4)	1.551(8)
C(5)-C(6)	1.378(7)	C(5)-C(10)	1.376(9)
C(6)-C(7)	1.381(11)	C(7)-C(8)	1.357(13)
C(8)-C(9)	1.378(10)	C(9)-C(10)	1.364(11)
C(11)-C(12)	1.388(13)	C(11)-C(16)	1.366(9)
C(12)-C(13)	1.375(12)	C(13)-C(14)	1.354(14)
C(14)-C(15)	1.350(17)	C(15)-C(16)	1.391(12)

**b) Bond angles**

O(3)-Te(1)-C(5)	88.1(2)	O(3)-Te(1)-O(3a)	167.3(2)
C(5)-Te(1)-O(3a)	83.6(2)	C(5)-Te(1)-C(5a)	98.9(3)
O(1)-Te(2)-C(11)	84.3(2)	O(1)-Te(2)-O(1a)	165.9(2)
C(11)-Te(2)-O(1a)	86.7(2)	C(11)-Te(2)-C(11a)	101.2(3)
Te(2)-O(1)-C(1)	113.1(4)	Te(1)-O(3)-C(3)	114.3(3)
O(1)-C(1)-O(2)	127.5(6)	O(1)-C(1)-C(2)	111.8(6)
O(2)-C(1)-C(2)	120.7(5)	Cl(1)-C(2)-Cl(2)	110.2(5)
Cl(1)-C(2)-Cl(3)	109.4(4)	Cl(2)-C(2)-Cl(3)	107.3(3)
Cl(1)-C(2)-C(1)	112.2(4)	Cl(2)-C(2)-C(1)	111.1(5)
Cl(3)-C(2)-C(1)	106.4(6)	O(3)-C(3)-O(4)	126.6(6)
O(3)-C(3)-C(4)	112.2(5)	O(4)-C(3)-C(4)	121.2(6)
Cl(4)-C(4)-Cl(5)	108.2(5)	Cl(4)-C(4)-Cl(6)	109.5(4)
Cl(5)-C(4)-Cl(6)	109.4(4)	Cl(4)-C(4)-C(3)	112.9(5)
Cl(5)-C(4)-C(3)	109.5(4)	Cl(6)-C(4)-C(3)	107.3(6)
Te(1)-C(5)-C(6)	119.2(5)	Te(1)-C(5)-C(10)	120.7(4)
C(6)-C(5)-C(10)	120.2(6)	C(5)-C(6)-C(7)	119.2(7)
C(6)-C(7)-C(8)	120.4(6)	C(7)-C(8)-C(9)	120.4(8)
C(8)-C(9)-C(10)	119.8(8)	C(5)-C(10)-C(9)	120.1(5)
Te(2)-C(11)-C(12)	117.9(4)	Te(2)-C(11)-C(16)	120.3(6)
C(12)-C(11)-C(16)	121.6(7)	C(11)-C(12)-C(13)	117.3(8)
C(12)-C(13)-C(14)	121.4(12)	C(13)-C(14)-C(15)	121.3(9)
C(14)-C(15)-C(16)	119.3(8)	C(11)-C(16)-C(15)	119.1(9)



**Table 3.8:** Infra-red ( $\text{cm}^{-1}$ ) and  $^1\text{H}$ -n.m.r. (ppm) data

M,R	$\nu_{asym}$	$\nu_{symm}$	$\Delta\nu$	Int	$\delta$
Sn,CH <sub>3</sub> [6]	1610	1335	265	10,5.8	7.5-8.0,2.0
Sn,CH <sub>2</sub> Cl [7]	1620	1240	380	10,3.8	7.5-8.0,4.2
Sn,CHCl <sub>2</sub>	1670	1330	340	10,1.7	7.5-8.0,6.1
Te,CH <sub>3</sub>	1640 <sup>a</sup>	1290 <sup>a</sup>	350	10,6.0	7.5-8.0,2.0
Te,CHCl <sub>2</sub>	1660 <sup>a</sup>	1310 <sup>a</sup>	350	10,2.0	7.5-8.0,5.9
Te,CCl <sub>3</sub> [8]	1705	1270 <sup>a</sup>	435	-	7.5-8.0

a - average

## References

- 1) A. Cahours, *Ann.*, 1860, **114**, 354.
- 2) P. Kulmiz, *J. Prakt. Chem.*, 1860, **80**, 60.
- 3) Y. Maeda, R. Okawara, *J. Organomet. Chem.*, 1967, **10**, 247.
- 4) P.J. Smith, *Organomet. Chem. Rev. (A)*, 1970, **5**, 373.
- 5) T.N. Mitchell, *J. Organomet. Chem.*, 1973, **59**, 189.
- 6) W. McFarlane, J.C. Maire, M. Delmas, *J. Chem. Soc., Dalton*, 1972, 1862.
- 7) A.G. Davies, P.G. Harrison, J.D. Kennedy, T.N. Mitchell, R.J. Puddephatt, W. McFarlane, *J. Chem. Soc. (C)*, 1969, 1136.
- 8a) M. Yokoo, J. Ogura, T. Kanzawa, *J. Polymer Science (B)*, 1967, **5**, 57.
- 8b) C.J. Evans, S. Karpel, *J. Organomet. Chem. Libr.*, 1985, **16**, 1.
- 9) T.P. Lockhart, J.C. Calabrese, F. Davidson, *Organomet.*, 1987, **6**, 2479.
- 10) S.P. Narula, S.K. Bharadwaj, *Proceedings of the 6th ICOCC of Ge, Sn and Pb*, Brussels, 1989.
- 11) R.H. Vernon, *J. Chem. Soc.*, 1920, **117**, 86.
- 12) H.D.K. Drew, *J. Chem. Soc.*, 1926, 3069.
- 13) S.B. Bulgarevich, B.B. Rivkin, N.G. Furmanova, O.O. Exner, D. Ya Movshovich, T.A. Yusman, I.D. Sadekov, V.I. Minkin, *J. Structural Chem.*, 1984, **25**, 85.

- 14) N.W. Alcock, W.D. Harrison, C. Howes, *J. Chem. Soc., Dalton*, 1984, 1709.
- 15) G.B. Deacon, R.J. Phillips, *Coord. Chem. Rev.*, 1980, **33**, 227.
- 16) A. Bondi, *J. Phys. Chem.*, 1964, **68**, 441.
- 17) J. Hilton, E.K. Nunn, S.C. Wallwork, *J. Chem. Soc., Dalton*, 1973, 173.
- 18) N.W. Alcock, J.F. Sawyer, *J. Chem. Soc., Dalton*, 1977, 1090.
- 19) P.T. Greene, R.F. Bryan, *J. Chem. Soc. (A)*, 1971, 2549.
- 20) R.J. Gillespie (1972). *Molecular Geometry*, Van Nostrand-Reinhold, Princeton, New Jersey.
- 21) E. Shustorovich, P.A. Dobosh, *J. Am. Chem. Soc.*, 1979, **101**, 4090.
- 22) M.G.B. Drew, J.M. Kisenyi, G.R. Willey, *J. Chem. Soc., Dalton*, 1982, 1729.
- 23) M. Schmidt, R. Bender, Ch. Burschken, *Z. Anorg. Allg. Chem.*, 1979, **454**, 160.
- 24) G.M. Sheldrick (1983). *SHELXTL Users Manual*, Nicolet XRD Corporation, Madison, Wisconsin.
- 25) *International Tables for X-ray Crystallography* (1974). Vol. IV. Birmingham: Kynoch Press. (Present distributor D. Reidel, Dordrecht.)

## CHAPTER 4

### The Crystal Structure of Three Diphenyltellurium(IV) Bisdithiocarbamates

#### 4.1 Introduction

Relatively few complexes have been studied with Te(IV) and S-donor ligands, though much has been done with Te(II) dithiocarbamates and related compounds due to their use industrially for the stabilisation of rubber<sup>1</sup>. The first diorgano tellurium bis-dithiocarbamate was synthesised in 1979 by Srivastava et al.<sup>2</sup>. Structurally only eighteen Te(IV) compounds have been characterised with bidentate sulphur ligands and of these only two,  $\text{Me}_2\text{Te}(\text{S}_2\text{COMe})_2$ <sup>3</sup> and  $\text{Ph}_2\text{Te}(\text{S}_2\text{P}(\text{OMe})_2)_2$ <sup>4</sup>, are diorgano compounds. The xanthate complex forms a pentagonal bipyramidal structure around the central tellurium via a secondary bond to a neighbouring sulphur. This is similar in structure to its halo analogues,  $\text{I}_2\text{Te}(\text{S}_2\text{CN}(\text{EtOH})_2)_2$ <sup>5</sup> and  $\text{Br}_2\text{Te}(\text{S}_2\text{CNEt}_2)_2$ <sup>6</sup>, which also form seven coordinate systems. The phosphinate complex is a monomeric six coordinate structure, probably due to the more bulky ligands. One aryl tellurium dithiocarbamate complex has been reported,  $\text{PhTe}(\text{S}_2\text{CNEt}_2)_3$ <sup>7</sup> which exists in the solid state as a pentagonal bipyramidal structure with a non-sterically active lone pair. The phenyl group has a very strong trans effect. Several diorganotin bis-dithiocarbamates structures have been published<sup>8-11</sup>, these all having distorted octahedral geometries, with the sulphur atoms in the equatorial plane. Thus, it was of interest to extend the knowledge about  $\text{R}_2\text{Te}(\text{dithiocarbamate})_2$  complexes and compare them with their tin analogues and, to this end, three diphenyltellurium bisdithiocarbamates have been synthesised and characterised. They include the N,N-diethyl, [9], the N-ethyl-N-phenyl, [10] and the N,N-diphenyl, [11], dithiocarbamate complexes.

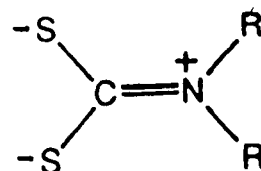
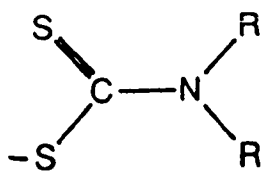
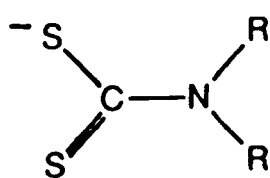
#### 4.2 Results and Discussion

Structures [9], [10] and [11] all have the same geometry around the tellurium. Their structures are very similar to that of [8],  $\text{Ph}_2\text{Te}(\text{OCOCCl}_3)_2$  (Chapter 3), but these complexes form monomers (Figures 4.1, 4.3 and 4.5). The geometry can be thought of in two ways. Firstly, as in [8], as a distorted octahedral complex, where the lone pair is sterically inactive and the dithiocarbamates are bidentate, or secondly, as a distorted trigonal bipyramid with a lone pair and

unidentate dithiocarbamates. In [8] the former description was preferred due to the fact that dimerisation prevented the lone pair from being active. Here this restriction no longer holds, the nearest intermolecular Te-S contact being 5.459Å for [9], and the geometry is probably best described as a mixture of both possibilities, i.e. a partially active lone pair.

If the lone pair were present and the complex five coordinate, the C-Te-C angle would be expected to be near 120°, since the sulphur atoms should take up the axial positions of the trigonal bipyramidal geometry. In fact the angles are near 90° (89.0(1), 95.1(2) and 96.7(8) for [9], [10] and [11] respectively). Also the lone pair would be expected to push the secondary bonded sulphurs further away from the tellurium center, due to repulsive electronic effects. The furthest away though (3.214Å, Table 4.8) is still well below the Van der Waals distance (Te-S=3.86Å)<sup>12</sup>. If the former explanation is closer to the truth, i.e. the lone pair is non-stereo active, then the second sulphur would be expected to be trans to a phenyl group. This is indeed the case, with the maximum mean deviation from the plane S-C-S-Te-C (Table 4.9) being just under 0.1Å in [9]. In the absence of electronic interactions, then there would be no reason for the sulphur to lie on or near this plane. The distortion from octahedral geometry arises purely from the secondary bonded sulphur atoms not being in the equatorial plane, which is a consequence of the small bite angle of a four membered chelate ring. A further indication of the lack of lone pair involvement comes from the fact that the tellurium compounds would be expected to adopt a similar geometry to their tin analogues if the lone pair were not sterically active. This is indeed the case with the tin compounds forming distorted octahedral complexes, but with the S-atoms in the equatorial plane and the R-groups axial.

The dithiocarbamate ligands are anisobidentate, with the difference in C-S bond lengths ranging between 0.058Å for [10] to 0.105Å for [11]. This indicates that the ligand C-S  $\pi$ -electron density is not fully delocalised but has some modest single and double bond character. This is usual for main group compounds, with the shorter M-S bond being associated with the longer C-S bond, and vice versa. Transition and f-block complexes tend to have isobidentate chelation of the dithiocarbamates. The bonding in the ligand can be thought of in terms of a simple valence bond description<sup>13,14</sup>. This accounts for the short C-N bond usually seen in the dithiocarbamates.



The partial double bond character between the C and N should also keep the  $\text{NCS}_2$  group planar, and the maximum deviation found is only  $0.0091\text{\AA}$  for [11] (Table 4.9). The largest deviation is expected in [11] since electronegative groups attached to the N will cause the lone pair on the N to become less available. This is supported by the C-N bond lengths where the distances for [9] and [10] are approximately equal, and both are shorter than for [11] (Table 4.8). The C-S1 and C-S2 bond lengths are within the ranges reported by Holt et al.<sup>15</sup> for a variety of dithiocarbamate complexes.

Figures 4.2, 4.4 and 4.6 show the packing diagrams for [9], [10] and [11]. Figures 4.4 and 4.6 show the disordered solvent in the lattice and also the phenyl-phenyl interactions in the cell.

### **4.3 Experimental**

#### **4.3.1 Preparation Of Compounds**

##### **Diphenyl Tellurium Dichloride**

$\text{TeCl}_4$  (3.8g, 0.014moles) and  $\text{Ph}_2\text{Hg}$  (5.0g, 0.014moles) were refluxed in dry benzene ( $100\text{cm}^3$ ) for 24hrs. After this time the solution was hot filtered and removed by rotary evaporation. The product was recrystallised from hot ethanol.

##### **Diethyldithiocarbamate, Potassium salt for [9]**

$\text{K}[\text{S}_2\text{CNET}_2]$  was prepared by the method of Graziani et al<sup>16</sup>. To a mixture of  $\text{CS}_2$  (7.6g, 0.1 moles) and  $\text{H}_2\text{O}$  ( $25\text{cm}^3$ ) containing KOH (5.6g, 0.1 moles) was added dropwise, with cooling and stirring,  $\text{Et}_2\text{NH}$  (7.3g, 0.1 moles). The solution was left stirring for 1.5hrs during which time it turned yellow. The solvent was then removed and the product dried in vacuo.

##### **Ethylphenyldithiocarbamate, Potassium salt for [10]**

The above preparation was followed substituting  $\text{EtPhNH}$  for  $\text{Et}_2\text{NH}$ . The solution turned a pale orange.  $\text{H}_2\text{O}_2$  was added dropwise until no further reaction was visible. A yellow precipitate formed. The solvent was removed under reduced pressure and the solid dried in vacuo.

### **Diphenyldithiocarbamate, Lithium salt for [11]**

Ph<sub>2</sub>NH (1.69g, 0.01 moles) was stirred, under N<sub>2</sub>, in dry hexane (25cm<sup>3</sup>) until dissolved. The solution was cooled in a dry ice/acetone bath and BuLi (6.25cm<sup>3</sup>, 0.01 moles, 1.6M in hexanes) was added dropwise via a syringe. The solution was allowed to warm up to room temperature to react then cooled to -78° again. CS<sub>2</sub> (0.6cm<sup>3</sup>, 0.01 moles) was added slowly and the solution allowed to warm up again. The solution turned yellow. The solvent was removed and the product stored under N<sub>2</sub>.

### **Diphenyl Tellurium Dithiocarbamate**

Ph<sub>2</sub>TeCl<sub>2</sub> (3.52g, 0.01 moles) and the respective dithiocarbamate (0.02 moles) were stirred in acetone for 3hrs. The yellow precipitate was filtered off and recrystallised from hot toluene. The needle crystals were used directly for structure determination.

#### **4.3.2 X-Ray Crystallography**

All data sets were recorded at 293K with Mo-K $\alpha$  radiation at 0.71069Å. Standard reflections were recorded every 200 reflections and showed slight changes (1,4 and 10% for [9], [10] and [11] respectively). The data sets were processed using profile analysis and corrected for Lorentz, polarisation and absorption effects, the last by the Gaussian method. The cell parameters were calculated from 15 reflections with 2 $\theta$  between 20 and 22°. Hydrogen atoms were inserted at calculated positions and not refined, their temperature factors fixed at 0.07Å<sup>2</sup>. Methyl groups were treated as rigid CH<sub>3</sub> units, their initial orientation taken from the strongest peaks on a difference Fourier synthesis. Computing was with SHELXTL<sup>17</sup> on a Data General DG30 for [9] and [10]. [11] was initially refined using SHELXTL then finished using SHELXTL PLUS<sup>18</sup> on a DEC MicroVax II. Scattering factors in the analytical form were taken from International Tables<sup>19</sup>. Crystallographic parameters are in Table 4.1. Atomic coordinates are in Tables 4.2-4.4 and bond lengths and angles in Tables 4.5-4.7 for [9], [10] and [11] respectively. Views of the molecules and packing diagrams are in Figures 4.1-4.6.

### **Diphenyl Tellurium Bis-diethyldithiocarbamate**

Systematic absences,  $hkl$ ;  $h+k=2n+1$  and  $hol$ ;  $h,l=2n+1$ , gave the space group as either  $Cc$  or  $C2/c$ . Analysis of the E-statistics indicated a centrosymmetric space group, the density calculation gave 4 molecules per unit cell and the Patterson synthesis gave the heavy atom position at  $0,y,1/2$ . Thus  $C2/c$  was chosen, and proved correct by good refinement. All non-hydrogen atoms were refined anisotropically.

#### **Diphenyl Tellurium Bis-ethylphenyldithiocarbamate**

Analysis of the data gave no systematic absences indicating the space group to be  $P1$  or  $P\bar{1}$ .  $P\bar{1}$  was chosen on the basis of density calculations and proved correct. All the non-hydrogen atoms were refined anisotropically except for those in the solvent toluene. This was very disordered and was refined at half occupancy. It is centred around  $(1/2, 1/2, 1/2)$ . The remaining electron density is all located around the solvent.

#### **Diphenyl Tellurium Bis-diphenyldithiocarbamate**

Systematic absences  $h0l$ ;  $l=2n+1$  and  $0k0$ ;  $k=2n+1$  gave the space group as  $P2_1/c$ . All the non-hydrogen atoms except C31 and solvent molecules were refined anisotropically. The solvent toluenes were disordered and were refined as rigid hexagons. The methyl group on the toluene was not located. Residual electron density is located close to the tellurium and the solvent. The high R-factor is probably a consequence of the presence of disordered solvent.



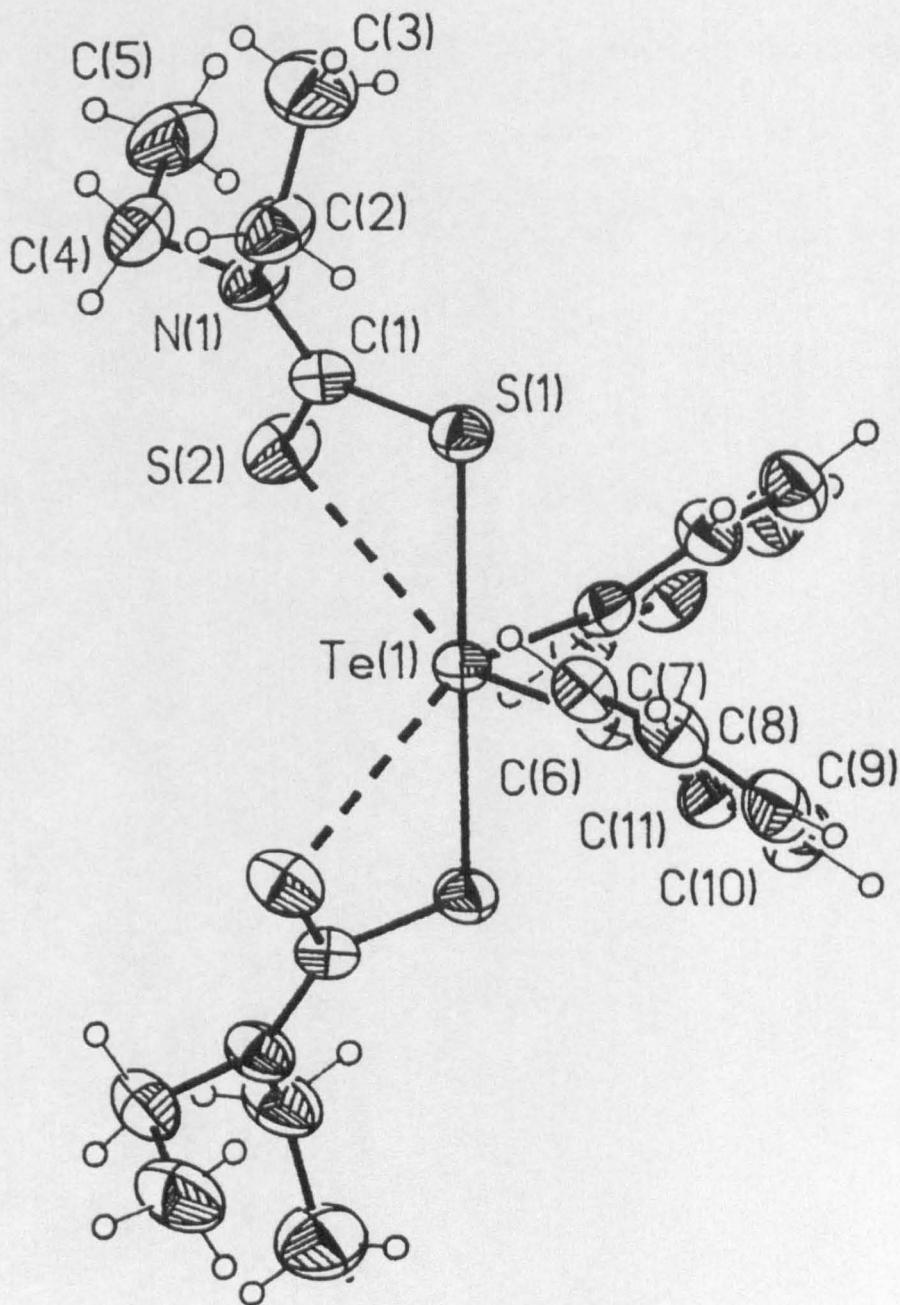


FIGURE 4.1 View of the molecule of [9], showing atomic numbering scheme.

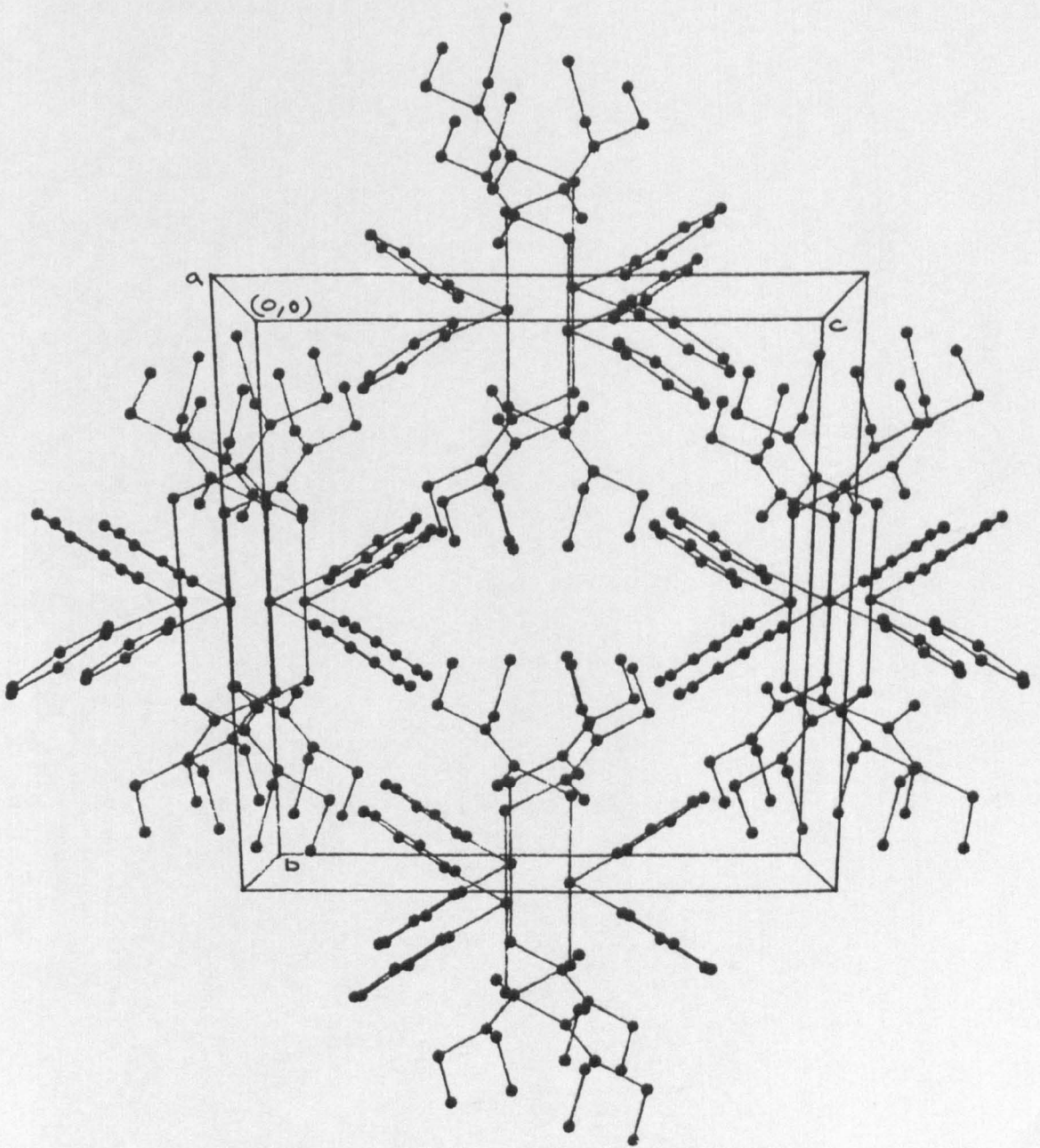


FIGURE 4.2 Packing diagram for [9].

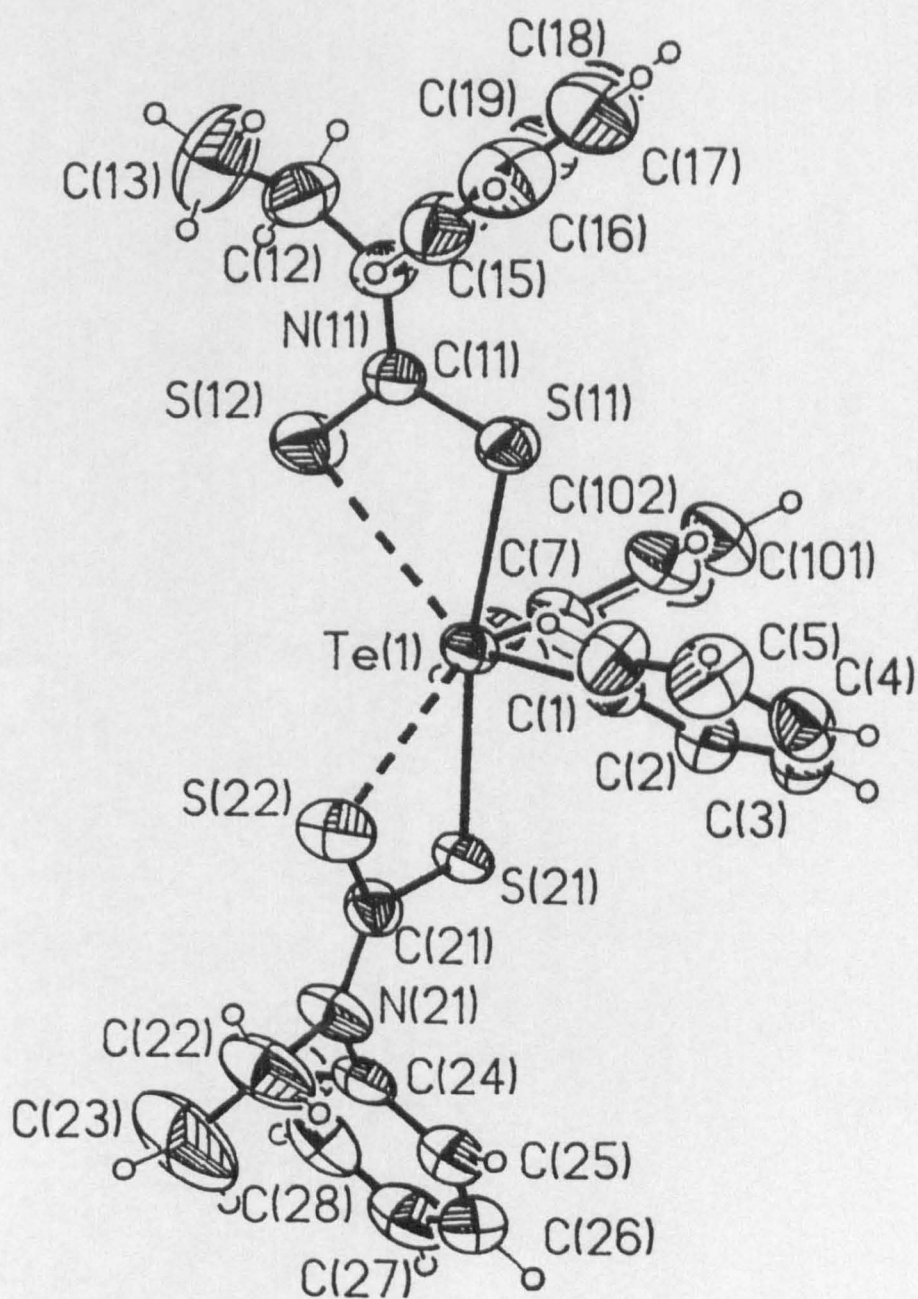


FIGURE 4.3 View of the molecule of [10], showing atomic numbering scheme.



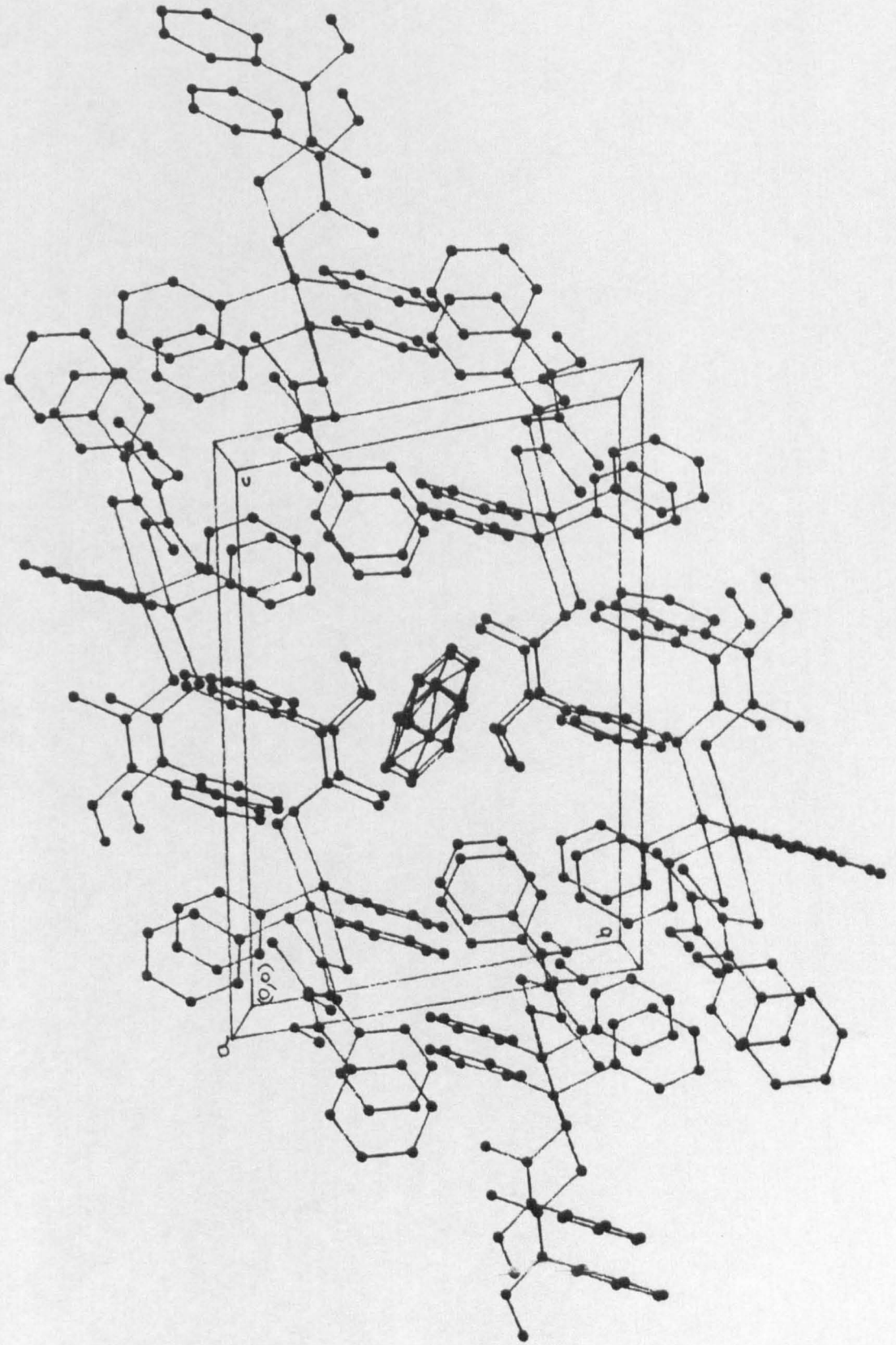


FIGURE 4.4 Packing diagram for [10].

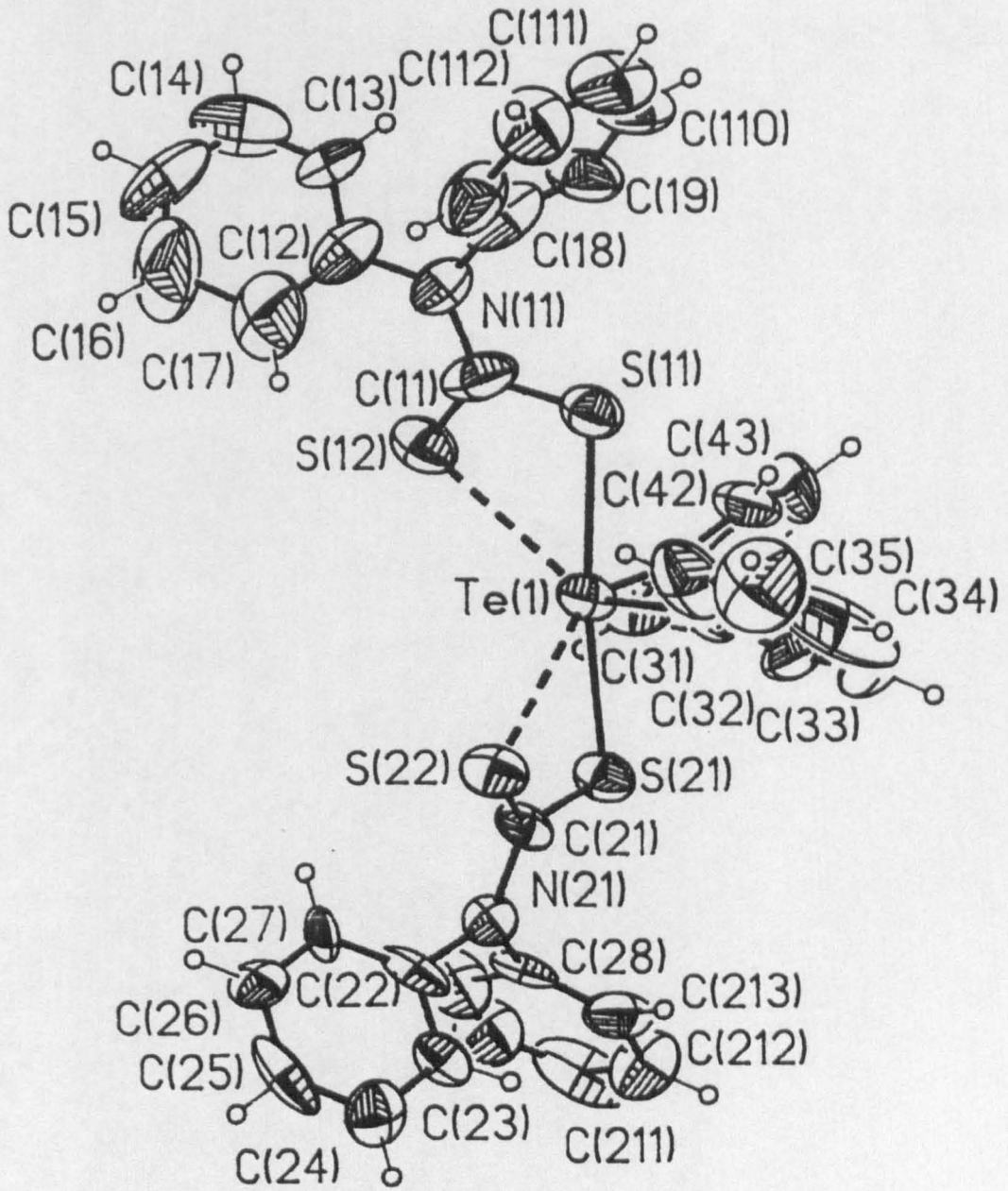


FIGURE 4.5 View of the molecule of [11], showing atomic numbering scheme.

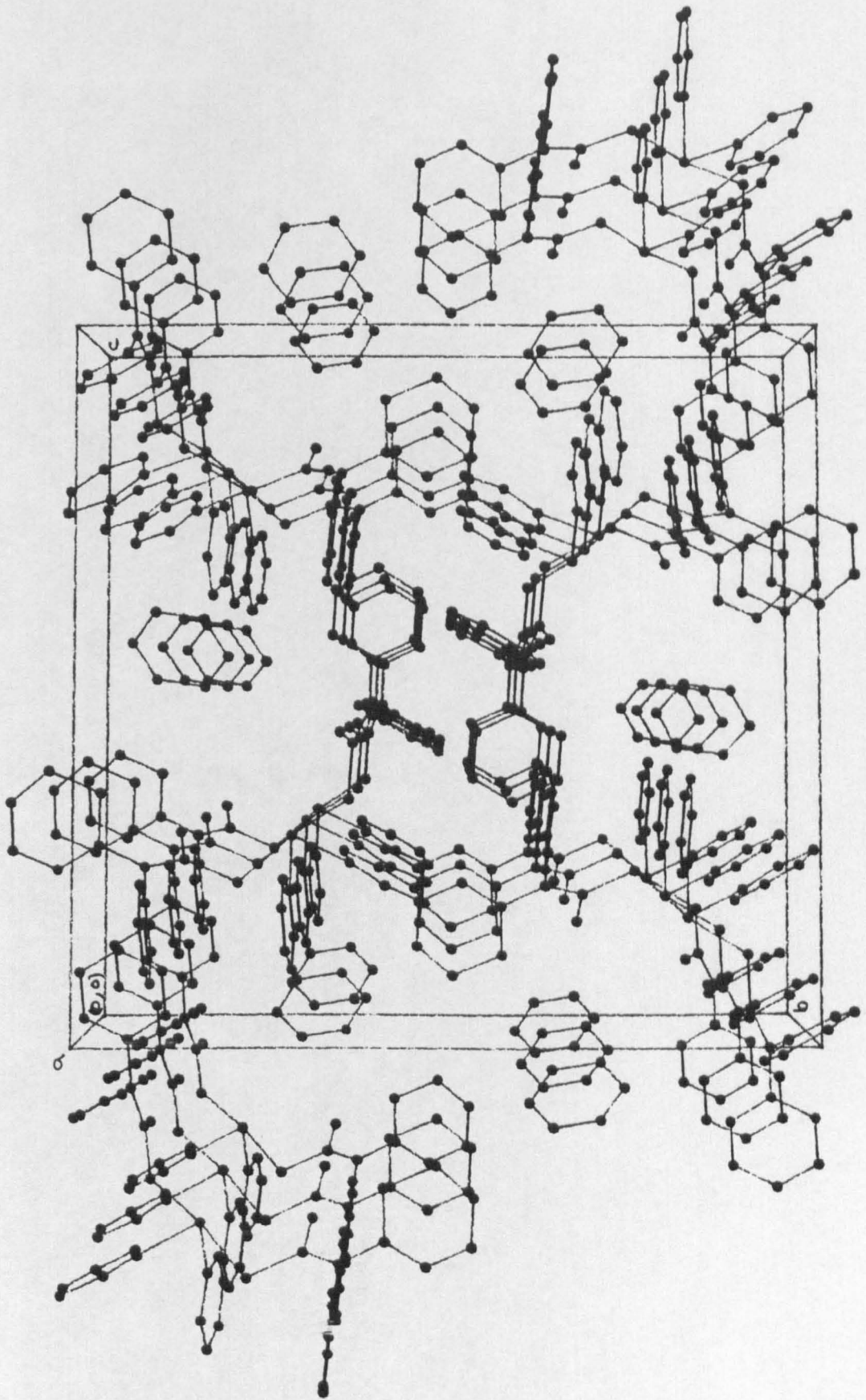


FIGURE 4.6 Packing diagram for [11].

**Table 4.1: Crystal data and data collection parameters**

<b>Compound</b>	<b>[9]</b>	<b>[10]</b>	<b>[11]</b>
Formula	$C_{22}H_{30}N_2ClS_4Te$	$C_{30}H_{30}N_2S_4Te \cdot 0.5C_7H_8$	$C_{38}H_{30}N_2S_4Te \cdot 2C_7H_8$
Mass	578.34	720.49	954.79
$D_{calc.}$ ( $gcm^{-3}$ )	1.56	1.42	1.37
Z	4	2	4
Crystal System	Monoclinic	Triclinic	Monoclinic
Systematic Absences	hkl $h+k=2n+1$ h0l $h,l=2n+1$	none	h0l $l=2n+1$ 0k0 $k=2n+1$
Space Group	C2/c	$P\bar{1}$	$P2_1/c$
a(Å)	16.538(5)	9.804(2)	9.613(2)
b(Å)	14.380(4)	11.156(3)	22.453(7)
c(Å)	12.169(3)	16.274(5)	21.552(7)
$\alpha$ (°)	-	79.33(2)	-
$\beta$ (°)	121.57(2)	74.46(2)	93.92(2)
$\gamma$ (°)	-	84.48(2)	-
U(Å <sup>3</sup> )	2465.6(1.3)	1683.2(0.7)	4637.5(2.4)
$\mu$ ( $cm^{-1}$ )	15.8	11.7	8.7
F(000)	1168	716	1952
Crystal Size	0.2×0.2×0.6	0.4×0.2×0.2	0.4×0.2×0.2
Max. Trans.	0.8272	0.9313	0.9361
Min. Trans.	0.7618	0.8622	0.8845
Scan Range(°)	+/- 1.0	+/- 1.1	+/- 1.1
Scan Rate(°min <sup>-1</sup> )	4.0	3.0	3.0
Max. 2 $\theta$ (°)	50	50	50
Refs. Collected	2350	5972	6179
Refs. Observed	1854	4014	2863
R(final)	0.0255	0.0454	0.0908
$R_w$	0.0277	0.0459	0.0939
g	0.00039	0.00083	0.00284
Max. on final Fourier	+/- 0.35	+/- 0.5	+/- 1.5
Max. $\delta/\sigma$	0.001	0.006	0.006
No. of Parameters	138	352	421

TABLE 4.2

Atomic coordinates ( $\times 10^4$ ) for [9] (with standard deviations in parentheses).

atom	x	y	z	U
Te(1)	00.0	5529.4(2)	7500.0	32(1)*
S(1)	-1589.0(6)	5545.0(6)	7480.2(8)	40(1)*
S(2)	-1667.6(7)	4268.9(7)	5493.1(9)	51(1)*
N(1)	-2727(2)	4075(2)	6525(3)	46(1)*
C(1)	-2061(2)	4565(2)	6470(3)	38(1)*
C(2)	-2998(3)	4234(3)	7491(4)	61(2)*
C(3)	-3999(3)	4505(3)	6906(6)	85(3)*
C(4)	-3156(3)	3247(3)	5699(4)	55(2)*
C(5)	-3895(3)	3487(3)	4314(4)	77(2)*
C(6)	515(2)	6547(2)	9006(3)	37(1)*
C(7)	379(2)	6396(2)	10021(3)	44(2)*
C(8)	767(3)	7015(3)	11047(3)	52(2)*
C(9)	1288(3)	7764(3)	11061(4)	55(2)*
C(10)	1418(3)	7916(3)	10049(4)	57(2)*
C(11)	1032(2)	7301(2)	9019(3)	47(2)*

\* Equivalent isotropic U defined as one third of the trace of the orthogonalised  $U_{ij}$  tensor.



TABLE 4.3

Atomic coordinates ( $\times 10^4$ ) for [10] (with standard deviations in parentheses).

atom	x	y	z	U
Te(1)	2057.6(4)	2062.3(3)	2134.6(2)	46(1)*
S(11)	2530.9(20)	1340.6(14)	3643.9(10)	59(1)*
S(12)	778.7(24)	3685.7(16)	3618.1(12)	77(1)*
S(21)	1958.3(16)	2634.2(14)	496.5(9)	47(1)*
S(22)	-386.3(21)	1030.6(17)	1565.4(11)	69(1)*
N(11)	1492(6)	2398(4)	4995(3)	59(2)*
N(21)	-159(5)	2127(5)	-54(3)	62(2)*
C(1)	3308(7)	439(5)	1857(4)	49(2)*
C(2)	4512(7)	445(5)	1190(4)	55(3)*
C(3)	5339(8)	-621(6)	1074(5)	69(3)*
C(4)	4944(8)	-1685(6)	1614(5)	71(3)*
C(5)	3731(9)	-1719(6)	2266(5)	86(4)*
C(6)	2894(8)	-644(5)	2397(4)	69(3)*
C(7)	3808(6)	3214(5)	1748(4)	48(2)*
C(8)	3614(7)	4410(5)	1354(4)	66(3)*
C(9)	4741(8)	5179(6)	1094(5)	79(4)*
C(10)	6025(8)	4784(6)	1252(5)	74(3)*
C(101)	6210(8)	3608(6)	1650(5)	74(3)*
C(102)	5102(7)	2814(6)	1902(4)	62(3)*
C(11)	1546(7)	2504(5)	4155(4)	53(2)*
C(12)	829(9)	3355(6)	5515(4)	77(3)*
C(13)	-436(10)	2950(8)	6170(7)	125(5)*
C(14)	2112(7)	1337(6)	5445(4)	63(3)*
C(15)	1404(9)	295(6)	5725(4)	77(3)*
C(16)	1984(11)	-728(7)	6160(5)	105(4)*
C(17)	3254(11)	-666(8)	6325(5)	120(5)*
C(18)	3922(10)	382(9)	6065(5)	119(5)*
C(19)	3379(8)	1441(7)	5615(5)	83(4)*
C(21)	390(6)	1920(5)	629(4)	49(2)*
C(22)	-1402(9)	1476(8)	-63(6)	103(5)*
C(23)	-2352(11)	2054(11)	-463(7)	152(7)*
C(24)	472(7)	2894(5)	-848(4)	52(2)*
C(25)	1351(7)	2390(6)	-1520(4)	67(3)*
C(26)	1883(8)	3141(8)	-2301(4)	83(4)*
C(27)	1538(9)	4375(8)	-2401(5)	79(4)*
C(28)	672(8)	4857(7)	-1728(5)	73(3)*
C(29)	129(7)	4132(5)	-950(4)	60(3)*
C(001)	6087(15)	4231(15)	5005(11)	190(19)
C(002)	5199(15)	5099(15)	5434(11)	106(6)
C(003)	4058(15)	5662(15)	5126(11)	129(12)
C(004)	3805(15)	5357(15)	4388(11)	143(8)
C(005)	4692(15)	4489(15)	3959(11)	111(6)
C(006)	5833(15)	3926(15)	4268(11)	142(8)

\* Equivalent isotropic U defined as one third of the trace of the orthogonalised  $U_{ij}$  tensor.

TABLE 4.4

Atomic coordinates ( $\times 10^4$ ) for [11] (with standard deviations in parentheses).

	x	y	z	U(eq)
Te	4501.1(1.4)	6938.5(6)	6953.5(6)	59.6(5)
S(11)	2726(6)	7575(3)	7536(3)	71(2)
S(12)	4697(6)	8356(3)	6909(3)	76(2)
S(21)	6350(5)	6236(2)	6512(2)	60(2)
S(22)	3868(5)	6326(3)	5612(2)	63(2)
N(11)	2301(18)	8708(8)	7312(8)	64(7)
N(21)	6350(14)	5968(6)	5330(6)	47(6)
C(11)	3226(23)	8259(9)	7238(9)	71(9)
C(12)	2341(22)	9272(12)	7032(13)	80(11)
C(13)	2311(20)	9787(11)	7328(11)	67(9)
C(14)	2277(27)	10322(13)	7058(15)	100(13)
C(15)	2228(36)	10338(13)	6430(19)	142(18)
C(16)	2247(46)	9857(17)	6083(15)	195(24)
C(17)	2321(33)	9292(13)	6385(15)	132(16)
C(18)	1137(24)	8653(10)	7691(12)	71(10)
C(19)	1418(24)	8590(11)	8314(12)	88(11)
C(110)	265(30)	8568(11)	8676(14)	114(13)
C(111)	-1073(32)	8571(13)	8466(18)	132(17)
C(112)	-1287(26)	8659(13)	7819(18)	130(16)
C(113)	-198(26)	8676(10)	7445(14)	98(12)
C(21)	5526(18)	6176(8)	5771(8)	51(7)
C(22)	5908(17)	5929(10)	4686(8)	46(7)
C(23)	5914(18)	5382(9)	4395(9)	52(8)
C(24)	5602(20)	5319(11)	3764(11)	68(9)
C(25)	5296(21)	5841(13)	3454(9)	72(10)
C(26)	5236(18)	6392(10)	3728(10)	60(8)
C(27)	5583(19)	6437(9)	4350(9)	54(8)
C(28)	7814(20)	5806(10)	5489(8)	55(8)
C(29)	8873(21)	6143(11)	5300(9)	79(10)
C(210)	10225(22)	5961(16)	5433(11)	98(13)
C(211)	10541(23)	5449(17)	5753(12)	102(15)
C(212)	9488(31)	5103(12)	5915(11)	95(12)
C(213)	8069(25)	5256(11)	5791(10)	77(10)
C(31)	3392(22)	6184(9)	7289(9)	49(5)
C(32)	4016(24)	5758(10)	7582(10)	71(9)
C(33)	3339(43)	5284(16)	7794(17)	131(18)
C(34)	1946(63)	5252(16)	7667(19)	175(28)
C(35)	1302(36)	5714(19)	7383(16)	142(19)
C(36)	1954(32)	6187(15)	7139(10)	108(14)
C(41)	6020(24)	7003(9)	7731(10)	70(9)
C(42)	5589(25)	6904(10)	8331(10)	80(9)
C(43)	6619(31)	6963(11)	8810(10)	79(10)
C(44)	7966(36)	7061(11)	8710(17)	108(15)
C(45)	8367(29)	7145(12)	8119(14)	102(13)
C(46)	7360(23)	7111(9)	7637(11)	71(9)

**TABLE 4.4 cont.**

C(61)	6244 (36)	1933 (24)	4980 (13)	232 (19)
C(62)	7162	2274	5363	237 (20)
C(63)	7952	2005	5853	226 (19)
C(64)	7824	1395	5960	206 (17)
C(65)	6905	1054	5578	278 (25)
C(66)	6115	1323	5087	341 (32)
C(71)	37 (50)	2168 (25)	4320 (22)	283 (25)
C(72)	1260	2336	4053	292 (27)
C(73)	2403	1951	4081	276 (24)
C(74)	2323	1400	4374	415 (39)
C(75)	1100	1232	4641	299 (27)
C(76)	-43	1616	4613	254 (22)

\* Equivalent isotropic U defined as one third of the trace of the  
orthogonalised  $U_{ij}$  tensor.

**TABLE 4.5**

**Bond lengths (Å) and angles (°) for [9]**

(standard deviations in parentheses).

**a) Bond lengths**

Te(1)-S(1)	2.165(1)	Te(1)-S(2)	3.130(1)
Te(1)-C(6)	2.143(3)	S(1)-C(1)	1.761(3)
S(2)-C(1)	1.682(4)	N(1)-C(1)	1.338(5)
N(1)-C(2)	1.478(7)	N(1)-C(4)	1.479(4)
C(2)-C(3)	1.473(7)	C(4)-C(5)	1.515(5)
C(6)-C(7)	1.383(6)	C(6)-C(11)	1.376(5)
C(7)-C(8)	1.387(5)	C(8)-C(9)	1.374(6)
C(9)-C(10)	1.374(7)	C(10)-C(11)	1.386(5)

**b) Bond angles**

S(1)-Te(1)-S(2)	61.8(1)	S(1)-Te(1)-C(6)	87.1(1)
S(2)-Te(1)-C(6)	148.9(1)	S(1)-Te(1)-S(1a)	179.0(1)
S(2)-Te(1)-S(1a)	118.8(1)	C(6)-Te(1)-S(1a)	92.3(1)
S(2)-Te(1)-S(2a)	109.2(1)	C(6)-Te(1)-S(2a)	86.3(1)
C(6)-Te(1)-C(6a)	93.9(2)	Te(1)-S(1)-C(1)	94.3(1)
Te(1)-S(2)-C(1)	79.1(1)	C(1)-N(1)-C(2)	123.9(3)
C(1)-N(1)-C(4)	120.3(4)	C(2)-N(1)-C(4)	115.3(3)
S(1)-C(1)-S(2)	120.1(2)	S(1)-C(1)-N(1)	117.5(3)
S(2)-C(1)-N(1)	122.4(3)	N(1)-C(2)-C(3)	113.0(4)
N(1)-C(4)-C(5)	113.1(3)	Te(1)-C(6)-C(7)	118.6(2)
Te(1)-C(6)-C(11)	120.9(3)	C(7)-C(6)-C(11)	120.3(3)
C(6)-C(7)-C(8)	119.3(3)	C(7)-C(8)-C(9)	120.3(4)
C(8)-C(9)-C(10)	120.3(3)	C(9)-C(10)-C(11)	119.7(4)
C(6)-C(11)-C(10)	120.1(4)		

**PAGE  
MISSING  
IN  
ORIGINAL**

TABLE 4.6

## Bond lengths (Å) and angles (°) for [10]

(standard deviations in parentheses).

## a) Bond lengths

Te(1)-S(11)	2.588(2)	Te(1)-S(21)	2.649(2)
Te(1)-C(1)	2.137(6)	Te(1)-C(7)	2.130(6)
S(11)-C(11)	1.744(6)	S(12)-C(11)	1.673(6)
S(21)-C(21)	1.743(7)	S(22)-C(21)	1.687(5)
N(11)-C(11)	1.337(8)	N(11)-C(12)	1.478(9)
N(11)-C(14)	1.444(8)	N(21)-C(21)	1.334(9)
N(21)-C(22)	1.482(11)	N(21)-C(24)	1.431(7)
C(1)-C(2)	1.372(8)	C(1)-C(6)	1.381(8)
C(2)-C(3)	1.387(9)	C(3)-C(4)	1.360(9)
C(4)-C(5)	1.364(10)	C(5)-C(6)	1.402(9)
C(7)-C(8)	1.388(8)	C(7)-C(102)	1.374(10)
C(8)-C(9)	1.391(10)	C(9)-C(10)	1.367(12)
C(10)-C(101)	1.370(9)	C(101)-C(102)	1.394(10)
C(12)-C(13)	1.449(11)	C(14)-C(15)	1.353(10)
C(14)-C(19)	1.363(12)	C(15)-C(16)	1.384(11)
C(16)-C(17)	1.352(15)	C(17)-C(18)	1.339(14)
C(18)-C(19)	1.408(12)	C(22)-C(23)	1.328(15)
C(24)-C(25)	1.372(9)	C(24)-C(29)	1.380(8)
C(25)-C(26)	1.387(9)	C(26)-C(27)	1.376(12)
C(27)-C(28)	1.357(11)	C(28)-C(29)	1.372(9)

## b) Bond angles

S(11)-Te(1)-S(21)	171.2(1)	S(11)-Te(1)-C(1)	82.4(2)
S(21)-Te(1)-C(1)	90.0(2)	S(11)-Te(1)-C(7)	91.3(2)
S(21)-Te(1)-C(7)	84.9(2)	C(1)-Te(1)-C(7)	95.0(2)
Te(1)-S(11)-C(11)	97.9(2)	Te(1)-S(21)-C(21)	96.1(2)
C(11)-N(11)-C(12)	122.7(5)	C(11)-N(11)-C(14)	121.3(5)
C(12)-N(11)-C(14)	116.0(5)	C(21)-N(21)-C(22)	121.4(5)
C(21)-N(21)-C(24)	123.0(6)	C(22)-N(21)-C(24)	115.4(6)
Te(1)-C(1)-C(2)	122.7(4)	Te(1)-C(1)-C(6)	117.6(4)
C(2)-C(1)-C(6)	119.6(5)	C(1)-C(2)-C(3)	120.5(5)
C(2)-C(3)-C(4)	119.9(6)	C(3)-C(4)-C(5)	120.6(6)
C(4)-C(5)-C(6)	120.0(6)	C(1)-C(6)-C(5)	119.3(6)
Te(1)-C(7)-C(8)	118.6(5)	Te(1)-C(7)-C(102)	121.8(4)
C(8)-C(7)-C(102)	119.5(6)	C(7)-C(8)-C(9)	119.7(7)
C(8)-C(9)-C(10)	120.7(6)	C(9)-C(10)-C(101)	119.5(7)
C(10)-C(101)-C(102)	120.7(7)	C(7)-C(102)-C(101)	119.8(6)
S(11)-C(11)-S(12)	122.0(4)	S(11)-C(11)-N(11)	115.0(4)
S(12)-C(11)-N(11)	123.0(5)	N(11)-C(12)-C(13)	111.9(7)
N(11)-C(14)-C(15)	120.1(7)	N(11)-C(14)-C(19)	118.2(6)
C(15)-C(14)-C(19)	121.7(7)	C(14)-C(15)-C(16)	120.6(8)
C(15)-C(16)-C(17)	119.3(8)	C(16)-C(17)-C(18)	119.3(9)
C(17)-C(18)-C(19)	123.4(10)	C(14)-C(19)-C(18)	115.6(8)
S(21)-C(21)-S(22)	122.0(4)	S(21)-C(21)-N(21)	115.8(4)
S(22)-C(21)-N(21)	122.2(5)	N(21)-C(22)-C(23)	119.5(8)
N(21)-C(24)-C(25)	120.1(5)	N(21)-C(24)-C(29)	119.6(5)
C(25)-C(24)-C(29)	120.3(5)	C(24)-C(25)-C(26)	119.1(7)
C(25)-C(26)-C(27)	120.5(7)	C(26)-C(27)-C(28)	119.6(7)
C(27)-C(28)-C(29)	121.0(7)	C(24)-C(29)-C(28)	119.6(6)

TABLE 4.7

## Bond lengths (Å) and angles (°) for [11]

(standard deviations in parentheses).

## a) Bond lengths

Te-S(11)	2.612 (6)	Te-S(21)	2.603 (5)
Te-C(31)	2.152 (20)	Te-C(41)	2.151 (21)
S(11)-C(11)	1.744 (21)	S(12)-C(11)	1.639 (23)
S(21)-C(21)	1.739 (17)	S(22)-C(21)	1.642 (18)
N(11)-C(11)	1.361 (28)	N(11)-C(12)	1.403 (32)
N(11)-C(18)	1.435 (30)	N(21)-C(21)	1.361 (23)
N(21)-C(22)	1.426 (22)	N(21)-C(28)	1.470 (24)
C(12)-C(13)	1.323 (36)	C(12)-C(17)	1.393 (42)
C(13)-C(14)	1.332 (39)	C(14)-C(15)	1.351 (53)
C(15)-C(16)	1.313 (48)	C(16)-C(17)	1.424 (47)
C(18)-C(19)	1.357 (37)	C(18)-C(113)	1.356 (34)
C(19)-C(110)	1.400 (39)	C(110)-C(111)	1.334 (42)
C(111)-C(112)	1.409 (55)	C(112)-C(113)	1.366 (43)
C(22)-C(23)	1.377 (29)	C(22)-C(27)	1.376 (28)
C(23)-C(24)	1.380 (29)	C(24)-C(25)	1.369 (36)
C(25)-C(26)	1.373 (35)	C(26)-C(27)	1.362 (27)
C(28)-C(29)	1.354 (30)	C(28)-C(213)	1.409 (33)
C(29)-C(210)	1.375 (31)	C(210)-C(211)	1.364 (47)
C(211)-C(212)	1.341 (41)	C(212)-C(213)	1.415 (37)
C(31)-C(32)	1.272 (29)	C(31)-C(36)	1.398 (37)
C(32)-C(33)	1.343 (43)	C(33)-C(34)	1.350 (72)
C(34)-C(35)	1.335 (56)	C(35)-C(36)	1.356 (50)
C(41)-C(42)	1.402 (31)	C(41)-C(46)	1.340 (32)
C(42)-C(43)	1.387 (33)	C(43)-C(44)	1.345 (46)
C(44)-C(45)	1.368 (47)	C(45)-C(46)	1.374 (36)

## b) Bond angles

S(11)-Te-S(21)	172.5(2)	S(11)-Te-C(31)	85.1(6)
S(21)-Te-C(31)	90.7(6)	S(11)-Te-C(41)	91.1(6)
S(21)-Te-C(41)	83.2(6)	C(31)-Te-C(41)	96.7(8)
Te-S(11)-C(11)	95.6(8)	Te-S(21)-C(21)	95.9(6)
C(11)-N(11)-C(12)	125.4(18)	C(11)-N(11)-C(18)	122.9(18)
C(12)-N(11)-C(18)	111.7(18)	C(21)-N(21)-C(22)	123.5(14)
C(21)-N(21)-C(28)	121.1(14)	C(22)-N(21)-C(28)	115.3(14)
S(11)-C(11)-S(12)	123.0(13)	S(11)-C(11)-N(11)	114.2(16)
S(12)-C(11)-N(11)	122.8(16)	N(11)-C(12)-C(13)	125.3(24)
N(11)-C(12)-C(17)	117.5(23)	C(13)-C(12)-C(17)	117.0(25)
C(12)-C(13)-C(14)	125.2(26)	C(13)-C(14)-C(15)	117.4(28)
C(14)-C(15)-C(16)	123.2(31)	C(15)-C(16)-C(17)	118.3(30)
C(12)-C(17)-C(16)	118.9(27)	N(11)-C(18)-C(19)	117.5(20)

TABLE 4.7 cont.

N(11)-C(18)-C(113)	121.8(23)	C(19)-C(18)-C(113)	120.6(24)
C(18)-C(19)-C(110)	116.4(22)	C(19)-C(110)-C(111)	126.3(30)
C(110)-C(111)-C(112)	114.1(30)	C(111)-C(112)-C(113)	121.5(26)
C(18)-C(113)-C(112)	120.8(28)	S(21)-C(21)-S(22)	123.4(11)
S(21)-C(21)-N(21)	114.7(12)	S(22)-C(21)-N(21)	121.9(13)
N(21)-C(22)-C(23)	119.3(17)	N(21)-C(22)-C(27)	120.3(17)
C(23)-C(22)-C(27)	120.3(16)	C(22)-C(23)-C(24)	122.3(19)
C(23)-C(24)-C(25)	114.7(21)	C(24)-C(25)-C(26)	125.1(20)
C(25)-C(26)-C(27)	118.3(20)	C(22)-C(27)-C(26)	119.3(19)
N(21)-C(28)-C(29)	121.3(19)	N(21)-C(28)-C(213)	117.2(18)
C(29)-C(28)-C(213)	121.2(20)	C(28)-C(29)-C(210)	119.4(23)
C(29)-C(210)-C(211)	122.1(24)	C(210)-C(211)-C(212)	118.3(23)
C(211)-C(212)-C(213)	123.0(25)	C(28)-C(213)-C(212)	115.8(21)
Te-C(31)-C(32)	122.0(17)	Te-C(31)-C(36)	115.0(17)
C(32)-C(31)-C(36)	122.9(22)	C(31)-C(32)-C(33)	122.7(26)
C(32)-C(33)-C(34)	118.0(32)	C(33)-C(34)-C(35)	118.3(39)
C(34)-C(35)-C(36)	125.0(38)	C(31)-C(36)-C(35)	112.5(26)
Te-C(41)-C(42)	118.7(16)	Te-C(41)-C(46)	120.1(16)
C(42)-C(41)-C(46)	121.1(20)	C(41)-C(42)-C(43)	115.5(22)
C(42)-C(43)-C(44)	122.8(24)	C(43)-C(44)-C(45)	120.5(29)
C(44)-C(45)-C(46)	117.9(26)	C(41)-C(46)-C(45)	122.0(23)



**Table 4.8: Selected bond lengths**

<b>Compound</b>	<b>[9]</b>	<b>[10]</b>	<b>[11]</b>
Te1-S11	2.615(1)	2.589(2)	2.612(6)
Te1-S12	3.130(1)	3.200(2)	3.189(6)
Te1-S21	-	2.650(2)	2.603(5)
Te1-S22	-	3.168(2)	3.214(6)
C11-S11	1.761(3)	1.743(6)	1.744(21)
C11-S12	1.682(4)	1.673(6)	1.639(23)
C21-S21	-	1.744(7)	1.739(17)
C21-S22	-	1.686(5)	1.642(18)
C11-N11	1.338(5)	1.339(8)	1.361(28)
C21-N21	-	1.335(9)	1.361(23)

**Table 4.9: Deviations from mean planes**

<b>Compound</b>	<b>[9]</b>	<b>[10]</b>	<b>[11]</b>
<b>Plane 1</b>	0.0982	0.0455	0.0687
<b>Plane 2</b>	0.0982	0.0202	0.0776
<b>Angle</b>			
<b>between 1,2</b>	76.7	93.6	96.7
<b>Plane 3</b>	0.0014	0.0060	0.0091
<b>Plane 4</b>	0.0014	0.0012	0.0085

## References

- 1) W.C. Cooper, *Tellurium*, New York, Van Nostrand-Reinhold, 1971.
- 2) T.N. Srivastava, R.C. Srivastava, A. Bhargava, *Indian J. Chem. (A)*, 1979, **18**, 236.
- 3) M. Wieber, E. Schmidt, C. Burschka, *Z. Anorg. Allg. Chem.*, 1985, **525**, 127.
- 4) R.K. Chadha, J.E. Drake, N.T. McManus, B.A. Quinlan, A.B. Sarkar, *Organometallics*, 1987, **6**, 813.
- 5) G.V.N. Appa Rao, M Seshasayee, G. Aravamudan, K. Radha, *Acta Cryst. (C)*, 1983, **39**, 1018.
- 6) W. Schnabel, K. Von Deuten, G. Klar, *Cryst. Struct. Commun.*, 1981, **10**, 1405.
- 7) S. Esperas, S. Husebye, *Acta Chem. Scand.*, 1972, **26**, 3293.
- 8) J.S. Morris, E.O. Schlemper, *J. Cryst. Mol. Struct.*, 1979, **9**, 13.
- 9) T.P. Lockhart, W.F. Manders, E.O. Schlemper, J.J. Zuckerman, *J. Am. Chem. Soc.*, 1986, **108**, 4074.
- 10) T. Kimura, N. Yasuaoka, N. Kasai, M. Kakudo, *Bull. Chem. Soc. Japan*, 1972, **45**, 1649.
- 11) T.P. Lockhart, W.F. Manders, E.O. Schlemper, *J. Am. Chem. Soc.*, 1985, **107**, 7451.
- 12) N.W. Alcock, *Adv. Inorg. Chem. Radiochem.*, 1972, **15**, 1.
- 13) G.M. Sheldrick, W.S. Sheldrick, R.F. Dalton, K. Jones, *J. Chem. Soc. (A)*,

1970, 493.

14) G.C. Rout, M. Seshasayee, G. Avaramudan, E. Radha, *Acta Cryst. (C)*, 1984, **40**, 1142.

15) E. Holt, F.A.K. Nasser, A. Wilson Jr., J.J. Zuckerman, *Organometallics*, 1985, **4**, 2073.

16) R. Graziani, B. Zarli, A. Cassol, G. Bombieri, *Inorg. Chem.*, 1970, **9**, 2116.

17) G.M. Sheldrick (1983). *SHELXTL Users Manual*, Nicolet XRD Corporation, Madison, Wisconsin.

18) G.M. Sheldrick (1986). *SHELXTL PLUS Users Manual*, Nicolet XRD Corporation, Madison, Wisconsin.

19) *International Tables for X-ray Crystallography* (1974). Vol. IV. Birmingham: Kynoch Press. (Present distributor D. Reidel, Dordrecht.)

## CHAPTER 5

### The Crystal Structures of Six Hydrolysis Products of Organotin Compounds

#### 5.1 Introduction

Organotin compounds have been known to form cluster compounds, or organostannoxanes, based on Sn-O-Sn bonding since the work of Lambourne<sup>1,2</sup>, who reported condensation products from alkylstannoic acids and carboxylic acids of the form  $[\text{MeSn}(\text{OCOR})(\text{O})]_3$ , where R=Me,  $\text{CHCl}_2$  and  $[\text{MeSn}(\text{OCOR})(\text{O})]_6$ , where R=Et, Pr, <sup>i</sup>Pr. Little work was carried out in this area until the early 1970's when interest picked up again, mainly due to new methods of investigation becoming available, including X-ray diffraction and <sup>119</sup>Sn-n.m.r. The first structure reported was a tetrameric stannoxane from Graziani et al in 1977<sup>3</sup>. Several tetrameric stannoxanes have been determined since then<sup>4-11</sup> and also Holmes et al have synthesised and characterised a range of linear and cyclic hexameric compounds<sup>12,13</sup>. These compounds are usually formed from reactions involving organostannoic acids and organic acids, though tin-carbon cleavage has been mentioned by Peruzzo et al<sup>14</sup> and Poller et al<sup>15</sup>. Holmes et al have also recently studied the structures formed with phosphorus based acids<sup>16</sup>. Interest has also been shown in the correlation of these compounds with Al-N and Fe-S clusters, which has been reviewed by Holmes<sup>17</sup>.

During our investigations into tin chemistry, structures similar to the above mentioned tetramers and hexamers were synthesised. All the compounds shown below were synthesised by dearylation reactions rather from the parent organotin compound, except for [17], a hydroxy-bridged linear tetramer. [12] is the initial dearylation product of  $\text{Ph}_3\text{SnOCOCCl}_3$ , where a phenyl group has been replaced by a hydroxy group. [13] and [14] are tetrameric structural isomers, formed from the condensation of two molecules of [12], followed by dimerisation. [15] and [16] are hexameric tin structures, [15] is linear, while [16] is cyclic. They are formed from further condensation from the tetramers.

Structures [12] to [16] were all formed via a dearylation reaction from the parent tri- or di-phenyl tin. Tin-carbon bond cleavage has been noted before<sup>25,26</sup> and even used by Tagliavini<sup>14</sup> to produce organostannoxanes via the cleavage of the weak tin-vinyl bond. Aryl-tin bonds, though stronger than vinyl-tin, are also susceptible to cleavage, as shown by Ingham<sup>25</sup> and Peruzzo<sup>15</sup>. Cleavage of the bond is normally assumed to occur due to a strong organic acid present, and this

is probably true for the formation of [14] (Scheme 5.1). In the case of [12] the cleavage is most likely due to the action of H<sub>2</sub>O (Scheme 5.2), though it is possible to account for it by means of acid attack (Scheme 5.3). [13] and [16] can also be shown to form easily by the use of hydroxide or water attack rather than acid cleavage (Schemes 5.4 and 5.5), and [15] has been shown to form with [13] in solution. This may also explain why [13] and [14] have different structures, i.e. they were formed by different reaction pathways.

## 5.2 Results and Discussion

[12] is a dimeric unit in the solid state (Figure 5.1), the bridges formed by the hydroxy groups, to form a planar four-centre ring. The geometry of the tin atom is based on a trigonal bipyramid. The distortion arises from the small O11-Sn1-O11A angle (70.7°) in the four membered ring, which also opens up the C-Sn-C angle from 120° to 134.1°. The difference in the Sn-O11 bond lengths is 0.135Å, showing the bridges are almost symmetrical. The acyl oxygen in the carboxylate is involved in a hydrogen bond to the hydroxy hydrogen (O2-H11=1.872Å), to form a six membered ring, with a mean deviation from planarity of 0.11Å. This plane is at an angle of 8.6° to the central four membered ring. The difference in the C-O bond lengths in the carboxylate is small, at only 0.017Å, indicating delocalisation of the double bond.

Several R<sub>2</sub>Sn(X)(Y) structures have been determined. Those containing OH as a ligand<sup>18-21</sup> all crystallised as hydroxy-bridged dimers. Work carried out by Chapman et al<sup>22</sup> on [XR<sub>2</sub>Sn(OMe)]<sub>2</sub> also suggests bridging through the MeO moiety. [Me<sub>2</sub>Sn(OH)(NO<sub>3</sub>)]<sub>2</sub><sup>8</sup>, the only one to contain a possible bidentate ligand in addition to the hydroxide, does not form hydrogen bonds from the ligand to the hydroxide, as in [12]. Me<sub>2</sub>Sn(Cl)(S<sub>2</sub>NMe<sub>2</sub>)<sup>23</sup> and Me<sub>2</sub>Sn(Cl)(OCOCH<sub>3</sub>)<sup>24</sup> do not form bridges with the Cl ligands. The former exists as a monomeric species in the solid state and the latter as linear chains with bridging carboxylates, similar to [1] and [2] (Chapter 2).

[13] is also a dimer. The asymmetric unit contains two tin atoms joined by a μ<sup>3</sup>-oxygen. The geometry of both is based on the trigonal bipyramidal structure (Figure 5.2). There are two carboxylates, one unidentate and the other bidentate.

Around Sn1 the axial groups are the carboxylate oxygen, O22, and the μ<sup>3</sup>-bridging oxygen, O1A, and the equatorial groups are the two phenyl groups and the remaining μ<sup>3</sup>-oxygen, O1. There is also a long interaction between the tin and the carboxylate attached to Sn2 (Sn1-

O11A=2.886Å), which is shorter than the sum of the Van der Waals radii (3.52Å). This causes the C-Sn-C angle, between which O11 approaches, to open up to 149.6°, indicating quite a strong interaction.

The geometry around Sn2 is closer to trigonal bipyramidal than for Sn1. The two carboxylate oxygens, O11 and O21, form the axial groups, and the phenyl rings and the  $\mu^3$ -oxygen, O1, form the equatorial groups. Distortion arises from a long interaction between Sn2 and the acyl oxygen, O12, forming a weak bond (Sn2-O12=2.902Å). This causes the C-Sn-C angle to widen to 145.5° to accommodate it.

The bridging carboxylate is isobidentate, the difference in C-O bond lengths being only 0.003(11)Å and in Sn-O lengths, 0.073(5)Å. The unidentate carboxylate shows a much greater C-O difference (0.05(11)Å), as would be expected. There are no intermolecular contacts to the unidentate carboxylate.

[13] has the most common structure found for the tetrameric stannoxanes, comprising of two bidentate and two unidentate carboxylates. In some cases<sup>4,5</sup> this structure is stabilised by the formation of intermolecular bonds from the unidentate carboxylate to the neighbouring tetramer, creating an infinite linear chain in the solid state. [13] lacks this interaction, as do a number of other structures<sup>3,7</sup>.

[14] is a structural isomer of [13]. Here both carboxylates in the asymmetric unit are bidentate, bridging between Sn1 and Sn2. This creates six primary bonds around Sn1, to give it a distorted octahedral geometry, and five around Sn2, as before, giving it a trigonal bipyramidal geometry (Figure 5.5).

Distortions from octahedral geometry around Sn1 arise for two reasons. Firstly, the stannoxane unit, Sn<sub>2</sub>O<sub>2</sub>, at the centre of the tetramer, has small O-Sn1-O angles (76.1(4)°) and, secondly, the phenyl/phenyl interactions across the ring force the C-Sn1-C angle to close to 153.4(5)°. The distortion around Sn2 also arises from phenyl/phenyl interactions, here from phenyl groups on the same tin, causing the C-Sn2-C angle to open from 120° to 134.2(6)°. The angle between the axial groups is also slightly reduced from 180° to 171.6(5)°, due to the carboxylates being bidentate.

Unlike [13], the  $\mu^3$ -oxygen, O5, has almost equal length bonds in the stannoxane ring (2.138(10) and 2.131(8)Å for Sn1-O5 and Sn1A-O5) indicating that the tetramer is likely to exist in solution. The four bidentate carboxylates should confer greater stability on this structure over

[13], due to the greater delocalisation.

The carboxylates are isobidentate with respect to the C-O bond lengths, the differences being 0.004(22) and 0.008(24) for C1 and C3 respectively. The Sn-O bond lengths show a much greater variation, though, the differences being 0.225(14) and 0.201(14)Å for C1 and C3. Thus, from comparison with [2], one would expect to find another interaction to the carboxylate, possibly intermolecular, but the nearest contact is at 6.085Å from O2-Sn2'.

No other compounds have been reported to date with all four carboxylates being bidentate, as in [14], the closest being  $\{[\text{Me}_2\text{Sn}(\text{OAc})_2\text{O}]\}_2^8$ , which has three bidentate and one unidentate carboxylate.

The structure of [15] is also dimeric, situated around an inversion centre. The asymmetric unit comprises three phenyltin groups, bound together by two  $\mu^3$ -oxygens and five carboxylates, one of which is unidentate (Figure 5.8). At the centre of the molecule is a chain of three stannoxane units, forming a ladder like structure.

Each tin atom is octahedrally coordinated. Sn1 and Sn3 are coordinated to two carboxylates, one phenyl ring and three  $\mu^3$ -oxygens. Sn2 is bonded to one phenyl, one  $\mu^3$ -oxygen and four carboxylates. The distortions from octahedral geometry are again due to the small O-Sn-O angle in the stannoxane rings. Sn1, which is part of two rings, is the most distorted, the O11-Sn1-O12 angle being only 147.3(4)° instead of 180°. Sn2, which does not belong to any stannoxane rings, is the least distorted.

The four bidentate carboxylate groups all have small C-O bond length differences, the largest being 0.047(20)Å for C1 (Table 5.14). The differences in Sn-O bonds is small for C1, C3 and C5, at 0.057(11), 0.046(11) and 0.023(11)Å respectively, though larger for C7, at 0.160(11)Å. There appears to be no correlation between  $\Delta\text{C-O}$  and  $\Delta\text{Sn-O}$  bond lengths.

[16] is a hexameric molecule in the shape of a drum (Figure 5.10). There is an  $S_6$  axis passing through the centre of the molecule. The asymmetric unit contains one tin atom with one phenyl, one carboxylate and one  $\mu^3$ -oxygen. The drum has top and bottom faces constructed of  $\text{Sn}_3\text{O}_3$  rings. The sides are made from stannoxane units. The carboxylate groups are bidentate, bridging the tin atoms.

The geometry around the tin is nearly octahedral. Distortion arises from a large O-Sn-O angle in the  $\text{Sn}_3\text{O}_3$  plane (104.6(1)°) and a small O-Sn-O angle between the bridging carboxylates

(76.7(1)°). In the six membered ring the tin and oxygen atoms are staggered around the mean plane of the ring (+/- 0.1431Å), with the oxygens between the top and bottom faces and the tin atoms outside the faces (Figure 5.11).

The carboxylate is isobidentate, the differences in C-O and Sn-O bond lengths being both less than 0.008Å.

[17] is also dimeric around an inversion centre (Figure 5.12). The asymmetric unit contains two tin atoms, three carboxylates, four phenyl groups and a hydroxide. Sn1 and Sn2 have six and five coordination respectively. Distortion around Sn2 arises due to phenyl/phenyl interactions opening the C-Sn-C angle to 136.3(4)°.

The independent carboxylates in the molecule all have different bonding modes. The C1 carboxylate, joining the dimer together, is bidentate in a syn/anti fashion, as with [1] and [2]. The large  $\Delta$ Sn-O (0.156(7)Å) indicating anisobidentate behaviour. The C5 carboxylate is bridging in a syn/syn fashion with smaller  $\Delta$ C-O and  $\Delta$ Sn-O bond lengths indicating a closer approach to isobidentate behaviour. The C3 carboxylate is unidentate with a hydrogen bond from the acyl oxygen to the hydroxide. The  $\Delta$ C-O length is the largest for the three bonding types, at 0.052(11)Å, as would be expected from a unidentate carboxylate.

There are no reported analogues of [17] in the literature.

## 5.3 Experimental

### 5.3.1 Preparation of compounds

#### Dimeric $\mu$ -OH-trichloroacetato-diphenyltin [12]

[12] was prepared from [3] by recrystallisation from CCl<sub>4</sub>:hexane by the liquid diffusion method. Crystals formed at the interface after 12hrs and were used directly for structure determination.

#### Dimeric $\mu^2$ -oxo- $\mu$ -trichloroacetato-trichloroacetato-bisdiphenyltin [13]



$\text{Ph}_3\text{SnCl}$  (1.094g, 2.84mmol) in  $\text{CHCl}_3$  was shaken with  $\text{NaOH}$  (0.205g, 5.12mmol) in  $\text{H}_2\text{O}$  ( $5\text{cm}^3$ ). The resulting organic layer was separated and the solvent removed under reduced pressure. The product,  $(\text{Ph}_3\text{Sn})_2\text{O}$ , was stirred with  $\text{Cl}_3\text{CCOOH}$  (0.2195g, 1.34mmol) in aqueous  $\text{MeOH}$  ( $30\text{cm}^3$ ) for 3hrs. The solvent was removed and the product recrystallised from  $\text{CH}_2\text{Cl}_2$ :Pet. Ether (30/40°bpt.). The crystals produced were used directly for structure determination.

#### **Dimeric $\mu^3$ -oxo-bis( $\mu$ -trichloroacetato)-bisdiphenyltin [14]**

[14] was prepared from [3] by recrystallisation from  $\text{CCl}_4$ :Hexane solution by the liquid diffusion method. Clear crystals appeared at the interface after 12hrs. These were used directly for structure refinement.

#### **Dimeric bis- $\mu^3$ -oxo-(tetra- $\mu$ -trichloroacetato)-trichloroacetato-trisphenyltin benzene solvate [15]**

$\text{Ph}_3\text{SnOH}$  (1.056g, 2.88mmol) and  $\text{Cl}_3\text{CCOOH}$  (0.49g, 3mmol) were refluxed in benzene ( $50\text{cm}^3$ ) with a Dean-Stark separator attached. After 24hrs the solution was filtered and reduced to  $20\text{cm}^3$ . Hexane was added until precipitation started to occur. The product was redissolved by gentle warming, then the solution was left at  $0^\circ\text{C}$  for 24hrs, whereupon crystals formed. Examination under a microscope revealed two distinct crystal types - small clear rhomboids and larger cloudier cubes. The former proved to be identical to [13] by analysis of the unit cell dimensions. A full structure determination was carried out on the latter only.

#### **Hexameric $\mu^3$ -oxo- $\mu$ -trichloroacetato-phenyltin benzene solvate [16]**

$(\text{Ph}_2\text{SnO})_n$  (1.6g, 5.5mmol) and  $\text{Cl}_3\text{CCOOH}$  (1.87g, 11.5mmol) were refluxed in benzene ( $100\text{cm}^3$ ) fitted with a Dean-Stark separator, for 12hrs. Well formed rhombohedral crystals suitable for structure elucidation grew on the side of the reaction vessel. [16] was also obtained by a repetition of the reaction originally used for [14]; crystals grown from  $\text{CCl}_4$ :hexane solution by liquid diffusion proved to be rhombohedral ( $a=15.6\text{\AA}$ ,  $\alpha=91.4^\circ$ , unrefined). They are believed to be an unsolvated form of [6], as recrystallisation from hot benzene gave rhombohedral crystals ( $a=21.3\text{\AA}$ ,  $\alpha=43.2^\circ$ , unrefined) clearly identical to [16].

### Dimeric $\mu$ -OH-bis- $\mu$ -trichloroacetato-trichloroacetato-bis-diphenyltin [17]

$(\text{Ph}_2\text{SnO})_n$  (4.33g,15mmol) and  $\text{Cl}_3\text{CCOOH}$  (5g,30mmol) were stirred in hexane (30cm<sup>3</sup>) for 3hrs. The solvent was removed under reduced pressure and the product recrystallised from Dichloromethane:Pet Ether solution. Large colourless blocks formed after 12hrs. These were used directly for structure determination. [17] was also formed by recrystallising [3] in  $\text{CH}_2\text{Cl}_2$ / pet. ether (30-40° bpt.).

### 5.3.2 X-ray Crystallography

Accurate unit cell dimensions were determined by least squares fits to 15 high angle reflections ( $20^\circ < \theta < 22^\circ$ ) except for [13] where the reflections were measured between 25 and 29°. Data for [13], [14], [15], [16] and [17] were measured on a Syntex P2<sub>1</sub> 4-circle diffractometer, while the data for [12] was recorded on a Nicolet R3m. Intensities were measured using Mo-K $\alpha$  radiation (graphite crystal monochromator,  $\lambda=0.71069\text{\AA}$ ). Three check reflections were monitored every 200 reflections, the data being rescaled to account for any variation, 1,4,25,54,5 and 5% for [12] to [17] respectively. These are insignificant for [12], [13], [16] and [17], but serious for [14] and [15]. Intensities were corrected for Lorentz, polarisation and absorption effects, the last by the Gaussian method. Crystal data and a summary of the data collection parameters are given in Table 5.1.

All structures were solved using the heavy atom method, the positions of the tin atoms being determined from Patterson maps. The remaining non-hydrogen atoms were determined from successive difference Fourier syntheses. Hydrogen atoms were included at calculated positions (C-H = 0.96 $\text{\AA}$ , U=0.07 $\text{\AA}^2$ ). A weighting scheme of the form  $W=1/(\sigma^2(F)+gF^2)$  was used. All calculations for [13] to [17] were made using SHELXTL<sup>27</sup> on a Data General DG30, the structure of [12] was determined using SHELXTL PLUS<sup>28</sup> on a DEC MicroVax II. Scattering factors were taken from International Tables<sup>29</sup>. Final atomic coordinates are listed in Tables 5.2-5.7. Bond lengths and angles are listed in Tables 5.8-5.13. Structures are shown in Figures 5.1-5.13.

### Dimeric $\mu$ -OH-trichloroacetato-diphenyltin [12]

Systematic absences,  $h0l;l=2n+1$  and  $0k0;k=2n+1$ , indicated the space group  $P2_1/c$  uniquely. The hydroxy hydrogen, H11, was located on a difference Fourier map. Its position was

allowed to refine but the bond length was fixed at 0.85Å. All non-hydrogen atoms were refined anisotropically. The residual electron density is all located in the rotation cone of the trichloro groups.

#### **Dimeric $\mu^3$ -oxo- $\mu$ -trichloroacetato-trichloroacetato-bisdiphenyltin [13]**

The systematic absences,  $h0l;h+l=2n+1$  and  $0k0;k=2n+1$ , indicate space group  $P2_1/n$ . The Patterson synthesis showed two heavy atom positions. These were both inserted and refinement proceeded smoothly. All non-hydrogen atoms were refined anisotropically. Residual electron density is mostly located around the tin atoms.

#### **Dimeric $\mu^3$ -oxo-bis( $\mu$ -trichloroacetato)-bis-diphenyltin [14]**

The space group was determined as  $P2_1/c$  from the systematic absences. Two heavy atom positions were located from the Patterson synthesis and used for refinement. All non-hydrogen atoms were refined anisotropically. One trichloro group was refined as disordered over six sites with half occupancy chlorine atoms. The group was fixed as two staggered tetrahedral groups with the C-Cl distances fixed at 1.74Å. The residual electron density is mostly associated with this group. The high R-factor is probably a consequence of the decomposition (~25%) of the crystal in the X-ray beam.

#### **Dimeric bis- $\mu^3$ -oxo-(tetra- $\mu$ -trichloroacetato)- trichloroacetato-trisphenyltin benzene solvate [15]**

The space group was determined uniquely as  $P2_1/a$  from the systematic absences. This was rotated to the standard  $P2_1/c$  for the structure determination. One tin was located using the Patterson synthesis and the two others were found on further difference Fourier maps. One trichloroacetate group was very disordered with its acyl carbon, acyl oxygen and trichloro group all having alternative positions. The occupancy of the acyl carbon and oxygen atoms were refined to nearly 0.5. The trichloro group was refined as half occupancy over six sites as for [14]. All non-hydrogen atoms except C9, C9A, C10, O9, O10 and O10A, from the disordered carboxylate, and C12, C23, C33 and C44, from the phenyl rings, were refined anisotropically. The remaining electron density was mainly associated with the trichloro groups, the highest peaks being associated

with the disordered group. The high R-factor is probably due to the disorder in the crystal, since the decomposition of the crystal (~54%) appears not to have affected the structure solution.

#### **Hexameric $\mu^3$ -oxo- $\mu$ -trichloroacetato-phenyltin benzene solvate [16]**

The data was collected for a monoclinic cell and the systematic absences,  $hkl;h+k=2n+1$ ,  $h0l;h,l=2n+1$ , indicated space groups Cc or C2/c. From density calculations C2/c was chosen and the structure refined to  $R=0.0365$ . It was then noticed that the structure had an  $S_6$  axis, which indicated that the space group should have been rhombohedral. The cell and data were transformed, giving the new space group as  $R\bar{3}c$ . The structure was re-refined, giving  $R=0.0296$ , indicating this was the correct setting. Anisotropic thermal parameters were used for all non-hydrogen atoms. The highest peak left in the final difference Fourier was located on a special position, the rest was located in the rotation circle of the trichloro group.

#### **Dimeric $\mu$ -OH-bis- $\mu$ -trichloroacetato-trichloroacetato-bis-diphenyltin [17]**

No systematic absences indicated space groups P1 or  $P\bar{1}$ .  $P\bar{1}$  was chosen from density calculations. All non-hydrogen atoms were refined anisotropically. The residual electron density lies in the rotation circles of the three trichloro groups and also near the tin atoms.

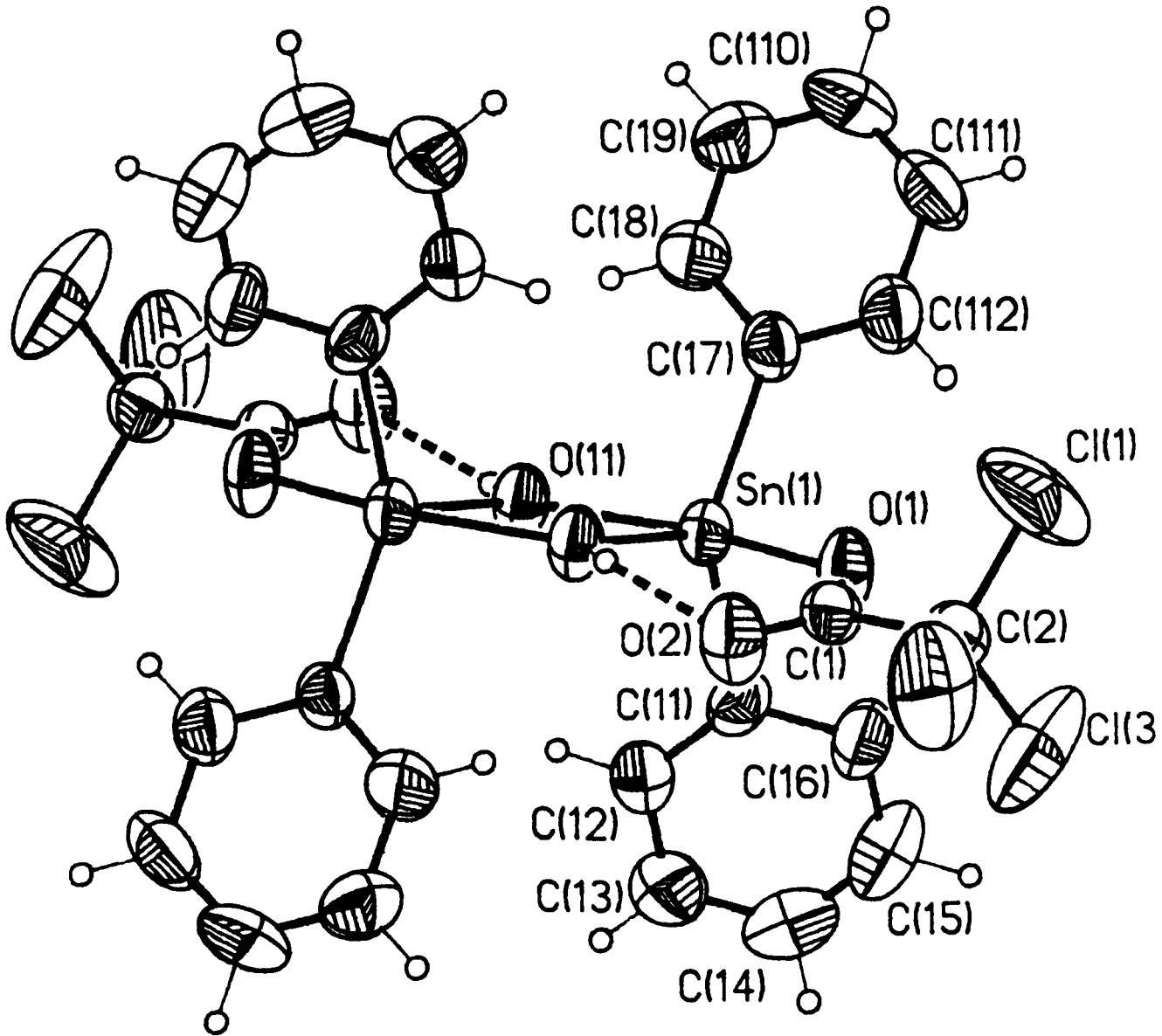


FIGURE 5.1 View of the dimer formed by [12].

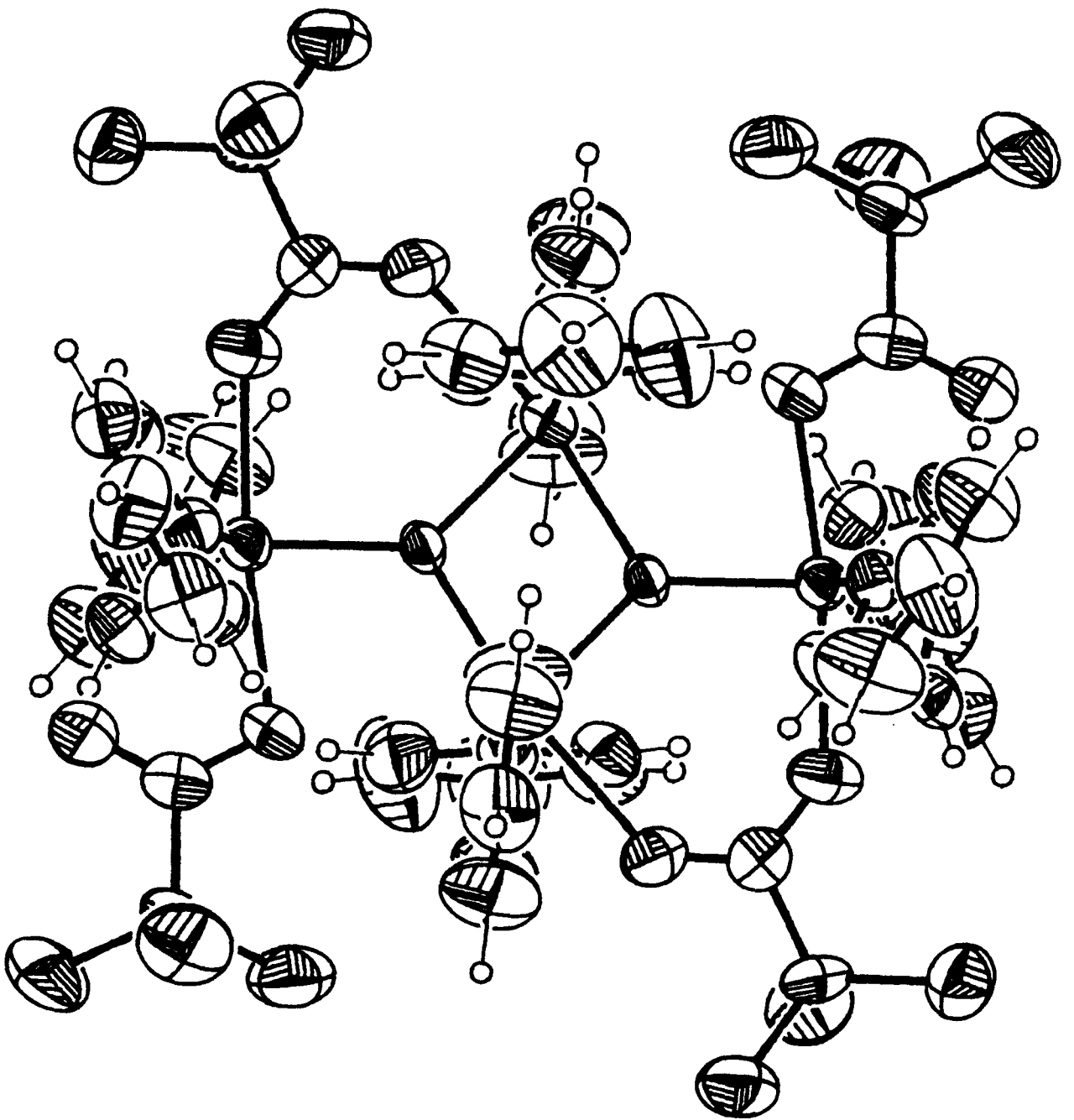


FIGURE 5.2 View of the dimer formed by [13].

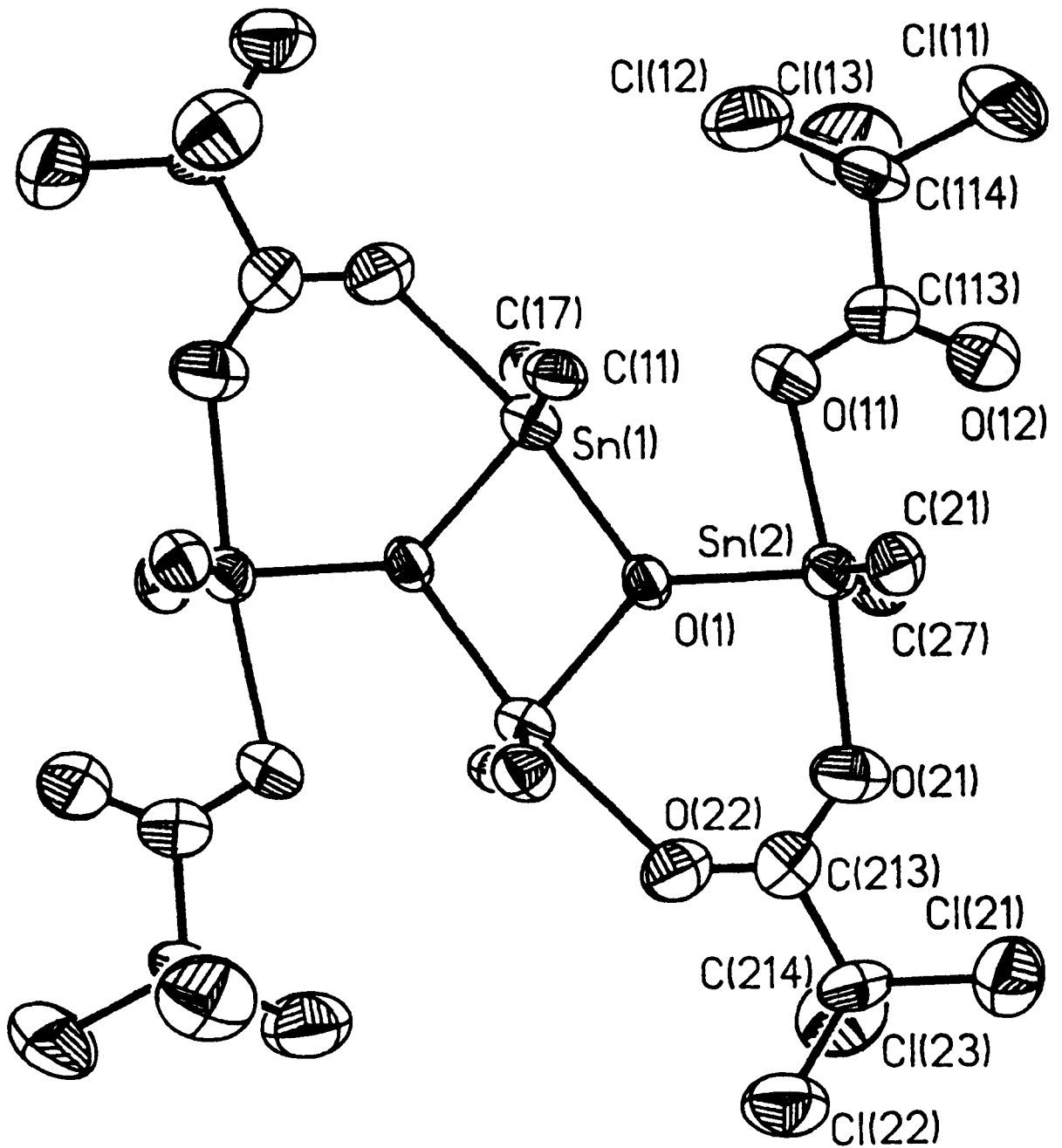


FIGURE 5.3 View of [13], phenyl groups removed, showing atomic numbering scheme.

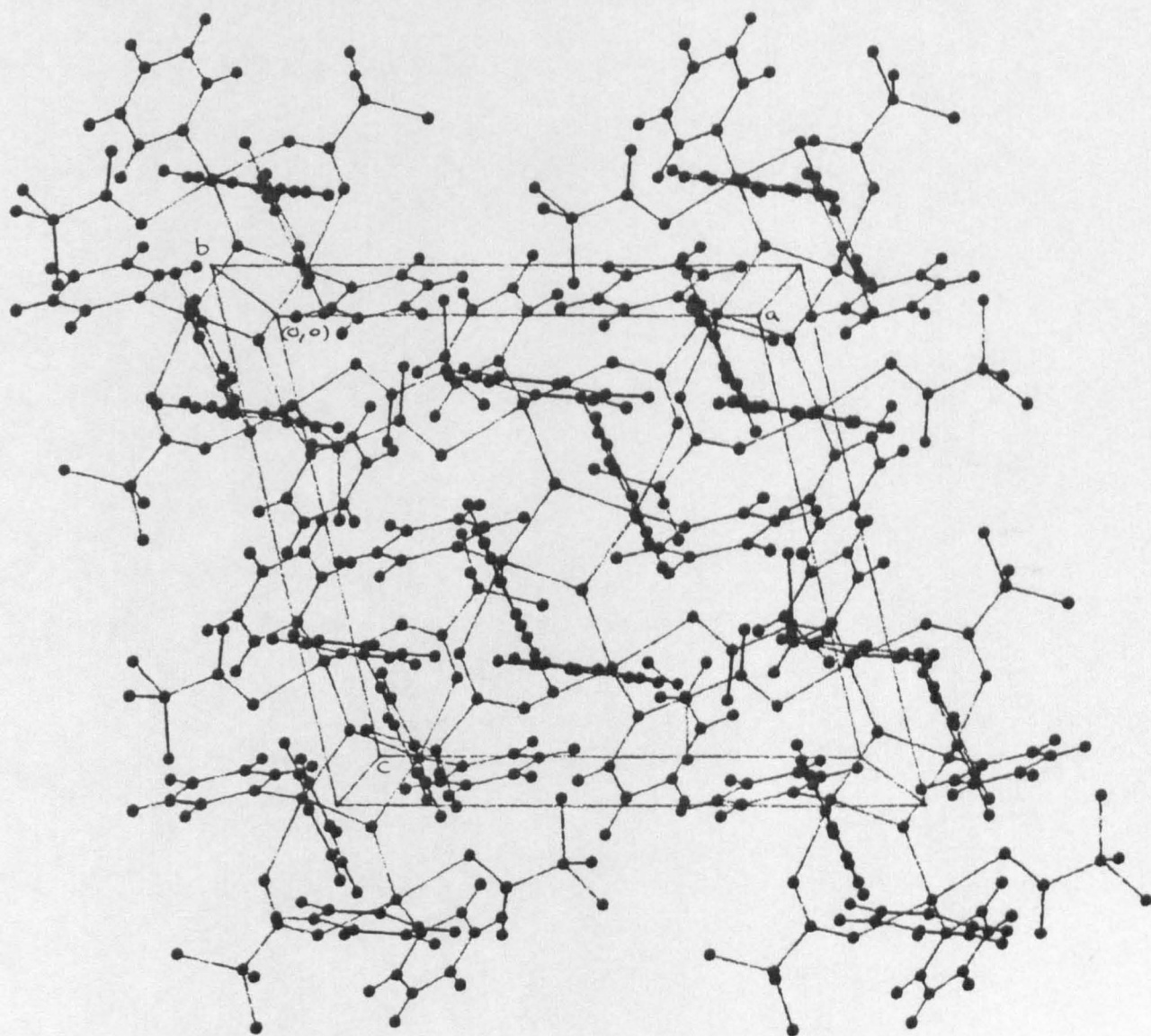


FIGURE 5.4 Packing diagram for [13].



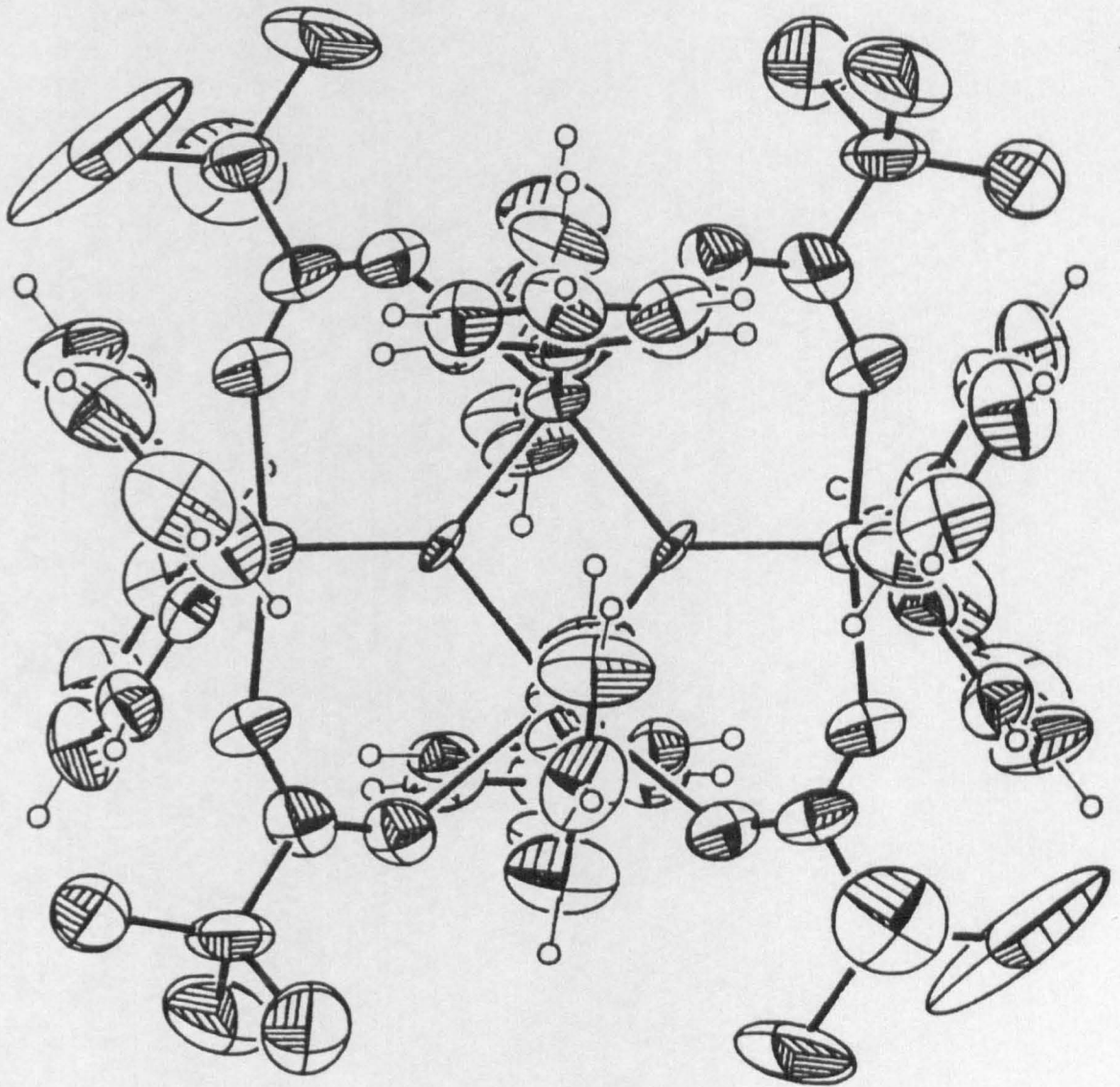


FIGURE 5.5 View of the dimer formed by [14].

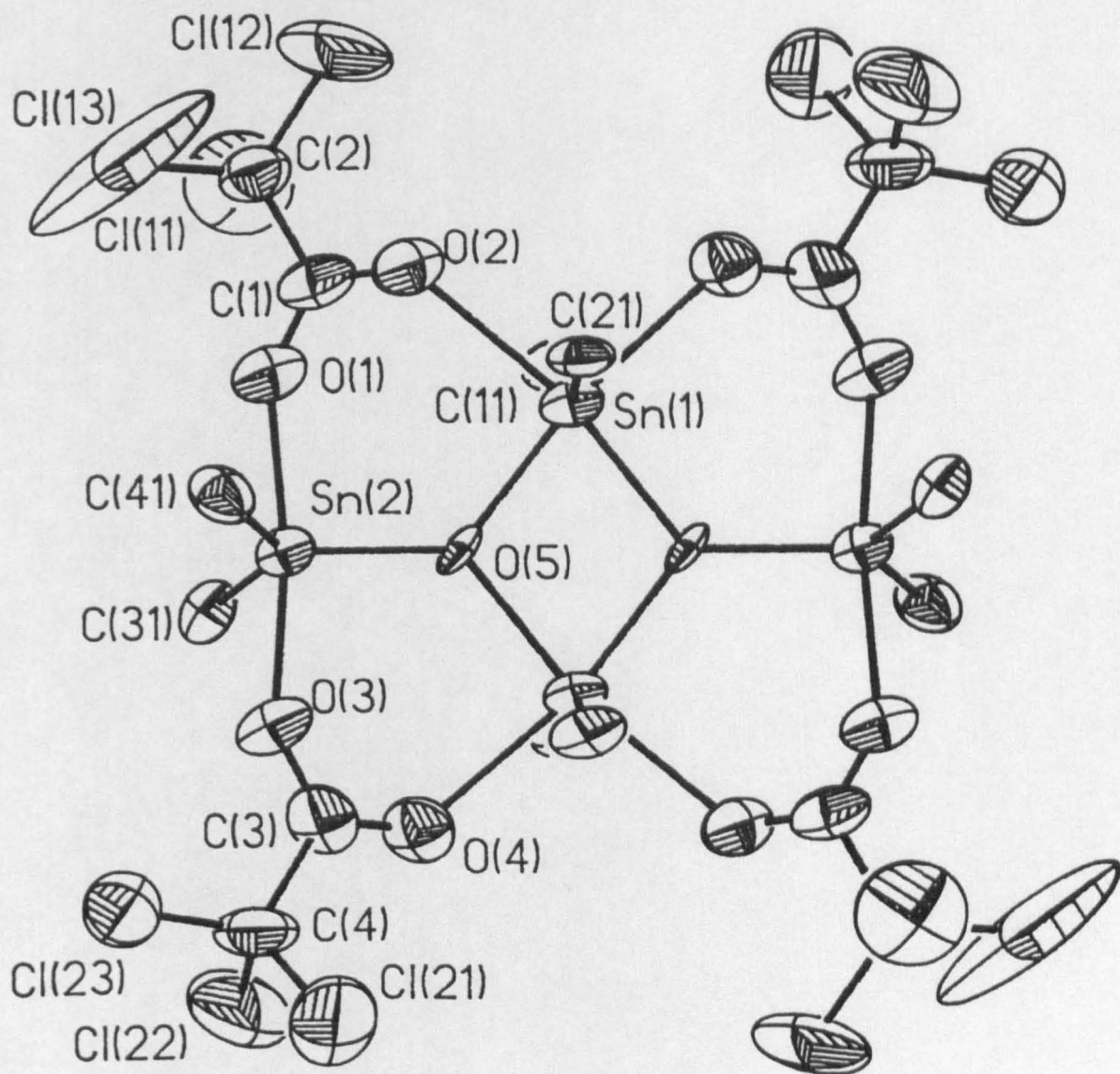


FIGURE 5.6 View of [14], phenyl groups removed, showing atomic numbering scheme.

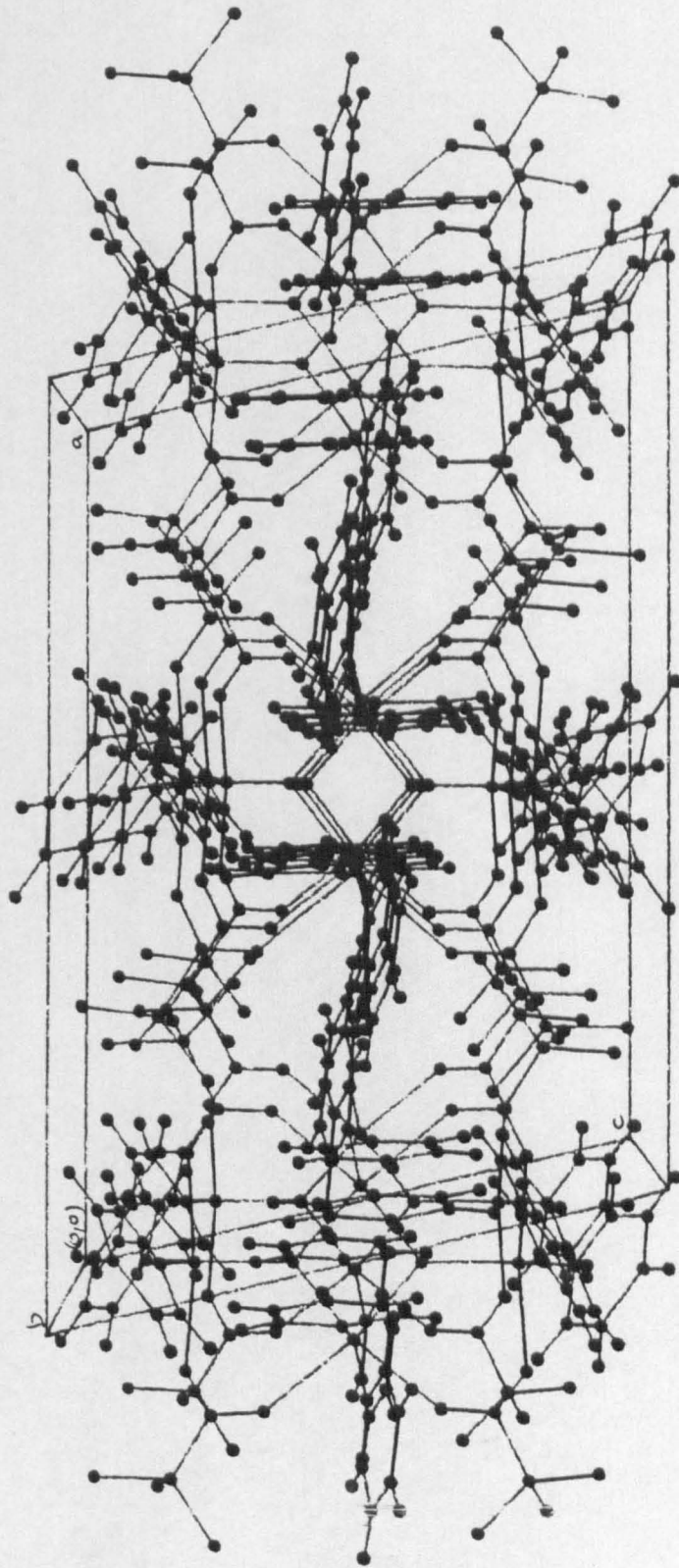


FIGURE 5.7 Packing diagram for [14].



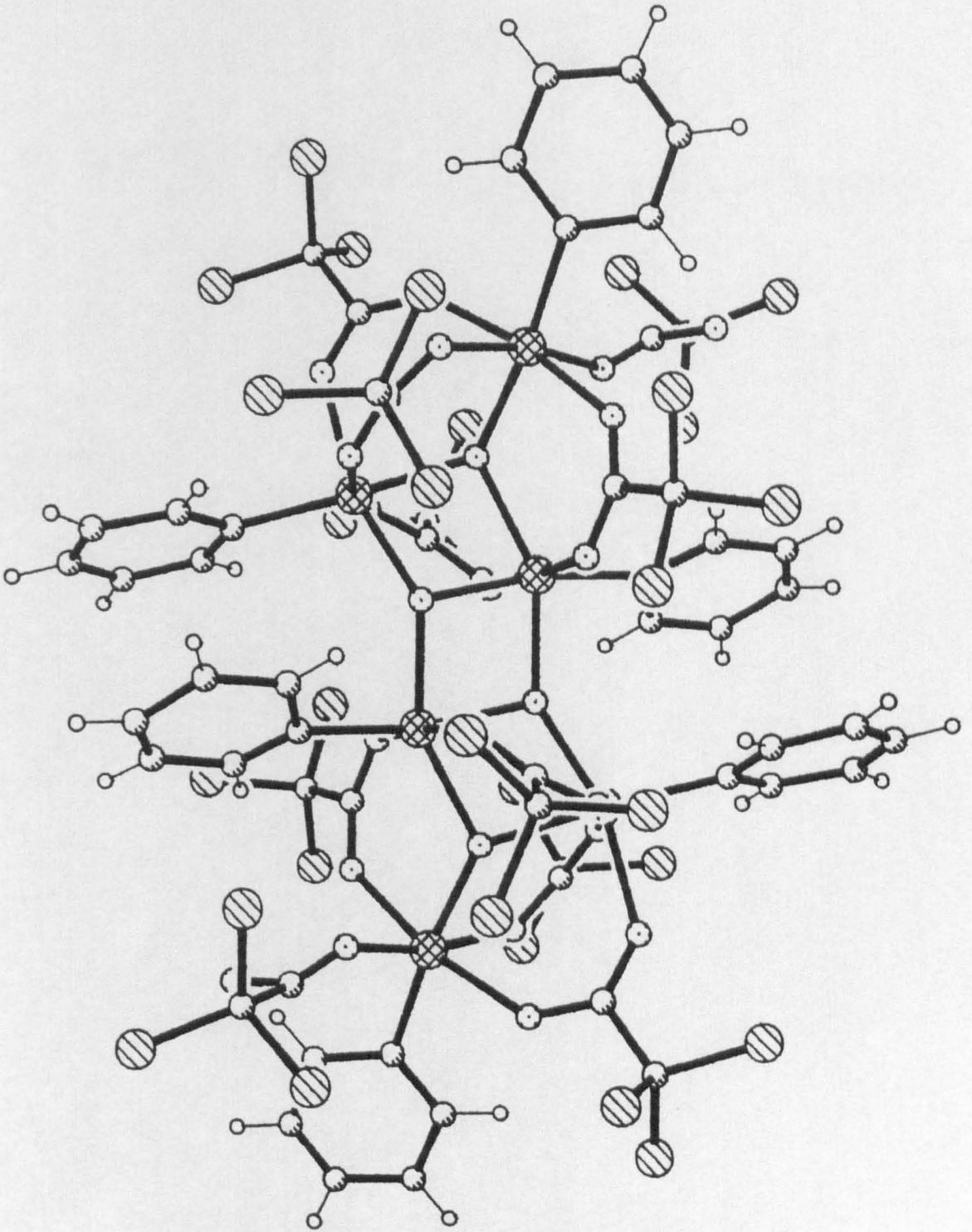
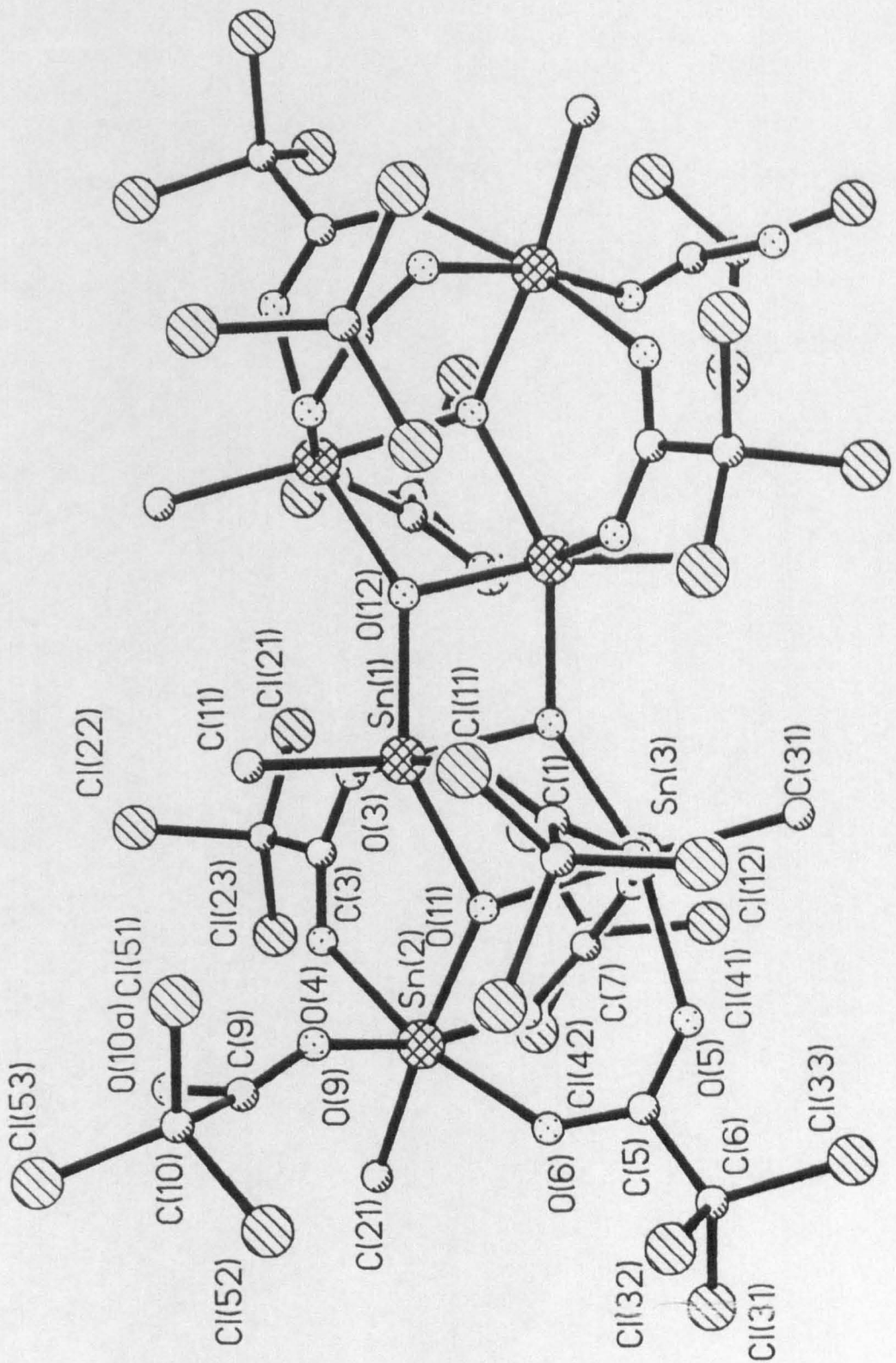


FIGURE 5.8 View of the dimer formed by [15].



**FIGURE 5.9** View of [15], phenyl groups removed, showing atomic numbering scheme.

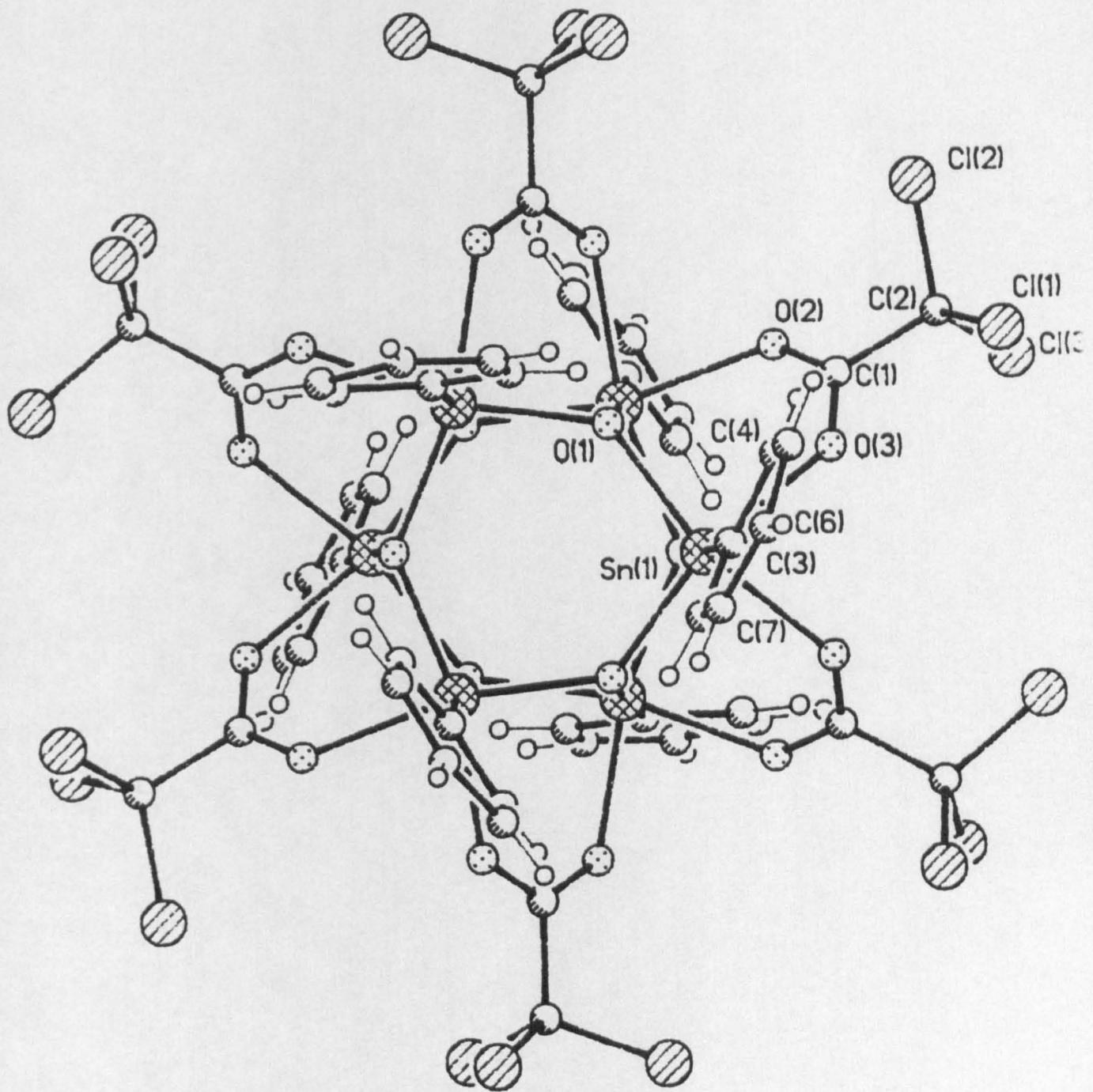


FIGURE 5.10 Top view of hexamer formed by [16], showing atomic numbering scheme.



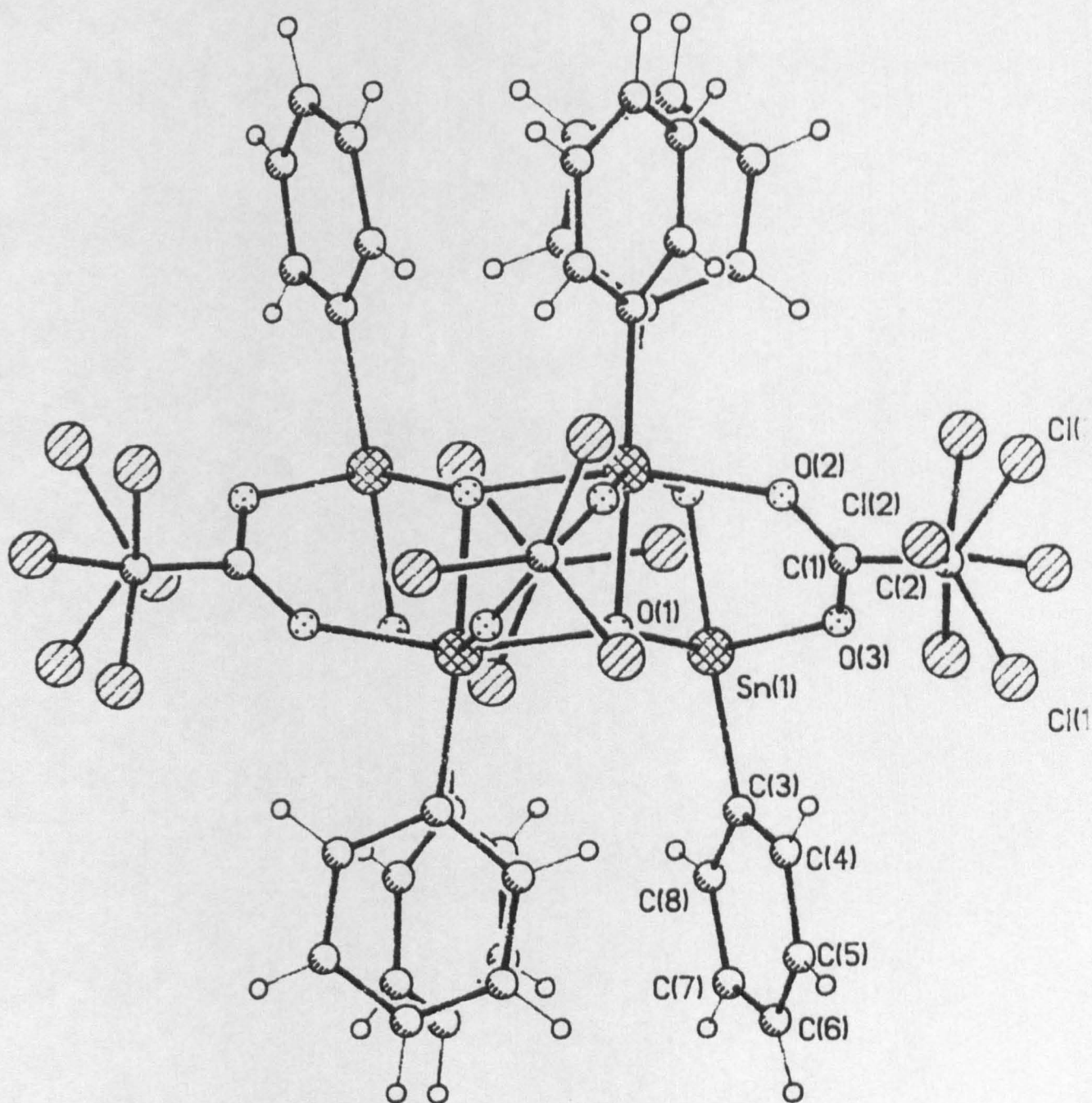


FIGURE 5.11 Side view of hexamer formed by [16], showing atomic numbering scheme.

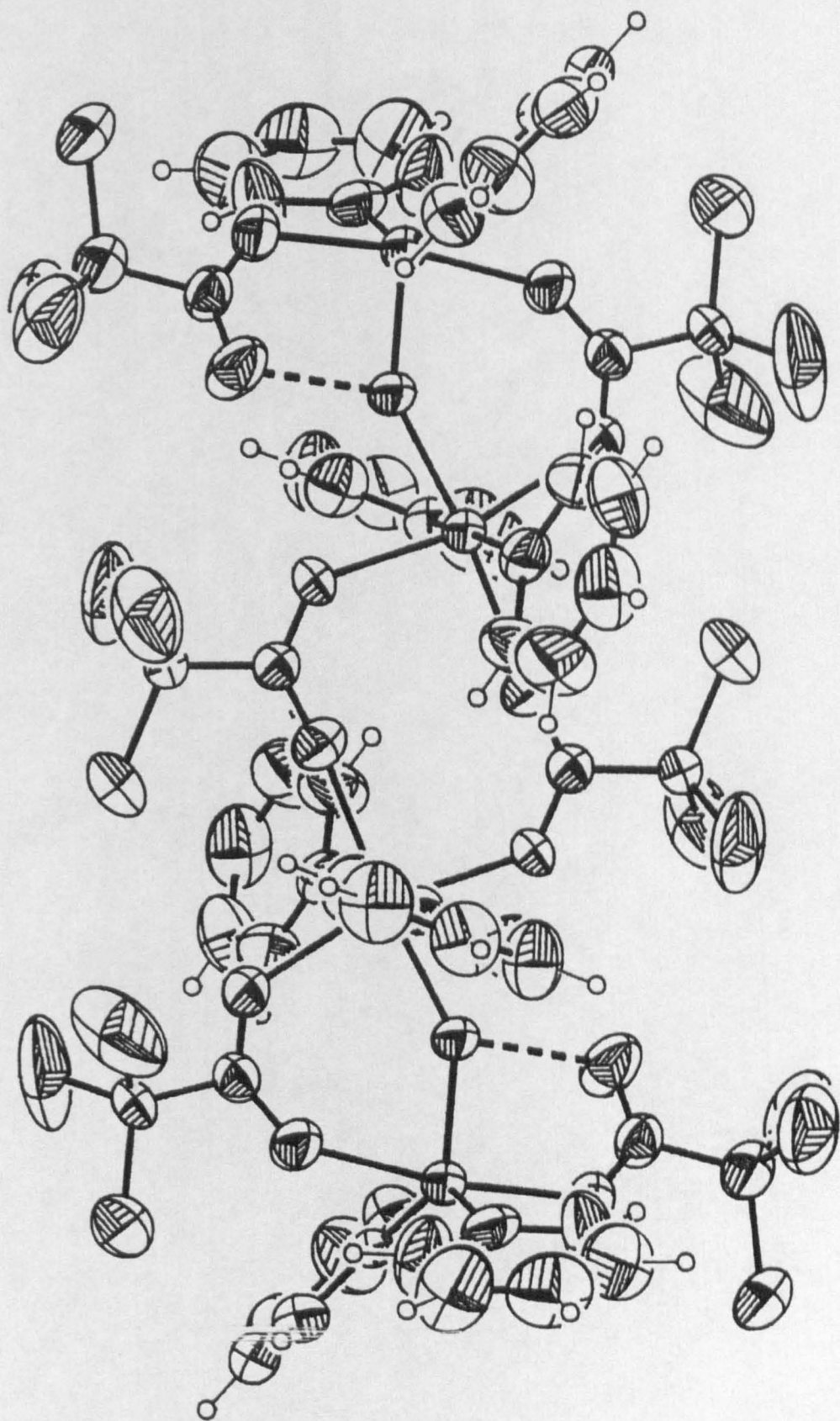


FIGURE 5.12 View of the dimer formed by [17].



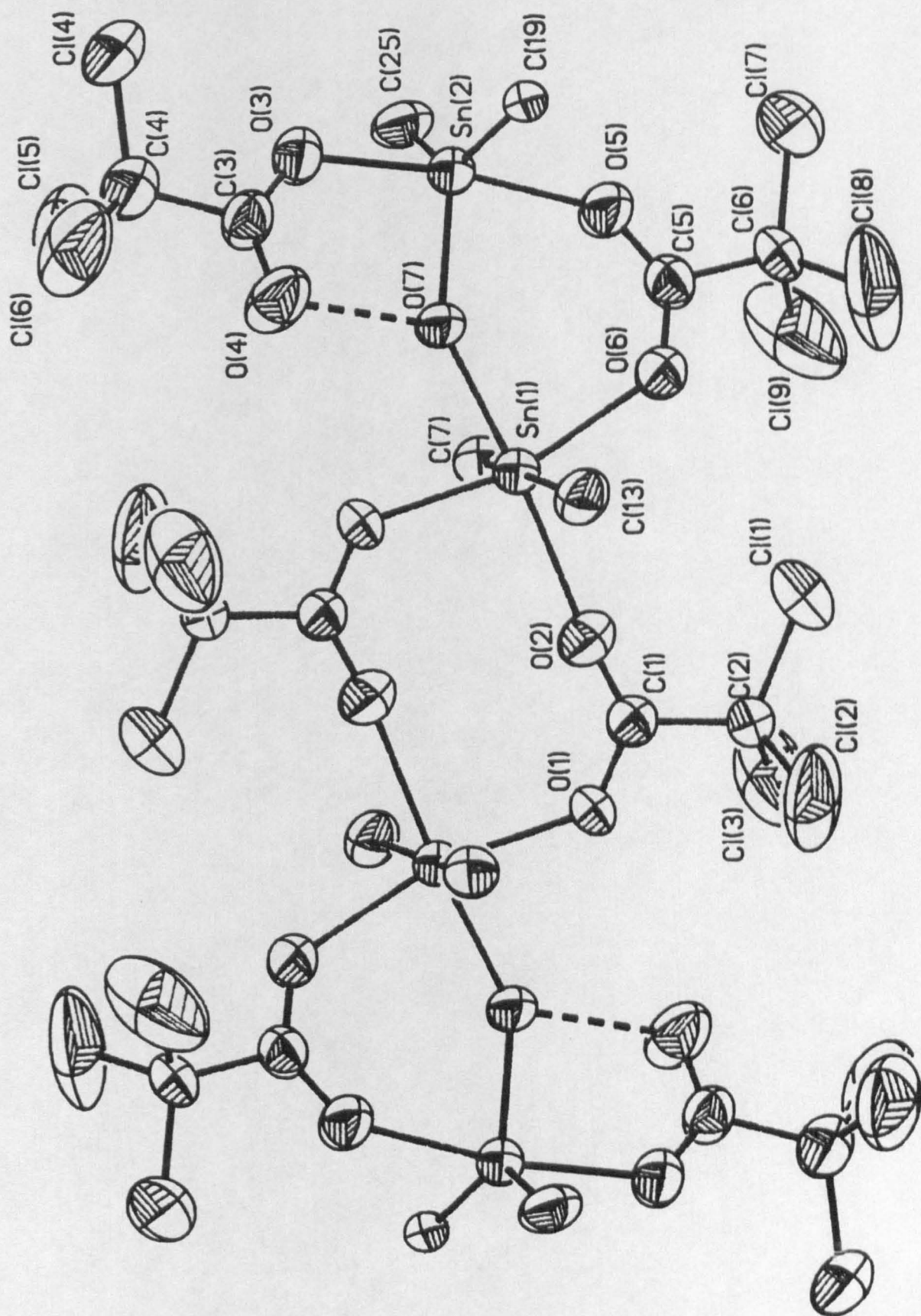


FIGURE 5.13 View of [17], phenyl groups removed, showing atomic numbering scheme.

**Table 5.1: Crystal data and data collection parameters**

Compound	[12]	[13]	[14]	[15]	[16]	[17]
Formula	$C_{20}H_{17}O_2Cl_3Sn.CH_3OH$	$C_{56}H_{40}O_{10}Cl_{12}Sn_4$	$C_{56}H_{30}O_{24}Cl_{30}Sn_6.2C_6H_6$	$C_{56}H_{40}O_{10}Cl_{12}Sn_4$	$C_{60}H_{42}O_{14}Cl_{18}Sn_4$	$C_{48}H_{30}O_{18}Cl_{18}Sn_6.3C_6H_6$
Mass	544.48	1773.33	3019.66	1773.33	2100.38	2402.12
$D_{calc}$	1.563	1.850	1.932	1.895	1.787	1.881
Z	4	2	2	2	1	2
Crystal System	Monoclinic	Monoclinic	Monoclinic	Monoclinic	Triclinic	Trigonal
Systematic Absences	$h0l\ l=2n+1$ $0k0\ k=2n+1$	$h0l\ l=2n+1$ $0k0\ k=2n+1$	$h0l\ l=2n+1$ $0k0\ k=2n+1$	$h0l\ h+l=2n+1$ $0k0\ k=2n+1$	none	$hkl\ h+k=2n+1$ $h0l\ h,l=2n+1$
Space Group	$P2_1/c$	$P2_1/c$	$P2_1/c$	$P2_1/n$	$\bar{P}1$	$R\bar{3}c$
a	10.196(2)	13.172(3)	15.714(4)	12.818(3)	10.008(4)	21.770(4)
b	12.672(2)	12.697(5)	14.054(4)	18.241(4)	10.696(4)	-
c	17.913(3)	19.561(5)	23.575(4)	13.651(3)	18.878(7)	-
$\alpha$	-	-	-	-	80.71(3)	42.33(1)
$\beta$	91.59(2)	103.32(2)	94.59(2)	103.24(2)	78.30(3)	-
$\gamma$	-	-	-	-	85.89(3)	-
U	2313.6(8)	3183.5(1.7)	5189.8(2.3)	3107.0(1.1)	1951.3(1.3)	4240.0(1.8)
$\mu$	14.74	21.19)	22.69	21.71	19.48	23.81
$F(000)$	1076	1720	2896	1720	1018	2388
Crystal Size	0.2×0.2×0.4	0.1×0.2×0.5	0.1×0.3×0.2	0.3×0.3×0.3	0.2×0.1×0.3	0.2×0.2×0.4
Max. Trans.	0.7915	0.8120	0.7971	0.78	0.8653	0.6914
Min. Trans.	0.7464	0.6115	0.7540	0.66	0.7109	0.5486
Scan Range	+/- 0.95	+/- 1.0	+/-1.1	+/- 1.0	+/-1.5	+/-0.95
Scan Rate	4.0°	2.0°	3.5°	3.0°	2.0°	2.0°
Max. 2 $\theta$	50°	50°	45°	50°	45°	50°
Refs. Collected	4440	5353	7301	5925	5140	8449
Refs. Observed	1770	3185	2556	3132	3111	1921
Weight	0.00041	0.00235	0.00114	0.00072	0.00049	0.00057
R(final)	0.0296	0.0918	0.0521	0.0379	0.0454	0.0296
$R_w$	0.0327	0.1017	0.0509	0.0385	0.0451	0.0330
Max. on final Fourier	+/- 0.3	+/- 3.2	+/-0.8	+/- 0.5	+/- 0.7	+/- 0.7
Max. $\delta/\sigma$	0.105	0.08	0.075	0.013	0.030	0.003
No. of Parameters	259	382	555	370	433	164

TABLE 5.2

Atomic coordinates ( $\times 10^4$ ) for [12] (with standard deviations in parentheses).

	x	y	z	U(eq)
Sn(1)	4378.5(4)	1262.7(5)	550.0(2)	48(1)
C1(1)	-221(4)	1200(5)	936(3)	184(3)
C1(2)	-123(3)	-1993(4)	1302(2)	127(2)
C1(3)	1337(3)	145(6)	2221(2)	146(2)
O(11)	5945(5)	818(6)	-28(3)	53(2)
O(1)	2600(5)	846(6)	956(3)	63(2)
O(2)	2195(6)	-1677(7)	711(4)	75(2)
C(1)	1971(6)	-395(8)	954(3)	48(2)
C(2)	786(7)	-251(8)	1351(4)	58(2)
C(11)	5514(7)	1046(8)	1564(4)	53(2)
C(12)	6657(7)	202(8)	1676(4)	59(2)
C(13)	7374(8)	97(11)	2346(5)	78(3)
C(14)	6956(10)	855(11)	2896(5)	77(3)
C(15)	5840(11)	1697(13)	2791(5)	88(4)
C(16)	5101(9)	1805(10)	2124(4)	67(3)
C(17)	3560(7)	3194(8)	-70(3)	48(2)
C(18)	4084(10)	3685(8)	-645(5)	69(3)
C(19)	3536(10)	4887(11)	-1055(5)	84(4)
C(110)	2475(10)	5652(10)	-906(6)	87(4)
C(111)	1944(9)	5234(10)	-319(5)	83(4)
C(112)	2502(9)	3991(9)	104(5)	66(3)

\* Equivalent isotropic U defined as one third of the trace of the orthogonalised  $U_{ij}$  tensor.

TABLE 5.3

Atomic coordinates ( $\times 10^4$ ) for [13] (with standard deviations in parentheses).

atom	x	y	z
Sn(1)	4560(1)	171(1)	3783(1)
Sn(2)	7431(1)	514(1)	4787(1)
Cl(11)	7361(3)	1415(2)	952(2)
Cl(12)	5294(2)	1071(2)	1263(2)
Cl(13)	6719(3)	-76(2)	1001(2)
Cl(21)	10072(2)	485(2)	7990(2)
Cl(22)	8601(2)	151(2)	9216(2)
Cl(23)	9296(2)	-973(1)	8042(2)
O(1)	5981(4)	183(3)	4986(3)
C(11)	4200(6)	1304(4)	3719(5)
C(12)	4895(8)	1848(5)	3617(7)
C(13)	4632(10)	2580(6)	3688(9)
C(14)	3668(10)	2764(6)	3883(9)
C(15)	2956(8)	2229(5)	4023(7)
C(16)	3220(7)	1509(5)	3937(6)
C(17)	4823(7)	-805(4)	3049(5)
C(18)	5202(9)	-1399(5)	3581(7)
C(19)	5352(9)	-2058(6)	3142(8)
C(110)	5113(8)	-2132(6)	2150(7)
C(111)	4704(10)	-1551(6)	1569(7)
C(112)	4558(9)	-893(6)	2012(7)
C(113)	7124(7)	743(4)	2658(6)
O(11)	6497(4)	579(3)	3212(4)
O(12)	8074(5)	862(4)	2937(4)
C(114)	6632(7)	806(5)	1508(6)
C(21)	7530(6)	1667(4)	5029(6)
C(22)	7426(8)	1938(5)	5934(7)
C(23)	7481(10)	2680(6)	6138(8)
C(24)	7620(9)	3159(5)	5412(9)
C(25)	7756(9)	2903(5)	4514(8)
C(26)	7722(7)	2182(5)	4337(7)
C(27)	8272(6)	-441(4)	4546(6)
C(28)	9196(7)	-656(5)	5223(7)
C(29)	9704(7)	-1300(5)	5070(7)
C(210)	9317(8)	-1717(5)	4262(8)
C(211)	8428(8)	-1524(5)	3594(8)
C(212)	7899(7)	-879(5)	3711(7)
C(213)	7997(7)	99(4)	7183(6)
O(21)	8190(5)	388(3)	6437(4)
O(22)	7127(5)	-107(4)	7294(4)
C(214)	8963(7)	-36(4)	8080(5)

\* Equivalent isotropic U defined as one third of the trace of  
the orthogonalised  $U_{ij}$  tensor.

TABLE 5.4

Atomic coordinates ( $\times 10^4$ ) for [14] (with standard deviations in parentheses).

atom	x	y	z	U
Sn(1)	5046.0(8)	5331.6(7)	4176.2(4)	40(1)*
Sn(2)	2415.1(9)	5271.9(7)	4582.7(5)	44(1)*
C(2)	2233(5)	5336(6)	2261(3)	68(7)*
C1(11)	1997(5)	4013(6)	2053(3)	138(8)*
C1(12)	3038(5)	5857(6)	1755(3)	182(13)*
C1(13)	1057(5)	6020(6)	2090(3)	433(31)*
C1(14)	896(5)	5523(6)	2149(3)	176(12)*
C1(15)	2467(5)	4087(6)	1966(3)	371(27)*
C1(16)	2729(5)	6281(6)	1782(3)	592(35)*
C1(21)	2759(6)	5572(8)	7575(3)	146(4)*
C1(22)	1772(7)	3688(8)	6998(4)	158(5)*
C1(23)	848(5)	5656(7)	6542(3)	124(3)*
O(1)	2297(10)	5075(8)	3446(5)	61(4)*
O(2)	3642(9)	5820(9)	3184(5)	61(4)*
O(3)	2286(11)	5508(10)	5673(6)	74(5)*
O(4)	3511(11)	4556(9)	6378(6)	61(5)*
O(5)	3980(7)	5117(7)	4839(4)	41(3)*
C(1)	2783(15)	5434(12)	3050(8)	59(6)*
C(3)	2676(17)	5055(14)	6241(9)	63(7)*
C(4)	2039(19)	5081(18)	6810(9)	86(9)*
C(11)	4849(14)	3848(10)	3657(7)	50(6)*
C(12)	4558(17)	2977(11)	3987(8)	71(8)*
C(13)	4376(22)	2010(14)	3642(11)	102(11)*
C(14)	4493(18)	1918(18)	2966(11)	102(10)*
C(15)	4786(20)	2801(15)	2623(11)	109(11)*
C(16)	4927(18)	3787(14)	2988(10)	81(9)*
C(21)	5251(12)	6987(11)	4210(7)	48(6)*
C(22)	6294(14)	7425(12)	4367(8)	57(6)*
C(23)	6384(16)	8491(11)	4425(8)	65(7)*
C(24)	5505(16)	9129(12)	4354(10)	69(7)*
C(25)	4572(16)	8741(13)	4201(10)	69(7)*
C(26)	4405(14)	7679(11)	4129(8)	52(6)*
C(31)	1581(13)	3777(12)	4545(8)	53(6)*
C(32)	1750(18)	3036(14)	4033(10)	78(9)*
C(33)	1253(19)	2119(14)	4006(12)	91(10)*
C(34)	614(19)	1905(15)	4497(14)	99(11)*
C(35)	500(16)	2627(15)	4959(13)	85(9)*
C(36)	1008(14)	3581(14)	4983(10)	64(7)*
C(41)	1943(14)	6870(12)	4416(9)	58(6)*
C(42)	1323(15)	7155(14)	3764(10)	71(8)*
C(43)	1031(21)	8155(19)	3643(12)	104(12)*
C(44)	1319(25)	8916(19)	4138(16)	130(16)*
C(45)	1985(25)	8670(19)	4794(16)	126(16)*
C(46)	2284(17)	7607(13)	4917(13)	81(9)*

\* Equivalent isotropic U defined as one third of the trace of the orthogonalised  $U_{ij}$  tensor.

TABLE 5.5

Atomic coordinates ( $\times 10^4$ ) for [15] (standard deviations in parentheses).

atom	x	y	z
Sn(1)	4586.4(7)	5942.8(8)	4664.7(6)
Sn(2)	2410.8(8)	6378.8(9)	3993.0(7)
Sn(3)	3037.9(7)	4966.9(9)	5283.2(6)
Cl(11)	4756(4)	8367(4)	6184(3)
Cl(12)	3402(4)	7521(5)	6753(3)
Cl(13)	3044(4)	8401(4)	5670(4)
Cl(21)	4837(4)	3864(4)	2979(3)
Cl(22)	4806(5)	5726(5)	2553(3)
Cl(23)	3283(4)	4622(6)	2453(3)
Cl(31)	-315(3)	6411(5)	4883(4)
Cl(32)	726(4)	7764(4)	5520(3)
Cl(33)	441(5)	5947(5)	5958(4)
Cl(41)	1664(4)	2253(4)	4236(4)
Cl(42)	1434(4)	3341(5)	3204(3)
Cl(43)	3115(4)	2802(4)	3652(3)
C(10)	3105(5)	9344(5)	3911(5)
Cl(51)	4029(5)	9403(5)	4376(5)
Cl(52)	2217(5)	9640(5)	4279(5)
Cl(53)	3190(5)	10145(5)	3350(5)
Cl(54)	2338(5)	10247(5)	3830(5)
Cl(55)	3653(5)	9268(5)	3295(5)
Cl(56)	3828(5)	9603(5)	4494(5)
O(1)	3312(7)	6195(7)	5815(5)
O(2)	4516(6)	6740(7)	5469(5)
O(3)	4500(6)	5145(7)	3878(5)
O(4)	3360(7)	5833(8)	3433(5)
O(5)	1761(6)	5520(8)	5271(6)
O(6)	1526(8)	6621(9)	4614(6)
O(7)	2004(7)	4817(9)	3957(6)
O(8)	2600(7)	3941(7)	4663(5)
O(9)	2995(9)	7705(10)	4065(7)
O(10)	2300(26)	8320(32)	4236(22)
O(10a)	3107(25)	8190(29)	3257(20)
O(11)	3231(6)	5920(7)	4622(5)
O(12)	5730(6)	5219(6)	4886(5)
C(1)	3898(10)	6792(11)	5749(8)
C(2)	3803(13)	7695(12)	6095(10)
C(3)	3985(10)	5304(12)	3469(8)
C(4)	4209(11)	4872(14)	2904(9)
C(5)	1367(10)	6231(14)	5057(9)
C(6)	598(12)	6593(12)	5326(9)
C(7)	2226(10)	4051(12)	4199(10)
C(8)	2106(11)	3132(15)	3818(10)
C(9)	2950(28)	8403(32)	3846(24)
C(9a)	3303(44)	7950(51)	3590(36)

**TABLE 5.5 cont.**

C(11)	5156(10)	7171(11)	4345(8)
C(12)	5105(11)	7403(14)	3798(10)
C(13)	5565(16)	8205(20)	3619(13)
C(14)	6029(20)	8724(18)	3959(13)
C(15)	6144(12)	8452(14)	4536(11)
C(16)	5699(12)	7690(14)	4738(10)
C(21)	1482(12)	6575(14)	3324(9)
C(22)	1738(13)	6909(17)	2823(12)
C(24)	364(25)	6847(26)	2386(16)
C(25)	55(21)	6465(26)	2855(16)
C(26)	644(13)	6359(18)	3352(13)
C(31)	2779(10)	4148(12)	5990(8)
C(32)	2981(17)	4437(16)	6537(11)
C(33)	2793(16)	3850(18)	6976(14)
C(34)	2370(13)	3049(16)	6887(11)
C(35)	2131(16)	2755(18)	6375(11)
C(36)	2367(12)	3302(14)	5911(11)
C(41)	1470(21)	4875(32)	1287(20)
C(42)	1239(26)	4726(37)	767(22)
C(43)	592(15)	4252(18)	631(14)
C(44)	111(17)	4086(30)	1046(22)
C(45)	117(30)	4116(25)	1587(26)
C(46)	919(28)	4653(25)	1658(22)

\* Equivalent isotropic U defined as one third of the trace of the  
orthogonalised  $U_{ij}$  tensor.

**TABLE 5.6**

**Atomic coordinates ( $\times 10^4$ ) for [16] (standard deviations in parentheses).**

atom	x	y	z	U
Sn(1)	3673.1(2)	5519.0(2)	6404.4(2)	35(1)*
C1(1)	1676.2(15)	4086.0(16)	10031.8(12)	88(3)*
C1(2)	2641.2(17)	2237.5(13)	10037.7(12)	103(3)*
C1(3)	1025.0(14)	3887.1(20)	9455.3(16)	106(4)*
O(1)	4878(2)	4101(2)	6473(2)	36(4)*
O(2)	3316(3)	3384(3)	7874(2)	48(5)*
O(3)	2767(2)	4722(3)	7919(2)	46(5)*
C(1)	2800(3)	3913(4)	8291(4)	40(6)*
C(2)	2072(4)	3539(4)	9416(4)	51(7)*
C(3)	3803(4)	5837(4)	7003(4)	47(7)*
C(4)	3743(6)	5198(6)	7974(5)	86(13)*
C(5)	3882(7)	5370(7)	8357(6)	111(18)*
C(6)	3986(7)	6222(7)	7813(7)	108(18)*
C(7)	4071(9)	6813(8)	6889(8)	160(28)*
C(8)	3982(7)	6623(6)	6470(6)	111(18)*
C(9)	-276(9)	5552(9)	2559(9)	169(27)*
C(10)	586(9)	4969(9)	2624(7)	136(25)*
C(11)	1117(10)	4143(11)	2573(14)	201(38)*

\* Equivalent isotropic U defined as one third of the trace of the orthogonalised  $U_{ij}$  tensor.



TABLE 5.7

Atomic coordinates ( $\times 10^4$ ) for [17] (standard deviations in parentheses).

atom	x	y	z	U
Sn(1)	9508.8(7)	347.8(6)	6332.9(3)	46(1)*
Sn(2)	9122.1(7)	-638.9(6)	8440.7(3)	48(1)*
C1(1)	8059(5)	3694(3)	5347(2)	131(2)*
C1(2)	9576(5)	4147(3)	3896(3)	149(2)*
C1(3)	6947(4)	3191(4)	4180(3)	134(2)*
C1(4)	11619(4)	-4493(3)	9406(2)	92(1)*
C1(5)	10569(5)	-5182(3)	8244(3)	139(2)*
C1(6)	13361(4)	-4596(4)	8030(2)	145(2)*
C1(7)	6164(5)	3066(4)	8644(2)	130(2)*
C1(8)	7792(5)	4437(3)	7409(3)	176(3)*
C1(9)	5603(4)	3112(5)	7251(3)	171(3)*
O(1)	9423(7)	1399(6)	3970(3)	60(3)*
O(2)	9071(7)	1197(6)	5164(4)	68(3)*
O(3)	10299(7)	-2392(6)	8612(4)	62(3)*
O(4)	11833(8)	-2326(7)	7586(4)	91(4)*
O(5)	7899(7)	1087(6)	8118(3)	65(3)*
O(6)	8453(7)	1923(6)	6948(3)	57(3)*
O(7)	9944(6)	-581(5)	7366(3)	50(2)*
C(1)	9039(9)	1787(9)	4568(5)	44(4)*
C(2)	8466(10)	3161(9)	4503(5)	56(4)*
C(3)	11266(10)	-2832(9)	8175(5)	54(4)*
C(4)	11739(11)	-4213(10)	8456(6)	70(5)*
C(5)	7856(9)	1900(9)	7588(5)	49(4)*
C(6)	6920(11)	3093(9)	7735(5)	64(5)*
C(7)	7577(10)	-413(9)	6492(5)	55(4)*
C(8)	7438(11)	-1674(10)	6828(6)	72(5)*
C(9)	6165(12)	-2189(11)	6990(7)	94(6)*
C(10)	5033(12)	-1472(12)	6834(7)	90(6)*
C(11)	5206(13)	-268(12)	6503(7)	102(7)*
C(12)	6436(11)	261(11)	6336(6)	75(5)*
C(13)	11251(10)	1449(9)	6048(5)	56(4)*
C(14)	12112(12)	1496(12)	5383(6)	82(6)*
C(15)	13225(13)	2231(12)	5200(7)	109(7)*
C(16)	13500(14)	2931(12)	5685(8)	98(7)*
C(17)	12693(12)	2893(11)	6359(8)	87(6)*
C(18)	11557(11)	2159(10)	6549(6)	68(5)*
C(19)	10374(12)	458(8)	8828(5)	52(4)*
C(20)	11788(15)	423(11)	8553(7)	84(6)*
C(21)	12643(15)	1128(13)	8777(8)	105(7)*
C(22)	12144(18)	1907(13)	9252(8)	89(7)*
C(23)	10811(18)	2001(11)	9543(6)	85(6)*
C(24)	9914(12)	1275(10)	9311(5)	68(5)*
C(25)	7286(11)	-1580(10)	8868(5)	63(5)*
C(26)	7253(12)	-2873(11)	8957(7)	93(6)*
C(27)	6069(16)	-3476(14)	9242(8)	115(8)*
C(28)	4901(15)	-2781(14)	9452(8)	111(8)*
C(29)	4898(15)	-1532(17)	9382(8)	120(8)*
C(30)	6104(12)	-912(11)	9076(7)	94(6)*

\* Equivalent isotropic U defined as one third of the trace of the

orthogonalised  $U_{ij}$  tensor.

TABLE 5.8

Bond lengths (Å)

and angles (°) for [12] (standard deviations in parentheses).

a) Bond lengths

Sn(1)-O(11)	2.162 (5)	Sn(1)-O(1)	2.162 (5)
Sn(1)-C(11)	2.106 (7)	Sn(1)-C(17)	2.115 (7)
Cl(1)-C(2)	1.721 (7)	Cl(2)-C(2)	1.748 (8)
Cl(3)-C(2)	1.707 (8)	O(1)-C(1)	1.239 (8)
O(2)-C(1)	1.222 (9)	C(1)-C(2)	1.564 (9)
C(11)-C(12)	1.375 (10)	C(11)-C(16)	1.385 (10)
C(12)-C(13)	1.376 (11)	C(13)-C(14)	1.372 (12)
C(14)-C(15)	1.350 (14)	C(15)-C(16)	1.380 (13)
C(17)-C(18)	1.379 (11)	C(17)-C(112)	1.383 (11)
C(18)-C(19)	1.353 (11)	C(19)-C(110)	1.355 (13)
C(110)-C(111)	1.385 (14)	C(111)-C(112)	1.395 (11)

b) Bond angles

O(1)-Sn(1)-O(11)	158.2(2)	C(11)-Sn(1)-O(11)	96.1(2)
C(11)-Sn(1)-O(1)	91.8(2)	C(17)-Sn(1)-O(11)	96.4(2)
C(17)-Sn(1)-O(1)	92.4(2)	C(17)-Sn(1)-C(11)	134.1(3)
C(1)-O(1)-Sn(1)	128.7(4)	O(2)-C(1)-O(1)	128.2(6)
C(2)-C(1)-O(1)	113.3(6)	C(2)-C(1)-O(2)	118.4(6)
Cl(2)-C(2)-Cl(1)	107.2(4)	Cl(3)-C(2)-Cl(1)	112.9(5)
Cl(3)-C(2)-Cl(2)	107.8(4)	C(1)-C(2)-Cl(1)	107.5(5)
C(1)-C(2)-Cl(2)	112.0(5)	C(1)-C(2)-Cl(3)	109.5(5)
C(12)-C(11)-Sn(1)	121.6(5)	C(16)-C(11)-Sn(1)	118.6(6)
C(16)-C(11)-C(12)	119.8(7)	C(13)-C(12)-C(11)	119.8(7)
C(14)-C(13)-C(12)	119.9(8)	C(15)-C(14)-C(13)	120.8(9)
C(16)-C(15)-C(14)	120.1(9)	C(15)-C(16)-C(11)	119.6(9)
C(18)-C(17)-Sn(1)	120.5(5)	C(112)-C(17)-Sn(1)	120.2(5)
C(112)-C(17)-C(18)	119.3(7)	C(19)-C(18)-C(17)	120.6(8)
C(110)-C(19)-C(18)	121.0(8)	C(111)-C(110)-C(19)	120.4(7)
C(112)-C(111)-C(110)	118.9(8)	C(111)-C(112)-C(17)	119.8(8)

**TABLE 5.9**

**Bond lengths (Å) and angles (°) for [13]**

(standard deviations in parentheses).

**a) Bond lengths**

Sn(1)-O(1)	2.154(4)	Sn(1)-C(11)	2.115(8)
Sn(1)-C(17)	2.107(8)	Sn(1)-O(1a)	2.062(5)
Sn(1)-O(22a)	2.323(6)	Sn(2)-O(1)	2.031(5)
Sn(2)-O(11)	2.212(5)	Sn(2)-C(21)	2.129(7)
Sn(2)-C(27)	2.113(8)	Sn(2)-O(21)	2.250(5)
Cl(11)-C(114)	1.735(10)	Cl(12)-C(114)	1.740(10)
Cl(13)-C(114)	1.765(9)	Cl(21)-C(214)	1.738(9)
Cl(22)-C(214)	1.752(9)	Cl(23)-C(214)	1.766(9)
O(1)-Sn(1a)	2.063(5)	C(11)-C(12)	1.362(13)
C(11)-C(16)	1.408(13)	C(12)-C(13)	1.386(15)
C(13)-C(14)	1.364(19)	C(14)-C(15)	1.378(16)
C(15)-C(16)	1.368(13)	C(17)-C(18)	1.332(11)
C(17)-C(112)	1.388(12)	C(18)-C(19)	1.376(14)
C(19)-C(110)	1.325(14)	C(110)-C(111)	1.355(14)
C(111)-C(112)	1.376(15)	C(113)-O(11)	1.259(11)
C(113)-O(12)	1.209(10)	C(113)-C(114)	1.556(10)
C(21)-C(22)	1.365(13)	C(21)-C(26)	1.393(12)
C(22)-C(23)	1.380(14)	C(23)-C(24)	1.363(16)
C(24)-C(25)	1.361(17)	C(25)-C(26)	1.336(13)
C(27)-C(28)	1.381(11)	C(27)-C(212)	1.384(12)
C(28)-C(29)	1.382(13)	C(29)-C(210)	1.338(14)
C(210)-C(211)	1.334(13)	C(211)-C(212)	1.385(14)
C(213)-O(21)	1.222(11)	C(213)-O(22)	1.219(11)
C(213)-C(214)	1.548(10)		

**b) Bond angles**

O(1)-Sn(1)-C(11)	99.2(2)	O(1)-Sn(1)-C(17)	99.9(2)
C(11)-Sn(1)-C(17)	149.6(3)	O(1)-Sn(1)-O(1a)	76.4(2)
C(11)-Sn(1)-O(1a)	103.2(3)	C(17)-Sn(1)-O(1a)	104.1(3)
O(1)-Sn(1)-O(22a)	170.0(2)	C(11)-Sn(1)-O(22a)	82.0(2)
C(17)-Sn(1)-O(22a)	83.3(3)	O(1)-Sn(2)-O(11)	80.7(2)
O(1)-Sn(2)-C(21)	107.3(3)	O(11)-Sn(2)-C(21)	95.6(2)
O(1)-Sn(2)-C(27)	106.9(3)	O(11)-Sn(2)-C(27)	94.3(2)
C(21)-Sn(2)-C(27)	145.5(3)	O(1)-Sn(2)-O(21)	92.0(2)
O(11)-Sn(2)-O(21)	172.7(2)	C(21)-Sn(2)-O(21)	87.1(2)
C(27)-Sn(2)-O(21)	87.3(3)	Sn(1)-O(1)-Sn(2)	122.8(2)
Sn(1)-O(1)-Sn(1a)	103.6(2)	Sn(2)-O(1)-Sn(1a)	133.7(2)
Sn(1)-C(11)-C(12)	125.1(7)	Sn(1)-C(11)-C(16)	116.7(6)
C(12)-C(11)-C(16)	117.6(8)	C(11)-C(12)-C(13)	121.4(10)
C(12)-C(13)-C(14)	119.7(11)	C(13)-C(14)-C(15)	120.7(10)
C(14)-C(15)-C(16)	118.9(10)	C(11)-C(16)-C(15)	121.6(9)

**TABLE 5.9 cont.**

Sn(1)-C(17)-C(18)	120.4(6)	Sn(1)-C(17)-C(112)	123.7(6)
C(18)-C(17)-C(112)	115.8(8)	C(17)-C(18)-C(19)	122.9(9)
C(18)-C(19)-C(110)	120.8(10)	C(19)-C(110)-C(111)	119.1(10)
C(110)-C(111)-C(112)	119.9(9)	C(17)-C(112)-C(111)	121.5(9)
O(11)-C(113)-O(12)	126.1(7)	O(11)-C(113)-C(114)	117.2(7)
O(12)-C(113)-C(114)	116.8(8)	Sn(2)-O(11)-C(113)	108.6(4)
Cl(11)-C(114)-Cl(12)	110.1(5)	Cl(11)-C(114)-Cl(13)	108.9(5)
Cl(12)-C(114)-Cl(13)	109.0(5)	Cl(11)-C(114)-C(113)	110.7(6)
Cl(12)-C(114)-C(113)	111.6(6)	Cl(13)-C(114)-C(113)	106.4(5)
Sn(2)-C(21)-C(22)	118.9(6)	Sn(2)-C(21)-C(26)	125.0(6)
C(22)-C(21)-C(26)	116.0(8)	C(21)-C(22)-C(23)	121.8(9)
C(22)-C(23)-C(24)	119.4(10)	C(23)-C(24)-C(25)	120.0(10)
C(24)-C(25)-C(26)	119.7(10)	C(21)-C(26)-C(25)	123.0(9)
Sn(2)-C(27)-C(28)	121.3(6)	Sn(2)-C(27)-C(212)	120.8(6)
C(28)-C(27)-C(212)	118.0(8)	C(27)-C(28)-C(29)	120.1(8)
C(28)-C(29)-C(210)	120.6(8)	C(29)-C(210)-C(211)	120.8(10)
C(210)-C(211)-C(212)	120.6(9)	C(27)-C(212)-C(211)	120.0(8)
O(21)-C(213)-O(22)	127.0(7)	O(21)-C(213)-C(214)	116.8(8)
O(22)-C(213)-C(214)	116.2(7)	Sn(2)-O(21)-C(213)	139.0(6)
C(213)-O(22)-Sn(1a)	133.0(5)	Cl(21)-C(214)-Cl(22)	110.1(4)
Cl(21)-C(214)-Cl(23)	108.7(5)	Cl(22)-C(214)-Cl(23)	109.2(4)
Cl(21)-C(214)-C(213)	112.1(6)	Cl(22)-C(214)-C(213)	110.1(6)
Cl(23)-C(214)-C(213)	106.6(5)		

**TABLE 5.10**

**Bond lengths (Å) and angles (°) for [14]**

(standard deviations in parentheses).

**a) Bond lengths**

Sn(1)-O(2)	2.432(10)	Sn(1)-O(5)	2.138(10)
Sn(1)-C(11)	2.127(13)	Sn(1)-C(21)	2.118(14)
Sn(1)-O(4a)	2.400(14)	Sn(1)-O(5a)	2.131(8)
Sn(2)-O(1)	2.207(11)	Sn(2)-O(3)	2.199(12)
Sn(2)-O(5)	2.015(9)	Sn(2)-C(31)	2.186(16)
Sn(2)-C(41)	2.126(16)	C(2)-Cl(11)	1.740
C(2)-Cl(12)	1.740	C(2)-Cl(13)	1.740
C(2)-Cl(14)	1.740	C(2)-Cl(15)	1.740
C(2)-Cl(16)	1.740	C(2)-C(1)	1.552(15)
Cl(21)-C(4)	1.697(20)	Cl(22)-C(4)	1.856(25)
Cl(23)-C(4)	1.700(24)	O(1)-C(1)	1.202(22)
O(2)-C(1)	1.206(22)	O(3)-C(3)	1.251(20)
O(4)-C(3)	1.243(24)	C(3)-C(4)	1.540(32)
C(11)-C(12)	1.378(22)	C(11)-C(16)	1.338(25)
C(12)-C(13)	1.394(24)	C(13)-C(14)	1.373(34)
C(14)-C(15)	1.406(32)	C(15)-C(16)	1.432(27)
C(21)-C(22)	1.448(24)	C(21)-C(26)	1.399(22)
C(22)-C(23)	1.361(21)	C(23)-C(24)	1.394(27)
C(24)-C(25)	1.294(28)	C(25)-C(26)	1.369(22)
C(31)-C(32)	1.428(26)	C(31)-C(36)	1.290(27)
C(32)-C(33)	1.331(28)	C(33)-C(34)	1.442(39)
C(34)-C(35)	1.319(34)	C(35)-C(36)	1.380(26)
C(41)-C(42)	1.394(24)	C(41)-C(46)	1.355(26)
C(42)-C(43)	1.332(30)	C(43)-C(44)	1.358(36)
C(44)-C(45)	1.412(40)	C(45)-C(46)	1.410(29)

**b) Bond angles**

O(2)-Sn(1)-O(5)	91.8(4)	O(2)-Sn(1)-C(11)	81.9(5)
O(5)-Sn(1)-C(11)	98.7(5)	O(2)-Sn(1)-C(21)	80.8(4)
O(5)-Sn(1)-C(21)	101.8(5)	C(11)-Sn(1)-C(21)	153.4(5)
O(2)-Sn(1)-O(4a)	99.2(4)	O(5)-Sn(1)-O(4a)	168.9(3)
C(11)-Sn(1)-O(4a)	81.9(6)	C(21)-Sn(1)-O(4a)	81.2(5)
O(2)-Sn(1)-O(5a)	168.0(4)	O(5)-Sn(1)-O(5a)	76.1(4)
C(11)-Sn(1)-O(5a)	100.2(4)	C(21)-Sn(1)-O(5a)	101.0(4)
O(4a)-Sn(1)-O(5a)	92.8(4)	O(1)-Sn(2)-O(3)	171.6(5)
O(1)-Sn(2)-O(5)	94.1(4)	O(3)-Sn(2)-O(5)	94.3(4)
O(1)-Sn(2)-C(31)	87.1(5)	O(3)-Sn(2)-C(31)	90.0(5)
O(5)-Sn(2)-C(31)	113.6(5)	O(1)-Sn(2)-C(41)	90.2(6)
O(3)-Sn(2)-C(41)	86.2(6)	O(5)-Sn(2)-C(41)	112.2(5)
C(31)-Sn(2)-C(41)	134.2(6)	Cl(11)-C(2)-Cl(12)	109.5
Cl(11)-C(2)-Cl(13)	109.5	Cl(12)-C(2)-Cl(13)	109.5
Cl(14)-C(2)-Cl(15)	109.5	Cl(14)-C(2)-Cl(16)	109.5
Cl(15)-C(2)-Cl(16)	109.5	Cl(11)-C(2)-C(1)	109.1(6)

**TABLE 5.10 cont.**

Cl(12)-C(2)-C(1)	109.3(8)	Cl(13)-C(2)-C(1)	110.0(7)
Cl(14)-C(2)-C(1)	109.9(8)	Cl(15)-C(2)-C(1)	109.0(6)
Cl(16)-C(2)-C(1)	109.5(7)	Sn(2)-O(1)-C(1)	133.0(10)
Sn(1)-O(2)-C(1)	124.9(10)	Sn(2)-O(3)-C(3)	133.7(13)
C(3)-O(4)-Sn(1a)	128.7(12)	Sn(1)-O(5)-Sn(2)	127.8(4)
Sn(1)-O(5)-Sn(1a)	103.9(4)	Sn(2)-O(5)-Sn(1a)	128.3(5)
C(2)-C(1)-O(1)	114.5(14)	C(2)-C(1)-O(2)	116.6(14)
O(1)-C(1)-O(2)	128.8(14)	O(3)-C(3)-O(4)	126.0(20)
O(3)-C(3)-C(4)	116.7(18)	O(4)-C(3)-C(4)	117.2(15)
Cl(21)-C(4)-Cl(22)	105.5(10)	Cl(21)-C(4)-Cl(23)	113.8(13)
Cl(22)-C(4)-Cl(23)	105.5(13)	Cl(21)-C(4)-C(3)	111.0(16)
Cl(22)-C(4)-C(3)	106.4(14)	Cl(23)-C(4)-C(3)	113.9(13)
Sn(1)-C(11)-C(12)	120.2(11)	Sn(1)-C(11)-C(16)	119.3(11)
C(12)-C(11)-C(16)	120.2(14)	C(11)-C(12)-C(13)	121.0(17)
C(12)-C(13)-C(14)	119.7(20)	C(13)-C(14)-C(15)	119.8(20)
C(14)-C(15)-C(16)	118.5(20)	C(11)-C(16)-C(15)	120.6(18)
Sn(1)-C(21)-C(22)	119.7(11)	Sn(1)-C(21)-C(26)	121.8(11)
C(22)-C(21)-C(26)	118.3(13)	C(21)-C(22)-C(23)	117.4(16)
C(22)-C(23)-C(24)	121.0(18)	C(23)-C(24)-C(25)	121.7(15)
C(24)-C(25)-C(26)	121.4(18)	C(21)-C(26)-C(25)	120.2(16)
Sn(2)-C(31)-C(32)	115.9(13)	Sn(2)-C(31)-C(36)	120.7(12)
C(32)-C(31)-C(36)	123.3(17)	C(31)-C(32)-C(33)	116.7(22)
C(32)-C(33)-C(34)	119.8(20)	C(33)-C(34)-C(35)	120.0(20)
C(34)-C(35)-C(36)	120.2(23)	C(31)-C(36)-C(35)	119.9(19)
Sn(2)-C(41)-C(42)	118.5(12)	Sn(2)-C(41)-C(46)	120.8(13)
C(42)-C(41)-C(46)	120.6(16)	C(41)-C(42)-C(43)	119.6(18)
C(42)-C(43)-C(44)	122.0(22)	C(43)-C(44)-C(45)	120.2(23)
C(44)-C(45)-C(46)	117.2(23)	C(41)-C(46)-C(45)	120.3(21)

TABLE 5.11

Bond lengths (Å) and angles (°) for [15]  
(standard deviations in parentheses).

a) Bond lengths

Sn(1)-O(2)	2.213(12)	Sn(1)-O(3)	2.162(12)
Sn(1)-O(11)	2.124(9)	Sn(1)-O(12)	2.094(9)
Sn(1)-C(11)	2.111(16)	Sn(1)-O(12a)	2.030(10)
Sn(2)-O(4)	2.208(12)	Sn(2)-O(6)	2.126(14)
Sn(2)-O(7)	2.285(12)	Sn(2)-O(9)	2.080(14)
Sn(2)-O(11)	1.994(10)	Sn(2)-C(21)	2.080(20)
Sn(3)-O(1)	2.156(11)	Sn(3)-O(5)	2.149(10)
Sn(3)-O(8)	2.125(11)	Sn(3)-O(11)	2.095(11)
Sn(3)-C(31)	2.092(19)	Sn(3)-O(12a)	2.024(10)
Cl(11)-C(2)	1.768(20)	Cl(12)-C(2)	1.738(25)
Cl(13)-C(2)	1.795(21)	Cl(21)-C(4)	1.728(20)
Cl(22)-C(4)	1.768(21)	Cl(23)-C(4)	1.768(19)
Cl(31)-C(6)	1.725(20)	Cl(32)-C(6)	1.715(19)
Cl(33)-C(6)	1.779(23)	Cl(41)-C(8)	1.756(23)
Cl(42)-C(8)	1.748(22)	Cl(43)-C(8)	1.726(20)
C(10)-Cl(51)	1.750	C(10)-Cl(52)	1.749
C(10)-Cl(53)	1.749	C(10)-Cl(54)	1.749
C(10)-Cl(55)	1.751	C(10)-Cl(56)	1.750
C(10)-C(9)	1.352(46)	O(1)-C(1)	1.265(19)
O(2)-C(1)	1.218(20)	O(3)-C(3)	1.227(20)
O(4)-C(3)	1.228(20)	O(5)-C(5)	1.260(22)
O(6)-C(5)	1.223(25)	O(7)-C(7)	1.255(22)
O(8)-C(7)	1.212(24)	O(9)-C(9)	1.109(50)
O(9)-C(9a)	1.301(85)	O(10)-C(9)	1.433(72)
O(10a)-C(9)	1.460(74)	O(10a)-C(9a)	0.887(91)
C(1)-C(2)	1.523(26)	C(3)-C(4)	1.531(28)
C(5)-C(6)	1.498(27)	C(7)-C(8)	1.576(29)
C(11)-C(12)	1.327(30)	C(11)-C(16)	1.412(26)
C(12)-C(13)	1.420(34)	C(13)-C(14)	1.269(39)
C(14)-C(15)	1.410(39)	C(15)-C(16)	1.385(29)
C(21)-C(22)	1.362(35)	C(21)-C(26)	1.358(28)
C(22)-C(23)	1.363(38)	C(23)-C(24)	1.257(47)
C(24)-C(25)	1.355(54)	C(25)-C(26)	1.440(44)
C(31)-C(32)	1.366(31)	C(31)-C(36)	1.358(25)
C(32)-C(33)	1.374(40)	C(33)-C(34)	1.316(34)
C(34)-C(35)	1.303(35)	C(35)-C(36)	1.411(35)
C(41)-C(42)	1.268(68)	C(41)-C(46)	1.316(65)
C(42)-C(43)	1.236(49)	C(43)-C(44)	1.305(54)
C(44)-C(45)	1.274(81)	C(45)-C(46)	1.468(60)

TABLE 5.11 cont.

## b) Bond angles

O(2)-Sn(1)-O(3)	173.5(4)	O(2)-Sn(1)-O(11)	85.9(4)
O(3)-Sn(1)-O(11)	87.6(4)	O(2)-Sn(1)-O(12)	97.7(4)
O(3)-Sn(1)-O(12)	87.5(4)	O(11)-Sn(1)-O(12)	147.3(4)
O(2)-Sn(1)-C(11)	86.8(6)	O(3)-Sn(1)-C(11)	96.7(6)
O(11)-Sn(1)-C(11)	116.6(5)	O(12)-Sn(1)-C(11)	96.1(5)
O(2)-Sn(1)-O(12a)	85.9(4)	O(3)-Sn(1)-O(12a)	91.7(4)
O(11)-Sn(1)-O(12a)	74.1(4)	O(12)-Sn(1)-O(12a)	73.8(4)
C(11)-Sn(1)-O(12a)	166.6(5)	O(4)-Sn(2)-O(6)	168.0(5)
O(4)-Sn(2)-O(6)	168.0(5)	O(4)-Sn(2)-O(7)	81.1(4)
O(6)-Sn(2)-O(7)	89.0(5)	O(4)-Sn(2)-O(9)	92.6(5)
O(6)-Sn(2)-O(9)	96.2(6)	O(7)-Sn(2)-O(9)	169.9(5)
O(4)-Sn(2)-O(11)	84.6(4)	O(6)-Sn(2)-O(11)	87.6(5)
O(7)-Sn(2)-O(11)	83.0(4)	O(9)-Sn(2)-O(11)	88.5(5)
O(4)-Sn(2)-C(21)	93.4(7)	O(6)-Sn(2)-C(21)	92.5(7)
O(7)-Sn(2)-C(21)	85.6(6)	O(9)-Sn(2)-C(21)	102.8(7)
O(11)-Sn(2)-C(21)	168.6(6)	O(1)-Sn(3)-O(5)	82.0(4)
O(1)-Sn(3)-O(8)	168.7(4)	O(5)-Sn(3)-O(8)	89.4(4)
O(1)-Sn(3)-O(11)	83.5(4)	O(5)-Sn(3)-O(11)	87.1(4)
O(8)-Sn(3)-O(11)	88.8(4)	O(1)-Sn(3)-C(31)	91.2(6)
O(5)-Sn(3)-C(31)	88.2(6)	O(8)-Sn(3)-C(31)	95.9(6)
O(11)-Sn(3)-C(31)	173.3(6)	O(1)-Sn(3)-O(12a)	93.9(4)
O(5)-Sn(3)-O(12a)	161.9(4)	O(8)-Sn(3)-O(12a)	92.0(4)
O(11)-Sn(3)-O(12a)	74.8(4)	C(31)-Sn(3)-O(12a)	109.6(5)
Cl(51)-C(10)-Cl(52)	109.5	Cl(51)-C(10)-Cl(53)	109.5
Cl(52)-C(10)-Cl(53)	109.5	Cl(54)-C(10)-Cl(55)	109.5
Cl(54)-C(10)-Cl(56)	109.5	Cl(55)-C(10)-Cl(56)	109.5
Cl(51)-C(10)-C(9)	104.5(20)	Cl(52)-C(10)-C(9)	98.4(21)
Cl(53)-C(10)-C(9)	124.5(24)	Cl(54)-C(10)-C(9)	125.5(19)
Cl(55)-C(10)-C(9)	86.6(24)	Cl(56)-C(10)-C(9)	113.1(22)
Sn(3)-O(1)-C(1)	125.0(12)	Sn(1)-O(2)-C(1)	126.2(10)
Sn(1)-O(3)-C(3)	124.8(11)	Sn(2)-O(4)-C(3)	138.0(12)
Sn(3)-O(5)-C(5)	136.1(11)	Sn(2)-O(6)-C(5)	134.9(12)
Sn(2)-O(7)-C(7)	137.8(11)	Sn(3)-O(8)-C(7)	129.9(11)
Sn(2)-O(9)-O(10)	102.4(19)	Sn(2)-O(9)-C(9)	138.0(27)
O(10)-O(9)-C(9)	65.7(33)	Sn(2)-O(9)-C(9a)	111.0(34)
O(10)-O(9)-C(9a)	114.5(39)	Sn(1)-O(11)-Sn(2)	128.0(6)
Sn(1)-O(11)-Sn(3)	100.3(4)	Sn(2)-O(11)-Sn(3)	129.6(5)
Sn(1)-O(12)-Sn(1a)	106.2(4)	Sn(1)-O(12)-Sn(3a)	146.0(6)
Sn(1a)-O(12)-Sn(3a)	106.1(4)	O(1)-C(1)-O(2)	130.3(15)
O(1)-C(1)-C(2)	112.5(16)	O(2)-C(1)-C(2)	117.2(14)
Cl(11)-C(2)-Cl(12)	109.5(12)	Cl(11)-C(2)-Cl(13)	106.9(10)
Cl(12)-C(2)-Cl(13)	107.6(11)	Cl(11)-C(2)-C(1)	113.0(14)
Cl(12)-C(2)-C(1)	114.8(13)	Cl(13)-C(2)-C(1)	104.5(14)
O(3)-C(3)-O(4)	129.6(18)	O(3)-C(3)-C(4)	115.4(15)
O(4)-C(3)-C(4)	114.6(16)	Cl(21)-C(4)-Cl(22)	106.5(10)
Cl(21)-C(4)-Cl(23)	109.6(11)	Cl(22)-C(4)-Cl(23)	107.2(11)
Cl(21)-C(4)-C(3)	113.9(14)	Cl(22)-C(4)-C(3)	107.8(13)
Cl(23)-C(4)-C(3)	111.6(13)	O(5)-C(5)-O(6)	124.7(17)
O(5)-C(5)-C(6)	119.2(18)	O(6)-C(5)-C(6)	115.8(16)
Cl(31)-C(6)-Cl(32)	112.2(11)	Cl(31)-C(6)-Cl(33)	105.5(11)
Cl(32)-C(6)-Cl(33)	106.7(12)	Cl(31)-C(6)-C(5)	110.7(15)
Cl(32)-C(6)-C(5)	110.9(13)	Cl(33)-C(6)-C(5)	110.5(13)



**TABLE 5.11 cont.**

O(7)-C(7)-O(8)	128.1(17)	O(7)-C(7)-C(8)	115.3(18)
O(8)-C(7)-C(8)	116.0(15)	Cl(41)-C(8)-Cl(42)	110.1(10)
Cl(41)-C(8)-Cl(43)	110.5(12)	Cl(42)-C(8)-Cl(43)	111.2(13)
Cl(41)-C(8)-C(7)	106.9(15)	Cl(42)-C(8)-C(7)	111.8(14)
Cl(43)-C(8)-C(7)	106.2(12)	C(10)-C(9)-O(9)	143.9(49)
C(10)-C(9)-O(10)	97.9(36)	O(9)-C(9)-O(10)	69.5(34)
C(10)-C(9)-O(10a)	105.5(38)	O(9)-C(9)-O(10a)	104.7(39)
O(9)-C(9a)-O(10a)	137.4(79)	Sn(1)-C(11)-C(12)	123.6(13)
Sn(1)-C(11)-C(16)	116.0(14)	C(12)-C(11)-C(16)	119.9(17)
C(11)-C(12)-C(13)	119.3(20)	C(12)-C(13)-C(14)	123.3(27)
C(13)-C(14)-C(15)	118.4(26)	C(14)-C(15)-C(16)	120.9(21)
C(11)-C(16)-C(15)	117.9(20)	Sn(2)-C(21)-C(22)	117.7(14)
Sn(2)-C(21)-C(26)	124.0(18)	C(22)-C(21)-C(26)	118.3(21)
C(21)-C(22)-C(23)	119.0(21)	C(22)-C(23)-C(24)	124.4(32)
C(23)-C(24)-C(25)	121.0(35)	C(24)-C(25)-C(26)	117.1(30)
C(21)-C(26)-C(25)	120.1(27)	Sn(3)-C(31)-C(32)	122.9(14)
Sn(3)-C(31)-C(36)	119.6(15)	C(32)-C(31)-C(36)	117.5(20)
C(31)-C(32)-C(33)	119.0(22)	C(32)-C(33)-C(34)	122.1(28)
C(33)-C(34)-C(35)	121.5(26)	C(34)-C(35)-C(36)	118.1(22)
C(31)-C(36)-C(35)	121.6(22)	C(42)-C(41)-C(46)	116.9(38)
C(41)-C(42)-C(43)	120.4(45)	C(42)-C(43)-C(44)	114.5(38)
C(43)-C(44)-C(45)	141.8(36)	C(44)-C(45)-C(46)	94.0(41)
C(41)-C(46)-C(45)	130.5(47)		

**TABLE 5.12**

**Bond lengths (Å) and angles (°) for [16]**

(standard deviations in parentheses).

**a) Bond lengths**

Sn(1)-O(1)	2.089(3)	Sn(1)-O(3)	2.183(3)
Sn(1)-C(3)	2.104(13)	Sn(1)-O(1a)	2.095(7)
Sn(1)-O(1b)	2.075(3)	Sn(1)-O(2a)	2.191(3)
Cl(1)-C(2)	1.757(12)	Cl(2)-C(2)	1.736(5)
Cl(3)-C(2)	1.744(11)	O(1)-Sn(1a)	2.076(3)
O(1)-Sn(1c)	2.095(7)	O(2)-C(1)	1.240(11)
O(2)-Sn(1c)	2.190(3)	O(3)-C(1)	1.244(10)
C(1)-C(2)	1.549(6)	C(3)-C(4)	1.391(11)
C(3)-C(8)	1.343(17)	C(4)-C(5)	1.387(29)
C(5)-C(6)	1.368(21)	C(6)-C(7)	1.308(17)
C(7)-C(8)	1.406(35)	C(9)-C(10)	1.327(25)
C(9)-C(9a)	1.332(60)	C(10)-C(11)	1.269(31)
C(11)-C(11a)	1.326(80)		

**b) Bond angles**

O(1)-Sn(1)-O(3)	86.6(1)	O(1)-Sn(1)-C(3)	101.0(2)
O(3)-Sn(1)-C(3)	90.4(2)	O(1)-Sn(1)-O(1a)	77.3(2)
O(3)-Sn(1)-O(1a)	86.2(2)	C(3)-Sn(1)-O(1a)	176.2(1)
O(1)-Sn(1)-O(1b)	104.6(1)	O(3)-Sn(1)-O(1b)	157.4(2)
C(3)-Sn(1)-O(1b)	106.2(2)	O(1a)-Sn(1)-O(1b)	77.5(2)
O(1)-Sn(1)-O(2a)	158.1(2)	O(3)-Sn(1)-O(2a)	76.7(1)
C(3)-Sn(1)-O(2a)	93.3(3)	O(1a)-Sn(1)-O(2a)	87.4(2)
O(1b)-Sn(1)-O(2a)	87.0(1)	Sn(1)-O(1)-Sn(1a)	131.5(2)
Sn(1)-O(1)-Sn(1c)	100.6(2)	Sn(1a)-O(1)-Sn(1c)	101.2(2)
C(1)-O(2)-Sn(1c)	127.7(4)	Sn(1)-O(3)-C(1)	129.4(4)
O(2)-C(1)-O(3)	128.6(4)	O(2)-C(1)-C(2)	115.8(7)
O(3)-C(1)-C(2)	115.5(7)	Cl(1)-C(2)-Cl(2)	108.8(5)
Cl(1)-C(2)-Cl(3)	108.9(3)	Cl(2)-C(2)-Cl(3)	109.5(6)
Cl(1)-C(2)-C(1)	112.0(7)	Cl(2)-C(2)-C(1)	110.6(3)
Cl(3)-C(2)-C(1)	106.9(6)	Sn(1)-C(3)-C(4)	119.9(9)
Sn(1)-C(3)-C(8)	122.6(9)	C(4)-C(3)-C(8)	117.5(14)
C(3)-C(4)-C(5)	120.4(11)	C(4)-C(5)-C(6)	119.7(11)
C(5)-C(6)-C(7)	120.0(21)	C(6)-C(7)-C(8)	120.7(17)
C(3)-C(8)-C(7)	121.3(10)	C(10)-C(9)-C(9a)	121.1(16)
C(9)-C(10)-C(11)	116.1(29)	C(10)-C(11)-C(11a)	122.7(19)

**TABLE 5.13**

**Bond lengths (Å) and angles (°) for [17]**

(standard deviations in parentheses).

**a) Bond lengths**

Sn(1)-O(2)	2.361(7)	Sn(1)-O(6)	2.277(6)
Sn(1)-O(7)	2.155(6)	Sn(1)-C(7)	2.098(10)
Sn(1)-C(13)	2.104(10)	Sn(1)-O(1a)	2.185(6)
Sn(2)-O(3)	2.157(6)	Sn(2)-O(5)	2.212(6)
Sn(2)-O(7)	2.021(5)	Sn(2)-C(19)	2.083(12)
Sn(2)-C(25)	2.108(11)	Cl(1)-C(2)	1.739(10)
Cl(2)-C(2)	1.709(10)	Cl(3)-C(2)	1.746(12)
Cl(4)-C(4)	1.750(11)	Cl(5)-C(4)	1.762(13)
Cl(6)-C(4)	1.712(11)	Cl(7)-C(6)	1.725(10)
Cl(8)-C(6)	1.698(11)	Cl(9)-C(6)	1.747(13)
O(1)-C(1)	1.244(12)	O(1)-Sn(1a)	2.185(6)
O(2)-C(1)	1.204(11)	O(3)-C(3)	1.255(11)
O(4)-C(3)	1.203(11)	O(5)-C(5)	1.220(11)
O(6)-C(5)	1.232(10)	C(1)-C(2)	1.535(13)
C(3)-C(4)	1.561(14)	C(5)-C(6)	1.556(13)
C(7)-C(8)	1.399(14)	C(7)-C(12)	1.364(15)
C(8)-C(9)	1.381(16)	C(9)-C(10)	1.377(17)
C(10)-C(11)	1.344(17)	C(11)-C(12)	1.349(18)
C(13)-C(14)	1.367(14)	C(13)-C(18)	1.396(17)
C(14)-C(15)	1.364(18)	C(15)-C(16)	1.351(21)
C(16)-C(17)	1.358(19)	C(17)-C(18)	1.382(16)
C(19)-C(20)	1.405(18)	C(19)-C(24)	1.355(14)
C(20)-C(21)	1.349(22)	C(21)-C(22)	1.321(20)
C(22)-C(23)	1.339(23)	C(23)-C(24)	1.404(21)
C(25)-C(26)	1.368(16)	C(25)-C(30)	1.359(16)
C(26)-C(27)	1.359(19)	C(27)-C(28)	1.363(21)
C(28)-C(29)	1.321(23)	C(29)-C(30)	1.391(19)

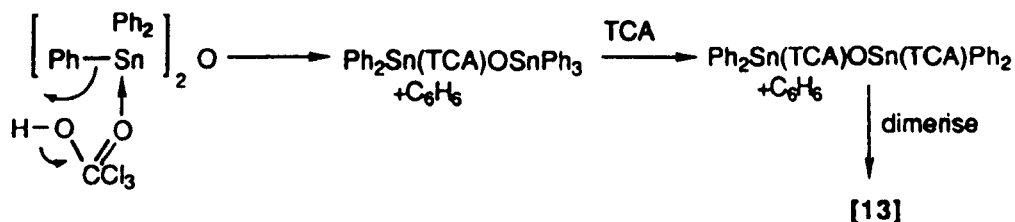
**b) Bond angles**

O(2)-Sn(1)-O(6)	98.0(2)	O(2)-Sn(1)-O(7)	175.1(2)
O(6)-Sn(1)-O(7)	86.6(2)	O(2)-Sn(1)-C(7)	84.0(3)
O(6)-Sn(1)-C(7)	86.9(3)	O(7)-Sn(1)-C(7)	94.8(3)
O(2)-Sn(1)-C(13)	86.1(3)	O(6)-Sn(1)-C(13)	87.1(3)
O(7)-Sn(1)-C(13)	95.7(3)	C(7)-Sn(1)-C(13)	167.6(4)
O(2)-Sn(1)-O(1a)	96.9(2)	O(6)-Sn(1)-O(1a)	165.0(2)
O(7)-Sn(1)-O(1a)	78.4(2)	C(7)-Sn(1)-O(1a)	93.1(3)
C(13)-Sn(1)-O(1a)	95.5(3)	O(3)-Sn(2)-O(5)	172.1(3)
O(3)-Sn(2)-O(7)	86.3(2)	O(5)-Sn(2)-O(7)	86.9(2)
O(3)-Sn(2)-C(19)	95.9(3)	O(5)-Sn(2)-C(19)	89.8(3)
O(7)-Sn(2)-C(19)	104.8(3)	O(3)-Sn(2)-C(25)	91.0(3)
O(5)-Sn(2)-C(25)	88.6(3)	O(7)-Sn(2)-C(25)	118.7(3)

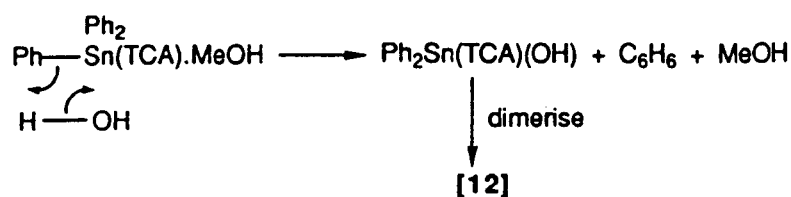
**TABLE 5.13 cont.**

C(1)-O(1)-Sn(1a)	132.5(6)	Sn(1)-O(2)-C(1)	167.5(7)
Sn(2)-O(3)-C(3)	128.3(6)	Sn(2)-O(5)-C(5)	139.6(6)
Sn(1)-O(6)-C(5)	131.1(6)	Sn(1)-O(7)-Sn(2)	137.8(3)
O(1)-C(1)-O(2)	126.8(9)	O(1)-C(1)-C(2)	113.9(8)
O(2)-C(1)-C(2)	119.4(9)	Cl(1)-C(2)-Cl(2)	110.6(6)
Cl(1)-C(2)-Cl(3)	107.0(5)	Cl(2)-C(2)-Cl(3)	108.8(5)
Cl(1)-C(2)-C(1)	112.1(7)	Cl(2)-C(2)-C(1)	111.0(6)
Cl(3)-C(2)-C(1)	107.2(7)	O(3)-C(3)-O(4)	128.0(9)
O(3)-C(3)-C(4)	113.4(8)	O(4)-C(3)-C(4)	118.5(9)
Cl(4)-C(4)-Cl(5)	107.6(5)	Cl(4)-C(4)-Cl(6)	109.8(7)
Cl(5)-C(4)-Cl(6)	109.8(6)	Cl(4)-C(4)-C(3)	112.5(7)
Cl(5)-C(4)-C(3)	104.6(8)	Cl(6)-C(4)-C(3)	112.3(7)
O(5)-C(5)-O(6)	129.6(9)	O(5)-C(5)-C(6)	116.0(8)
O(6)-C(5)-C(6)	114.5(7)	Cl(7)-C(6)-Cl(8)	110.8(6)
Cl(7)-C(6)-Cl(9)	106.9(6)	Cl(8)-C(6)-Cl(9)	107.7(6)
Cl(7)-C(6)-C(5)	113.4(6)	Cl(8)-C(6)-C(5)	110.7(7)
Cl(9)-C(6)-C(5)	107.0(8)	Sn(1)-C(7)-C(8)	117.3(7)
Sn(1)-C(7)-C(12)	124.5(8)	C(8)-C(7)-C(12)	118.1(10)
C(7)-C(8)-C(9)	119.4(10)	C(8)-C(9)-C(10)	120.9(11)
C(9)-C(10)-C(11)	118.2(12)	C(10)-C(11)-C(12)	122.3(12)
C(7)-C(12)-C(11)	121.2(11)	Sn(1)-C(13)-C(14)	122.2(9)
Sn(1)-C(13)-C(18)	119.7(7)	C(14)-C(13)-C(18)	118.1(10)
C(13)-C(14)-C(15)	121.6(12)	C(14)-C(15)-C(16)	119.8(11)
C(15)-C(16)-C(17)	120.7(12)	C(16)-C(17)-C(18)	120.0(14)
C(13)-C(18)-C(17)	119.7(10)	Sn(2)-C(19)-C(20)	119.5(8)
Sn(2)-C(19)-C(24)	124.4(9)	C(20)-C(19)-C(24)	116.0(11)
C(19)-C(20)-C(21)	121.9(12)	C(20)-C(21)-C(22)	119.7(14)
C(21)-C(22)-C(23)	122.5(16)	C(22)-C(23)-C(24)	118.2(12)
C(19)-C(24)-C(23)	121.6(11)	Sn(2)-C(25)-C(26)	121.3(8)
Sn(2)-C(25)-C(30)	120.5(9)	C(26)-C(25)-C(30)	118.2(10)
C(25)-C(26)-C(27)	121.0(11)	C(26)-C(27)-C(28)	119.4(13)
C(27)-C(28)-C(29)	121.2(14)	C(28)-C(29)-C(30)	119.4(14)
C(25)-C(30)-C(29)	120.7(12)		

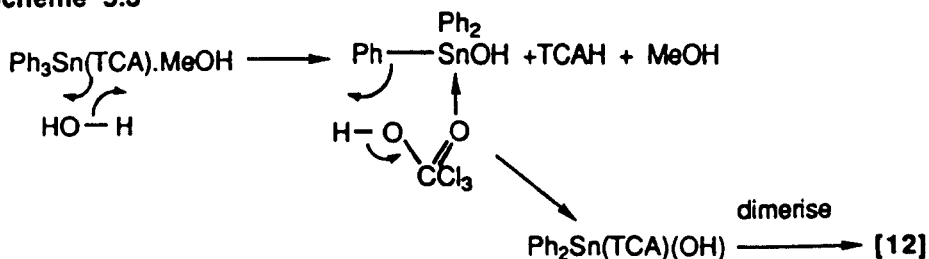
Scheme 5.1



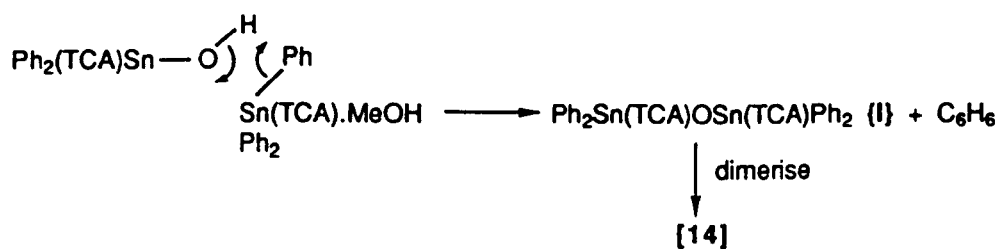
Scheme 5.2



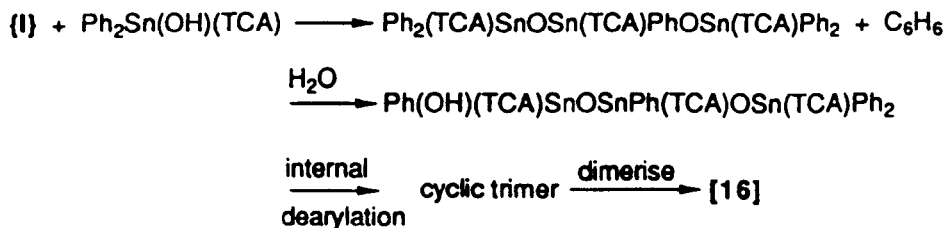
Scheme 5.3



Scheme 5.4



Scheme 5.5



Schemes 5.1-5.5: Hydrolysis pathways for [12] to [16].

## References

- 1) H. Lambourne, *J. Chem. Soc.*, 1922, **121**, 2533.
- 2) H. Lambourne, *J. Chem. Soc.*, 1924, **125**, 2013.
- 3) R. Graziani, G. Bombieri, E. Forsellini, P. Furlan, V. Peruzzo, G. Tagliavini, *J. Organomet. Chem.*, 1977, **125**, 43.
- 4) G. Valle, V. Peruzzo, G. Tagliavini, P. Ganis, *J. Organomet. Chem.*, 1984, **276**, 325.
- 5) R. Faggiani, J.P. Johnson, I.D. Brown, T. Birchall, *Acta Cryst. (B)*, 1978, **34**, 3743.
- 6) J.F. Vollano, R.O. Day, R.R. Holmes, *Organometallics*, 1984, **3**, 745.
- 7) S.P. Narula, S.K. Bharadwaj, H.K. Sharma, G. Mairesse, P. Barbier, G. Nowogrocki, *J. Chem. Soc., Dalton*, 1988, 1719.
- 8) T.P. Lockhart, W.F. Manders, E.M. Holt, *J. Am. Chem. Soc.*, 1986, **108**, 6611.
- 9) P.G. Harrison, M.J. Begley, K.C. Molloy, *J. Organomet. Chem.*, 1980, **186**, 213.
- 10) R. Graziani, V. Casellato, G. Plazzogna, *Acta Cryst. (C)*, 1983, **39**, 1188.
- 11) D. Dakternieks, R.W. Gable, B.F. Hoskins, *Inorg. Chim. Acta*, 1984, **85**, L43.
- 12) R.R. Holmes, C.G. Schmid, V. Chandrasekhar, R.O. Day, J.M. Holmes, *J. Am. Chem. Soc.*, 1987, **109**, 1408.
- 13) V. Chandrasekhar, C.G. Schmid, S.D. Burton, J.M. Holmes, R.O. Day, R.R.

Holmes, *Inorg. Chem.*, 1987, **26**, 1050.

- 14) V. Peruzzo, G. Tagliavini, *J. Organomet. Chem.*, 1974, **66**, 437.
- 15) R.C. Poller, J.N.R. Ruddick, B. Taylor, D.L.B. Toley, *J. Organomet. Chem.*, 1970, **24**, 341.
- 16) R.O. Day, V. Chandrasekhar, K.C.K. Swamy, J.M. Holmes, S.D. Burton, R.R. Holmes, *Inorg. Chem.*, 1988, **27**, 2887.
- 17) R.R. Holmes, *Acc. Chem. Res.*, 1989, **22**, 190.
- 18) A.M. Domingos, G.M. Sheldrick, *J. Chem. Soc., Dalton*, 1974, 475.
- 19) C. Lecompte, J. Protas, M. Devaud, *Acta Cryst. (B)*, 1976, **32**, 923.
- 20) J.C. Barnes, H.A. Sampson, T.J.R. Weakly, *J. Chem. Soc., Dalton*, 1980, 949.
- 21) H. Puff, H. Hevendehl, K. Hofer, H. Reuter, W. Schuh, *J. Organomet. Chem.*, 1985, **287**, 163.
- 22) A.C. Chapman, A.G. Davies, P.G. Harrison, W. McFarlane, *J. Chem. Soc. (C)*, 1970, 821.
- 23) D.W. Allen, I.W. Nowell, J.S. Brooks, R.W. Clarkson, *J. Organomet. Chem.*, 1981, **219**, 29.
- 24) K. Furue, T. Kimura, N. Yasuoka, N. Kasai, M. Kakudo, *Bull. Chem. Soc. Jpn.*, 1970, **43**, 1661.
- 25) B.F.E. Ford, J.R. Sams, *Inorg. Chim. Acta*, 1978, **28**, L173.
- 26) R.K. Ingham, S.D. Rosenberg, H. Gilman, *Chem. Rev.*, 1960, **60**, 459.

27) G.M. Sheldrick (1983). *SHELXTL Users Manual*, Nicolet XRD Corporation, Madison, Wisconsin.

28) G.M. Sheldrick (1986). *SHELXTL PLUS Users Manual*, Nicolet XRD Corporation, Madison, Wisconsin.

29) *International Tables for X-ray Crystallography* (1974). Vol. IV. Birmingham: Kynoch Press. (Present distributor D. Reidel, Dordrecht.)



## CHAPTER 6

### Experimental Section

#### 6.1 Choice Of Crystal

It is most important that a good crystal be chosen to measure the data on. This is simply due to the fact that a poor crystal will give a poor diffraction pattern and hence will not give good results. There are two main criteria for the choice of a crystal, the first being that it should be single, and secondly, that it should be of appropriate size.

A simple method for deducing whether a crystal is single or not is by the use of a polarising microscope. If a crystal is rotated on an axis perpendicular to the plane of a polarising filter then the crystal should appear continuously dark, for any rotation, or be bright and extinguish to darkness every 90°. Crystals that have bright and dark patches at the same time are not single and thus should not be used.

The size of a crystal is also important and is dependent on a number of factors. On modern diffractometers there is a plateau of uniform X-ray intensity, of approximately 0.8 by 0.8mm. For best results the crystal should not move out of this region and so, allowing for difficulties in centering the crystal perfectly, this sets an upper limit of about 0.6mm in any dimension of the crystal. Another factor is the absorption of the X-rays by the crystal itself. In any absorption process the intensity is reduced according to the Beer-Lambert Law:

$$I = I_0 e^{-\mu\tau} \quad 6.1$$

where  $\mu$  is the linear absorption coefficient, and is dependent on the atoms in the crystal, and  $\tau$  is the thickness of the crystal. Thus a small crystal would be expected to be chosen, to minimise the absorption effects. However a third factor is also present. The intensity of the diffracted X-rays are dependent on the amount of material present to diffract the primary beam, i.e. on the volume of the crystal, and thus, there would be an advantage in having as large a crystal as possible. There is an optimum thickness that arises from the combination of these two conflicting factors, given by:

$$t_{opt} = \frac{2}{\mu} \quad 6.2$$

In practice, crystals of dimensions between 0.3 and 0.5mm are generally used.

## 6.2 Crystal Mounting And Data Collection Procedure

A suitable crystal, as outlined above, is chosen and mounted on a fibre. This is most easily done with the use of a high power stereo microscope. The crystal is positioned at the edge of a glass slide and glued on to the end of a quartz fibre, which is mounted in a grub screw with wax, by the use of Araldite glue. Quartz and Araldite are used because they are both amorphous materials, and so will not affect the diffraction pattern.

The grub screw is screwed into a goniometer head (Figure 6.1) and the unit is transferred to the diffractometer<sup>1</sup>. The position of the crystal on the head is adjusted in three dimensions, by means of adjusting screws 1,2 and 3, until the crystal is centred in the X-ray beam and does not move away from this point when rotated in any of the three circles  $\omega$ ,  $\phi$  and  $\chi$  (Figure 6.2)<sup>2</sup>. This is achieved with the aid of a microscope that has been pre-aligned and focused on the centre point.

Once the crystal has been centred a *rotation photograph* is recorded. The crystal is moved to  $0^\circ$  on all the circles, and then rotated in  $\omega$  while the beam is on and the photograph is exposed. An example of the diffraction pattern observed is shown in Figure 6.3. A series of six to eight points ( $2x,2y$ ) are measured from the photograph and input to the control program.  $\chi$  and  $2\theta$  can then be calculated for each point by the following equations:

$$\chi = \tan^{-1} \left[ \frac{y}{x} \right] \quad 2\theta = \cos^{-1} \left[ \frac{2d}{(x^2+y^2+4d^2)^{1/2}} \right] \quad 6.3$$

where  $d$  is the distance from the crystal to the centre of the photograph. The crystal is then moved to the calculated  $\chi$  and  $2\theta$  position and rotated in  $\omega$  until the reflection is found. The program then centres on the reflection by the iterative half-height method.

Once all the reflections have been centred the smallest primitive triclinic cell that is compatible with the data is found. Thus the more data points used, the greater the confidence that can be attached to the result. The minimum number of reflections needed is three, to define the three axes of the cell.

The cell thus produced is then checked to see if there is a higher symmetry cell available. If this is the case, then the data is transformed to the new cell, since higher symmetry cells usually involve less data collection. Photographs are then taken of each axis of the cell. These are used to

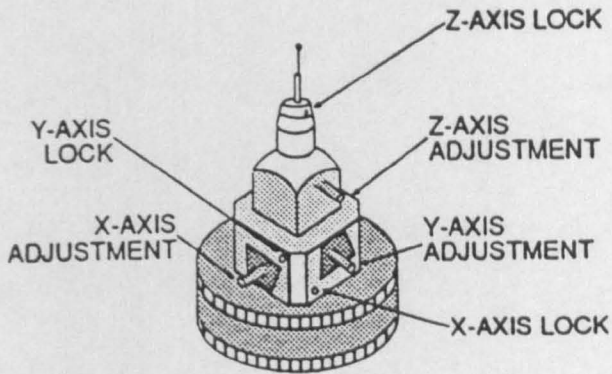
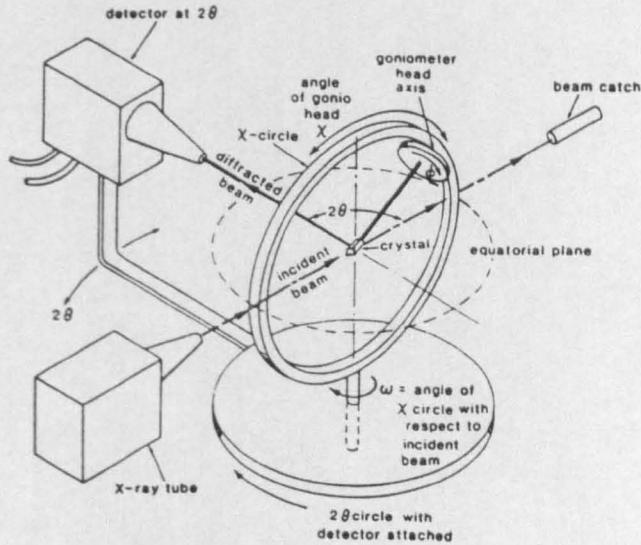


Figure 6.1 Goniometer head.



- $\phi$  = spindle axis of goniometer head
- $2\theta$  = angle between directions of incident and diffracted beams
- $\chi$  = angle detector has to be rotated to intercept diffracted beam
- $\omega$  = angle between diffracted vector and plane of X-circle
- $\chi$  = angle between  $\phi$  axis (gonio. head) and diffractometer axis (equatorial plane)

Figure 6.2 Four circles of the diffractometer.

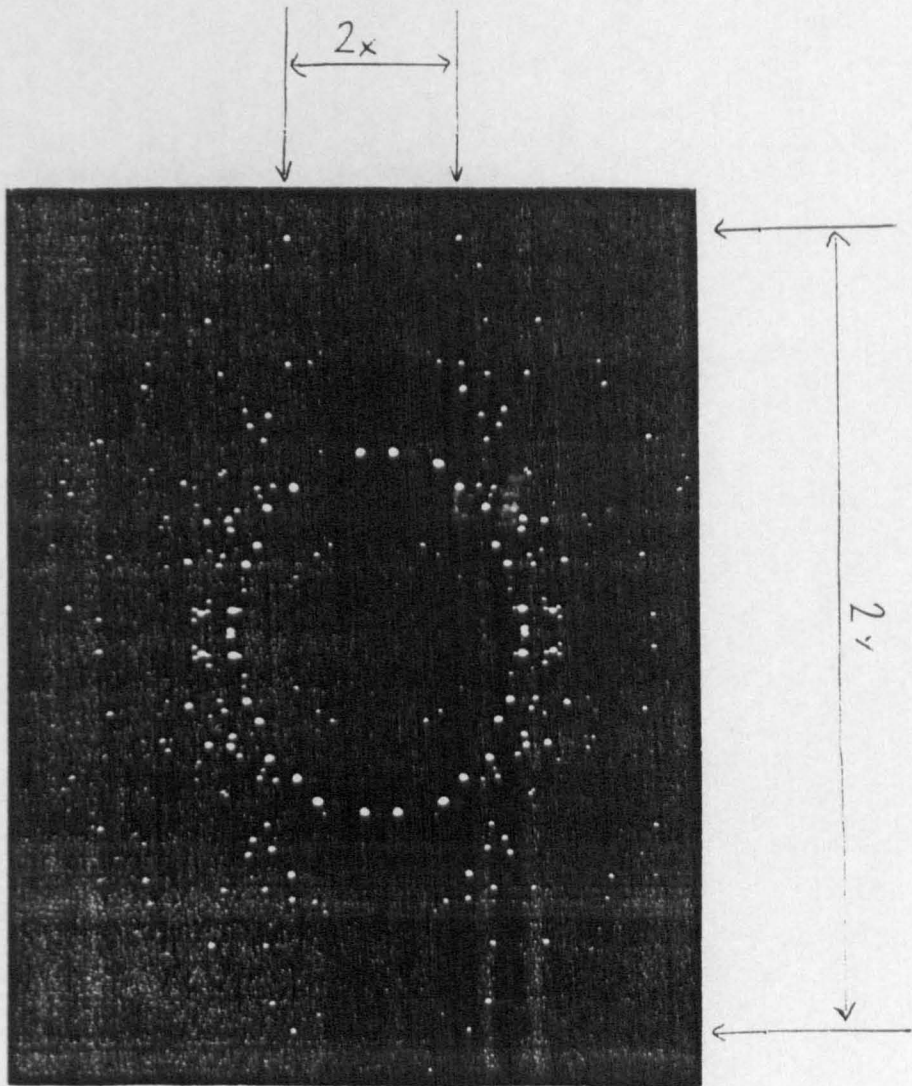


Figure 6.3 Example of a Rotation photograph.

check three points. Firstly, that the cell has the required symmetry, i.e. for a monoclinic cell the b-axis photograph should show mirror symmetry, secondly, to check that there is no twinning, evidenced by double spots on the photograph where one spot is not on the layer line, and thirdly, to check for doubling of the cell dimensions, a problem which occurs if the original points taken from the rotation photograph form a consistent subset of the actual diffraction pattern.

The indices (*hkl*) of the reflections collected are then calculated in a least squares program, which also calculates the cell parameters and the orientation matrix<sup>3</sup>. More accurate cell parameters are calculated by using reflections with higher  $2\theta$  values. To achieve this a rapid data collection is run in the region  $20 < 2\theta < 22^\circ$ . From the output fifteen of the most intense points are chosen and centred on as before. The final cell parameters, error margins and the orientation matrix are calculated from these reflections. The rapid data scan is also useful for checking whether the cell is centred or not prior to the full data collection.

At this point the crystal is removed from the diffractometer to be measured. This is done by the method of Alcock<sup>4</sup>. Accurate measurement of the crystal shape is important for calculating the path length of any particular beam through the crystal, and thus the extent to which absorption may affect its intensity. This is especially important for needle and plate crystals which can have very different path lengths through them. It is useful to measure the crystal before the data collection, because during the data collection the edges may become less distinct, due to solvent loss for example.

The crystal is then replaced on the diffractometer and the full data collection started. Using the information obtained from the least squares program, the angles at which any reflection will occur can be calculated. The program systematically measures each reflection. The geometry used is a  $\omega/2\theta$  scan, where the  $\omega$  circle, which rotates the crystal, moves at half the angular rate of the detector, located on the  $2\theta$  circle. A pre-scan estimates the intensity of each reflection and determines the scan speed for each, fast for a strong reflection and slow for a weak one. Intensity measurements are taken at either side of the reflection to determine the background accurately. Three standard reflections are measured every 200 reflections. These are used to determine if any systematic decrease in diffracted intensity occurs over the data collection time, if so the data can be scaled to account for it. The data is transferred directly to the MicroVax II for structure solution.

The ambient temperature around the crystal is held at 18°C by means of an air conditioning unit. If cooler temperatures are required, to counteract thermal vibration for instance, the crystal can be bathed in a stream of cold, dry nitrogen. The temperature of the stream can be adjusted to

access any temperature down to approximately 150K, by means of stream heaters.

Structure solution was carried out using the SHELXTL PLUS<sup>5</sup> suite of programs on the DEC MicroVax II. In all cases the Patterson routines were used to find the heavy atoms in the molecules, though Direct Methods strategies have been used in the solution of other structures, notably organic compounds.

## References

- 1) Nicolet Instrument Corporation, *SHELXTL PLUS users manual*, 1988.
- 2) J.P. Glusker, K.N. Trueblood,  
*Crystal Structure Analysis - A Primer*, 2<sup>nd</sup> ed., Oxford University Press, Oxford, 1985.
- 3) R.A. Sparks in *Crystallographic Computing Techniques*, ed. F.R. Ahmed, Munksgaard, Copenhagen, 1976.
- 4) N.W. Alcock, *Acta Cryst.(A)*, 1970, **26**, 437.

## CHAPTER 7

### Conclusions and Areas of Further Study

#### 7.1 Conclusions

In Chapter 2 it was noted that bulky groups were needed to force triorgano carboxylates to be four coordinate. This has been demonstrated by the increase in the steric bulk from the monochlorocarboxylate to the trichlorocarboxylate, where the mono and dichloro complexes are five coordinate polymeric compounds and the trichloro complex is a monomeric four coordinate unit. Also reported were two dicarboxylate complexes, showing these to be monomeric in the crystal as well as in solution and not polymeric as suggested by infra-red evidence.

The compounds reported in Chapter 5, which are mostly hydrolysis and dearylation products, show how moisture sensitive the tin compounds are in the presence of a strong acid. A point worth noting from this Chapter is the difference in structure of the isomers [13] and [14], which can only be ascribed to differences in crystallisation due to the solvent. This highlights the fact that some lattice effects are due to the solvent, whether or not it is present in the lattice.

The diorgano tellurium dithiocarbamate structures all show the absence of a sterically active lone pair in the coordination sphere and thus their geometry is similar to that of analogous tin compounds. The non-sterically active lone pair is a characteristic of the lower right hand corner of the periodic table. Systematic changes in the dithiocarbamate ligands, from the diethyl to the diphenyl, do not show any systematic changes in the bond lengths around the tellurium that may have been expected from electronic effects. The lone pair is also absent in the dicarboxylate complex allowing two molecules to dimerise. In the case of the monocarboxylate the lone pair is active though, two molecules dimerising as edge-edge octahedra. The differences here may be due to the fact that the triorganotellurium complex is predominantly ionic.

From studying the bond lengths (Table 7.1), it is clear that the Te-C bond lengths are longer in the dithiocarbamate complexes than the carboxylates. This is probably due to the steric bulk of the coordinated sulphur atoms. The Te-O bond lengths are longer than the Sn-O bond lengths in the dicarboxylate complexes, which is probably due to the carboxylates being bidentate bridging in this case.



## 7.2 Areas for Further Study

In our knowledge of structural tin carboxylate chemistry there is still a large hole in relation to the tricarboxylates. This is mainly due to difficulties in crystallisation of the compounds. These should show seven coordination, from comparison with  $\text{PhSn}(\text{S}_2\text{CNEt}_2)_3$ . Further work also needs to be carried out on the dicarboxylates to investigate under what circumstances, if any, they form polymeric units rather than monomers.

The hydrolysis/dearylation reactions also need to be studied in greater detail to pinpoint the conditions required for the reactions to occur. Especially in respect to the amount of water present in the solvent, the strength of the carboxylic acid used and the temperature of the reaction, to see if it occurs during the synthesis or the recrystallisation.

Finally, the effect of varying the ligands in the tin and tellurium analogues could be further investigated by the use of monothiocarboxylates ( $\text{RCOS}$ ) and monothiocarbamates ( $\text{R}_2\text{NCOS}$ ).

**Table 7.1: Selected Bond Lengths**

<b>Compound</b>	<b>M-C</b>	<b>M-O</b>	
<b>Ph<sub>3</sub>Sn(OCOR)</b>	2.117(4)	2.195(3)	
	2.134(4)		
	2.134(4)	2.221(4)	
	2.116(6)		
	2.121(5)		
	2.121(6)		
	2.102(6)	2.168(3)	
	2.115(3)		
2.120(4)	2.19(2)		
<b>average</b>		2.12(1)	
<b>Ph<sub>3</sub>Te(OCOR)</b>	2.106(4)		
	2.127(4)		
	2.104(4)		
	<b>average</b>		2.11(1)
<b>Ph<sub>2</sub>Sn(OCOR)<sub>2</sub></b>	2.119(5)	2.079(4)	
	2.110(6)	2.076(4)	
	2.105(6)	2.101(6)	
	2.118(6)	2.090(6)	
	<b>average</b>	2.113(6)	2.09(1)
<b>Ph<sub>2</sub>Te(OCOR)<sub>2</sub></b>	2.106(6)	2.149(4)	
	2.114(7)	2.163(4)	
	<b>average</b>	2.11(1)	2.156(7)
<b>Ph<sub>2</sub>Te(dtc)<sub>2</sub></b>	2.143(3)		
	2.137(6)		
	2.130(6)		
	2.152(20)		
	2.151(21)		
	<b>average</b>		2.143(8)

## APPENDIX A

### Crystallographic Theory and Structure Solution

#### A.1 Diffraction of X-rays

A crystal is a three dimensional array of repeating units. When struck by X-rays, which have a wavelength comparable to the interatomic spacing in the crystal, the crystal acts as a three dimensional diffraction grating and diffracts the X-rays. This was first noted by Laue in 1912<sup>1</sup>. In the same year Bragg noted the similarity to reflection from a plane and deduced a simple equation to explain it<sup>2</sup>. With reference to Figure A.1, incident beams 1 and 2, which are parallel and in phase, pass through the planes  $P_1$  and  $P_2$ . The electromagnetic field of the X-rays force the electrons in the planes to vibrate and, as vibrating charges, to re-radiate the energy in a spherical waveform.

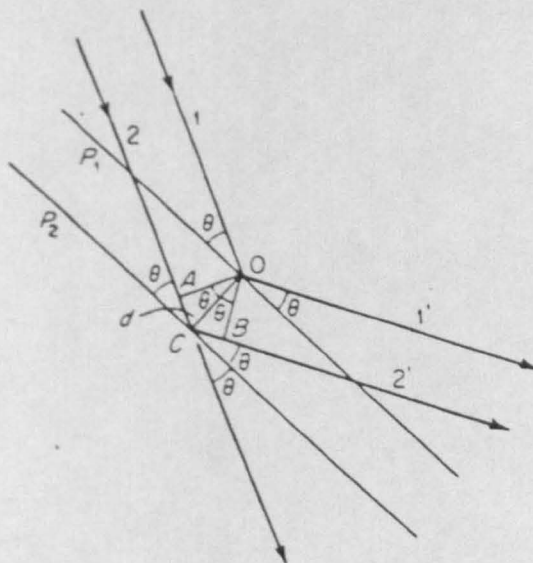


Figure A.1 Diffraction of X-rays from crystal planes.

For the particular direction where the parallel secondary waves are emitted ( $1'$  and  $2'$ ) at angle  $\theta$ , a peak of intensity will occur if the rays are in phase. This will be true if the distance  $ACB=n\lambda$ . From the construction  $AC=CB$  and so diffraction occurs if  $2AC=n\lambda$ , and since  $AC=d\sin\theta$ ,

$$2d \sin \theta = n \lambda$$

This is termed Braggs Law. In the construction outlined above this process was envisaged as having a fixed set of planes and varying the angle of the incident radiation until diffraction occurs. The general experimental set up, though mathematically identical, has the diffraction occurring by moving the set of planes, i.e. the crystal, through a stationary beam.

In the derivation the assumption is made that the electrons that scatter the rays are in the planes. This is clearly not the case, but the derivation is still valid because it can be shown<sup>3</sup> that waves scattered from electrons not lying in the plane can be added to give a resultant, as if from the plane. It is the variation of these resultants, since electrons will be different distances away from different planes, that gives rise to the different intensities of reflection.

The family of planes that give rise to a reflection are described by their Miller indices ( $hkl$ ). This plane intersects the  $a, b$  and  $c$  axes of the cell at  $a/h, b/k$  and  $c/l$  respectively (Figure A.2)<sup>4</sup>.

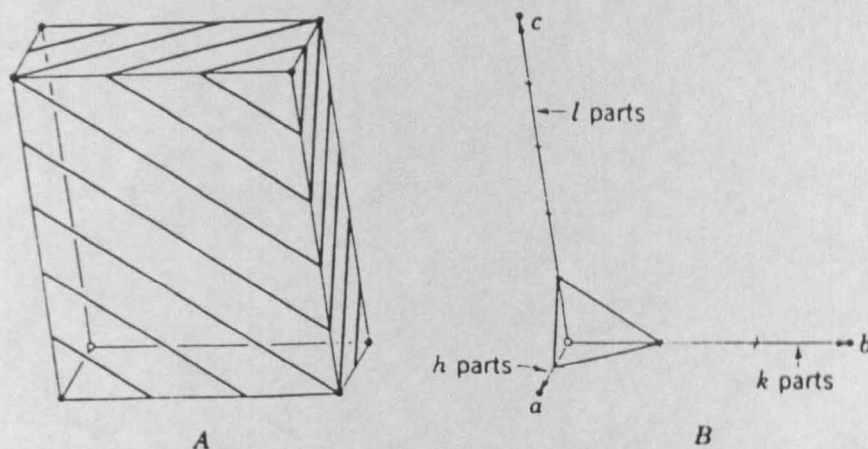


**Figure A.2 Derivation of Miller Indices for any plane of reflection**

Crystals have a virtually infinite periodic array of diffracting planes, when considering the relation of the bulk size of the crystal versus the distance between the planes. This would be expected to result in infinitely narrow diffraction peaks, by simple analogy with diffraction gratings. The peaks observed have a finite breadth, though, due to the mosaic structure of the crystals. All 'perfect' crystals are constructed of slightly misaligned microcrystals, this is called the mosaic structure. This is a desirable quality since it enhances the diffraction intensity because there is less primary extinction (section A.5).

## A.2 Symmetry and Space Groups

The first step in the determination of the structure of a crystal is to determine the space group it belongs to. In the first instance, the crystal system needs to be found. This can be one of a possible seven (Table A.1)<sup>5</sup>, and is determined by the diffraction symmetry of the cell.

<i>Crystal system</i>	<i>No. independent parameters</i>	<i>Parameters</i>	<i>Lattice symmetry</i>
Triclinic	6	$a \neq b \neq c; \alpha \neq \beta \neq \gamma$	$\bar{1}$
Monoclinic	4	$a \neq b \neq c; \alpha = \gamma = 90^\circ$	$2/m$
Orthorhombic	3	$a \neq b \neq c; \alpha = \beta = \gamma = 90^\circ$	$mmm$
Tetragonal	2	$a = b \neq c; \alpha = \beta = \gamma = 90^\circ$	$4/mmm$
Rhombohedral	2	$a = b = c; \alpha = \beta = \gamma$	$\bar{3}m$
Hexagonal	2	$a = b \neq c; \alpha = \beta = 90^\circ; \gamma = 120^\circ$	$6/mmm$
Cubic	1	$a = b = c; \alpha = \beta = \gamma = 90^\circ$	$m\bar{3}m$

**Table A.1 The seven crystal systems.**

When these systems have lattice centering included, i.e. more than one lattice point per cell, a possible fourteen lattices can be constructed (Figure A.3)<sup>6</sup>. These were first recognised by Bravais and consist of seven primitive lattices with one lattice point per cell and seven non-primitive lattices which have more than one lattice point per cell. The centering, either A, B, C, I or F, can be deduced from the systematic absences in the data collection:

P= no absence

C=  $h+k=2n+1$

I=  $h+k+l=2n+1$

F=  $h+k=2n+1, k+l=2n+1, h+l=2n+1$

Convention dictates that A- or B-centred lattices are rotated to be C-centred, except for orthorhombic space groups 38-41 inclusive, for which the standard setting is A-centred. It should be noted that a B-centred monoclinic lattice can always be reduced to a primitive cell of half the volume. In addition to the centering, each space group contains a unique set of symmetry elements. These can be split into two groups, those which do not cause systematic absences to occur and those which do. The former group include mirror planes, rotation axes and rotation inversion axes and are collected under the term point symmetry elements. The latter group, called translational symmetry elements, includes screw axes and glide planes. Combining these symmetry elements with the fourteen Bravais lattices creates a total of 230 space groups, many of which can be

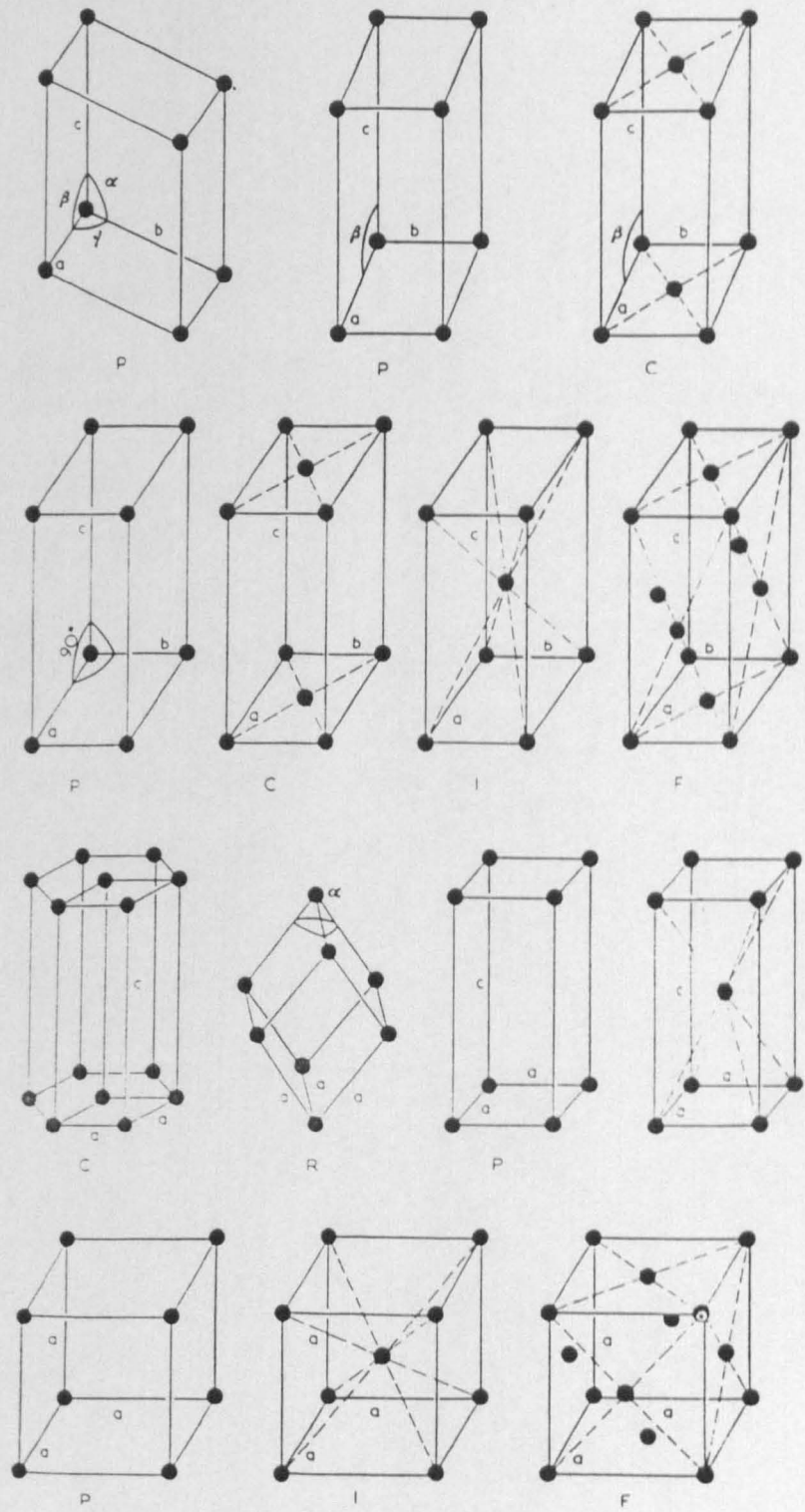


Figure A.3 The fourteen Bravais lattices.

determined uniquely by the systematic absences they produce.

A screw axis ( $M_n$ ) describes the positions of a set of atoms around an axis. The net translation in the direction of the axis is given by  $n/M$  and the clockwise rotation about the axis by  $360/M$ . Thus after  $M$  translations, the point is in its original position, displaced by one unit cell. For instance a  $2_1$  screw axis rotates a point by  $180^\circ$  while translating it along the axis by  $1/2$  of the axis length. It would be recognised by absences produced in either  $h00$ ,  $0k0$  or  $00l$ , depending on the axis involved.

A glide plane is a combination of a mirror plane and a translation parallel to the reflecting plane. Usually the translation is one half the cell length. The glide plane is designated a, b or c. The systematic absence produced by a c-glide normal to the b-axis would be  $h0l$ ,  $l=2n+1$ .

### A.3 Data Reduction

Data reduction is the term used for the manipulation of the raw intensity data,  $I(hkl)$ , collected from the diffractometer, to usable structure factors,  $F(hkl)$ . The structure factor is proportional to the square root of the intensity and the relationship between them is dependent on a number of factors. The structure factor is given as

$$|F_{hkl}| = \left[ \frac{kI_{hkl}}{Lp} \right]^{1/2} \quad \text{A.2}$$

where  $L$  = Lorentz factor and  $p$  = polarisation factor such that

$$L = \frac{1}{\sin 2\theta} \quad \text{A.3}$$

$$p = \left[ f \left[ \frac{1 + \cos^2 2\theta_m \cos^2 2\theta_c}{1 + \cos^2 2\theta_m} \right] + (1-f) \left[ \frac{1 + \cos 2\theta_m \cos^2 2\theta_c}{1 + \cos^2 2\theta_m} \right] \right] \quad \text{A.4}$$

where  $m$  and  $c$  refer to the monochromator and the crystal respectively.

$k$  depends on the crystal size and beam intensity and thus is a constant for any particular set of measurements. This is termed the scaling factor.

The polarisation factor arises due to the fact that the diffracted X-ray beam will be partially polarised. In the primary beam, which is unpolarised, the electric vectors of the photons can point in any direction. When diffracting from a crystal though, those with their electric vectors parallel to the reflecting plane are reflected *independent* of  $2\theta$ , whereas those with vectors perpendicular to the plane depend on  $2\theta$  and at  $90^\circ$  their intensity reduces to zero. Thus the photons with

parallel vectors will be represented in greater intensity than those perpendicular vectors. If a graphite crystal is used to monochromate the X-ray beam then this effect is enhanced by reflection from the monochromator and must be accounted for.

The Lorentz factor arises because the time that a plane is in the reflecting position is not constant. All points on the Ewald sphere rotate with the same angular velocity, but the further a point is from the origin ( $2\theta=0^\circ$ ) the greater linear velocity it will have. The greater linear velocity a point has, the less time it spends in the reflecting position and thus the weaker the intensity from that point.

During the data collection the beam often causes slight decay in the crystal. This can be followed by recording several standard reflections throughout the data collection. The decay can then be accounted for by scaling the data such that the standard reflections have the same intensity throughout.

The data reduction program also checks for any weak reflections. Those with intensity  $I/\sigma(I) < 2.0$  are eliminated from the data file. Reflections with bad background counts, i.e. one side much larger than the other, are also discarded. These are calculated by

$$B_l - B_r > 10(B_l + B_r + 0.002(P - B_l - B_r))^{1/2} \quad \text{A.5}$$

where  $B_l$  and  $B_r$  are the backgrounds measured either side of the peak,  $P$ .

One further correction that is applied to the data is the absorption correction. This is normally accounted for near the end of the refinement procedure, once the structure has been elucidated since it depends on the material in the crystal. It is most important for needle or platy crystals, where there may be a large path length difference, and hence absorption, between two reflections, and for crystals containing heavy atoms, which absorb strongly. This correction is performed using the Gaussian integration method in SHELXTL PLUS. The attenuation of the incident radiation is given by

$$I = I_0 e^{-\mu} \quad \text{A.6}$$

where

$$\mu = \sum (\sigma_i n_i) \times \frac{Z}{V} \quad \text{A.7}$$

where  $\sigma_i$  = the mass absorption coefficient and  
 $n_i$  = the number of such atoms in the unit cell.



#### A.4 The Structure Factor and Patterson Function

The X-ray beam scattered in the direction  $hkl$  by the  $j$  atoms of the unit cell is a combination of an amplitude and a phase and is particular to the reflection  $hkl$ . It is known as the Structure Factor,  $F(hkl)$ . It is the Fourier transform of the electron density at the point  $hkl$  and can be written as

$$F(hkl) = \sum_j f_j e^{i\alpha_j} = \sum_j f_j \cos\alpha_j + i \sum_j f_j \sin\alpha_j \quad \text{A.8}$$

where  $f_j$  is the atomic scattering factor for the atom  $j$  and  $\alpha_j$  is the phase of the scattered wave, which can be shown to be  $2\pi(hx+ky+lz)$  radians, relative to the phase of the wave scattered from the origin<sup>7</sup>.

In order to calculate the electron density distribution in three dimensions a three dimensional Fourier summation must be carried out. The electron density at a given point  $(xyz)$  is then given by

$$\rho(xyz) = \frac{1}{V_c} \sum_h \sum_k \sum_l F(hkl) \exp[-2\pi i(hx+ky+lz)] \quad \text{A.9}$$

Thus if the structure factor is known, then the electron density at any point in the cell can be calculated and the structure solved. However, although the amplitude can be measured directly from the experiment, the phase cannot be. This is called the Phase Problem. The phase,  $\alpha$ , must be derived, either from trial structures or by purely analytical methods.

One such analytical method, the Patterson Function<sup>8</sup>, has been used throughout this thesis. All the compounds studied in the thesis have (at least) one heavy atom in them, either tin or tellurium. The Patterson Function is able to calculate the positions of the heavy atoms without the need for phase information. Since the heavy atoms dominate the scattering of the X-rays, location of these usually allows the structure to be solved. The Patterson method consists of evaluating a Fourier series using only the indices  $(hkl)$  and the  $|F|^2$  value of each diffracted beam. No phase information is needed since  $|F|^2$  is independent of phase. The Patterson function is given by

$$P(UVW) = \frac{1}{V_c} \sum_h \sum_k \sum_l |F|^2 \cos 2\pi(hU+kV+lW) \quad \text{A.10}$$

A peak  $(UVW)$  in the resultant map corresponds to the vector between a pair of atoms in the unit cell, with  $U=x_2-x_1$ ,  $V=y_2-y_1$  and  $W=z_2-z_1$ . The height of the peaks is dependent on the product of the number of electrons in the atoms between which the vector occurs. Thus the

highest peaks will correspond to the vectors between the heaviest atoms. Since there is a vector between every pair of atoms in the unit cell the Patterson diagram rapidly becomes very congested and uninformative. This situation can be improved in two ways. Firstly by the use of a sharpened Patterson function. In a normal Patterson synthesis the width of the vector peaks are large, since they are dependent on the sum of the widths of the atom peaks in the cell. In the sharpened Patterson all the scattering power is placed at the nucleus, thus producing much narrower peaks in the Patterson diagram. Secondly, the results can be made more clear by the removal of the origin peak in the Patterson map. This tends to be a very intense and very broad peak which is generated by each atom having a vector to itself.

The heavy atom can be located by the use of Harker lines and planes<sup>9</sup>. For instance, if there is a mirror plane perpendicular to the b-axis in a cell then every atom  $x,y,z$  will have a partner  $x,-y,z$ . Thus there will be number of vectors  $(0,2y,0)$  in the Patterson. The most intense peak with this vector corresponds to the heavy atom. Therefore the y-coordinate for the heavy atom can be found. This can also be done to find the x and z coordinates using other symmetry elements.

### A.5 Structure Solution and Refinement

Since the heavy atoms dominate the scattering, a set of calculated structure factors,  $F_c$ , based on the heavy atoms alone will be useful as a starting model for the structure. The lighter atoms can then be found by calculating a difference Fourier map,  $\Delta F$ , from the observed and calculated structure factors

$$\Delta F = |F_o| - |F_c| \quad \text{A.11}$$

This will produce a map with peaks corresponding to the positions of the remaining lighter elements. These are then included in the model and the process repeated until all atoms have been located.

Refinement of the structure is carried out by least squares methods to minimise a function  $Q$ , given by

$$Q = \sum w(hkl) [|F_o| - |F_c|]^2 \quad \text{A.12}$$

where  $w(hkl)$  is a weighting factor for each reflection  $hkl$ . The closeness of the agreement between the model structure and reality is indicated by the difference between the observed and calculated structure factors, the smaller the difference the greater the agreement. This is followed

by calculating the Residual factor R, given by

$$R = \frac{\sum ||F_o| - |F_c||}{\sum |F_o|} \quad \text{A.13}$$

A major effect that needs to be allowed for is the thermal motion of the atoms in the crystal. Since the atoms are thermally vibrating the electron clouds associated with each atom become more diffuse than they would be for an atom at rest. This has the effect of increasing the rate at which scattering from the atom falls off by a factor which is proportional to the amplitude of vibration. In the early stages of refinement each atom is treated as if the thermal motion is spherical. Thus  $f_o$ , the proper scattering factor for the atom at rest, is replaced by

$$f = f_o e^{-B_{iso}(\sin^2\theta)/\lambda^2} \quad \text{A.14}$$

where  $B_{iso}$  is related to the mean square amplitude of vibration,  $\bar{U}^2$  by

$$B_{iso} = 8\pi^2\bar{U}^2 \quad \text{A.15}$$

A more precise description of the thermal motion is introduced towards the end of the refinement. This is the *anisotropic* temperature factor,  $B_{aniso}$ , where the thermal motion is modeled by an ellipsoid rather than a sphere. Thus

$$\bar{U}^2 = U_{11}h^2a^*{}^2 + U_{22}k^2b^*{}^2 + U_{33}l^2c^*{}^2 + 2U_{12}hka^*b^* + 2U_{13}hla^*c^* + 2U_{23}klb^*c^* \quad \text{A.16}$$

where the  $U_{ii}$  terms describes the three principal axes of the ellipsoid and the  $U_{ij}$  terms describe the orientation of the ellipsoid to the crystallographic axes.

One effect that may need to be corrected for is extinction. There are two forms of this, primary and secondary. Primary extinction relates to a destructive interference effect that reduces the intensity of the incident beam as it travels through the crystal. From Figure A.4<sup>10</sup>, it is clear that reflected rays are in a position to reflect once more, to finish pointing in the same direction as the incident beam, but with a phase difference of  $\pi$ . Thus destructive interference can occur. This is only a major effect in near perfect crystals, with the normal mosaic spread of crystallites usually encountered this effect becomes negligible.

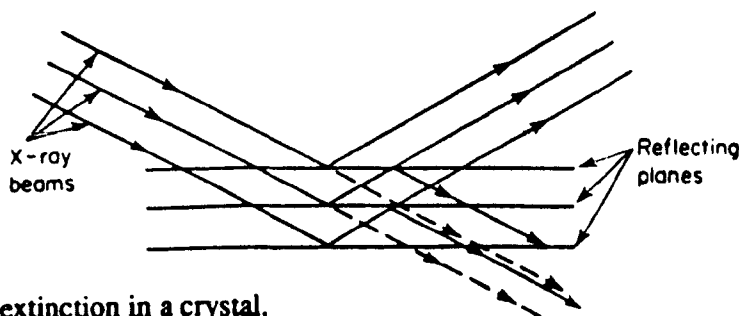


Figure A.4 Primary extinction in a crystal.

Secondary extinction, on the other hand, can be quite important for normal crystals. It arises when reflection from the first few planes the incident beams strikes is very strong. This causes a noticeable reduction in the intensity of the incident beam and thus reflections from deeper in the crystal are weaker. This effect is more pronounced for low angle reflections and leads to intensities which are smaller than would be expected.

## References

- 1) M.J. Buerger, *Contemporary Crystallography*, McGraw-Hill, New York, 1970, p1.
- 2) G.H. Stout, L.H. Jensen, *X-Ray Structure Determination - A Practical Guide*, Macmillan, New York, 1968, p22.
- 3) G.H. Stout, L.H. Jensen, *X-Ray Structure Determination - A Practical Guide*, Macmillan, New York, 1968, p221-226.
- 4) M.J. Buerger, *Contemporary Crystallography*, McGraw-Hill, New York, 1970, p31.
- 5) G.H. Stout, L.H. Jensen, *X-Ray Structure Determination - A Practical Guide*, Macmillan, New York, 1968, p39.
- 6) J.M. Bijvoet, N.H. Kolkmeier, C.H. Macgillavry, *X-ray Analysis of Crystals*, Butterworths, London, 1951. p14.
- 7) G.H. Stout, L.H. Jensen, *X-Ray Structure Determination - A Practical Guide*, Macmillan, New York, 1968, p217-218.
- 8) J.P. Glusker, K.N. Trueblood, *Crystal Structure Analysis - A Primer*, Oxford University Press, Oxford, 1985, p113-127.
- 9) G.H. Stout, L.H. Jensen, *X-Ray Structure Determination - A Practical Guide*, Macmillan, New York, 1968, p279-280.
- 10) G.H. Stout, L.H. Jensen, *X-Ray Structure Determination - A Practical Guide*, Macmillan, New York, 1968, p410.

## **APPENDIX B**

### **Anisotropic Displacement Parameters**

**Table B.1: Anisotropic displacement parameters for [1]**  
( $\text{\AA}^2 \times 10^3$ )

Atom	$U_{11}$	$U_{22}$	$U_{33}$	$U_{23}$	$U_{13}$	$U_{12}$
Sn(1)	31.9(2)	27.8(1)	31.6(2)	-0.2(1)	-0.0(1)	2.2(1)
Cl(1)	52.0(7)	67.3(8)	54.8(7)	9.6(6)	13.5(6)	-1.7(6)
O(1)	35.2(15)	29.5(15)	51.5(17)	3.1(13)	1.7(13)	2.2(12)
O(2)	44.8(16)	33.2(15)	38.1(16)	-0.6(13)	4.8(13)	3.9(13)
C(1)	39(2)	28(2)	33(2)	-3(2)	-5(2)	-4(2)
C(2)	57(3)	49(3)	54(3)	11(2)	19(2)	6(2)
C(11)	34(2)	25(2)	37(2)	4(2)	4(2)	-1(2)
C(12)	42(2)	47(3)	39(2)	-5(2)	-2(2)	4(2)
C(13)	64(3)	52(3)	52(3)	-20(2)	7(2)	5(3)
C(14)	46(3)	49(3)	82(4)	-2(3)	21(3)	9(2)
C(15)	41(3)	73(4)	77(4)	-14(3)	-8(3)	17(3)
C(16)	40(3)	56(3)	56(3)	-12(2)	-10(2)	10(2)
C(21)	29(2)	38(2)	34(2)	-2(2)	-3(2)	-2(2)
C(22)	57(3)	40(2)	40(2)	4(2)	-5(2)	1(2)
C(23)	58(3)	60(3)	41(3)	12(2)	-3(2)	-1(2)
C(24)	52(3)	74(4)	33(2)	-6(2)	3(2)	-2(3)
C(25)	66(3)	46(3)	46(3)	-17(2)	1(2)	0(2)
C(26)	52(3)	36(2)	44(3)	1(2)	-1(2)	8(2)
C(31)	39(2)	28(2)	38(2)	4(2)	-1(2)	1(2)
C(32)	49(3)	44(3)	42(2)	-1(2)	-3(2)	4(2)
C(33)	71(3)	54(3)	45(3)	3(2)	-10(2)	6(3)
C(34)	64(3)	55(3)	59(3)	9(3)	-29(3)	1(3)
C(35)	37(3)	75(4)	87(4)	19(3)	-9(3)	3(3)
C(36)	40(2)	65(3)	54(3)	13(2)	1(2)	4(2)

$$-2\pi^2(h^2 a^* U_{11} + \dots + 2hka^* b^* U_{12})$$

The anisotropic displacement exponent takes the form:

**Table B.2: Anisotropic displacement parameters for [2]**  
( $\text{\AA}^2 \times 10^3$ )

atom	$U_{11}$	$U_{22}$	$U_{33}$	$U_{23}$	$U_{13}$	$U_{12}$
Sn(1)	35.0(2)	34.6(2)	30.4(2)	2.2(2)	9.6(2)	-1.0(2)
Cl(1)	130(2)	70(1)	129(2)	-51(1)	-2(2)	18(1)
Cl(2)	79(1)	167(3)	123(2)	-61(2)	33(2)	-63(2)
O(1)	51(2)	42(2)	27(2)	-1(2)	12(2)	-3(2)
O(2)	55(2)	44(2)	32(2)	5(2)	12(2)	-6(2)
C(1)	47(3)	32(3)	36(3)	1(2)	19(3)	2(2)
C(2)	80(5)	44(3)	34(3)	-4(3)	14(3)	-11(3)
C(11)	45(3)	36(3)	42(3)	3(3)	24(3)	6(2)
C(12)	46(3)	47(3)	60(4)	5(3)	19(3)	0(3)
C(13)	79(5)	54(4)	89(6)	6(4)	40(4)	-16(4)
C(14)	117(7)	52(4)	76(5)	22(4)	48(5)	6(5)
C(15)	89(5)	81(5)	45(4)	21(4)	11(4)	19(4)
C(16)	67(4)	49(4)	40(3)	5(3)	13(3)	8(3)
C(21)	40(3)	43(3)	29(3)	-3(2)	11(2)	4(3)
C(22)	46(4)	60(4)	71(5)	11(3)	23(3)	6(3)
C(23)	39(4)	95(6)	98(6)	7(5)	25(4)	8(4)
C(24)	54(4)	121(7)	79(6)	14(5)	7(4)	48(5)
C(25)	87(6)	89(6)	54(4)	30(4)	29(4)	48(5)
C(26)	56(4)	57(4)	47(4)	7(3)	22(3)	11(3)
C(31)	38(3)	42(3)	39(3)	8(3)	9(3)	-1(2)
C(32)	64(4)	66(5)	88(6)	-33(4)	33(4)	-30(4)
C(33)	78(5)	73(5)	117(7)	-23(5)	32(5)	-40(4)
C(34)	45(4)	87(6)	97(6)	28(5)	15(4)	-21(4)
C(35)	45(4)	104(6)	85(6)	9(5)	32(4)	-2(4)
C(36)	46(3)	61(4)	63(4)	-2(3)	19(3)	-4(3)

The anisotropic displacement exponent takes the form:

$$-2\pi^2(h^2a^*U_{11} + \dots + 2hka^*b^*U_{12})$$



**Table B.3: Anisotropic displacement parameters for [3]**  
( $\text{\AA}^2 \times 10^3$ )

atom	$U_{11}$	$U_{22}$	$U_{33}$	$U_{23}$	$U_{13}$	$U_{12}$
Sn(1)	34.4(2)	33.9(2)	41.1(9)	2.2(2)	1.1(2)	2.3(1)
C1(1)	102.5(11)	36.7(7)	100.0(27)	3.1(10)	14.0(12)	-5.0(7)
C1(2)	50.3(8)	75.7(10)	125.1(30)	17.3(12)	30.1(11)	1.0(7)
C1(3)	125.0(15)	98.1(13)	46.1(32)	2.0(14)	-3.0(15)	-21.0(11)
O(1)	46.0(18)	39.6(17)	46.6(54)	7.0(22)	10.9(21)	-0.1(13)
O(2)	51(2)	57(2)	56(6)	4(3)	14(2)	14(2)
C(1)	53(3)	37(2)	41(8)	2(3)	-1(3)	-1(2)
C(2)	40(3)	40(2)	18(9)	1(3)	-7(3)	-2(2)
C(5)	170(9)	91(6)	80(15)	2(8)	34(8)	-20(6)
C(6)	184(10)	131(9)	30(12)	-25(9)	27(9)	-90(7)
C(7)	108(6)	120(7)	49(15)	17(8)	-18(6)	-58(6)
C(8)	71(4)	81(4)	21(12)	17(5)	-16(5)	-27(3)
C(3)	55(3)	44(3)	24(8)	1(4)	8(4)	-11(2)
C(10)	47(3)	72(4)	73(9)	-1(4)	10(4)	19(3)
C(11)	71(4)	103(6)	121(11)	5(6)	29(5)	38(4)
C(12)	132(7)	85(5)	103(12)	21(6)	46(7)	61(5)
C(13)	169(8)	40(3)	91(12)	-7(5)	55(7)	17(4)
C(14)	91(4)	40(3)	72(10)	-1(4)	30(5)	1(3)
C(9)	52(3)	46(3)	16(8)	7(3)	-2(3)	15(2)
C(18)	46(3)	73(4)	45(9)	8(4)	-3(4)	8(2)
C(19)	44(3)	99(5)	58(15)	30(6)	-14(5)	6(3)
C(20)	66(4)	79(4)	70(16)	34(6)	-39(6)	-6(3)
C(17)	43(3)	38(2)	26(10)	3(3)	2(4)	3(2)
O(3)	53(2)	55(2)	40(6)	23(3)	-10(2)	-13(2)
C(16)	68(4)	64(4)	93(10)	19(5)	-13(5)	-14(3)

The anisotropic displacement exponent takes the form:

$$-2\pi^2(h^2 a^{*2} U_{11} + \dots + 2hka^* b^* U_{12})$$

**Table B.4: Anisotropic displacement parameters for [4]**

(Å<sup>2</sup>×10<sup>3</sup>)

	U <sub>11</sub>	U <sub>22</sub>	U <sub>33</sub>	U <sub>23</sub>	U <sub>13</sub>	U <sub>12</sub>
Sn(1)	40(1)	45(1)	39(1)	14(1)	12(1)	11(1)
Cl(1)	79(1)	79(1)	217(2)	71(1)	63(1)	18(1)
Cl(2)	99(1)	139(2)	228(3)	117(2)	-40(2)	19(1)
Cl(3)	293(4)	62(1)	171(2)	17(1)	123(3)	55(2)
O(1)	63(2)	48(1)	57(2)	17(1)	24(1)	17(1)
O(2)	96(3)	64(2)	67(2)	25(2)	41(2)	28(2)
C(1)	42(2)	47(2)	53(2)	13(2)	6(2)	11(2)
C(2)	56(3)	47(2)	78(3)	26(2)	19(2)	14(2)
C(11)	44(2)	44(2)	49(2)	7(2)	15(2)	13(2)
C(12)	59(3)	75(3)	79(3)	33(3)	3(2)	18(2)
C(13)	55(3)	83(4)	110(5)	29(3)	7(3)	30(3)
C(14)	44(3)	90(4)	96(4)	-4(3)	6(3)	25(3)
C(15)	56(3)	106(4)	70(3)	6(3)	34(3)	5(3)
C(16)	52(2)	81(3)	46(2)	7(2)	14(2)	7(2)
C(21)	45(2)	46(2)	40(2)	14(2)	10(2)	10(2)
C(22)	54(2)	90(3)	45(2)	19(2)	16(2)	28(2)
C(23)	75(3)	107(4)	46(2)	28(3)	20(2)	32(3)
C(24)	68(3)	84(3)	49(2)	24(2)	-3(2)	22(3)
C(25)	53(2)	70(3)	63(3)	18(2)	5(2)	26(2)
C(26)	50(2)	57(2)	52(2)	13(2)	14(2)	19(2)
C(31)	38(2)	48(2)	41(2)	14(2)	7(1)	9(2)
C(32)	57(2)	53(2)	46(2)	14(2)	17(2)	10(2)
C(33)	62(3)	76(3)	51(2)	18(2)	21(2)	8(2)
C(34)	66(3)	77(3)	54(3)	5(2)	21(2)	26(2)
C(35)	87(4)	57(3)	64(3)	3(2)	18(3)	32(3)
C(36)	67(3)	47(2)	63(3)	15(2)	22(2)	16(2)

The anisotropic displacement exponent takes the form:

$$-2\pi^2(h^2a^{*2}U_{11} + \dots + 2hka^*b^*U_{12})$$

**Table B.5: Anisotropic displacement parameters for [5]**  
( $\text{\AA}^2 \times 10^3$ )

	$U_{11}$	$U_{22}$	$U_{33}$	$U_{23}$	$U_{13}$	$U_{12}$
Te(1)	37.7(2)	41.2(2)	34.5(2)	-2.4(1)	5.5(1)	0.2(1)
Cl(1)	75.7(8)	82.9(8)	43.0(6)	10.9(5)	13.3(5)	8.4(6)
Cl(2)	91.6(1.0)	92.8(1.0)	73.5(8)	3.6(8)	5.6(7)	43.4(8)
Cl(3)	97.2(1.0)	96.1(1.0)	69.6(8)	11.3(8)	-16.0(7)	-49.5(8)
O(1)	63(2)	80(2)	41(2)	9(1)	3(1)	-11(2)
O(2)	53(2)	90(2)	59(2)	3(2)	2(1)	-10(2)
C(1)	56(2)	41(2)	42(2)	-5(2)	4(2)	-3(2)
C(2)	51(2)	52(2)	39(2)	3(2)	4(2)	-3(2)
C(11)	43(2)	45(2)	42(2)	4(2)	0(2)	-5(2)
C(12)	55(2)	47(2)	62(3)	2(2)	1(2)	-1(2)
C(13)	67(3)	47(2)	72(3)	11(2)	-2(2)	-14(2)
C(14)	58(3)	80(3)	57(3)	15(2)	0(2)	-26(2)
C(15)	54(2)	79(3)	49(2)	0(2)	-5(2)	-12(2)
C(16)	54(2)	57(2)	45(2)	-5(2)	7(2)	-2(2)
C(21)	43(2)	44(2)	42(2)	-2(2)	-7(2)	-4(2)
C(22)	55(2)	41(2)	54(2)	0(2)	5(2)	-1(2)
C(23)	71(3)	45(2)	59(3)	-10(2)	9(2)	-9(2)
C(24)	61(3)	77(3)	56(3)	-16(2)	0(2)	-15(2)
C(25)	60(3)	70(3)	50(3)	-1(2)	-8(2)	-2(2)
C(26)	53(2)	52(2)	54(2)	2(2)	-4(2)	-2(2)
C(31)	45(2)	45(2)	36(2)	-1(2)	5(2)	-3(2)
C(32)	54(3)	69(3)	60(3)	18(2)	13(2)	1(2)
C(33)	74(3)	70(3)	63(3)	26(2)	3(2)	-5(2)
C(34)	71(3)	61(3)	59(3)	8(2)	-4(2)	9(2)
C(35)	53(2)	66(3)	58(3)	-2(2)	7(2)	9(2)
C(36)	44(2)	54(2)	50(2)	4(2)	7(2)	-4(2)

The anisotropic displacement exponent takes the form:

$$-2\pi^2(h^2a^*U_{11} + \dots + 2hka^*b^*U_{12})$$

**Table B.6: Anisotropic displacement parameters for [6]**  
( $\text{\AA}^2 \times 10^3$ )

atom	$U_{11}$	$U_{22}$	$U_{33}$	$U_{23}$	$U_{13}$	$U_{12}$
Sn(1)	41.8(2)	43.9(2)	37.8(2)	-1.6(2)	1.0(2)	-4.2(2)
O(1)	67(3)	58(2)	58(2)	-7(2)	-0(2)	4(3)
O(2)	54(2)	60(2)	50(2)	-6(2)	-9(2)	-1(2)
O(3)	60(2)	50(2)	60(2)	-0(2)	0(2)	4(2)
O(4)	77(3)	58(2)	76(3)	-8(2)	-7(3)	-18(2)
C(1)	53(4)	61(4)	38(3)	-10(3)	-2(3)	-5(3)
C(2)	82(5)	91(5)	70(4)	-37(4)	-5(4)	-14(5)
C(3)	70(4)	44(3)	64(4)	-6(3)	8(4)	-11(3)
C(4)	129(7)	49(4)	101(6)	-10(4)	-13(6)	2(5)
C(11)	51(3)	38(2)	38(3)	-2(2)	-1(2)	-9(2)
C(12)	52(3)	59(4)	48(3)	-7(3)	5(3)	1(3)
C(13)	68(4)	78(4)	47(3)	-7(3)	18(3)	-8(4)
C(14)	96(6)	83(4)	43(3)	12(4)	8(4)	-26(4)
C(15)	87(5)	57(3)	62(4)	16(3)	-6(4)	-4(4)
C(16)	66(4)	52(3)	50(3)	-1(3)	2(3)	8(3)
C(21)	39(3)	60(3)	60(3)	22(3)	-3(3)	-4(3)
C(22)	57(4)	78(4)	51(3)	14(3)	-18(3)	5(4)
C(23)	69(5)	125(7)	74(5)	40(5)	-32(4)	20(6)
C(24)	62(5)	131(8)	136(8)	60(7)	-39(5)	21(6)
C(25)	47(4)	111(7)	157(9)	29(7)	-1(5)	-8(4)
C(26)	53(4)	80(5)	92(5)	-6(4)	-20(4)	-13(4)
C(27)	58(4)	64(4)	69(5)	-22(4)	18(4)	-0(4)
C(12)	52(3)	59(4)	48(3)	-7(3)	5(3)	1(3)

The anisotropic displacement exponent takes the form:

$$-2\pi^2(h^2a^{*2}U_{11} + \dots + 2hka^*b^*U_{12})$$

Table B.7: Anisotropic displacement parameters for [7]

( $\text{\AA}^2 \times 10^3$ )

Atom	$U_{11}$	$U_{22}$	$U_{33}$	$U_{23}$	$U_{13}$	$U_{12}$
Sn(1)	30.2(3)	31.4(4)	28.3(4)	-0.4(2)	0.1(3)	2.0(1)
Cl(1)	37.1(11)	57.2(16)	92.5(24)	8.7(15)	-2.6(8)	11.1(7)
Cl(2)	41.8(10)	55.6(15)	92.0(22)	-7.3(14)	-1.8(13)	13.3(10)
O(1)	41(2)	54(3)	47(3)	-1(2)	3(2)	10(2)
O(2)	33(3)	41(2)	36(3)	-6(2)	7(2)	2(2)
O(3)	29(2)	47(2)	44(3)	10(3)	-7(2)	0(2)
O(4)	44(2)	50(3)	34(2)	-0(2)	-3(2)	12(2)
C(21)	26(3)	41(4)	48(4)	-14(3)	2(3)	-3(2)
C(22)	44(4)	55(4)	61(4)	-23(3)	-1(3)	2(3)
C(23)	30(3)	47(4)	37(3)	15(2)	-3(2)	1(3)
C(24)	40(4)	55(4)	65(5)	23(4)	1(3)	9(3)
C(1)	26(3)	34(3)	29(3)	-1(2)	6(2)	-1(2)
C(2)	23(2)	55(3)	38(3)	7(3)	12(3)	-4(2)
C(3)	53(4)	55(4)	56(4)	-11(3)	2(3)	-12(3)
C(4)	62(4)	30(4)	58(4)	8(3)	13(4)	0(3)
C(5)	54(4)	43(4)	84(6)	15(4)	-21(4)	-4(3)
C(6)	54(4)	48(5)	62(4)	4(4)	-15(3)	0(3)
C(7)	26(3)	31(3)	34(3)	-3(2)	-12(2)	3(2)
C(8)	35(3)	47(3)	35(3)	-6(3)	-10(3)	-4(2)
C(9)	48(3)	56(4)	38(3)	8(3)	-1(3)	-11(3)
C(10)	80(5)	25(4)	57(4)	-1(3)	-26(4)	-11(3)
C(11)	58(4)	44(4)	69(5)	-22(4)	18(4)	-0(4)
C(12)	29(3)	53(5)	62(5)	-1(4)	7(3)	9(3)

The anisotropic displacement exponent takes the form:

$$-2\pi^2(h^2 a^{*2} U_{11} + \dots + 2hka^* b^* U_{12})$$

The anisotropic displacement exponent takes the form:

$$-2\pi^2(h^2 a^{*2} U_{11} + \dots + 2hka^* b^* U_{12})$$

Table B.8: Anisotropic displacement parameters for [8]

(Å<sup>2</sup>×10<sup>3</sup>)

Atom	U <sub>11</sub>	U <sub>22</sub>	U <sub>33</sub>	U <sub>23</sub>	U <sub>13</sub>	U <sub>12</sub>
Te(1)	37.0(3)	61.4(4)	57.0(3)	0.0	24.2(3)	0.0
Te(2)	47.3(3)	61.0(4)	51.2(3)	0.0	28.3(3)	0.0
Cl(1)	161(3)	223(3)	96(2)	-18(2)	93(2)	-71(2)
Cl(2)	131.9(21)	129.9(19)	69.0(12)	-28.3(12)	42.3(13)	-24.8(15)
Cl(3)	121.6(21)	150.4(23)	92.1(16)	16.9(16)	7.5(15)	42.9(19)
Cl(4)	68.5(12)	127.3(19)	140.4(20)	14.8(15)	49.6(13)	-30.8(13)
Cl(5)	95(2)	120(2)	341(4)	-43(2)	142(2)	-6(2)
Cl(6)	60.1(13)	421.7(56)	65.7(13)	35.7(23)	14.9(11)	-33.4(23)
O(1)	63(3)	77(3)	49(2)	-1(2)	29(2)	-9(2)
O(2)	105(4)	96(4)	58(3)	-5(2)	33(3)	-36(3)
O(3)	35(2)	70(3)	76(3)	12(2)	28(2)	3(2)
O(4)	61(3)	83(3)	85(3)	23(2)	46(3)	6(2)
C(1)	48(3)	88(5)	47(3)	-3(3)	23(3)	1(3)
C(2)	80(5)	92(5)	60(4)	-2(4)	34(4)	-10(4)
C(3)	44(3)	81(4)	48(3)	-2(3)	28(3)	-4(3)
C(4)	48(4)	97(5)	71(4)	6(4)	33(3)	-6(4)
C(5)	47(3)	58(3)	61(3)	-0(3)	36(3)	-1(3)
C(6)	48(4)	91(5)	64(4)	-10(4)	31(3)	-2(3)
C(7)	59(4)	117(6)	69(4)	-21(4)	37(4)	-12(4)
C(8)	115(7)	98(5)	92(6)	-27(5)	81(6)	-22(5)
C(9)	105(6)	71(5)	99(6)	5(4)	77(6)	15(4)
C(10)	74(4)	79(5)	67(4)	13(3)	48(4)	14(4)
C(11)	44(3)	60(4)	65(4)	11(3)	30(3)	3(3)
C(12)	66(4)	77(5)	104(5)	-5(4)	58(4)	-3(4)
C(13)	89(6)	101(6)	168(9)	7(6)	102(7)	4(5)
C(14)	53(5)	99(6)	166(9)	10(6)	53(6)	-10(5)
C(15)	70(5)	77(5)	100(6)	-9(5)	23(4)	-16(4)
C(16)	54(4)	79(4)	76(4)	-4(4)	32(3)	-3(4)

The anisotropic displacement exponent takes the form:

$$-2\pi^2(h^2a^{*2}U_{11} + \dots + 2hka^*b^*U_{12})$$



**Table B.9: Anisotropic displacement parameters for [9]**

( $\text{\AA}^2 \times 10^3$ )

atom	$U_{11}$	$U_{22}$	$U_{33}$	$U_{23}$	$U_{13}$	$U_{12}$
Te(1)	28.8(2)	33.8(2)	34.9(2)	0.0	17.8(1)	0.0
S(1)	35.2(4)	42.1(4)	47.4(4)	-3.3(4)	25.5(4)	-1.7(4)
S(2)	51.5(5)	65.3(6)	46.6(5)	-12.7(4)	33.5(4)	-14.5(4)
N(1)	42.2(16)	54.5(17)	50.9(16)	-6.0(14)	31.3(14)	-10.3(14)
C(1)	28.9(15)	46.3(18)	37.3(16)	-0.5(14)	15.9(13)	-1.4(14)
C(2)	55(2)	71(3)	72(3)	-12(2)	44(2)	-17(2)
C(3)	72(3)	94(4)	114(4)	-14(3)	66(3)	2(3)
C(4)	58(2)	52(2)	64(2)	-13(2)	38(2)	-17(2)
C(5)	58(3)	92(3)	69(3)	-25(2)	26(2)	-24(2)
C(6)	32.5(16)	40.2(17)	36.4(16)	-0.7(14)	17.6(13)	4.6(14)
C(7)	44.9(19)	44.5(19)	41.2(18)	2.3(15)	22.3(16)	6.3(15)
C(8)	53(2)	59(2)	42(2)	-0(2)	25(2)	13(2)
C(9)	55(2)	51(2)	49(2)	-16(2)	20(2)	5(2)
C(10)	53(2)	50(2)	62(2)	-13(2)	27(2)	-11(2)
C(11)	47(2)	49(2)	52(2)	-8(2)	30(2)	-8(2)

The anisotropic displacement exponent takes the form:

$$-2\pi^2(h^2a^*U_{11} + \dots + 2hka^*b^*U_{12})$$

**Table B.10: Anisotropic displacement parameters for [10]**

( $\text{\AA}^2 \times 10^3$ )

atom	$U_{11}$	$U_{22}$	$U_{33}$	$U_{23}$	$U_{13}$	$U_{12}$
Te(1)	53.0(3)	44.9(2)	42.2(2)	-6.1(2)	-20.0(2)	0.8(2)
S(11)	76.4(12)	57.9(9)	41.9(8)	-7.8(7)	-24.7(8)	20.9(9)
S(12)	111.6(17)	62.3(11)	66.2(11)	-16.8(9)	-47.6(12)	32.3(11)
S(21)	47.1(9)	57.3(9)	41.4(8)	-1.4(7)	-20.1(7)	-9.4(7)
S(22)	72.9(13)	77.5(12)	56.8(10)	1.1(9)	-17.7(9)	-30.5(10)
N(11)	76(4)	59(3)	40(3)	-10(2)	-17(3)	12(3)
N(21)	62(4)	73(4)	60(3)	1(3)	-35(3)	-22(3)
C(1)	55(4)	48(3)	51(3)	-11(3)	-21(3)	-1(3)
C(2)	53(4)	52(4)	59(4)	-9(3)	-10(3)	-5(3)
C(3)	57(5)	70(4)	84(5)	-31(4)	-14(4)	3(4)
C(4)	72(5)	55(4)	100(6)	-27(4)	-39(4)	13(4)
C(5)	119(7)	45(4)	85(5)	2(4)	-21(5)	4(4)
C(6)	82(5)	53(4)	60(4)	-4(3)	-4(4)	0(4)
C(7)	56(4)	46(3)	50(3)	-5(3)	-27(3)	-7(3)
C(8)	68(5)	50(4)	93(5)	-0(3)	-56(4)	1(3)
C(9)	88(6)	47(4)	115(6)	11(4)	-57(5)	-21(4)
C(10)	82(5)	56(4)	96(6)	-1(4)	-44(5)	-23(4)
C(101)	72(5)	70(5)	97(6)	-16(4)	-47(4)	-3(4)
C(102)	77(5)	50(4)	69(4)	-5(3)	-39(4)	-4(3)
C(11)	59(4)	57(4)	47(3)	-11(3)	-19(3)	4(3)
C(12)	98(6)	76(5)	55(4)	-15(4)	-18(4)	9(5)
C(13)	119(9)	92(6)	153(10)	-59(6)	8(7)	1(6)
C(14)	73(5)	80(4)	31(3)	-8(3)	-12(3)	13(4)
C(15)	86(6)	80(5)	56(4)	-0(4)	-11(4)	7(4)
C(16)	155(9)	80(5)	64(5)	12(4)	-23(5)	7(6)
C(17)	152(9)	125(7)	73(6)	18(5)	-50(6)	41(7)
C(18)	98(7)	173(9)	96(7)	-30(6)	-59(6)	53(7)
C(19)	78(6)	108(6)	68(5)	-16(4)	-28(4)	7(5)
C(21)	52(4)	46(3)	52(4)	-10(3)	-19(3)	3(3)
C(22)	88(7)	130(8)	106(7)	9(6)	-58(6)	-48(6)
C(23)	85(7)	221(14)	163(11)	24(9)	-67(8)	-75(8)
C(24)	50(4)	70(4)	44(3)	-2(3)	-27(3)	-9(3)
C(25)	68(5)	78(5)	62(4)	-14(4)	-32(4)	8(4)
C(26)	69(5)	132(7)	52(4)	-25(4)	-21(4)	13(5)
C(27)	83(6)	94(6)	63(5)	10(4)	-38(5)	-15(5)
C(28)	73(5)	62(4)	92(6)	6(4)	-50(5)	-1(4)
C(29)	59(4)	63(4)	67(4)	-14(3)	-33(4)	3(3)

The anisotropic displacement exponent takes the form:

$$-2\pi^2(h^2a^*U_{11} + \dots + 2hka^*b^*U_{12})$$



**Table B.11: Anisotropic displacement parameters for [11]**

( $\text{\AA}^2 \times 10^3$ )

	$U_{11}$	$U_{22}$	$U_{33}$	$U_{23}$	$U_{13}$	$U_{12}$
Te	60.4(9)	62.2(9)	57.8(8)	-12.5(8)	15.1(6)	1.2(9)
S(11)	76(4)	70(4)	72(4)	-8(3)	28(3)	2(3)
S(12)	70(4)	86(4)	76(4)	-9(4)	26(3)	5(4)
S(21)	49(3)	77(4)	55(3)	-10(3)	4(3)	6(3)
S(22)	36(3)	83(4)	70(4)	-8(3)	8(3)	8(3)
N(11)	64(12)	63(13)	63(12)	2(10)	-8(10)	19(11)
N(21)	38(9)	57(10)	48(10)	6(8)	7(8)	-1(9)
C(11)	88(17)	58(15)	63(13)	-25(11)	-16(13)	36(13)
C(12)	63(16)	72(19)	101(21)	-7(17)	-17(14)	30(14)
C(13)	48(14)	45(14)	111(19)	-12(15)	13(13)	9(13)
C(14)	87(20)	82(24)	132(26)	-35(21)	14(20)	-9(17)
C(15)	206(37)	45(18)	176(35)	10(22)	29(32)	-6(21)
C(16)	381(62)	127(30)	72(21)	0(23)	-21(29)	42(39)
C(17)	207(34)	77(20)	105(24)	12(19)	-31(24)	7(22)
C(18)	59(16)	68(16)	86(18)	-26(14)	7(15)	23(14)
C(19)	59(15)	105(21)	105(20)	-33(17)	29(15)	3(15)
C(110)	102(22)	95(21)	155(26)	-37(19)	72(22)	-15(20)
C(111)	88(24)	93(23)	227(39)	-34(26)	113(29)	-37(20)
C(112)	38(16)	125(26)	235(39)	18(29)	62(24)	39(17)
C(113)	72(19)	54(15)	167(26)	18(16)	1(19)	15(15)
C(21)	41(11)	62(13)	54(12)	-14(10)	25(10)	-19(10)
C(22)	22(10)	80(15)	37(11)	-9(11)	14(9)	9(11)
C(23)	48(13)	61(14)	47(13)	-4(11)	6(10)	-7(11)
C(24)	48(14)	76(17)	79(18)	-22(14)	2(12)	-16(14)
C(25)	60(15)	120(22)	36(12)	-8(15)	11(11)	3(16)
C(26)	42(12)	77(16)	61(15)	16(13)	6(11)	34(12)
C(27)	52(13)	68(15)	44(13)	0(11)	6(11)	1(12)
C(28)	40(13)	81(16)	44(12)	-24(12)	8(10)	9(13)
C(29)	38(13)	129(21)	73(15)	18(14)	13(12)	-13(15)
C(210)	19(14)	197(33)	75(18)	10(20)	-11(12)	-11(17)
C(211)	20(14)	222(39)	63(17)	-40(20)	-7(13)	6(21)
C(212)	82(19)	111(23)	90(19)	7(16)	-16(16)	54(20)
C(213)	69(18)	77(18)	87(17)	-22(14)	26(14)	-11(15)
C(32)	79(16)	50(14)	90(17)	4(13)	36(14)	4(14)
C(33)	174(36)	87(27)	140(29)	-1(21)	74(31)	-19(27)
C(34)	320(71)	55(23)	164(39)	-46(24)	121(48)	-100(39)
C(35)	115(26)	137(32)	185(39)	-54(30)	95(28)	-58(29)
C(36)	133(27)	144(28)	46(15)	-27(16)	1(16)	-1(23)
C(41)	80(17)	54(13)	74(15)	-37(13)	-3(13)	14(14)
C(42)	93(17)	93(18)	52(13)	-8(14)	-4(14)	17(17)
C(43)	113(21)	78(16)	46(13)	0(14)	-1(15)	9(20)
C(44)	119(27)	63(18)	135(29)	-39(19)	-55(23)	20(19)
C(45)	80(19)	126(26)	95(20)	-21(18)	-14(19)	-30(17)
C(46)	53(14)	82(18)	81(16)	-8(13)	17(14)	12(13)

The anisotropic displacement exponent takes the form:

$$-2\pi^2(h^2a^*U_{11} + \dots + 2hka^*b^*U_{12})$$

**Table B.12: Anisotropic displacement parameters for [12]**  
( $\text{\AA}^2 \times 10^3$ )

	$U_{11}$	$U_{22}$	$U_{33}$	$U_{23}$	$U_{13}$	$U_{12}$
Sn(1)	50.7(3)	49.7(4)	48.0(3)	0.6(2)	21.0(2)	8.3(2)
Cl(1)	111(2)	200(4)	269(6)	149(4)	114(3)	106(3)
Cl(2)	88(2)	117(2)	193(4)	-22(2)	75(2)	-28(2)
Cl(3)	115(2)	257(5)	77(2)	-44(3)	51(2)	-42(3)
O(11)	57(3)	50(2)	60(3)	-6(2)	29(2)	0(2)
O(1)	59(3)	62(3)	79(4)	-10(3)	40(3)	0(2)
O(2)	80(4)	57(3)	100(5)	-7(3)	46(3)	-2(3)
C(1)	39(3)	55(4)	53(4)	9(3)	16(3)	6(3)
C(2)	52(4)	60(4)	68(4)	12(3)	21(3)	6(3)
C(11)	61(4)	57(4)	48(4)	4(3)	24(3)	-4(3)
C(12)	60(4)	59(4)	57(4)	-5(3)	13(3)	10(3)
C(13)	70(5)	89(6)	77(5)	11(5)	16(4)	15(4)
C(14)	88(6)	85(5)	56(5)	10(4)	4(4)	-24(5)
C(15)	95(7)	108(7)	68(6)	-27(5)	34(5)	-20(6)
C(16)	79(5)	69(4)	60(5)	-9(4)	33(4)	3(4)
C(17)	53(4)	41(3)	52(4)	-5(3)	15(3)	3(3)
C(18)	87(6)	55(4)	70(5)	13(4)	26(4)	10(4)
C(19)	117(8)	76(5)	64(5)	19(5)	30(5)	9(5)
C(110)	97(7)	56(4)	104(7)	31(5)	6(6)	20(5)
C(111)	84(5)	59(5)	107(7)	11(5)	21(5)	33(4)
C(112)	81(5)	51(4)	71(5)	-1(4)	32(4)	8(3)

The anisotropic displacement exponent takes the form:

$$-2\pi^2(h^2 a^{*2} U_{11} + \dots + 2hka^* b^* U_{12})$$

**Table B.13: Anisotropic displacement parameters for [13]**

(Å<sup>2</sup>×10<sup>3</sup>)

	U <sub>11</sub>	U <sub>22</sub>	U <sub>33</sub>	U <sub>23</sub>	U <sub>13</sub>	U <sub>12</sub>
Sn(1)	45(1)	41(1)	33(1)	3(1)	12(1)	2(1)
Sn(2)	40(1)	39(1)	39(1)	5(1)	11(1)	0(1)
C1(11)	130(3)	119(3)	80(2)	39(2)	29(2)	-35(2)
C1(12)	86(2)	115(2)	60(2)	15(2)	2(1)	18(2)
C1(13)	136(3)	89(2)	74(2)	-35(2)	27(2)	-4(2)
C1(21)	68(2)	86(2)	85(2)	7(2)	7(1)	-18(2)
C1(22)	89(2)	104(2)	46(1)	-3(1)	3(1)	2(2)
C1(23)	87(2)	61(2)	94(2)	12(1)	6(2)	21(2)
O(1)	35(3)	39(3)	33(3)	-3(2)	14(2)	-6(2)
O(11)	46(5)	49(5)	31(4)	9(4)	7(4)	6(4)
O(12)	60(7)	71(7)	81(7)	15(6)	10(5)	14(6)
O(13)	132(12)	47(7)	181(13)	34(8)	79(10)	16(7)
O(14)	148(12)	42(6)	146(11)	10(7)	42(9)	25(7)
O(15)	93(8)	64(7)	73(7)	4(5)	26(6)	36(6)
O(16)	71(7)	59(6)	59(6)	10(5)	22(5)	8(5)
O(17)	56(6)	45(5)	37(4)	-8(4)	13(4)	-9(4)
O(18)	131(10)	42(6)	56(6)	-13(5)	-3(6)	31(6)
O(19)	119(10)	68(8)	85(8)	1(6)	22(7)	17(7)
O(110)	98(9)	85(8)	78(7)	-48(6)	40(7)	-14(6)
O(111)	141(11)	82(8)	55(6)	-26(6)	18(7)	-1(8)
O(112)	113(9)	64(7)	53(6)	-11(5)	22(6)	-6(6)
O(113)	66(6)	36(5)	42(5)	0(4)	10(4)	9(4)
O(11)	60(4)	48(3)	41(3)	6(3)	19(3)	7(3)
O(12)	68(4)	86(5)	53(4)	-3(3)	18(3)	-2(4)
O(114)	81(7)	55(6)	34(4)	4(4)	17(5)	-8(5)
O(21)	47(5)	34(4)	50(5)	0(4)	12(4)	-7(4)
O(22)	120(10)	56(6)	67(6)	5(5)	37(6)	12(6)
O(23)	177(13)	62(7)	82(8)	-31(6)	41(8)	12(8)
O(24)	126(11)	37(6)	136(11)	2(6)	61(9)	-3(6)
O(25)	120(10)	36(6)	91(8)	4(6)	35(7)	-8(6)
O(26)	78(7)	46(6)	66(6)	7(5)	28(5)	-3(5)
O(27)	46(5)	37(5)	51(5)	11(4)	13(4)	10(4)
O(28)	56(6)	54(6)	59(6)	18(5)	19(5)	-7(5)
O(29)	54(7)	59(7)	99(8)	26(6)	22(6)	17(5)
O(210)	72(7)	55(7)	129(9)	2(6)	22(7)	25(6)
O(211)	97(9)	51(6)	100(8)	-17(6)	38(7)	12(6)
O(212)	55(6)	66(6)	67(6)	7(5)	15(5)	15(5)
O(213)	53(6)	32(5)	52(5)	-10(4)	11(4)	2(4)
O(21)	81(5)	65(4)	44(4)	9(3)	8(3)	-1(3)
O(22)	52(4)	89(5)	49(4)	1(3)	4(3)	4(4)
O(214)	61(6)	52(6)	35(4)	1(4)	-7(4)	1(4)

The anisotropic displacement exponent takes the form:

$$-2\pi^2(h^2a^{*2}U_{11} + \dots + 2hka^*b^*U_{12})$$



**Table B.14: Anisotropic displacement parameters for [14]**

(Å<sup>2</sup>×10<sup>3</sup>)

atom	U <sub>11</sub>	U <sub>22</sub>	U <sub>33</sub>	U <sub>23</sub>	U <sub>13</sub>	U <sub>12</sub>
Sn(1)	57.5(7)	36.1(5)	26.5(5)	-0.7(4)	7.3(4)	1.1(5)
Sn(2)	52.1(7)	45.5(6)	33.1(5)	2.8(4)	7.1(4)	3.2(5)
C(2)	77(13)	84(13)	40(9)	3(8)	6(9)	-7(11)
C1(11)	172(16)	118(11)	120(13)	-70(10)	28(11)	-42(12)
C1(12)	185(19)	324(30)	59(9)	-0(14)	70(12)	-25(21)
C1(13)	568(66)	585(59)	66(13)	-68(21)	-87(22)	475(56)
C1(14)	50(7)	370(32)	86(12)	-56(15)	-32(7)	9(13)
C1(15)	263(33)	626(71)	147(20)	-254(34)	-107(20)	254(42)
C1(16)	673(70)	678(67)	220(29)	349(41)	-321(39)	-596(63)
C1(21)	110(5)	259(10)	65(4)	-58(5)	15(4)	29(6)
C1(22)	158(8)	195(8)	145(7)	79(6)	81(6)	8(6)
C1(23)	95(5)	206(8)	75(4)	5(4)	30(3)	42(5)
O(1)	83(9)	57(6)	39(6)	2(5)	5(6)	-6(6)
O(2)	71(8)	66(7)	43(6)	5(5)	6(5)	-5(6)
O(3)	87(10)	87(8)	39(6)	8(6)	-1(6)	5(7)
O(4)	71(9)	61(7)	55(7)	-10(5)	21(6)	6(6)
O(5)	30(5)	55(5)	29(5)	14(4)	-10(4)	15(5)
C(1)	91(14)	45(8)	39(8)	8(6)	8(8)	16(9)
C(3)	72(13)	70(11)	52(10)	-34(9)	24(10)	-3(10)
C(4)	112(18)	111(15)	43(10)	20(10)	33(11)	28(13)
C(11)	84(12)	37(7)	26(7)	-17(5)	9(7)	16(8)
C(12)	128(17)	44(9)	38(8)	-4(6)	13(10)	9(10)
C(13)	185(27)	48(10)	80(14)	6(9)	47(16)	5(13)
C(14)	108(18)	107(16)	81(15)	-54(12)	-0(13)	33(15)
C(15)	172(25)	96(15)	63(13)	-47(12)	37(15)	-21(17)
C(16)	128(19)	58(10)	76(13)	-5(9)	61(13)	-16(12)
C(21)	66(11)	52(8)	29(7)	17(6)	15(7)	7(8)
C(22)	71(12)	59(10)	44(9)	22(7)	20(8)	19(9)
C(23)	92(14)	41(8)	55(10)	5(7)	4(10)	-10(9)
C(24)	97(15)	37(8)	82(12)	10(8)	41(11)	-0(10)
C(25)	83(14)	48(9)	74(12)	6(8)	18(10)	13(10)
C(26)	53(10)	45(8)	56(9)	10(7)	11(8)	2(8)
C(31)	48(10)	58(9)	46(9)	-2(7)	-4(7)	1(8)
C(32)	116(18)	65(11)	65(12)	-8(9)	44(12)	-2(12)
C(33)	131(21)	39(10)	103(17)	-10(9)	25(15)	13(11)
C(34)	98(18)	59(12)	143(22)	2(12)	34(17)	-26(12)
C(35)	68(14)	68(12)	122(18)	-8(12)	28(13)	-19(11)
C(36)	57(11)	63(10)	77(12)	4(9)	22(10)	-2(9)
C(41)	63(12)	52(9)	66(10)	21(8)	30(9)	6(9)
C(42)	71(13)	61(10)	78(13)	12(9)	11(10)	17(10)
C(43)	153(25)	82(15)	70(14)	39(12)	13(15)	30(17)
C(44)	173(29)	74(15)	173(28)	72(17)	101(25)	50(17)
C(45)	170(30)	66(14)	158(27)	-10(16)	68(25)	-27(17)
C(46)	89(15)	48(10)	114(16)	-21(10)	40(13)	0(10)

The anisotropic displacement exponent takes the form:

$$-2\pi^2(h^2a^{*2}U_{11} + \dots + 2hka^*b^*U_{12})$$

Table B.15: Anisotropic displacement parameters for [15]

( $\text{\AA}^2 \times 10^3$ )

atom	$U_{11}$	$U_{22}$	$U_{33}$	$U_{23}$	$U_{13}$	$U_{12}$
Sn(1)	39.3(7)	29.3(7)	28.5(10)	2.8(8)	5.6(7)	0.8(6)
Sn(2)	45.9(8)	44.3(8)	40.8(11)	3.6(9)	1.0(8)	7.8(7)
Sn(3)	38.9(7)	35.9(7)	35.3(9)	1.7(9)	7.7(7)	-2.8(6)
C1(11)	99(4)	67(4)	99(6)	-46(4)	32(4)	-35(3)
C1(12)	137(6)	103(5)	91(6)	-50(5)	67(5)	-26(4)
C1(13)	130(6)	74(4)	206(10)	-18(6)	-28(7)	32(4)
C1(21)	125(5)	110(5)	67(5)	-17(5)	3(5)	53(4)
C1(22)	162(7)	149(7)	76(6)	26(6)	67(6)	36(5)
C1(23)	102(5)	194(7)	75(6)	-71(6)	-32(5)	51(5)
C1(31)	49(3)	174(7)	187(9)	-104(7)	13(5)	-14(4)
C1(32)	93(4)	78(4)	125(7)	-37(5)	26(5)	5(3)
C1(33)	199(8)	130(6)	159(9)	40(7)	129(8)	72(6)
C1(41)	140(6)	58(4)	149(8)	-29(5)	39(6)	-28(4)
C1(42)	93(4)	133(6)	77(6)	-52(5)	-23(4)	-1(4)
C1(43)	77(4)	103(5)	114(7)	-43(5)	28(5)	20(4)
C1(51)	90(9)	69(9)	201(24)	-57(13)	-12(12)	-28(8)
C1(52)	96(11)	70(9)	534(48)	4(20)	54(20)	38(8)
C1(53)	527(51)	59(12)	442(52)	91(22)	-19(43)	10(19)
C1(54)	462(54)	378(52)	870(108)	279(62)	401(64)	263(43)
C1(55)	176(18)	358(33)	238(30)	216(28)	92(20)	82(22)
C1(56)	548(59)	222(36)	361(54)	-156(36)	272(48)	-104(36)
O(1)	66(8)	44(7)	47(10)	-14(8)	35(8)	-23(6)
O(2)	36(7)	45(7)	45(10)	-20(8)	20(7)	-1(6)
O(3)	47(7)	50(7)	31(9)	2(8)	-10(7)	11(6)
O(4)	57(8)	71(9)	37(10)	-8(9)	8(8)	31(7)
O(5)	40(7)	59(8)	70(12)	-5(9)	17(8)	5(6)
O(6)	72(9)	96(10)	57(12)	-10(10)	37(9)	45(8)
O(7)	65(8)	71(9)	67(12)	-4(10)	-14(9)	-3(7)
O(8)	60(8)	40(7)	42(10)	-5(8)	0(7)	-9(6)
O(11)	31(6)	37(6)	29(8)	5(7)	-1(6)	-2(5)
O(12)	48(7)	24(6)	33(9)	-5(7)	20(7)	-7(5)
O(2)	96(16)	44(13)	77(20)	-15(15)	-1(16)	5(11)
O(3)	55(12)	57(12)	34(15)	-2(12)	29(12)	11(10)
O(4)	66(13)	82(15)	51(17)	7(15)	4(13)	33(12)
O(5)	28(10)	108(17)	54(17)	-41(15)	19(11)	26(10)
O(6)	87(15)	54(13)	57(18)	-9(14)	40(15)	15(11)
O(7)	52(11)	41(11)	77(19)	0	0	0
O(8)	57(13)	100(17)	71(20)	-28(16)	12(14)	-24(12)
O(11)	62(12)	30(10)	28(14)	9(11)	-3(12)	-1(9)
O(13)	116(23)	195(34)	58(25)	62(25)	17(20)	-53(22)
O(14)	188(34)	79(20)	106(33)	56(22)	14(25)	-23(19)
O(15)	62(13)	99(17)	135(27)	20(20)	1(17)	-51(13)
O(16)	94(16)	102(17)	47(18)	-7(16)	26(15)	-40(14)
O(21)	71(14)	71(14)	53(17)	4(15)	-4(14)	7(12)
O(22)	56(14)	152(23)	148(31)	-6(24)	-27(18)	32(16)

Table B.15 cont.

C(24)	229(45)	177(38)	110(38)	49(31)	-72(32)	52(30)
C(25)	101(22)	171(36)	169(44)	19(35)	-46(31)	59(25)
C(26)	54(14)	158(25)	127(28)	46(25)	-25(19)	0(16)
C(31)	58(12)	49(11)	29(14)	13(13)	9(11)	1(10)
C(32)	233(31)	68(16)	67(22)	17(18)	-38(23)	-76(19)
C(34)	108(18)	127(21)	79(22)	65(19)	16(18)	-7(16)
C(35)	154(24)	118(23)	96(25)	18(21)	-4(22)	-48(19)
C(36)	98(17)	80(16)	81(22)	31(17)	17(17)	-13(14)
C(41)	51(17)	165(32)	446(86)	89(55)	-84(36)	-10(20)
C(42)	174(41)	264(51)	308(71)	197(54)	-120(39)	-60(35)
C(43)	108(21)	194(31)	159(33)	-109(29)	-20(23)	35(21)
C(44)	63(19)	498(69)	686(104)	0(74)	0(41)	0(32)
C(45)	383(74)	150(39)	535(105)	116(52)	88(74)	-116(43)
C(46)	229(49)	99(31)	169(55)	-41(36)	-35(47)	63(32)

The anisotropic displacement exponent takes the form:

$$-2\pi^2(h^2a^*U_{11} + \dots + 2hka^*b^*U_{12})$$



**Table B.16: Anisotropic displacement parameters for [16]**

( $\text{\AA}^2 \times 10^3$ )

atom	$U_{11}$	$U_{22}$	$U_{33}$	$U_{23}$	$U_{13}$	$U_{12}$
Sn(1)	34.4(2)	33.7(2)	31.8(2)	-14.9(2)	-13.0(1)	-13.3(2)
C1(1)	110.7(14)	110.0(14)	49.4(9)	-39.9(9)	-4.2(9)	-72.4(12)
C1(2)	131.5(18)	55.8(10)	50.9(9)	-0.5(8)	-40.0(11)	-43.1(11)
C1(3)	66.7(11)	168.1(22)	88.9(13)	-62.1(14)	-6.9(10)	-70.4(14)
O(1)	35.0(17)	31.2(16)	36.4(17)	-14.8(14)	-16.5(14)	-10.9(14)
O(2)	47(2)	43(2)	41(2)	-20(2)	-9(2)	-23(2)
O(3)	47(2)	44(2)	36(2)	-17(2)	-10(2)	-24(2)
C(1)	36(3)	40(3)	35(3)	-11(2)	-17(2)	-17(2)
C(2)	49(3)	56(3)	36(3)	-17(2)	-10(2)	-30(3)
C(3)	51(3)	44(3)	50(3)	-25(2)	-21(2)	-17(2)
C(4)	127(7)	99(5)	65(4)	-14(4)	-47(4)	-71(5)
C(5)	169(9)	158(8)	70(5)	-36(5)	-48(5)	-100(7)
C(6)	156(8)	118(7)	117(7)	-57(6)	-70(6)	-56(6)
C(7)	325(15)	139(9)	151(9)	15(6)	-150(11)	-160(10)
C(8)	211(10)	95(6)	87(6)	-0(4)	-84(6)	-98(7)
C(9)	226(14)	144(10)	155(9)	-81(8)	-112(10)	-35(8)
C(10)	163(11)	181(11)	104(7)	-51(8)	-50(7)	-99(9)
C(11)	130(11)	209(16)	308(19)	-178(16)	-127(12)	19(10)

The anisotropic displacement exponent takes the form:

$$-2\pi^2(h^2 a^{*2} U_{11} + \dots + 2hka^* b^* U_{12})$$

**Table B.17: Anisotropic displacement parameters for [17]**

( $\text{\AA}^2 \times 10^3$ )

atom	$U_{11}$	$U_{22}$	$U_{33}$	$U_{23}$	$U_{13}$	$U_{12}$
Sn(1)	59.1(5)	38.2(4)	35.1(4)	-4.3(3)	-2.0(4)	4.4(4)
Sn(2)	60.9(5)	40.1(4)	36.7(4)	-3.9(3)	0.5(4)	4.5(4)
C1(1)	233(5)	79(2)	83(2)	-44(2)	-25(3)	34(3)
C1(2)	167(4)	51(2)	174(4)	16(2)	69(3)	-6(2)
C1(3)	114(3)	126(3)	186(4)	-67(3)	-70(3)	57(3)
C1(4)	126(3)	71(2)	68(2)	12(2)	-18(2)	20(2)
C1(5)	221(5)	61(2)	161(4)	-13(2)	-95(4)	-14(3)
C1(6)	128(3)	119(3)	135(3)	26(3)	33(3)	74(3)
C1(7)	194(4)	102(3)	72(2)	-24(2)	10(2)	69(3)
C1(8)	189(5)	48(2)	248(6)	-31(3)	68(4)	-15(3)
C1(9)	133(4)	236(6)	179(5)	-125(4)	-80(3)	117(4)
O(1)	92(5)	42(4)	41(4)	-13(3)	-2(4)	14(4)
O(2)	87(6)	61(5)	50(5)	1(4)	-15(4)	14(4)
O(3)	74(5)	48(4)	54(4)	-1(4)	0(4)	11(4)
O(4)	92(6)	84(6)	66(5)	18(4)	19(4)	29(5)
O(5)	78(5)	58(5)	48(4)	-0(3)	1(4)	22(4)
O(6)	70(5)	48(4)	46(4)	-3(3)	1(3)	9(4)
O(7)	62(4)	48(4)	33(3)	-2(3)	0(3)	10(3)
C(1)	46(6)	44(6)	44(6)	-5(5)	-8(5)	-2(5)
C(2)	82(8)	42(6)	42(6)	-9(5)	-12(6)	10(6)
C(3)	56(7)	45(6)	55(7)	1(5)	-1(6)	-3(5)
C(4)	81(8)	59(7)	64(7)	0(6)	-11(6)	9(6)
C(5)	51(6)	45(6)	48(6)	-11(5)	-2(5)	2(5)
C(6)	93(9)	46(6)	49(6)	-18(5)	0(6)	14(6)
C(7)	63(7)	53(6)	45(6)	-6(5)	-1(5)	-2(5)
C(8)	60(8)	73(8)	76(8)	-3(6)	-4(6)	-13(6)
C(9)	88(10)	67(9)	124(12)	-7(8)	-14(8)	-12(7)
C(10)	70(9)	92(10)	108(10)	-17(8)	-14(8)	-14(7)
C(11)	64(9)	107(11)	130(13)	-18(9)	-12(9)	3(8)
C(12)	62(8)	69(8)	84(9)	-1(7)	-5(7)	0(7)
C(13)	65(7)	47(6)	54(6)	1(5)	-9(6)	-11(5)
C(14)	94(10)	88(9)	56(8)	-18(7)	15(7)	-26(8)
C(15)	113(11)	114(12)	83(10)	-20(8)	42(8)	-43(9)
C(16)	75(10)	79(10)	131(13)	-9(9)	4(9)	-18(8)
C(17)	66(9)	75(9)	130(12)	-38(9)	-23(8)	-5(7)
C(18)	64(8)	77(8)	58(7)	-13(6)	-1(6)	-3(7)
C(19)	93(9)	32(5)	28(6)	-3(5)	-9(6)	2(6)
C(20)	111(12)	68(9)	72(9)	-16(7)	-11(8)	-11(8)
C(21)	106(11)	100(11)	118(12)	-37(9)	-23(9)	-25(9)
C(22)	128(14)	73(10)	73(10)	-2(8)	-39(9)	-32(10)
C(23)	151(14)	47(8)	52(8)	-4(6)	-15(9)	1(9)
C(24)	96(9)	59(7)	44(6)	-3(6)	-3(6)	-5(7)
C(25)	75(8)	70(8)	35(6)	4(5)	-0(5)	3(6)
C(26)	91(10)	51(8)	122(11)	-25(7)	27(8)	-14(7)
C(27)	150(15)	81(11)	107(12)	-10(9)	4(11)	-59(11)
C(28)	87(11)	132(14)	103(12)	-3(10)	6(9)	-47(10)
C(29)	76(11)	119(14)	137(14)	8(12)	17(10)	13(10)
C(30)	80(9)	61(8)	116(11)	13(8)	22(8)	-2(7)

The anisotropic displacement exponent takes the form:

$$-2\pi^2(h^2a^{*2}U_{11} + \dots + 2hka^*b^*U_{12})$$



## **APPENDIX C**

### **Final Structure Factor Tables**

The structure factor tables for structures [3], [13], [14], [15], [16] and [17] have already been deposited. The tables for the remaining structures will be deposited when they are published. All tables are available on request.